

The copyright of this thesis vests in the author. No quotation from it or information derived from it is to be published without full acknowledgement of the source. The thesis is to be used for private study or non-commercial research purposes only.

Published by the University of Cape Town (UCT) in terms of the non-exclusive license granted to UCT by the author.

UNIVERSITY OF CAPE TOWN



PROBABILISTIC MODELLING FOR DURABILITY DESIGN OF REINFORCED CONCRETE STRUCTURES

NAME: RACHEL NJERI MUIGAI
STUDENT NUMBER: MGXRAC001
PROGRAMME (2007): EMOO1
CIV: 5000
DATE: 22/09/2008

Submitted to the Faculty of Engineering and Built Environment, University of Cape Town, on the 22nd September, in partial fulfilment of the requirements for the degree of Master of Science in Civil Engineering

CAPE TOWN, 2008

DECLARATION

This dissertation is being submitted in partial fulfilment for the Degree of Masters of Science in Engineering at the University of Cape Town. It has not been submitted before for any degree or examination at any other university. In addition, I know the meaning of plagiarism and declare that all the work in the document, save for that which is properly acknowledged, is my own.

22nd Day of September 2008

ABSTRACT

The purpose of this study was to create a framework for the development of a probabilistic model for durability design of reinforced concrete (RC) structures in South African marine conditions. Durability design of RC structures is mainly concerned with ensuring the ability of the concrete to resist the penetration of aggressive agents during the concrete's intended service life. RC structures in the marine environment may be attacked by aggressive chloride ions which penetrate concrete mainly through the diffusion mechanism. The chloride ions accumulate at the steel level and, upon reaching a critical concentration, cause corrosion to initiate which if not intercepted leads to the eventual deterioration of the entire structure.

The study involved modelling the chloride ingress mechanism using modified Fick's second law of diffusion. The model includes: environmental parameters (surface chloride concentration and critical chloride content derived from both field and laboratory tests); material parameter (diffusion coefficient which was derived from the chloride conductivity test) and geometric parameter (cover depth from field measurements of existing bridge structures).

The model parameters were all found to be variable and taken into account as stochastic quantities (represented in terms of mean, coefficients of variation and probability distributions). Between these parameters a mathematical relationship or limit state function (LSF) was formulated to describe the durability limit state (i.e. the point at which corrosion initiates).

The statistical information for each parameter was exploited in this study to provide improved uncertainty estimates of the output, which was expressed in terms of the probability of durability failure. An example was illustrated of the use of Monte Carlo simulation (MCS) techniques i.e. both parametric and non-parametric bootstrapping methods in calculating the reliability against depassivation of reinforcement for a given choice of the LSF parameters.

Finally, a sensitivity analysis was carried out to show the influence of each of the parameters to the probability of durability failure. The cover depth was found to be the most sensitive parameter in the durability design. This shows that it is important to work out the thickness of concrete cover that will provide adequate protection of the structure in the marine environment. The study found other factors such as water-cement ratio and protection condition to each affect the quality of concrete cover.

Key words: Reinforced concrete durability, probabilistic modelling, chloride-induced corrosion, Variability

Thesis Supervisor: Assoc. Prof. Pilate Moyo

Co-Supervisor: Prof. Mark Alexander

ACKNOWLEDGEMENTS

I would like to express my sincere gratitude to my supervisors: Professor Pilate Moyo and Professor Mark Alexander for their assistance throughout this research.

And to my parents, sister and brothers for their continued support and assistance.

University of Cape Town

TABLE OF CONTENTS

<u>Contents</u>	<u>page</u>
DECLARATION	ii
ABSTRACT	iii
ACKNOWLEDGEMENTS	iv
TABLE OF CONTENTS	v
LIST OF FIGURES	viii
LIST OF TABLES	xi
LIST OF TERMS, DEFINITIONS AND SYMBOLS	xv
CHAPTER 1: INTRODUCTION	1
1.1 BACKGROUND.....	1
1.2 RESEARCH MOTIVATION.....	4
1.3 RESEARCH HYPOTHESIS AND OBJECTIVES.....	8
1.4 LAYOUT OF THESIS	12
1.5 REFERENCES.....	13
CHAPTER 2: LITERATURE REVIEW	17
2.1 BACKGROUND.....	17
2.1.1 Introduction	17
2.1.2 Factors influencing penetrability.....	18
2.1.3 Chloride ion penetrability.....	21
2.2 FICKIAN DIFFUSION MODELS	25
2.2.1 Collepari's model	25
2.2.2 Time-dependent diffusivity models	26
2.3 DIFFUSION COEFFICIENTS	29
2.3.1 Non-Steady State Migration Tests	30
2.3.2 Steady-State Conduction Tests.....	34
2.3.3 Summary of diffusion coefficient used in the study.....	40
2.4 DURABILITY DESIGN.....	41
2.4.1 General	41
2.4.2 Approaches to Service Life Design.....	42
2.5 SUMMARY	56
2.6 REFERENCES.....	57

CHAPTER 3: METHODOLOGY	67
3.1 INTRODUCTION.....	67
3.2 OBJECTIVES OF THE STUDY	67
3.3 LIMIT-STATE DURABILITY DESIGN	69
3.3.1 Introduction	69
3.3.2 Durability Design Procedure.....	71
3.3.3 Limit-State Function Parameters.....	76
3.3.4 Material Parameters.....	77
3.3.5 Environmental Parameter	82
3.3.6 Structural Parameter: Cover depth	85
3.4 FITTING DISTRIBUTIONS TO DATA.....	87
3.4.1 Uncertainty in LSF parameters.....	87
3.4.2 Main Descriptors of Random Variables	89
3.4.3 Goodness-of-fit-tests	91
3.4.4 Tail sensitivity	91
3.5 MONTE-CARLO SIMULATION	92
3.6 SENSITIVITY ANALYSIS.....	94
3.7 REFERENCES.....	96
CHAPTER 4: STATISTICAL QUANTIFICATION and RELIABILITY ANALYSIS	101
4.1 INTRODUCTION.....	101
4.2 SURFACE CHLORIDE CONCENTRATION	102
4.2.1 Collection of data	102
4.2.2 Classification of data.....	104
4.2.3 Statistical quantification of C_s data	109
4.2.4 How C_s distribution compares to others in literature	112
4.2.5 Summary of C_s results.....	114
4.3 CRITICAL CHLORIDE CONTENT.....	115
4.4 CHLORIDE CONDUCTIVITY & DIFFUSION COEFFICIENT	116
4.4.1 Collection and Classification of Chloride Diffusion Data	116
4.4.2 Statistical quantification of chloride diffusion data	122
4.4.3 Summary of D_i results	126
4.5 COVER DEPTH	126
4.6 MODEL UNCERTAINTIES	128

4.7	RELIABILITY ANALYSIS	129
4.7.1	Monte Carlo Simulations	129
4.7.2	Example: Reliability Analysis of a RC Pier	130
4.7.3	Method of Sensitivity Analysis	135
4.8	CONCLUSION	140
4.8.1	Discussion	140
4.8.2	Specific Conclusions	143
4.8.3	General conclusion	143
4.9	REFERENCES	145
	CHAPTER 5: CONCLUSION and RECOMMENDATIONS	150
5.1	SUMMARY	150
5.1.1	Service Life Prediction	150
5.1.2	Importance of the study	153
5.2	LIMITATIONS AND FUTURE RESEARCH	154
5.2.1	Limitations in analysis	154
5.2.2	Limitations in the service life prediction model	155
5.3	CONCLUSIONS	156
5.4	RECOMMENDATIONS	157
5.4.1	Bayesian updating of probability distribution functions	157
5.4.2	Validating the probabilistic model	157
5.4.3	Probabilistic carbonation model	157
5.5	REFERENCES	159
	APPENDIX A: Surface Chloride Concentration Data	160
	APPENDIX B: Fitting Distributions to surface chloride Data	165
	APPENDIX C: Diffusion Coefficient Data	168
	APPENDIX D: Goodness-of-Fit Test	176
	APPENDIX E: MCS Program Documentation	183
	APPENDIX F: Durability Index Tests	186
	APPENDIX G: First Order Reliability Method (FORM)	188
	APPENDIX H: Service Life Design Examples	195
	APPENDIX I: Ethics form	202

LIST OF FIGURES


<u>Figure</u>	<u>page</u>
Figure 1.1: Range of design making values due to uncertainty in concrete materials	6
Figure 2.1: The corrosion process based (adopted from: Liu <i>et al.</i> , 1998)	23
Figure 2.2: Tang and Nilsson migration cell (source: Hooton <i>et al.</i> , 2001)	31
Figure 2.3: Nord test setup (source: Hooton <i>et al.</i> , 2001)	33
Figure 2.4: Chloride Conductivity Test (Alexander <i>et al.</i> , 1999).....	35
Figure 2.5: Illustrative cost-benefit analysis (Phoon, 2000).....	49
Figure 2.6: Relation between characteristic values, design values and partial factors of safety.....	53
Figure 2.7: Summary of service life design approaches.....	55
Figure 3.1: Flow chart of the methodology followed in the study	69
Figure 3.2: Illustration of the decrease of resistance with time and increase of load with time (Rostam, 2005)	70
Figure 3.3: Flow chart of the durability design procedure (<i>Adapted from</i> Sarja, 2002).....	72
Figure 3.4: Illustration of PDF showing relation of the action effect, resistance and probability of failure	75
Figure 3.5: Illustration of decrease in diffusion coefficient (log-scale) with time (normal scale) for different binder types	81
Figure 3.6: Chloride profile with fitted curves for C_s (Song <i>et al.</i> , 2008).....	84
Figure 3.7: Cover depth  measurements	85
Figure 3.8: Complex reinforcement detailing which does not allow for adequate compaction (Rostam, 2005).....	86
Figure 3.9: Cover meter (Song and Saraswathy, 2007).....	87
Figure 3.10: Types of uncertainty	88
Figure 3.11: Flow chart of the MCS procedure service-life design	94
Figure 4.1: Detail of the geographical locations of the marine structures investigated and sample exposure sites along the Cape Peninsula and environs	103
Figure 4.2: Illustration of box and whisker plot.....	107
Figure 4.3: Comparative box-plots of C_s data for PC concrete structures in XS3b [#] marine zone.....	107

Figure 4.4: Comparative box-plots of C_s data for PC concrete structures in XS3a [#] marine zone.....	108
Figure 4.5: Comparative box-plots of C_s data for PC concrete structures in XS1 marine zone.....	108
Figure 4.6: Histogram of surface chloride concentration of OPC concrete in XS1 marine environment	110
Figure 4.6: Histogram and distribution fit of surface chloride concentration of OPC concrete in very severe spray marine environment.....	111
Figure 4.7: Correlation of 28-day chloride conductivity and D_i for CSF.....	118
Figure 4.8: Correlation of 28-day chloride conductivity and D_i for FA.....	118
Figure 4.9: Correlation of 28-day chloride conductivity and D_i for FA.....	119
Figure 4.10: Correlation of 28-day chloride conductivity and D_i for FA.....	119
Figure 4.11: Correlation of 28-day chloride conductivity and corresponding D_i for FA	120
Figure 4.12: Histogram of chloride conductivity of CSF concrete cured with a curing compound based on 999 non-parametric simulations.....	125
Figure 4.13: Histogram of diffusion coefficient of CSF concrete cured with a curing compound based on 999 non-parametric simulations.....	125
Figure 4.14: Scatterplot for cover depth data in South African (Ronne, 2005).....	127
Figure 4.15: CDF of probability of failure for diffusion coefficient values	134
Figure 4.16: Sensitivity of cover depth to probability of corrosion initiation.....	135
Figure 4.17: Sensitivity of surface chloride concentration to probability of corrosion initiation.....	137
Figure 4.18: Sensitivity of critical chloride content to probability of corrosion initiation.....	138
Figure 4.19: Sensitivity of diffusion coefficient to probability of corrosion initiation	139
Figure B.1: Histogram and distribution fit of surface chloride concentration of OPC concrete in extreme tidal and splash marine environment.....	165
Figure B.2: Histogram and distribution fit of surface chloride concentration of OPC concrete in very severe tidal and splash (XS3a) marine environment.....	167
Figure E.1: Flow chart of the MCS program used for the reliability analysis	183
Figure E.2: Flow chart of the FORM program used for the reliability analysis.....	184
Figure F.1: Water sorptivity test apparatus (Page and Badenhorst, 2007)	186

Figure F.2: Oxygen permeability test set-up (Durability index testing manual, 2007)..... 187
Figure G.1: Illustration of the reliability index β (Ljungquist, 2005; Holichky, 2007) 190
Figure H.1: Extension of the service life of a concrete structure with corrosion
inhibitor treatment (Laamenen *et al.*, 1996). 198

University of Cape Town

LIST OF TABLES

Table	page
Table 2.1: Repeatability and reproducibility of tests given in terms of the coefficient of variation (%) (Castellote <i>et al.</i> , 2006).....	33
Table 2.2: Repeatability and reproducibility of steady state test (Stanish <i>et al.</i> , 2006)	36
Table 2.3: Recommended Service Life for Different Structure Types (EN 1990:2000).....	41
Table 2.4: Guideline for selection of factor values for concrete (Hovde, 2005)	45
Table 2.5: Relationship between reliability index β and probability of failure P_f (Melchers, 1999).....	48
Table 2.6: Indicative values of P_{target} and β_{target} at ILS for 100 years service life design.....	49
Table 3.1: Marine Environmental Classes (Natural environments only) (after EN206-1 <i>as cited in</i> Alexander <i>et al.</i> , 2001)	73
Table 3.2: Basic random variables in the initiation limit-state function	77
Table 3.3: Chloride diffusion coefficient reduction factor	80
Table 3.4: Critical chloride content levels.....	82
Table 4.1: Basic random variables in the initiation limit-state function	101
Table 4.2: Concrete Structures investigated for surface chloride concentration (Mackechnie, 1996)	102
Table 4.3: Marine exposure categories for South African conditions (<i>Adopted from:</i> SABS 1992, <i>as cited in</i> Mackechnie, 1996)	104
Table 4.4: Marine Environmental Classes EN206-1 Vs SABS-2 (1992).....	105
Table 4.5: Chi-squared tests of two distributions for OPC concrete in XS1 marine environment	111
Table 4.6: Summary of statistics for surface chloride concentration parameter	112
Table 4.7: Concrete Structures investigated for surface chloride concentration	113
Table 4.8: Statistical quantities of surface chloride concentration from literature for OPC.....	113
Table 4.9: Statistical quantities for surface chloride concentration regression parameters (Duracrete, 2000) (Values given in % by weight of binder)	114

Table 4.10: Statistical quantities of critical chloride content for OPC binder (% by mass of cement)	115
Table 4.11: Mix proportions (kg/m^3) of concrete (<i>adopted from Du Preez, 2002</i>).....	116
Table 4.12: Summary of statistical quantities of chloride conductivity values (mS/cm) for w/c=0.5.....	122
Table 4.13: Summary of statistical quantities of effective diffusion coefficients (m^2/s) for w/c=0.5.....	123
Table 4.14: Suggested COV values for various standards of control for typical British construction practice (Sharp, 1997 as cited in Ronne and Beushausen, 2008).....	127
Table 4.15: COV of cover depths (mm) from South African data (Ronne, 2005)	128
Table 4.16: Statistical quantities of cover depth (mm) in mm for this study.....	128
Table 4.17: Assumed factor for conversion of chloride conductivity to diffusion coefficient	129
Table 4.18: Summary of statistics for LSF variables	130
Table 4.19: Input parameters for reliability analysis of RC pier	132
Table 4.20: Maximum Chloride Conductivity Values (mS/cm) for Different Classes and Binder Types: Deemed to Satisfy Approach – Monumental Structures (Cover = 50 mm) (Alexander <i>et al.</i> , 2007)	134
Table 4.21: Range of parameters for sensitivity analysis.....	135
Table 4.22: Sensitivity of concrete cover depth to P_f	136
Table 4.23: Sensitivity of surface chloride concentration to P_f	137
Table 4.24: Sensitivity of critical chloride content to P_f	138
Table 4.25: Sensitivity of diffusion coefficient to P_f	139
Table 4.26: Sensitivity of parameters to P_f	140
Table 5.2: Carbonation Exposure Classes (Natural environments only) (after EN206-1 as cited in Alexander <i>et al.</i> , 2001)	158
Table A.1: Surface chloride concentration of CEM I + Slag concrete in extreme splash and tidal environment	160
Table A.2: Surface chloride concentration of OPC + FA concrete in extreme splash and tidal environment	160

Table A.3: Mix composition of OPC concrete structures in extreme splash and tidal environment (adopted from Mackechnie, 1996).....	161
Table A.4: Mix composition of LASRC concrete structures in extreme splash and tidal environment (adopted from Mackechnie, 1996).....	161
Table A.5: Mix composition of OPC concrete structures in very severe splash and tidal marine environment (adopted from Mackechnie, 1996).....	162
Table A.6: Mix composition of PC concrete structures in very severe spray environment (adopted from Mackechnie, 1996).....	163
Table A.7: Mix composition of OPC concrete structures in severe spray environment (adopted from Mackechnie, 1996).....	164
Table A.8: Surface chloride concentration of submerged OPC concrete.....	164
Table A.9: Surface chloride concentration of submerged OPC + FA concrete.....	164
Table B.1: Computation of Chi-square tests of three distributions of OPC concrete in extreme tidal and splash marine environment.....	165
Table B.2: Computation of Chi-square tests of three distributions for OPC concrete in very severe tidal and splash (XS3a) marine environment	167
Table C.1: Steady state (Effective) diffusion coefficient of moist cured OPC+ CSF concrete.....	168
Table C.2: Steady state (Effective) diffusion coefficient of moist cured OPC+ FA concrete.....	168
Table C.3: Steady state (Effective) diffusion coefficient of moist cured OPC+ GGBS concrete.....	169
Table C.4: Steady state (Effective) diffusion coefficient of dry cured OPC+ CSF concrete.....	169
Table C.5: Steady state (Effective) diffusion coefficient of dry cured OPC+ FA concrete.....	170
Table C.6: Steady state (Effective) diffusion coefficient of dry cured OPC+ GGBS concrete.....	170
Table C.7: Steady state (Effective) diffusion coefficient of wet cured OPC+ CSF concrete.....	171
Table C.8: Steady state (Effective) diffusion coefficient of wet cured OPC+ FA concrete.....	171
Table C.9: Steady state (Effective) diffusion coefficient of wet cured OPC+ GGBS concrete.....	172

Table C.10: Steady state (Effective) diffusion coefficient of non-cured OPC+ CSF concrete.....	172
Table C.11: Steady state (Effective) diffusion coefficient of non-cured OPC+ FA concrete.....	173
Table C.12: Steady state (Effective) diffusion coefficient of non cured OPC+ GGBS concrete.....	173
Table C.13: Steady state (Effective) diffusion coefficient of OPC+ CSF concrete cured using a curing compound.....	174
Table C.14: Steady state (Effective) diffusion coefficient of OPC+ FA concrete cured using a curing compound.....	174
Table C.15: Steady state (Effective) diffusion coefficient of OPC+ GGBS concrete cured using a curing compound.....	175
Table D.1: Critical Values χ^2 of the Distribution at Probability Level α (Ang and Tang, 2007).....	180
Table G.1: Polynomial expansion coefficients.....	189
Table H.3: Design requirements.....	195
Table H.2: Deemed-to-satisfy parameters (Alexander <i>et al.</i> , 2007).....	196
Table H.3: Recommended material values (Table H.2).....	196
Table H.4: Characteristic values for input parameters in the LSF.....	199
Table H.5: Partial factors for parameters (adopted from Edvardsen, 1999).....	199
Table H.6: Design values for input parameters in the LSF.....	200

LIST OF TERMS, DEFINITIONS AND SYMBOLS

μ	→ Mean value of population
σ	→ Standard deviation of population
s	→ Standard deviation of sample
T_D	→ Design service life
P_f	→ Probability of failure
Beta-D	→ Beta distribution
COV	→ Coefficient of variation (ratio of standard deviation and mean value in percentage)
D	→ Diffusion coefficient
x	→ Cover depth
Gamma-D	→ Gamma distribution
ILS	→ Initiation limit state
Lognormal-D	→ Lognormal distribution
LSF	→ Limit state function
MCS	→ Monte Carlo simulation
mm	→ millimeters
N	→ Normal distribution
RBD	→ Reliability based design
RC	→ Reinforced concrete
SL	→ Service Life
SLD	→ Service life design
SLP	→ Service life prediction
UCT	→ University of Cape Town
w.r.t	→ With respect to

CHAPTER 1: INTRODUCTION

1.1 BACKGROUND

The International Standards Organisation defines durability as the capability of a structure to perform its intended function over a specified period of time under the influence of agents anticipated in service (ISO 15686-8:2008). The influencing agents include live loading and environmental loading. Durability design is concerned with predicting the longevity of structures, comparing life cycle costs, mitigating deterioration and optimising the selection of material.

The durability of reinforced concrete (RC) depends on the interactions with the service environment, in which penetration of deleterious substances is highly significant. The ingress of various ions, liquids and gases from the environment is responsible for the deterioration of concrete directly or indirectly. For instance, the ingress of chlorides or carbon dioxide would depassivate the steel in concrete, and in the presence of oxygen and water, steel may start corroding (Basheer *et al.*, 2001). Durability design of RC structures is concerned with ensuring the ability of the concrete to resist the penetration of aggressive agents during its intended service life. This largely involves controlling the quality and thickness of the cover layer protecting the reinforcement (Alexander and Stanish, 2001). The cover layer is most susceptible to poor construction practices (such as poor curing and inadequate compaction) which in turn increases the penetration of aggressive agents from the environment. Thus, designing for durability requires (Tikal'sky *et al.*, 2005):

- (i) Advanced knowledge of material transport mechanisms that describe the ingress of deleterious agents from the service environment into concrete.
- (ii) Properties and methods of production of construction material.
- (iii) Structural design and detailing to provide sufficient cover to reinforcement and quality control practices that should be implemented during construction.

Conventional structural design procedures provide for durability by prescribing limiting values for material specifications depending on the environmental conditions and life span of the structure. For example, BS (8110-1:1997) and SANS 10100 (2005) give the limiting values of the concrete cover to be provided to all reinforcement, 28-day compressive strength and cement content in order to achieve a durable concrete for a range of water-cement ratios (Table 3.3 and 4.8 of BS 8110-1, 1997 and Table 2 of SANS 10100-2, 2005). This approach to design is termed prescriptive approach and has a role to play in durability design but it cannot fulfil the need in certain instances. Firstly, the approach does not provide a means to verify or control the presumed concrete durability quality which is measured by the ability of the concrete to prevent ingress of aggressive agents using durability tests. Secondly, the prescriptive approach does not adequately define the material limit state or the deterioration mechanisms a structure is subjected to during its lifetime. The limit state in this case is the border that separates desired states from the undesired or adverse states under exposure conditions, which a RC structure may be subjected to during its lifetime (Edvardsen and Mohr, 1999). Ultimate limit state (ULS) depicts the point at which the safety of the RC structure is considered (for example the risk of collapse), serviceability limit state (SLS), is the point where the functionality of the structure is considered (for example the limitation of crack widths), and the initiation limit state (ILS), precedes both the occurrence of ULS and SLS, and is used to describe the onset of deterioration such as corrosion initiation. Lastly, the prescriptive approach considers concrete strength as the main indicator of durability (Stanish *et al.*, 2007), postulating that a stronger concrete is more durable (Kwan and Wong, 2006). However, this is not always the case, especially when high-strength concrete (HSC) is used for resistance against freezing and thawing action and certain forms of chemical attack. In such cases, HSC has been shown to lead to the development of shrinkage cracks, making the structure vulnerable to deterioration (Mehta, 2006). For these reasons the prescriptive approach has been increasingly refined to address durability requirements.

The European code, EN 206-1, addresses the shortcomings of the prescriptive approach by introducing sub-classes of exposure conditions and corresponding deterioration mechanisms on concrete (EN 206, 2000). When determining limiting values of concrete composition, the designer is forced to consider the most onerous condition, that the concrete structure or element will be exposed to (Richardson, 2002). The expanded suite of exposure classes is more likely to reflect specific deterioration mechanisms which allow the designer to prescribe

more reliable specifications (Richardson, 2002). In addition, EN 206- 1 introduces a further improvement to the prescriptive approach by allowing the method to be combined with performance tests and indicators. The performance tests quantify the cover layer transport properties of RC structures and are required to be reliable, repeatable and reproducible (Baroghel-Bouny, 2002; Mehta and Burrows, 2001).

In South Africa (SA), durability indexes (DI's) have been adopted as engineering measures of the potential resistance of concrete cover to the transport mechanisms of gaseous diffusion, water absorption and chloride diffusion (Alexander *et al.*, 1999). The DI's are derived from three tests; the chloride conductivity test, where chloride ion resistance is important, the oxygen permeability test to establish carbonation resistance, and a sorptivity test to examine concrete for water absorption. DI's characterise the macrostructure of the cover concrete and have been shown to be sensitive to material parameters such as binder type, processing influences such as type and degree of curing, and environmental influences such as temperature and relative humidity (Stanish *et al.*, 2007). The DI tests also serve as valuable inputs to service life prediction (SLP) models.

SLP models provide an alternative method to improving prescriptive durability design and rely heavily on durability tests output characterising the material quality, and also take into account the geometric properties and the environmental load on the structure in assessing performance. In SA, two corrosion initiation prediction models have been developed, related to carbonation-induced corrosion and chloride-induced corrosion, and derived from measurements and correlations of short-term durability index values, aggressiveness of the environment and actual deterioration rates monitored over periods of up to 10 years (Stanish *et al.*, 2007). The SLP models allow the expected service life of a structure to be predicted based on considerations of environmental conditions, cover thickness and concrete quality (Stanish *et al.*, 2007). The environmental classes used are related to the EN 206-1 classes, modified for South African conditions, while concrete quality is represented by the appropriate durability index parameter. The oxygen permeability index is used in the carbonation prediction model, while the chloride model utilises chloride conductivity to characterise material quality (Stanish *et al.*, 2007). The SA SLP models are used during the design and construction phases of new structures to give performance specifications, in the

form of appropriate combination of concrete quality (DI value) and cover , that provide sufficient resistance of the concrete to aggressive agents (Alexander *et al.*, 2003).

Heiyantuduwa *et al.* (2006) compared the SA SLP models to other existing SLP models (the Swedish ClinConc model, the European DuraCrete model and the North American 365 Life model) and noted that both the North American 365 Life model and the SA SLP models produce only a single deterministic time to corrosion initiation. This deterministic output contrasts with the well known fact that concrete properties are quite variable both throughout the structure and in terms of quality of construction and materials used (Bentz, 2003). This study therefore proposes the development of a probabilistic SLP model similar to the SA service life model for chloride-induced corrosion but differs in that it takes into account the range of possible values for each input parameter at the initiation limit state. The probabilistic SLP model would be able to predict a range of expected times to corrosion initiation rather than a single value so as to allow owners to make an easier and more accurate selection of durability parameters and economical decisions of structural concrete. It would thus assist in getting a balance of economy, durability as well as safety of the concrete material.

The modelling of the service life of RC structures using probabilistic models is made possible through the integration of reliability theory as used in structural load design (DuraCrete, 1998 and DuraCrete, 2000). Reliability theory incorporates statistical databases and probability theory to give a relative measure of the confidence in the ability of the RC structure to perform its function in a satisfactory manner (Puatatsananon and Saouma, 2006).

1.2 RESEARCH MOTIVATION

Much of South African infrastructure is situated in coastal areas and is thereby exposed to marine environments. The relatively harsh environment coupled with inadequate attention to durability with regard to both design and construction, has resulted in premature deterioration of RC structures in SA (Mackechnie, 1998). The main cause of deterioration has been related to reinforcement corrosion induced essentially by chlorides from the sea water penetrating into the concrete. Chloride ingress into concrete can occur by a number of transport mechanisms: diffusion under the influence of a concentration gradient, absorption due to capillary action, migration in an electric field, a pressure-induced flow and wick action resulting from combined water absorption and water vapour diffusion (Buenfield, 1997). Of

these transport mechanisms, diffusion is considered as the predominant mechanism for chloride penetration through concrete in marine structures based on the assumption that concrete is generally moist (Collepari *et al.*, 1972; Kropp, 1995). The chloride ions progressively diffuse into the concrete, and upon reaching a critical concentration at the reinforcement level, cause the depassivation of the steel oxide layer. Following which, corrosion initiates in the presence of oxygen and water (Youping, 1996).

Once corrosion is initiated, it tends to propagate itself if untreated. The pH within the rust film becomes progressively more acidic. The size of the corrosion activity site increases. As corrosion progresses, the corrosion by-product (rust) takes up more space than the original steel causing pressure within the concrete leading to concrete cracking and spalling. The cracks allow more chloride bearing water to enter the concrete, further intensifying corrosion activity (Pandey and Banerjee, 1998).

Owing to the problems associated with chloride-induced corrosion in RC structures, reliable prediction of chloride ingress in concrete is one of the key elements in durability design (Luping and Gulikers, 2007). The error function solution of 'Fick's second law of diffusion' (Crank, 1975) is used to model the diffusion of chloride ions into concrete (Equation 1-1).

$$C_{(x,t)} = C_s \left[1 - \operatorname{erf} \left(\frac{x}{2\sqrt{Dt}} \right) \right] \quad (1-1)$$

Where, $C_{x,t}$ is the chloride concentration at distance x (mm) from the exposed surface at a certain time t (s); C_s is the surface chloride concentration (% Cl^{-1} by mass of cement); D is the chloride diffusion coefficient (m^2/s) and erf is the error function. Derivation of this formula is given in Chapter 2.

The input parameters of the diffusion model (Equation 1-1) exhibit variability arising from material variability, construction tolerances, experimental error and modelling errors. The resulting uncertainties are termed as physical, statistical, and model uncertainties. The cover depth, x , exhibits physical uncertainty due to variations in concrete production, curing conditions, quality of workmanship in the construction site and occasionally the quality of design (Bentz, 2003). Statistical uncertainties result from measurement errors, number of samples tested, data handling and transcription errors depending on the quality assurance

observed during the test. Model uncertainties are associated with the use of simplified mathematical models or relationships between the basic variables to represent the actual physical phenomena of chloride ingress and corrosion initiation (Zhang and Lounis, 2006). This may be made due to lack of knowledge of the behaviour of materials in their service environment. For example, earlier research had postulated that concrete is inert and from this, made an assumption that the diffusion coefficient D is an intrinsic material constant. However, with advent of advanced materials technology it is now known that considerable chemical and physical interaction (continued hydration and cement binding) occurs between concrete and its environment, thereby making the diffusion coefficient a time and environmental-dependent property of the material (Mackechnie and Alexander, 1997). In addition, the diffusion model limits the number of basic variables, leaving out possibly an infinite set of parameters which during the model idealization were judged as secondary or of negligible importance to corrosion initiation. The aforementioned sources of uncertainty in concrete material affect the predictive ability of corrosion initiation models. The uncertainties make it difficult or rather impossible to say with any conviction that there is a uniquely defined value for corrosion initiation (Scott, 2004). It is more likely that there is a certain probability range of time values that the designer can design for as represented in Figure 1.1.

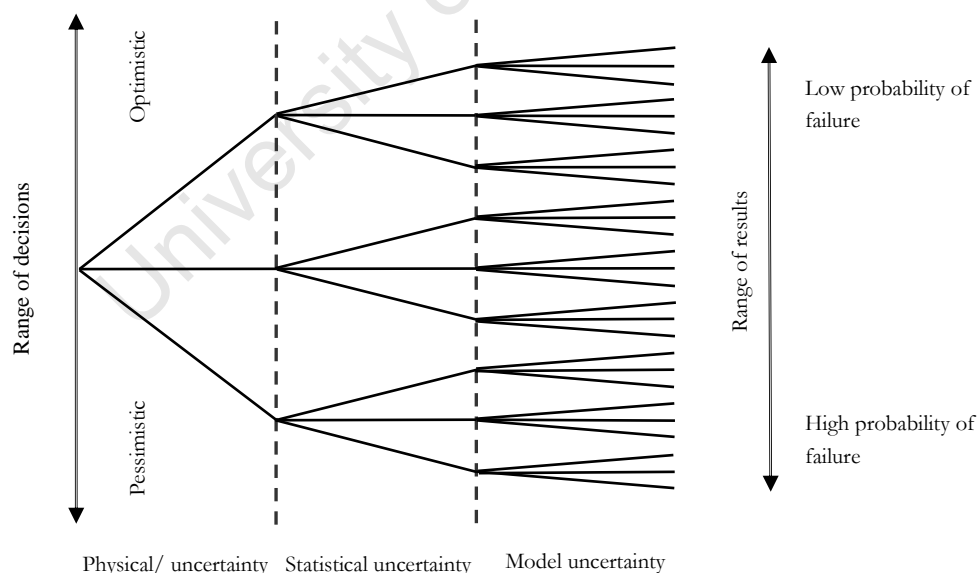


Figure 1.1: Range of design making values due to uncertainty in concrete materials

From Figure 1.1 it is clear that the design may result in a wide range of results depending on the optimism or pessimism of each decision made. A solution to this problem would be to

carry out an uncertainty analysis, which provides a formal and systematic framework of quantifying the uncertainty associated with the model output. The task of uncertainty analysis is to describe the degree of uncertainty of a single parameter or the uncertainty of the model itself with the use of a probability density function (PDF) and statistical moments (mean, standard deviation and skewness) (DuraCrete, 2000). The results of an uncertainty analysis still present an arduous task to the designer due to the range of possible values that individual parameters in the mathematical model may take. Furthermore, the distribution types of the parameters may also differ from each other. For this reason the designer has to rely on reliability analysis to determine uncertainty of the design outputs as a function of the uncertainties in the mathematical model itself and the stochastic variables involved. Reliability analysis is carried out by combining probability theory and reliability methods such as analytical methods, approximated approaches or direct integration methods. The selection of an appropriate reliability method depends on the nature of the problem at hand including availability of information, resource constraints, model complexity and type and accuracy of the results desired (Holický, 2007). Reliability analysis uses a durability limit-state function (Z-function) that defines the difference between variables contributing to capacity R and those contributing to demand S . The limit-state function is represented as:

$$Z = R - S \quad (1.2)$$

For a RC corrosion problem, the capacity might be defined as the chloride threshold required to depassivate the steel and the demand might be defined as the chloride concentration at the steel level at a given time.

The results of reliability analysis give a measure of performance in terms of a reliability index (β) marking the ability of the structure to fulfil its intended function during the established time of service (Au, 2005). If the structure cannot fulfil its functions at any time during its service life it is said to have failed (Equation 1-3) (Raizer, 2004). The probability that this occurs for any one load application is the probability of limit state violation, or simply the probability of failure P_f (Li, 2007).

$$P_f = p \{ Z < 0 \} \quad (1-3)$$

The probability of failure P_f is then checked against an acceptable probability of failure P_{target} corresponding to a specified design service life (Li, 2007) such that:

$$P_f = p \leq P_{target} \quad (1-4)$$

The acceptable limit is obtained by undertaking a risk analysis. This involves conducting a life cycle cost-benefit analysis of the variation of the initial cost, maintenance costs and the expected failure costs in order to achieve the most economical target probability of failure for design P_{target} (Holický, 2007). In some cases due to limitation in time and resources an implicit evaluation of P_{target} is not possible. In such situations, P_{target} is determined explicitly by setting a value at a performance level that is comparable with the failure rates estimated from actual case histories. These explicit values of the target levels for the design of different types of structural components have been reported in various national and international standards and codes such as EN 206 and it is up to the designer to select an appropriate level of reliability P_{target} under specified design configuration (design constraints and performance criteria).

In summary the three processes: uncertainty analysis, reliability analysis and risk analysis all make up probabilistic design. This study is concerned with only the first two processes, i.e. uncertainty and reliability analysis.

1.3 RESEARCH HYPOTHESIS AND OBJECTIVES

The hypothesis developed for this study is that probabilistic models can be effectively employed to predict the potential durability of RC up to the time of corrosion initiation. So far probabilistic models for durability design for RC structures have not been developed in SA. Currently in use is an empirical model developed by Mackechnie (1996) (Equation 1-5) to predict the time to initiation of corrosion in a marine environment. The model is derived from the error function solution of Fick's 2nd law with a time-dependent diffusion coefficient and constant surface chloride content. The prediction model uses the 28-day diffusion coefficient derived from the chloride conductivity test values, and allows for the long-term cementing reactions and chemical interactions between chloride ions and the concrete. From the model, time to corrosion activation may be estimated for different concrete types.

$$C_{(x,t)} = C_s \left[1 - \operatorname{erf} \left(\frac{x}{2\sqrt{D_i t^{(1-m)}}} \right) \right] \quad (1-5)$$

Most of the parameters in the model have been defined in Equation 1-1. However, in Equation 1-1 the diffusion coefficient was assumed to be constant, in this case (Equation 1-5) the change in diffusion coefficient with time is taken into account by the material coefficient m .

The m value allows for a changing diffusion coefficient with time, such that at any given time t the diffusion coefficient D_t can be represented as a function of:

$$D_t = D_i \left(\frac{t_i}{t} \right)^m \quad (1-6)$$

Where, D_i is the instantaneous diffusion coefficient at time t_i .

This study undertakes to further develop Mackechnie's model to a probabilistic model. The governing parameters in this model are the critical chloride content C_{crit} ; the surface chloride concentration C_s , which defines the environmental loads on the structural elements; diffusion coefficient D_i which defines the quality of material; and the concrete cover C . The criteria used to develop the probabilistic model will be first, to establish the statistical distributions of the models input parameters. That is, the single value measured from the deterministic model is supplemented with some statistical parameter (such as the mean or standard deviation) to be able to truly reflect the service life. The second part of the study involves substituting the statistical parameters into Equation 1-5 and rearranging the equation to give the time to corrosion depassivation t :

$$t = \frac{1}{1-m} \sqrt[1-m]{ \left[\left(\frac{2}{x} \operatorname{erf}^{-1} \left(1 - \frac{C_{crit}}{C_s} \right) \right)^{-2} \frac{1}{D_i} \right] } \quad (1-7)$$

Subsequently, a computation is made to give the probability of time to depassivation being less or equal to the design service life t_d . In order to meet the durability design

requirements, the probability of failure for the initiation limit state during the design service life of the RC structure/ component must be kept within an acceptable target probability value P_{target} . P_{target} corresponds to the operation and maintenance costs incurred as well as the degree or risk of failure that may occur during the design service life (Cheung and Kyle, 1996).

With this respect, design verification is carried out as illustrated in Equation 1-8 to ensure the feasibility of the design.

$$P_f = P(\leq T_D) \leq P_{target} \quad (1-8)$$

It should be noted that since there is a wide range of possible values that individual parameters in the model may take, the analysis is only possible through the use of reliability analysis. The results of such an analysis would be in terms of the probability of failure (i.e. the probability that the calculated time to initiation is less than the service life).

This model is similar to other existing models but a distinguishing factor is that it uses results from chloride conductivity test (durability index tests) to model the diffusion coefficient. The chloride conductivity test measures the electrical resistance of concrete when saturated with a standard, highly ionic chloride solution. The chloride conductivity parameter is related to chloride diffusion properties, and is very sensitive to binder type with blended binders containing, e.g. fly ash, slag, or silica fume, showing superior properties (Mackechnie and Alexander, 2000). The statistical variability of the other variables; surface chloride concentration and cover depth are based on published results of field measurements taken on existing structures in the Western Cape.

The primary objective of this study is therefore to develop a probabilistic model which will be used during the design and construction phases of new structures, to predict with an acceptable level of confidence the conditions leading to events defining the initiation limit state. In order to realize this, the following objectives need to be attained:

1. The first task in this study will be to define the limit-state function (LSF) for RC structures in a marine environment. The LSF is derived from modified Fick's second law and will be used to predict the time to corrosion initiation for new structures. The

parameters in the LSF are classified as environment, geometric or material parameters. The surface chloride concentration C_s represents the environment parameter. C_s is generated from the marine environment and is the force driving chlorides into the concrete towards the reinforcement. Determining a value of C_s for concrete elements in different marine environments is carried out through laboratory testing. The geometric parameter refers to the cover depth which is determined from in-situ testing of existing RC structures/elements. The diffusion coefficient D_i determines the potential resistance of concrete cover with respect to chloride diffusion and is used to represent the material parameter in the LSF. D_i is determined theoretically from the chloride conductivity values obtained from the chloride conductivity test which is one of South Africa's durability index tests.

2. The second step involves carrying out a statistical quantification of the variability in the LSF parameters by specifying their statistical distributions and associated parameters such as mean and standard deviation. The statistical quantification is carried out using data obtained from measurements and/or from literature.
3. The third step shows the application of structural reliability design philosophy to compute the probability of durability failure. The reliability-based design philosophy involves the use of probability theory and numerical techniques in evaluating the LSF. Monte Carlo simulation technique is used to analyse the durability LSF and to predict, with an acceptable level of confidence, the probability that corrosion is initiated during the service life of the RC structure. Results of the reliability-based design (RBD) give the design parameters (i.e. the chloride conductivity value and the cover depth) that will ensure the RC structure meets its performance requirements with a required probability level.
4. The final step involves carrying out an analysis of the sensitivity of LSF parameters to failure probability. The sensitivity analysis assigns sensitivity factors to each model parameter. The sensitivity factors give the designer insight to the parameters of the LSF that are more influential in the design. The designer can then use this information to define future research and development needs.

1.4 LAYOUT OF THESIS

Chapter 1: gives the research significance of carrying out durability design on RC structures. The chapter gives an overview of the various approaches to durability design and the reasons for paradigm shift made from prescriptive to performance based approach. This is shown to have resulted from the realisation that specifications based on prescriptive advice in codes of practice may have underestimated the requirements for durable concrete. The research motivation is then presented as: the need to convey the durability parameters in probability distribution functions due to their variability so as to achieve better designs. Finally, the research objective is clarified as the development of a framework for a probabilistic model for durability design.

Chapter 2: Identifies the factors influencing durability performance and the durability tests necessary for their quantification of parameters are summarised. A review is made of the various approaches available for service life design.

Chapter 3: Gives the research methodology to be used in developing the probabilistic model. First an uncertainty analysis will be carried out by quantifying the uncertainties in the input parameters in terms of their statistical distributions and respective statistical parameters.

Secondly, reliability analysis of the initiation limit state function will be carried out to get the reliability index and probability of failure. The framework for carrying out the probabilistic calculations is also given. Further, a sensitivity analysis is carried out to offer the designer useful insights of the importance of different input parameters to the overall failure probability. Such knowledge is essential in identifying the important parameters to which attention should be given to so as to have a better assessment of their values and, accordingly, to reduce the overall uncertainty of the failure probability.

Chapter 4: Gives the actual statistical quantification of the basic parameters in the model, reliability analysis and the sensitivity analysis of the parameters in the LSF using MCS techniques.

Chapter 5: Concludes the thesis and stresses on important issues concerning the application of the model to assess the durability of RC and further work that needs to be carried out.

1.5 REFERENCES

- Alexander M.G., Mackechnie J. R., (2003)**, Concrete mixes for durable marine structures, *Journal of the South African Institute of Civil Engineering*, 45(2), pp. 20-25.
- Alexander, M.G, Streicher, P.E and Mackechnie, J.R., (1999)**, Rapid Chloride Conductivity testing of Concrete, *Research Monograph, University of Cape Town*.
- Alexander, M.G., Stanish, K., (2001)**, Durability design and specification of reinforced concrete structures using a multi-factor approach, *Conference Proceedings in Honor of Sidney Mindess*.
- Baroghel-Bouny, V. (2002)**, Which toolkit for durability evaluation as regards chloride ingress into concrete? Part II, Development of a performance approach based on durability indicators and monitoring parameters, *In Proc. 3rd Int. RILEM Workshop, Testing and modelling chloride ingress into concrete, Madrid, Spain, 2004*, Eds. C. Andrade and J. Kropp, Bagnaux, RILEM Publication, PRO 38, pp.137-163.
- Basheer, L., Kropp, J., Cleland, D.J., (2001)**, Assessment of the Reliability of Concrete from its Permeation Properties: A Review, *Construction and Building Materials*, 15(2001), pp. 93-103.
- Bentz, E., (2003)**, Probabilistic modelling of Service Life for Structures Subjected to Chlorides, *American Concrete Institute Materials Journal*, Sept-Oct 2003, pp. 390-397.
- BS 8110-1:1997, (1997)**, *Structural use of concrete- Code of practice for design and construction*.
- Buenfield N.R., Shurafa-Daoudi, M.T., McLoughlin, I.M., (1997)**, Chloride transport due to wick action in concrete, Nilsson LO., Oliver, J.P. (Eds.), *Chloride penetration into concrete, Paris France*, pp. 302-324.
- Cheung M. S. and Kyle B. R., (1996)**, Service life prediction of concrete structures by reliability analysis, *Construction and Building Materials*, 10(1), pp. 45-55.
- Colleparidi, M., Marcialis, A., Turriziani, R., (1972)** Penetration of Chloride ions into Cement Pastes and Concretes, *Journal of American Concrete Society*, pp. 534-535.
- DuraCrete, (1998)**, *Modelling of degradation*, The European Union – Brite EuRam III, Project BE95-1347, Probabilistic Performance-Based Durability Design of Concrete Structures.

- Duracrete, (2000)**, *Statistical Quantification of the Variables in the Limit State Functions*, The European Union - Brite EuRam III, Project BE95-1347/R9, Probabilistic Performance-Based Durability Design of Concrete Structures.
- Edvardsen, C., Mohr, L., (1999)**, *DURACRETE – A Guideline for Durability Design of Concrete Structures*, COWI Consulting Engineers and Planners.
- EN 206 (2000)**, Concrete - Part 1: Specification, performance, production and conformity, British Standards Institution, 70 pp.
- Heiyantuduwa, R., Beushausen, H.D, Alexander M.G., and Mackechnie, J.R., (2006)**, Prediction Models for Concrete Durability, *Concrete Plant International*, pp. 80-88.
- Holický M., (2007)**, Probabilistic Design of Structures for Durability, *Proceedings of the SEMC Seminar*.
- ISO 13823-2006 (2006)**, *General Principles on the Design of Structures for Durability*, ISO TC98/SC2, Draft 10.
- ISO 15686-1:2000, (2000)**, *Buildings and constructed assets -- Service life planning -- Part 1: General Principles*.
- ISO 15686-8 (2008)**, *Buildings and Constructed Assets – Service life planning -Part 8: Reference service life and service life estimation*
- Kropp J., (1995)**, Chlorides in concrete, Performance Criteria for Concrete Durability (edited by Kropp and Hilsdorf), *RILEM Report 12*, 1st edition.
- Kwan and Wong Henry H.C., Albert, K.H., (2006)**, *Durability of Reinforced Concrete Structures, Theory vs. Practice*, Department of Civil Engineering, The University of Hong Kong, Hong Kong.
- Li, K., Chen, Z., Lian, H., (2007)**, *Concepts and Requirements of Durability Design for Concrete Structures*, An Extensive Review of CCES01.
- Luping, T., Gulikers, J., (2007)**, On the Mathematics of Time-Dependent Apparent Chloride Diffusion Coefficient in Concrete, *Cement and Concrete Research Journal* 37, pp. 589–595

- Mackechnie, J.R., (1996),** *Prediction of Reinforced Concrete Durability in the Marine Environment*, University of Cape Town, PhD Thesis.
- Mackechnie, J.R., (1998),** Observations from Case Studies of Marine Concrete Structures, *SAICE Journal*, 40(4), pp. 29-32.
- Mackechnie, J.R., Alexander, M.G., (2000),** Rapid Chloride Test Comparisons, *Concrete International*, 22(5), pp.40-46.
- Mackechnie, J.R., Alexander, M.G.,(1997),** Durability Findings from Case Studies of Marine Concrete Structures, *Cement, Concrete and Aggregates*, 19(1), pp. 22-25.
- Mehta, P. K., (2006),** *High-Performance, High-Volume Fly Ash Concrete for Sustainable Development*, University of California, Berkeley, USA.
- Mehta, P.K., and R.W. Burrows, (2001),** Building Durable Structures in the 21st Century, *Concrete International* 23(3), pp. 57-63.
- Pandey J.L. and Banerjee, M.K. (1998),** Concrete Corrosion and Control Practices-an Overview, *Anti-corrosion Methods and Materials*, 45(1), pp. 5-15.).
- Puatatsananon1, W., Saouma, V. E., (2006),** Reliability Analysis In Fracture Mechanics Using The First-Order Reliability Method And Monte Carlo Simulation, Blackwell Publishers Ltd. *Fatigue Fracture Engineering Materials and Structures* 29, pp. 959–975.
- Raizer, V., (2004),** Theory of Reliability in Structural Design, *Applied Mechanical Rev.* 57(1), pp. 1-21
- Richardson, M. G., (2002),** *Fundamentals of Durable Concrete*, First Edition, Spoon Press- Taylor and Francis group, pp. 38-50.
- Scott, A. N., (2004),** The Influence of Binder Type and Cracking on Reinforcing Steel Corrosion in Concrete, *Doctorate thesis University of Cape Town*.
- Stanish, K., Alexander, M. G., Ballim, Y., (2007),** A Framework for Use of Durability Indexes in Performance-based Design and Specifications for Reinforced Concrete Structures, *Materials and Structures Journal*, DOI 10.1617/s11527-007-9295-0

Tikalsky, P.J., David Pustka, D., Marek , P., (2005), Statistical Variations in Chloride Diffusion in Concrete Bridges, *American Concrete Institute Structural Journal*, May-June 2005 pp. 481-487

Youping, L., (1996), *Modelling the Time to Corrosion Cracking of the Cover Concrete in Chloride Contaminated Reinforced Concrete Structures*, Thesis Virginia Polytechnic Institute and State University.

Zhang, J., Lounis, Z., (2006), Sensitivity analysis of simplified diffusion-based corrosion initiation model of concrete structures exposed to chlorides, *Cement and Concrete Research*, 36(7), pp. 1312-1323.

University of Cape Town

CHAPTER 2: LITERATURE REVIEW

2.1 BACKGROUND

2.1.1 Introduction

Deterioration of concrete and hence its lack of durability results from reinforcement corrosion, alkali-silica reaction, chemical attack, leaching by non-basic (and non-alkaline) solutions, and high temperatures generated in case of fire (EN 1992-1, 2004; Baroghel-Bouny, 2002). With the exception of mechanical damage, all these adverse influences in the durability of concrete occur due to the transportation of aggressive agents such as water, oxygen, chlorides, sulphates and alkalis through the concrete (Mackechnie, 1996), for example harmful substances such as (Detwiler and Taylor, 2005);

- (i) water carries dissolved harmful ions into concrete, leaches calcium hydroxide from concrete and expands on freezing
- (ii) oxygen aids steel corrosion
- (iii) carbon-dioxide reduces pH and leads to carbonation
- (iv) chlorides promote corrosion
- (v) sulphates attack the aluminate compounds and
- (vi) alkalis react with reactive aggregates

This implies that if transportation of aggressive agents into concrete is limited then the durability of the concrete structure is enhanced. This can be achieved by first understanding the penetrability of aggressive agents into concrete.

Penetrability involves a number of transport processes (or mechanisms) namely the **diffusion** of ions under a concentration gradient, **permeation** of a solution under a hydrostatic head and the **capillary absorption** of liquids (Mikulic *et al.*, 2001). Transport mechanisms of concrete can be measured using standard test methods such as the durability index tests (DIs), namely

the water sorptivity test, chloride conductivity and the oxygen permeability test (Details of the DIs is given in Alexander *et al.*, 1999). Of concern in this study is the diffusion mechanism (diffusivity) of concrete, responsible for the penetration of gases and ions that lead to corrosion of most RC structures (Ferreira, 2006). For example, when carbon dioxide, CO_2 diffuses into concrete, it reacts with the dissolved cement paste $[Ca(OH)_2]$ to form calcium carbonate $[CaCO_3]$ and water. The presence of $CaCO_3$ lowers the alkalinity of the pore solution from pH 12.5 to pH 9. The reduction of alkalinity in the pore solution leads to the instability of the passive layer on the steel surface causing initiation of steel corrosion (Richardson, 2002). Similarly, chloride ion ingress in concrete causes the steel in the concrete to depassivate, leaving the steel susceptible to corrosion (Ferreira, 2006). Chloride-induced corrosion of reinforcing bars is the primary cause of deterioration of RC structures in onshore and offshore marine environments and results in the shortening of the service life of the structure.

A number of approaches to service life design have been put forward by current design codes of practice that aid in preventing the pre-mature failure of RC structures due to reinforcement corrosion. ISO 15686-1 (2000) gives a 'factor method' and the FIB Model Code (Service Life Design) gives additional approaches for service life design as: full probabilistic approach, partial factor design approach, deemed to satisfy approach, and avoidance of deterioration approach. These approaches are presented in this chapter with main focus given to the full probabilistic approach as it is the design methodology used in this study.

2.1.2 Factors influencing penetrability

Durability has been observed to be largely controlled by the quality of the thin cover layer protecting the reinforcement (also known as the covercrete) (Alexander and Stanish, 2001). The quality of the covercrete is measured in terms of its penetrability, which is defined as the ease with which ions or molecules in the form of liquids and gases move through the concrete (Paul *et al.*, 2005). Penetrability is one of the most important concrete characteristic affecting durability (Baykal, 2000). There is therefore a need to establish factors affecting penetrability of concrete, as this will in turn influence the durability of concrete.

The penetrability of concrete to a given agent, for example chloride ions is mainly affected by the pore structure of the cement paste. The pore structure refers to the size, distribution and continuity of pores within the cement paste. It is assumed to consist of capillary pores, gel pores and calcium silicate hydrate (C-S-H) inter-layers (Hansson *et al.*, 2007). Capillary pores are the remains of originally water-containing spaces between cement particles that have not been filled up by products of hydration (Ballim and Basson, 2001). They are of diameter 0.01 to 1 μm (McDonald, 1992), and their number and interconnectivity control the ingress of chloride ions, oxygen and moisture into concrete (Ballim, 2001). Gel pores and interlayer spaces are believed to be too small (\emptyset of 0.001 μm to 0.008 μm) and discontinuous to allow for the transport of aggressive agents into concrete. Concrete can be porous but still have a low penetrability as long as the pores are not interconnected (i.e. a closed pore system). On the other hand, it can have lower porosity but higher penetrability if the pores are connected (Zhang *et al.*, 2006). Hence, it is generally the interconnectivity of pores, rather than the total porosity that is essential in establishing the ease by which aggressive agents penetrates concrete (Zhang *et al.*, 2006).

Capillary porosity is influenced by the water content of the concrete. For lower water/cement ratios (below 0.38), the penetrability of the cement paste may be considerably reduced due to the greater extent of calcium-silicate-hydrate (C-S-H) gel formation which fills up the available pore space (Neville, 1995; McDonald, 1992; Ballim, 2001). For water/cement ratios between 0.38 and 0.6, the amount of C-S-H gel formation is usually significant enough to disrupt the continuity of the capillary pores, provided that complete hydration of the cement is allowed to occur. For water/cement ratios higher than 0.6, gel formation is insufficient to block the capillary pores even with complete hydration. Tests have shown that concrete penetrability decreases by up to four orders of magnitude as the water/cement ratio is reduced from 0.75 to 0.26 (Ballim, 2001).

The penetrability of concrete is also affected in a number of ways by aggregates. Firstly, the aggregates produce interfacial transition zones (ITZs) in the composite concrete material, thereby increasing the penetrability. Secondly, at sufficient aggregate volume concentration, the ITZ phases can become percolated, leading to an increase in penetrability. Percolation occurs due to the ITZs overlapping and thereby creating additional paths for penetration to

occur. Thirdly, aggregates tend to reduce the overall penetrability due to their own relatively low penetrabilities, sometimes called the dilution effect, and lastly, they influence the geometrical arrangement of the ITZ phases, introducing longer flow paths for moisture to circumvent the aggregate, thus reducing penetrability (Alexander and Mindess, 2006).

The use of mineral admixtures with pozzolanic characteristics influences both the gel and capillary porosity of the cement paste. Mineral admixtures, especially those of high fineness such as silica fume (SF), reduce the permeability of the cement paste and therefore affect the durability of concrete (Kwan and Wong, 2006). SF is a by-product resulting from the reduction of high-purity quartz with coal in electric arc furnaces in the manufacture of ferro-silicon and silicon metal. The fume contains between 85 and 98 percent Silicon Dioxide (SiO_2), and consists of extremely fine spherical glassy particles. Hamad and Itani (1998) stated that the average particle size of SF is 0.1 micro-metres or about two orders of magnitude finer than cement particles. Research indicates that the effects of silica fume on concrete durability are two-fold. Firstly, the mineral admixture is of high fineness and improves the packing of the cementitious materials and by so doing, reduces the pore volume and size in the bulk of cementitious products resulting in a denser pore structure (Kwan and Wong, 2006). Secondly, the silica content of the mineral admixtures reacts with the lime in the concrete to form additional gel products (this is known as pozzolanic reaction) thereby converting the soluble lime (which tends to leach out leaving behind pores in the concrete) to insoluble gel and reducing the porosity of the concrete (Kwan and Wong, 2006). An additional advantage can be attained if the mineral admixture used is fly ash (pozzolanic material). The particles of fly ash are spherical in shape, and thus have lower inter-particle friction than the angular cement particles. Therefore, less water is needed to attain a given slump resulting in fewer capillary pores. Typical water reduction ranges from 5 to 15% in comparison to concrete with Portland cement only (similar total amount of cementitious material) (Ballim, 2001).

Superplasticizers, also known as high-range water-reducing admixtures, are highly efficient water reducers. When added to concrete mixtures, the anionic long chain molecules of the admixture become adsorbed on the surface of the cement particles which are effectively dispersed in water through electrical repulsion. This results in a high fluidity at relatively low water contents. The hardened concrete due to its low porosity is generally characterized by

high durability (Mehta, 1999). From studies carried out by Borsoi *et al.* (2001) it was shown that superplasticized concretes with composite cements (25percent fly ash, 25percent ground slag, and 50 percent portland cement) perform very well in concrete mixtures in terms of excellent durability behaviour (negligible carbonation and very low chloride penetration).

Poor construction practices such as inadequate compaction, inappropriate curing of concrete, insufficient cover to the reinforcement, and leaking joints also affect the durability performance of a structure (Mehta *et al.*, 2001). Early age concrete (1day) exposed to an ambient environment undergoes a loss of water due to cement hydration resulting in the creation of empty capillary pores. In addition, as the concrete dries, shrinkage cracks develop through the C-S-H gel. These cracks separate capillary pores and render them once again continuous. Results from the field exposure tests carried out by Garboczi and Bentz (1996) show that proper curing can effectively terminate the hydration process as all remaining capillary water is removed from the concrete mass. Powers, (Powers *et al.*, 1947 as cited in Garboczi *et al.*, 1996) suggested that the best curing practice is to maintain surface saturated conditions until the capillary porosity depercolates, which occurs at different curing ages for different water/cement ratios, and then seal off the surface to prevent any moisture loss. Consolidation or compaction of concrete is also necessary for low permeability. Voids or excessive entrapped air resulting from poor placing practices, lack of vibration or congested reinforcement will increase permeability.

2.1.3 Chloride ion penetrability

Chlorides in concrete are obtained from various sources: First, chlorides may be introduced in the fresh concrete mix if the concrete-making materials are contaminated with chlorides. Secondly concrete in the marine environment would be exposed to chlorides from sea water. Thirdly concrete pavements may be exposed to de-icing agents (which contains calcium chloride and sodium chloride). Finally, chlorides may also be present in groundwater or the soil so that foundations or buried structures can be exposed to chloride ions (Kropp, 1995).

Depending on the exposure condition as well as the moisture content of the concrete, chloride ingress in or through concrete can occur by a number of mechanisms namely; diffusion, absorption or permeation, or a combination thereof (Kropp, 1995; Hobbs, 1996). Of these three mechanisms, diffusion is considered as the major mechanism for chloride ingress

through concrete in marine structures based on the assumption that concrete is generally moist (Kropp, 1995).

The diffusion process is defined as the motion of molecules from a point of higher concentration to a point of lower concentration through a concentration gradient (McDonald, 1992) When chlorides accumulate on the surface of the concrete, a concentration gradient of chloride ions is established within the cover layer with the result that chloride ions migrate toward the reinforcement in the concrete (McDonald, 1992; Nanukuttan, *et al.*, 2008). During the diffusion process some of the chlorides ions dissolved in the pore solution of the concrete (free chlorides) interact with products of hydration in a process referred to as chloride binding. During this process, the free ions are either fixed chemically to different extents on certain cement hydrates (C_3A and C_3AF) to form Friedels salt $\langle CaO.Al_2O_3.CaCl_2.10H_2O \rangle$ and calcium chloroferrite $\langle CaO.Fe_2O_3.CaCl_2.10H_2O \rangle$ or are physically adsorbed in the walls of the pores (Martin-Perez *et al.*, 2000).

HETEK-53 (1996) manual reports that chloride binding has dual benefits to RC. Firstly, the process lowers the rate at which chlorides penetrate by reducing the concentration of chloride ions in the pore solution available for transportation. The binding process is very effective, removing nearly all free chlorides from the pore solution. Secondly, the chloride binding process reduces the concentration of chlorides in concrete, translating to a longer time before the chloride concentration at the reinforcement level reaches a threshold level (0.4 % chlorides by mass of cement).

The remaining free chloride ions, which escape the chloride binding process, progressively diffuse into the concrete, to the reinforcement level where they continue to build up. Upon exceeding the critical chloride content, depassivation of steel oxide layer occurs. Depassivation cannot be detected by visual observation (Ann and Song, 2007; Gjrv, 1995) but is an important state in the RC material, in that from this point onwards corrosion of the steel would initiate provided there is sufficient supply of oxygen and presence of an electrolyte (Lindvall, 2006). After corrosion is initiated, it tends to propagate itself if left untreated. The pH within the rust film becomes progressively more acidic. The size of the corrosion activity site increases. As corrosion progresses, the corrosion by-product (rust) takes up more space than the original steel causing pressure within the concrete. Pressures

build up and ultimately cause cracking and spalling. The cracks allow more chloride bearing water to enter the concrete, further intensifying corrosion activity and eventually cause structural failure (Pandey and Banerjee, 1998).

The three periods to: corrosion initiation, propagation and final collapse of a RC structure represent respectively the durability, serviceability and ultimate limit states of the RC structure. The three limit states are marked respectively by depassivation of reinforcement, crack formation and spalling of concrete and are schematically presented in Figure 2.1. Service life of a structure can be defined w.r.t the relevant limit state. For this study the relevant limit state is the durability limit state (DLS) marked by reinforcement depassivation and is defined as the time during which the structure is able to meet its specified durability requirements with an acceptable level of safety (ACI, 1994).

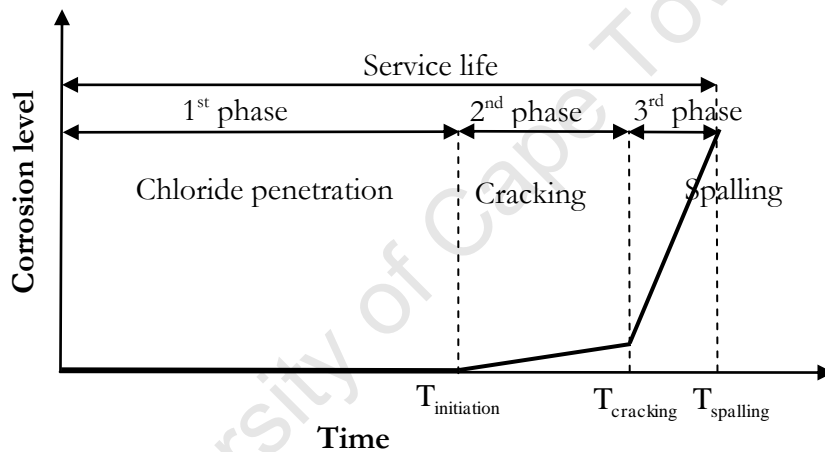


Figure 2.1: The corrosion process based (adopted from: Liu *et al.*, 1998)

Owing to the problems associated with chloride-induced corrosion in RC structures, reliable prediction of chloride ingress in concrete and time to depassivation, $T_{\text{initiation}}$, are the key elements for consideration in RC durability design (Luping and Gulikers, 2007). So far, mathematical models developed to predict $T_{\text{initiation}}$ are based on Fick's second law of diffusion (Streicher and Alexander, 1994):

$$\frac{\partial C_{(x,t)}}{\partial t} = -\frac{\partial}{\partial x} \left[D \frac{\partial C}{\partial x} \right] \quad (2-1)$$

where,

$\frac{\partial C_{(x,t)}}{\partial t} \Rightarrow$ rate of transfer of chloride ions per unit area of section of concrete sample

$\frac{\partial C}{\partial x} \Rightarrow$ concentration gradient, $\left(\frac{\text{mole}}{\text{m}^3 \text{m}}\right)$

$D \Rightarrow$ diffusion coefficient, $\left(\frac{\text{m}^2}{\text{s}}\right)$

$C \Rightarrow$ the chloride concentration $\left(\% \text{ Cl}^{-1} \text{ by mass of cement}\right)$

$x \Rightarrow$ space coordinate measured normal to the section

The negative sign in Equation 2-1 arises because diffusion occurs in the direction opposite to that of increasing concentration. The mathematical expression holds only for an isotropic medium, whose structure and diffusion properties in the neighbourhood of any point are the same relative to all directions (Crank, 1975). The partial differential of Equation 2-1 may be solved by applying the following boundary conditions and assumptions (Alexander *et al.*, 1999):

- (i) The surface chloride concentration $\left(C_s\right)$ reaches a constant value almost immediately

$$C_{(x,t)} = C_s \text{ at } x = 0 \text{ and } t > 0 \quad (2-2)$$

- (ii) The initial internal chloride concentration is zero $\left(C_0 = 0\right)$ at some point internally.

$$C_{(x,t)} = 0 \text{ at } x > 0 \text{ and } t = 0 \quad (2-3)$$

- (iii) The diffusivity of the material is constant with depth and time and is confined to one direction perpendicular to the surface.
- (iv) The concrete is saturated throughout the diffusion process
- (v) There is no significant interaction between diffusant and concrete.

Given these conditions, Crank's solution to Fick's second law takes up the following form:

$$C_{(x,t)} = C_s \left[1 - \operatorname{erf} \left(\frac{x}{2\sqrt{D_a t_i}} \right) \right] \quad (2-4)$$

where,

$C_{x,t}$ = total acid-soluble concentration of chloride in solution at time t and depth x ;

C_s = surface concentration $\left(\text{Cl}^{-1} \text{ by mass of cement} \right)$

x = concrete cover depth $\left(\text{mm} \right)$

t_i = initiation time to corrosion $\left(\text{yr} \right)$

D_a = apparent diffusion coefficient as it is only one of the transport mechanisms involved in chloride penetration. $\left(\text{m}^2 / \text{s} \right)$

erf = Gaussian error function which is equal to twice the cumulative distribution of the normal distribution with a mean of 0 and a variance of 0.5.

The Gaussian error function can be defined further by Equation 2-5:

$$\operatorname{erf} y = \frac{2}{\sqrt{\pi}} \int_0^y e^{-t^2} dt \quad (2-5)$$

Which if expanded takes up a power series of the form:

$$\operatorname{erf}(y) = \frac{2}{\sqrt{\pi}} \sum_{n=0}^{\infty} \frac{(-1)^n y^{2n+1}}{n! (2n+1)} \quad (2-6)$$

It should be noted that various researchers present different solutions to Equation 2-1 depending on the assumptions made on the variation of the boundary conditions with time.

2.2 FICKIAN DIFFUSION MODELS

2.2.1 Collepardi's model

Fick's second law (Equation 2-1) was derived by Adolf Fick in the year 1855 for the purpose of describing the diffusion of ionic species through permeable materials (Smith, 2004). It was not until the early 1970's that Collepardi *et al.* (1972) made the first attempt to use the law for

modelling chloride ingress through structural concrete. Collepardi's model was based on the assumption of a constant apparent diffusion coefficient and constant surface chloride content. The analytical solution obtained for these conditions was:

$$C_{(x,t)} = C_o + (C_s - C_o) \left[1 - \operatorname{erf} \left(\frac{x}{2\sqrt{D_{app}t}} \right) \right] \quad (2-7)$$

Where C_o is the initial chloride content in the concrete and other variables are as defined in Equation 2-4. The apparent diffusion coefficient D_{app} used in Collepardi's model is determined by fitting profiles of total acid-soluble chloride concentration versus depth with Cranks solution to Fick's second law of diffusion (Equation 2-4) (Nokken *et al.*, 2006). The apparent diffusion coefficient does not take into account that some chloride ions become chemically or physically bound as they penetrate through the pore system (Section 2.1.3). This phenomenon together with the alteration of the capillary pore system due to the formation of hydration products causes the diffusion coefficient to reduce with time (Mackechnie and Alexander, 1997). It can therefore be concluded that Collepardi's model over-estimates the chloride concentration.

2.2.2 Time-dependent diffusivity models

Takewaka and Mastumoto (1988) were the first to show the time-dependency of chloride diffusion coefficient on the exposure period. They used a purely empirical equation to describe the decrease of diffusion coefficient with time that is, the diffusion coefficient, D , is proportional to $t^{-0.1}$ (Luping and Gulickers, 2007).

Later in 1994, Mangat and Molloy (1994) proposed the use of an empirical material coefficient n to take account of the reduction in diffusion coefficient with time by use of the relationship:

$$D_t = D_i \left(\frac{t_i}{t} \right)^m \quad (2-8)$$

Where D_t and D_i are the apparent diffusion coefficients at time t and one second, respectively. In their experiments, they found m to be dependent on the type and grade of concrete. Mangat and Molloy (1994) then incorporated the time dependence of D_{app} into the standard model for chloride diffusion based on Fick's second law by substituting Equation 2-8 into Equation 2-1 (Streicher, 1997).

$$\frac{\partial C_{(x,t)}}{\partial t} = D_i t^{-m} \frac{\partial}{\partial x} \left[\frac{\partial C}{\partial x} \right] \quad (2-9)$$

$$\frac{1}{D_i t^{-m}} \frac{\partial C_{(x,t)}}{\partial t} = \frac{\partial}{\partial x} \left[\frac{\partial C}{\partial x} \right] \quad (2-10)$$

they then substituted

$$\partial T = D_i t^{-m} \partial t \quad (2-11)$$

into Equation 2-10 to get:

$$\frac{\partial C_{(x,t)}}{\partial T} = \frac{\partial}{\partial x} \left[\frac{\partial C}{\partial x} \right] \quad (2-12)$$

this has the standard solution:

$$C_{(x,t)} = C_s \left[1 - \operatorname{erf} \left(\frac{x}{2\sqrt{T}} \right) \right] \quad (2-13)$$

Upon integrating ∂T in Equation 2-11, they got:

$$T = \int_0^t D_i t^{-m} \partial t \quad (2-14)$$

$$= \frac{D_i}{1-m} t^{-(m-1)} \quad (2-15)$$

Finally, they substituted the value of T from Equation 2-15 into Equation 2-13 and found the final solution to be:

$$C_{(x,t)} = C_s \left[1 - \operatorname{erf} \left(\frac{x}{2 \sqrt{\frac{D_i}{1-m} t^{1-m}}} \right) \right] \quad (2-16)$$

Mackechnie (1996) established Equation 2-16 to be incorrect, if used on existing structures, as it assumed that the measured diffusion coefficient is the actual (instantaneous) diffusion coefficient at time t (D_t). This is not the case since measured diffusion coefficient is an integrated value over the entire period t ($t = 0$ to $t = t_{\text{current}}$). Mackechnie noted that Equation 2-16 would only be correct if D_i used is the instantaneous initial diffusion coefficient D_{ii} giving:

$$C_{(x,t)} = C_s \left[1 - \operatorname{erf} \left(\frac{x}{2 \sqrt{\frac{D_{ii}}{1-m} t^{1-m}}} \right) \right] \quad (2-17)$$

In other instances, the value for $C_{(x,t)}$ obtained would be over-estimated. For this reason, Mackechnie formulated a mathematical model that would correct for the error through the following steps:

Mackechnie compared Equations 2-4 and 2-16 to get:

$$D_a t = \frac{D_{ii}}{1-m} t^{1-m} \quad (2-18)$$

From this it was found that the integrated (measured) diffusion coefficient can be written as:

$$D_a = \frac{D_{ii}}{1-m} t^{-m} \quad (2-19)$$

And since measured diffusion coefficient D_a would be equal to the instantaneous diffusion coefficient D_t at the initial time $t = i$ then Equations 2-19 and 2-8 can be combined to give:

$$D_i t^{-m} = \frac{D_{ii}}{1-m} t^{-m} \quad (2-20)$$

Mackechnie therefore expressed the instantaneous diffusion coefficient as

$$D_i = \frac{D_{ii}}{1-m} \quad (2-21)$$

And upon substituting Equation 2-21 into Equation 2-17, Mackechnie was able to obtain the correct modified solution of Fick's law, which is expressed in terms of integrated (i.e. measured values):

$$C_{(x,t)} = C_s \left[1 - \operatorname{erf} \left(\frac{x}{2\sqrt{D_i t^{(1-m)}}} \right) \right] \quad (2-22)$$

The boundary conditions for this solution are that the m value may only vary from 0 to 1 (when $m = 0$, instantaneous and integrated diffusion coefficients are equal and constant whereas when $m = 1$, there is theoretically no ingress of chloride into concrete). Mackechnie (1996) stated that the advantage presented by the corrected modified solution of Fick's second law (Equation 2-22) was that future chloride levels could be predicted directly without having to factor the reduction of diffusion coefficient with time.

2.3 DIFFUSION COEFFICIENTS

In reality a wider range of degradation models exist other than those presented in Section 2.2.1 and 2.2.2. The degradation models are based on the concept of chloride transport into concrete by diffusion and initiation of reinforcement corrosion when chloride content at the steel surface exceeds a critical level (taken as 0.4 % chlorides by mass of cement). As aforementioned, these models differ from each other depending on the assumptions made of the variation of the boundary conditions with time (Section 2.1.3). In addition, the method of calculating the diffusion coefficient differs from model to model, which then creates a need for the designer to clarify the type of diffusion coefficient used in the SLP (de Rooij and Polder, 2004).

Apparent diffusion coefficients D_a may be determined by fitting the error function solution (Equation 2-4) to chloride profiles obtained from existing structures or from test samples stored under desired conditions. However, the procedure is relatively slow and time consuming hence accelerated penetration or migration tests are used to obtain diffusion coefficients (Marchand *et al.*, 1998). Standard migration tests have been developed worldwide and can be divided into two categories: steady state conduction experiments that deal with only the ionic transport of chloride ions through concrete and non-steady state (NSS) migration experiments which take into account the binding of chloride ions with cement phases (Castellote *et al.*, 2001).

A more detailed analysis for each of the tests and the procedure used in calculating the respective diffusion coefficients will be illustrated in the following sub-sections.

2.3.1 Non-Steady State Migration Tests

Non steady-state (NSS) migration tests account for chloride binding processes (Section 2.1.3). Various test methods worldwide have been developed to measure the non-steady state diffusion coefficient D_{NSS} . This includes the rapid migration test and the bulk diffusion test.

2.3.1.1 Rapid migration test

The rapid migration test (RMT) was developed by Tang and Nilsson (1992). In the test, a 50 mm thick 100 mm diameter sample is placed in a typical migration cell (Figure 2.2). The top surface of the sample is in contact with a reagent which is free of chlorides, whereas the bottom surface of the specimen is in contact with a chloride containing reagent. A 30V potential difference is applied across the specimen, to accelerate the migration process, for approximately 8 hours (this value is dependent on the measured initial current, for example, if the initial current value obtained for a concrete sample, is less than 5mA then the test duration would take 168 hours. However, if a higher value of say, 120mA is attained, then the test duration would be 4 hours (DuraCrete, 1999).

The specimen is then removed from the solution and split in two halves. A coulometric indicator (0.1 M silver nitrate solution) is then applied onto the split surface to detect the presence of chloride ions. Where chlorides have penetrated to at least approximately 0.07 N concentration, silver chloride will precipitate and cause that portion of the sample to turn

white, while the silver nitrate in the non-chloride penetrated zone turns brown (Tang and Nilsson, 1992). The test has the advantage that the results are not influenced by the pore fluid conductivity. This makes it applicable to concrete with calcium nitrite corrosion inhibitor (Hooton, 2001).

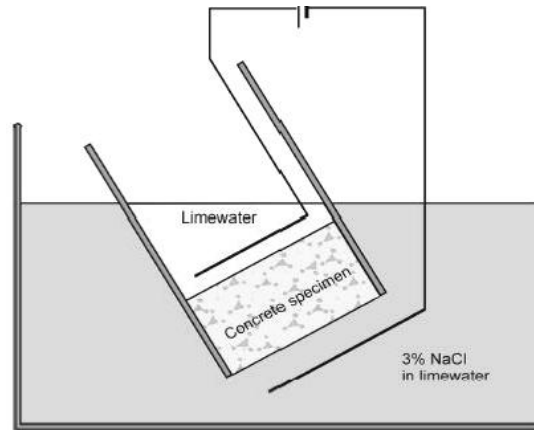


Figure 2.2: Tang and Nilsson migration cell (source: Hooton *et al.*, 2001)

The major drawbacks of this test are its inability to account for the current exclusively due to the flow of chloride ions out of the total current resulting from the flow of other ions. Furthermore, the high voltage applied across the sample induces heat in the sample, which in turn affects the rate of flow of chloride ions (Suryavanshi *et al.*, 2002).

Calculating Diffusion Coefficient from Non-Steady State Migration Tests

The non-steady diffusion coefficient, D_{nss} , is obtained from experiments that explicitly take into account binding, and can be used for predicting the initiation period of rebar corrosion provided that other factors, such as concrete ageing or chloride external concentration, are taken into account (Andrade *et al.*, 2000). The method of calculating D_{nss} from the RMT is based on substituting the measured depth of penetration x_d , specific voltage and time of exposure into Equation 2-23 (Duracrete, 1999).

$$D_{nss} = \frac{R \cdot T \cdot l}{zFE} \times \frac{x_d - \alpha \sqrt{x_d}}{t} \quad (2-23)$$

with:

$$\alpha = 2 \cdot \sqrt{\frac{R \cdot T}{zFE}} \cdot \operatorname{erf}^{-1} \left(1 - \frac{2c_d}{c_o} \right) \quad (2-24)$$

where:

- $R \Rightarrow$ Gas constant $R = 8.314 \text{ J} \cdot \text{K}^{-1} \cdot \text{mol}^{-1}$
- $T \Rightarrow$ Solution temperature (K)
- $z \Rightarrow$ Absolute value of ion valence, for chloride ions, $z = 1$
- $F \Rightarrow$ Faraday constant $F = 9.648 \cdot 10^4 \text{ C} \cdot \text{mol}^{-1}$
- $E \Rightarrow$ Absolute value of Voltage (V)
- $t \Rightarrow$ Test duration (s)
- $l \Rightarrow$ Thickness of the specimen (m)
- $x_d \Rightarrow$ Penetration depth (m)
- $c_d \Rightarrow$ Chloride concentration for indicator colour change ($0.07 \text{ mol} \cdot \text{l}^{-1}$)
- $c_o \Rightarrow$ Chloride concentration of reagents in the upstream cell ($\text{mol} \cdot \text{l}^{-1}$)

2.3.1.2 Bulk diffusion test (NordTest NT Build 443)

This is a Scandinavian test whereby samples are saturated with lime water and then sealed on all sides except the top face and submerged in a 2.8M NaCl solution for a minimum of 35 days (Figure 2.3). Chloride profiling is then carried out by grinding 0.5mm portions of the sample and measuring the amount of chlorides present at different depths. The chloride content of the profile is then determined in accordance with AASHTO T260 (1997). The error function solution of Fick's second law (Equation 2-4) is then fitted to the curve and a diffusion coefficient, D_{nss} , is determined.

The NordTest is usually extended up to 90 days depending on the quality of the concrete: this affects the results due to significant micro structural changes that might occur during the extension period, and it also makes the test unsuitable for quality control purposes.

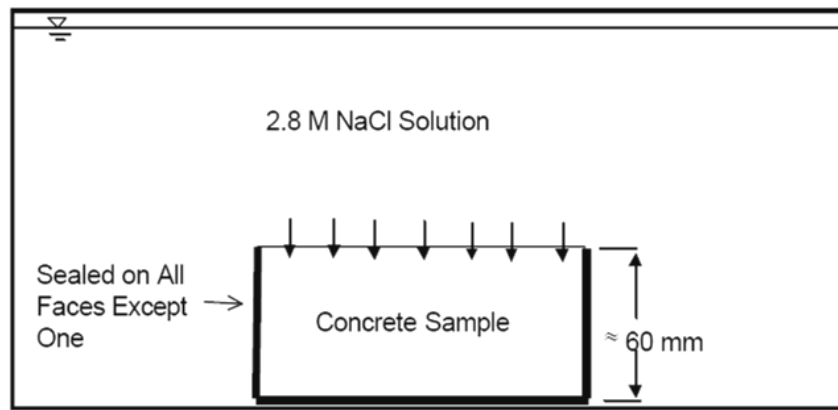


Figure 2.3: Nord test setup (source: Hooton *et al.*, 2001)

However, the test is not affected by the unknown implications of using an electric field to accelerate the diffusion process as is the case for the rapid migration test. As such it can be used in the calibration of other tests that are affected by an electric field as well as in long term research projects.

2.1.1.1 Summary of non-steady migration tests

A comparison is made of the effectiveness of the non-steady state accelerated test methods in determining D_{nss} using their repeatability and reproducibility characteristics (Table 2.1). Repeatability refers to the variability of test results within one laboratory (same operator, equipment and identical specimen) whereas reproducibility refers to the variability of the test results between different operators working in different laboratories using different equipment, and is determined through round-robin tests (Alexander *et al.*, 2001).

Table 2.1: Repeatability and reproducibility of tests given in terms of the coefficient of variation (%) (Castellote *et al.*, 2006)

Test:	Standard used [#]	Number of labs	Repeatability	Reproducibility
Rapid migration test (AASHTO T259 or NT Build492)	ISO 5725-2:1994	15	28%	47%
Bulk diffusion test (NordTest NT Build 443)		14	18%	36%

Standard used [#]= the standard followed in analysing the results

From Table 2.1 the precision of the test is stated and it is observed that among the two NSS methods, the bulk diffusion test in general gives the better precision in determining the NSS chloride diffusion coefficient of concrete.

2.3.2 Steady-State Conduction Tests

The steady-state process assumes that the flux of chloride ions across the specimen remains constant at all sections normal to the direction of diffusion, and that the activity of the chloride ion remains effectively unchanged at any location in the specimen (Truc *et al.*, 2000). To establish a steady state, the concentration gradient must be constant during the test. Therefore, the upstream and downstream cells have to be renewed frequently.

This section will cover the chloride conductivity test (CCT) as a steady state test used to obtain the effective diffusion coefficient D_i .

2.1.1.2 Chloride Conductivity Test (CCT)

Conduction refers to the movement of ions under an electric field (Streicher, 1997). Hence, the driving force with conduction is the electric field as opposed to a concentration gradient in the case of diffusion (Streicher *et al.*, 1995). Concrete is electrically conductive by virtue of an interconnected pore network which is partially or fully filled with water containing mobile ions. In steady state conduction the electric field is constant, and the charged ions are uniformly distributed.

Streicher (1997) developed a rapid chloride conductivity test (CCT) in which steady state conditions are achieved from the start by vacuum saturating 3 inch thick specimens in a 5M $NaCl$ solution for 24 hours. Prior to immersion the specimens are oven dried to avoid dilution of the solution. In the test, two concrete specimens are exposed on either side to 5M sodium chloride ($NaCl$) solution (Figure 2.4). A 10V potential difference is then applied that causes chlorides to migrate due to conduction (Gouws *et al.*, 2001).

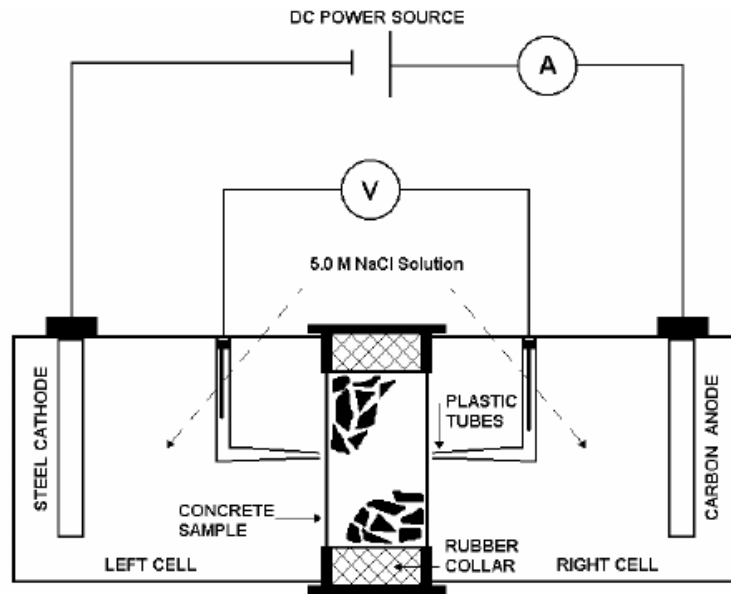


Figure 2.4: Chloride Conductivity Test (Alexander *et al.*, 1999)

The rate of conduction is characterised by conductivity σ , and is equal to the charge flux (current density) under a unit electric field. From the CCT a chloride conductivity value is determined by measuring the electric current flowing through the concrete specimen and applying Equation 2-25.

$$\sigma = \frac{i \cdot t}{V \cdot A} \quad (2-25)$$

where,

$\sigma \Rightarrow$ Chloride conductivity (mS/cm)

$i \Rightarrow$ Measured current (mA)

$V \Rightarrow$ voltage (V)

$t \Rightarrow$ Specimen thickness (cm)

$A \Rightarrow$ Cross-sectional area (cm^2)

The CCT is a steady state test and it is anticipated that the majority of chloride binding occurs during sample pre-saturation with 5M sodium chloride ($NaCl$) solution (Gardner, 2006).

Hence the conductivity reading only takes ion permeability into account and not ion-matrix interaction. It is possible that the CCT only accounts for the density of the microstructure and not the chloride binding capabilities of the binding system.

The CCT has a number of advantages; first, the electric field application has minimal impact on the chloride conductivity value obtained due to the relatively short test time (seconds) (Gardner, 2006). Secondly, the test is most rapid of all chloride tests developed to date (Streicher and Alexander, 1994). Lastly, results from a round-robin test carried out in South Africa, to determine the precision of the CCT (Table 2.2), indicated the CCT to be both repeatable and reproducible.

Table 2.2: Repeatability and reproducibility of steady state test (Stanish *et al.*, 2006)

Test:	Standard used [#]	Number of labs	Repeatability	Reproducibility
Chloride Conductivity Test (CCT)	ASTM C 802 (1987)	7	9.1%	21.1%

Standard used [#]= the standard followed in analysing the results

From Table 2.2 the observed variability in the CCT was attributed to the tolerances of the test apparatus. There were also indications that the procedures were not being followed correctly either due to lack of clarity in the procedures or the inexperience of the participating laboratories (Stanish *et al.*, 2006).

However, despite the merits of the test, it has been found unsuitable for some high performance concrete material due to the excessive micro-structural damage or inadequate saturation with the concentrated salt solution (Mackechnie and Alexander, 2002). In addition, the CCT does not adequately quantify long-term chemical interactions such as chloride binding and continued cement hydration, which change the concrete pore structure effectively (Mackechnie, 1996). A modification factor should thus be applied to the 28-day chloride conductivity value to estimate the potential long-term (2 years) chloride resistance of concrete.

2.1.1.3 Calculating Diffusion Coefficient from Conduction Tests

Conduction refers to the movement of electrons under an electric field, where an electron attains a net terminal velocity referred to as drift velocity v_d . Under a unit electric field the drift velocity v_d attained is the mobility of the ion μ . Conduction and diffusion are different ionic transport mechanisms, but at low ionic concentrations both are related by Einstein's relation (Streicher and Alexander, 1994):

$$\mu = zF \cdot \frac{D_o}{RT} \quad (2-26)$$

Where, z, F, R and T are as defined in Equation 2-24 and D_o is the ion diffusivity.

The v_d of the ion under specific electric field is obtained by multiplying μ by the magnitude of the electric field $\left(\frac{\partial E}{\partial x}\right)$.

$$\mu E = zF \cdot \frac{D_o}{RT} \times \frac{\partial E}{\partial x} \quad (2-27)$$

Total ionic flux by conduction J_c can be calculated by multiplying the drift velocity of the individual ions by ionic concentration c :

$$J_c = -c \cdot \mu \cdot \frac{\partial E}{\partial x} \quad (2-28)$$

Substituting Equation 2-27 into Equation 2-28 gives:

$$J_c = -D_o \cdot c \cdot \frac{ZF}{RT} \cdot \frac{E}{l} \quad (2-29)$$

where:

$J_c \Rightarrow$ Ion flux in steady state ($\text{mol} / \text{m}^2 \cdot \text{s}$)

$D_o \Rightarrow$ Ion diffusivity (m^2/s)

- $c \Rightarrow$ Concentration (mol/m^3)
 $Z \Rightarrow$ Electric charge ($z = 1$)
 $F \Rightarrow$ Faraday constant $F = 9.648 \cdot 10^4 \text{ C} \cdot \text{mol}^{-1}$
 $R \Rightarrow$ Gas constant $R = 8.314 \text{ J} \cdot \text{mol}^{-1} \cdot \text{K}^{-1}$
 $T \Rightarrow$ Absolute temperature (K)
 $\frac{E}{l} \Rightarrow$ Gradient of the electric field (V/m)

J_c is the ion flux in steady state due to conduction ($\text{mol} \cdot \text{m}^{-2} \cdot \text{s}^{-1}$) and can also be represented as (Streicher and Alexander, 1994):

$$J_c = \frac{i}{ZF} \quad (2-30)$$

where:

- $i \Rightarrow$ Current density ($\text{ampere} / \text{m}^2$)
 $Z \Rightarrow$ Valency of ion ($z = +1, +2, \dots$) (eq/mol)
 $F \Rightarrow$ Faraday constant (Coul/eq)

The knowledge of the ionic flux due to conduction (J_c) allows for the calculation of D_o from Equation 2-29 as:

$$D_o = \frac{RT}{ZF} \cdot \frac{l \cdot J_c}{E \cdot c} \quad (2-31)$$

Equation 2-31 is only applicable under ideal conditions (linear potential difference and constant temperature) in the determination of the ion diffusivity (Hooton *et al.*, 2001). The non-ideal nature of the ionic solutions affects this relationship (Alexander *et al.*, 1999).

The liquid through which the ionic species travels is constrained by the pore structure of the concrete material (Atkinson and Nickerson, 1984). Due to this constriction, the diffusion paths are tortuous and are unlikely to be of uniform cross-section due to the variable diameter

of the pores when compared to diffusion paths in the free liquid. These two effects are termed as tortuosity τ and constrictivity δ respectively and are used to relate the theoretical pore solution diffusivity, D_0 , to the actual pore solution diffusivity, D (Atkinson and Nickerson, 1984).

$$D = D_0 \left(\frac{\delta}{\tau^2} \right) \quad (2-32)$$

For experimental purposes, the properties τ and δ are expressed in terms of the average flux per unit area of the medium as opposed to the actual surface area of the fluid filled pores available for diffusion. This leads to another diffusion coefficient referred to as the effective diffusion coefficient D_i (Equation 2-33).

$$D_i = D \cdot \varepsilon = D_0 \left(\frac{\varepsilon \delta}{\tau^2} \right) \quad (2-33)$$

Where, ε is the volume fraction of porosity $\left(\frac{\text{m}^3_{\text{solution}}}{\text{m}^3_{\text{concrete}}} \right)$. The quantity $\frac{\varepsilon \delta}{\tau^2}$ is a material property that characterizes the pore structure and is known as the diffusibility of the medium, Q (Alexander *et al.*, 1999).

Q is also equal to the ratio between the conductivity of the chloride ion in the porous material to that of the same ion in the pore solution as described by Equation 2-34 (Streicher *et al.*, 1995).

$$Q = \frac{D_i}{D_0} = \frac{\sigma}{\sigma_0} \quad (2-34)$$

where,

$Q \Rightarrow$ Diffusibility ratio

$\sigma \Rightarrow$ Conductivity of concrete (calculated from Equation 2-25)

$\sigma_0 \Rightarrow$ Conductivity of the pore solution

$D_i \Rightarrow$ Effective diffusivity of chloride ions through concrete (m^2/s)

$D_o \Rightarrow$ Diffusivity of chloride ions in the pore solution (m^2/s)

The conductivity of the pore solution (σ_o) results from both the saturating salt solution and also from mobile ions such as K^+ , Na^+ and OH^- which are present in concrete pores. To measure the conductivity of the latter would involve pore expression measurements which are difficult and impractical for routine rapid testing, and hence the value of σ_o is assumed to be that of the 5M $NaCl$ saturating solution (Streicher, 1997). In summary, the effective diffusion coefficient would be given as:

$$D_i = \frac{D_o \sigma}{\sigma_o} \quad (2-35)$$

2.3.3 Summary of diffusion coefficient used in the study

The diffusion coefficients obtained from accelerated test methods are not comparable, due to differences in test methods, test conditions, and even calculation equations (Luping *et al.*, 2001). Hence one needs to be clear on the type of diffusion coefficient used and the corresponding test method during the characterisation of concrete material quality.

The effective chloride diffusion coefficient (D_i) used in this study indicates the concrete cover quality and is determined from the chloride conductivity test (Section 2.3.2). D_i is an important parameter as it not only indicates the quality of the cover concrete but can also be used as an input variable in the South African Fickian model for service life prediction (Equation 2-22). The service life in this case relates to the period up till when the durability limit state (DLS) is attained. This limit state is marked by reinforcement depassivation and defines the point where the RC structure ceases to meet its specified durability requirements.

It is important to define the DLS at the design stage of the RC structure so as to ensure that the correct material quality is selected that will allow for the longevity of the structure in its service environment. This process is considered under durability design.

2.4 DURABILITY DESIGN

2.4.1 General

Durability design of RC structures is concerned with ensuring the ability of the concrete to resist degradation under environmental conditions during its design working life without significant deterioration. The environmental conditions are taken to mean those actions i.e. the chemical and physical actions to which the structure or any part thereof is exposed, the consequences of which are not foreseen in the structural design (Cl. 4.1.2.2 of Eurocode 2, 1994). Whereas design working life T_d , is defined as the period for which the structure has to be used for its intended purpose with anticipated maintenance but without major repairs being necessary (DuraCrete, 1999). A guideline for typical values of T_d based on the actual building categories is provided by EN 1990 (2000) (see Table 2.3). For RC structures, the most relevant categories are 4 and 5, i.e. 50 or 100 years design life respectively (Alexander *et al.*, 2007)

Table 2.3: Recommended Service Life for Different Structure Types (EN 1990:2000)

Design Working Life Category	Indicative Design Working Life	Examples of Structures
1	10 years	Temporary
2	10 to 25 years	Replaceable Structural Parts
3	15 to 30 years	Agricultural and Similar Structures
4	50 years	Buildings and Other Common Structures
5	100 years	Monumental Building Structures, Bridges and other Civil Engineering Structures

Many RC structures in adverse environments fail to fulfill their design working life due to lack of understanding of the long-term performance of concrete and the impact of the severe environment on concrete material (Basheer *et al.*, 2001). As a result, owners have to spend an increasing percentage of their budgets on rehabilitation (or replacement) of existing RC structures. Thus, there is a financial incentive to extend the service life of existing structures, and to design new RC structures which will require less maintenance and repair over their lifetime.

Aforementioned, chloride-induced corrosion of reinforcing bars is the primary cause of deterioration of RC structures in onshore and offshore marine environments and results in the shortening of the service life of the structure. A number of approaches to service life design

have been put forward by current design codes of practice that aid in preventing the premature failure of RC structures due to reinforcement corrosion. ISO 15686-8 (2008) gives a 'reference factor method' and the FIB Model Code (Service Life Design) gives additional approaches for service life design as: full probabilistic approach, partial factor design approach, deemed to satisfy approach, and avoidance of deterioration approach.

2.4.2 Approaches to Service Life Design

2.4.2.1 Prescriptive Approach and Deemed-to-satisfy Approach

Conventional structural design codes specify the (prescriptive) requirements to obtain concrete durability. The design codes impose requirements on material constituents, construction practice as well as structural details on the basis of the exposure environment, expected service life and intended service life condition of the structure. For example, BS (8110-1:1997) and SANS 10100 (2005) give the limiting values of the concrete cover to be provided to all reinforcement, 28-day compressive strength and cement content in order to achieve a durable concrete for a range of water-cement ratios (Table 3.3 and 4.8 of BS 8110-1, 1997 and Table 2 of SANS 10100-2, 2005). This approach to design is termed prescriptive approach and has a role to play in durability design but it cannot fulfil the need in certain instances. Firstly, the approach does not provide a means to verify or control the presumed concrete durability quality which is measured by the ability of the concrete to prevent ingress of aggressive agents using durability tests. Secondly, the prescriptive approach does not adequately define the material limit state or the deterioration mechanisms a structure is subjected to during its lifetime. Lastly, the prescriptive approach considers concrete strength as the main indicator of durability (Stanish *et al.*, 2007), postulating that a stronger concrete is more durable (Kwan and Wong, 2006). However, this is not always the case, especially when high-strength concrete (HSC) is used for resistance against freezing and thawing action and certain forms of chemical attack. In such cases, HSC has been shown to lead to the development of shrinkage cracks, making the structure vulnerable to deterioration (Mehta, 2006). For these reasons the prescriptive approach has been increasingly refined to address durability requirements.

The European code, EN 206-1, addresses the shortcomings of the prescriptive approach by introducing sub-classes of exposure conditions and corresponding deterioration mechanisms on concrete (EN 206, 2000). When determining limiting values of concrete composition, the

designer is forced to consider the most onerous condition, that the concrete structure or element will be exposed to (Richardson, 2002). The expanded suite of exposure classes is more likely to reflect specific deterioration mechanisms which allow the designer to prescribe more reliable specifications (Richardson, 2002). In addition, EN 206- 1 introduces a further improvement to the prescriptive approach by allowing the method to be combined with performance tests and indicators. The performance tests quantify the cover layer transport properties of RC structures and are required to be reliable, repeatable and reproducible (Baroghel-Bouny, 2002; Mehta and Burrows, 2001).

In South Africa (SA), durability indexes (DI's) have been adopted as engineering measures of the potential resistance of concrete cover to the transport mechanisms of gaseous diffusion, water absorption and chloride diffusion (Alexander *et al.*, 1999). The DI's are derived from three tests; the chloride conductivity test, where chloride ion resistance is important, the oxygen permeability test to establish carbonation resistance, and a sorptivity test to examine concrete for water absorption (as given in Alexander *et al.*, 1999). DI's characterise the macrostructure of the cover concrete and have been shown to be sensitive to material parameters such as binder type, processing influences such as type and degree of curing, and environmental influences such as temperature and relative humidity (Stanish *et al.*, 2007).

The Deemed-to-satisfy approach in the FIB Model Code (Service Life Design) differs from the prescriptive service life design rules given by EN 206-1 or SANS 10100 (2005) in that it is based on calibrated results from SLD models as opposed to practical experience.

2.4.2.2 Avoidance-of-deterioration Approach

The avoidance-of-deterioration approach is one of the various options which enhance the durability of reinforced concrete by reducing the risk of reinforcement corrosion, through the use of materials that will not deteriorate, based on expert judgement. It is recognized that to reduce or negate the ingress of water, and water containing deleterious ions, the permeability of concrete must be decreased (Section 2.1.2). Engineers adopt several different methods to achieve this end. This includes (Shiessel, 1996):

1. Changing the micro-environment of the concrete component or structure, for example, through the application of corrosion inhibitors which prevent ingress of aggressive agents into concrete
2. Selection of non-reactive or inert materials such as stainless steel bars to provide maximum protection of the reinforcing steel.
3. Inhibiting the corrosion reaction through installation of a cathodic protection system.

Through the use of avoidance-of-deterioration techniques, there is an expected reduction in maintenance and repair costs. However, the initial costs of implementing the techniques are high; for example, corrosion resistance steel bars are six to nine times more expensive than the carbon reinforcing bars normally used (Knudsen *et al.*, 1998).

2.4.2.3 Reference Factor Method Approach

A third approach to service life design is the use of the reference factor method. The International Organization for Standardization (ISO) 15686-1 (2000) adopted the factor method from the work of both the Architectural Institute of Japan (1993) and Bourke and Davies (1997). The basic philosophy behind the Factor method (ISO 15686-8, 2008) is that for a given concrete material there is a Reference Service Life (RSL). RSL is that which a structure is expected (or is predicted) to have in a certain set of in-use conditions and should be based on experience, building codes or test results (ISO 15686-8:2008). The RSL can be adjusted by factors describing deviation from the estimated/prescribed value of RSL to the actual construction conditions. The factor method is defined by the expression:

$$ESL = RSL \times A \times B \times C \times D \times E \times F \times G \quad (2-36)$$

where,

RSL = Reference Service Life

ESL = Estimated Service Life

Factors defining the as-built performance level:

A = Quality of material

B = Design level

C = Workmanship level

Factors defining performance in service:

D = Internal environment

E = External environment

- F = In-use condition
G = Maintenance level

The factor method is used when there is limited knowledge of long term performance of the structure, in which factors are applied explicitly and implicitly (Equation 2-36) to compensate for neglecting the variability of quality in construction practices, concrete material constituent and environmental conditions. Examples of variability include (Bentz, 2003):

- The variability of concrete cover depth due to quality of construction, reinforcement geometry, and occasionally quality of design.
- The variation of environmental load from location to location within a structure, as well as between similar aged structures which are of similar material and are under similar environmental actions.

ISO 15686-1 (2000) provides some information on factors A–G (in an informative annex), but does not give explicit values. Hovde (2005) gives examples of some factor values (Table 2.4) which he suggests should be further developed by the designer based on existing knowledge or upon gaining further experience.

Table 2.4: Guideline for selection of factor values for concrete (Hovde, 2005)

Factor Value A	Qualities for selection of factor value	Factor Value D	Qualities for selection of factor value
3.0	High strength with reduced porosity	5.0	Dry climate, no pollution
1.5	Concrete with low w-c	3.0	Dry climate
0.2	Concrete with high w-c ratio and reactive aggregates		

w-c = water to cement ratio

Hovde, (2005) also suggests the application of a safety factor value of 1 if conditions are similar to RSL conditions or if a specific factor does not apply.

In general, using the factor approach leaves the designer with the task of determining a value for each of the modification factors before using the formula (Marteinsson, 2005). The factors can take on almost any value (except negative), depending on the difference between the intended use environment and that which the RSL is based on (Marteinsson, 2005). This tends to be disadvantageous due to the fact that the ESL, derived from the plain multiplication of factors, tends to be very sensitive to slight variations of each factor value. Hence, the ESL

calculated may vary widely (to even an unlimited number of years) depending on the designers' choice of safety factors. The multiplication also makes it hard to foresee the effect of changes in one or more of the factors (Marteinsson, 2005). It is clear that some practical and reliable choice of values for each of the factors should be developed.

Another setback to the reference factor method is that each factor is represented by a single deterministic figure. This deterministic value contrasts with the well known fact that concrete structures are quite variable in properties both throughout the structure and in terms of quality of construction and materials used (Bentz, 2003). In reality, each factor in Equation 2-36 can take on a range of possible values, with some of the values having a greater likelihood of occurring than others. The range of possible values and the different likelihood of realizations should be represented concisely by a probability distribution function or a probability density function (Bentz, 2003).

From this basis a probabilistic approach to service life design has been introduced by the FIB Model Code (Service Life Design). The approach allows for the assessment of all uncertainties caused by inherent random variabilities, insufficient data and lack of knowledge on durability parameters.

2.4.2.4 Probabilistic Approach

Probabilistic methods may be either full-probabilistic or semi probabilistic (partial factor method) and involve the use of reliability-based design and the limit state methodology.

The limit-states method (LSM) was developed by ISO 2394 (1998) and consequently adopted by various design standards and codes such as the ISO 13823 (2008) and FIB Model Code (Service Life Design). Although ISO 2394 includes durability in its principles, the LSM has not been developed for failures due to material deterioration to the extent that it has for failures due to gravity, wind, snow and earthquake (ISO 13823, 2008).

The LSM incorporates the use of mathematical models to describe the deterioration mechanisms in concrete material up till a specified limit state. The mathematical model is a function of a set of variables $X = \{X_1, X_2, X_3 \dots X_n\}$ that represent the loss of performance with time (Cheung, 1996). The variables include parameters defining material properties, geometric properties and environmental (load) properties. These variables are stochastic in

nature making it necessary to use a reliability-based design methodology (RBD) for analysing the mathematical model at a given limit state.

To carry out a reliability analysis at the initiation limit state (ILS), the variables are characterised further as either action effect, S_{C} or as an initiation limit, S_{lim} (ISO 13823, 2008). The basic requirement for the ILS defined at any time, t , during the design life of the RC structure/ component $\langle C_d \rangle$ can be generally characterised by an inequality that follows a service life format as was illustrated in Section 1.3 (Equation 1-8) or an inequality that follows a limit state format given by Equation 2-37 (ISO 13823, 2008):

$$S_{\text{lim}} > S_{\text{C}} \quad (2-37)$$

For chloride induced corrosion, S_{C} can be defined by Equation 2-22 where, $S_{\text{C}} = C_{\text{C},t}$ and S_{lim} is the critical chloride content level necessary to initiate corrosion $\langle C_{\text{crit}} \rangle$ (Section 3.3.4.3).

The designer selects design specifications that include concrete proportioning, bar arrangement, and placement conditions that are expected to meet requirements for the service life of the structure and members under the envisaged conditions of the deteriorative external forces using Equation 2-37 (Noguchi, *et al.*, 2006).

Subsequently, the designer carries out performance verification of a structure to ensure that the parameters so chosen for a concrete member are sufficient such that the specified limit-state is not reached within the design working life. The performance verification depends on the probabilistic approach used i.e. whether semi-probabilistic or full probabilistic.

Performance Verification using Full- Probabilistic Approach

With full probabilistic methods, mean values, statistical uncertainties and statistical distribution functions, are used to represent the variables of the functions S_{C} and S_{lim} . The condition in Equation 2-37 is represented in terms of a probability of failure $\langle P_f \rangle$:

$$P_f = P\{S_{lim} > S_{\Omega}\} \quad (2-38)$$

From Equation 2-38 the probability of failure appears to be comprehensible, however, it can be cumbersome to use when the value becomes very small, and for this reason, the reliability index is usually preferred (Phoon *et al.*, 2000). The reliability index, β , is defined by the expression given by Equation 2-39 (Faber *et al.*, 2002) and is actually the Z-score of $(1 - P_f)$.

$$P_f = \phi(-\beta) \quad (2-39)$$

Where ϕ is the standard normal cumulative distribution function.

The value of β is inversely related to the corresponding value of P_f i.e. as the probability of failure decreases the reliability index increases, but the variation is not linear (Table 2.5).

Table 2.5: Relationship between reliability index β and probability of failure P_f (Melchers, 1999)

Reliability index, β	1	1,2	1,4	1,6	1,8	2,0	2,2
Failure probability, P_f	0,159	0,115	0,0808	0,0548	0,0359	0,0228	0,0139

The performance verification is carried out by checking that the probability of failure, for a given choice of parameters, does not exceed an acceptable (target) probability of failure P_{target} such that (Li, 1997):

$$P_f = P\{S_{lim} > S_{\Omega} < 0\} < P_{target,ILS} \quad (2-40)$$

$P_{target,ILS}$ can be obtained in two of the following ways:

1. Implicitly by conducting a cost-benefit analysis, as shown in Figure 2.5. This involves studying the variation of the initial cost, maintenance costs and the expected failure costs to arrive at the most economical target probability of failure for design $P_{target,ILS}$ (Phoon *et al.*, 2000).

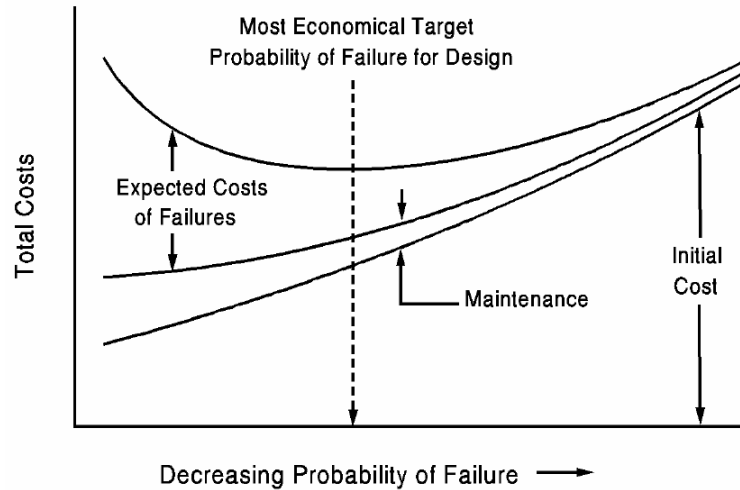


Figure 2.5: Illustrative cost-benefit analysis (Phoon, 2000)

2. Explicitly by setting a value at the initiation limit state that is comparable with the cost of repair values estimated from actual case histories. The explicit values of the target levels for the design have been reported in ISO 2394 (1998), fib Model Code for SLD and EN 1990 (2000), and are as illustrated in Table 2.6.

Table 2.6: Indicative values of P_{target} and β_{target} at ILS for 100 years service life design

Reference	$P_{target,ILS}$	$\beta_{target,ILS}$
Holický, 2007	0,05 to 0,20	0,8 to 1,6
EN 1990 (2000)	0,067	1,5
FIB Model Code (Service Life Design), 2006	0,04	1,8

ILS= Initiation limit state

In general, the acceptable probability of failure, $P_{target,ILS}$ given in Table 2.6, does not give the practical meaning of the failure involved. For example, to say whether the 100% probability of corrosion initiation can be interpreted as corresponding to a situation in which each square nanometre of the steel surface has been depassivated or to the situation when the concrete structure shows at least one corroding spot, is debatable and differs with different researchers. Thus, the specification of a target probability for durability related limit states is not an easy task.

To verify the performance requirements, statistical information of the variables in the LSF in terms of i.e., means, variances, correlation coefficients and probability distribution functions is available to the designer. The statistical information can be exploited to provide improved uncertainty estimates in the output, which is usually in terms of the probability that the output exceeds a prescribed threshold (Equation 2-40). There are many well-established methods of assessing the LSF. The first-order reliability method (FORM) and Monte Carlo simulation (MCS) are two such methods.

The FORM method was developed by Hasofer and Lind (1974) and has been modified over the years by Rackwitz and Fiessler (1978) and Liu and Der Kiureghian (1990). The term ‘first order’ indicates that the LSF is linearized in a standardised normal space (*u-space*). FORM requires the gradient of the linearized *LSF* with respect to the basic random variables and readily provides sensitivity measures that can be used to ascertain the relative importance of the underlying basic random variables (Cho, 2007). The FORM procedure is outlined in Appendix G.

The primary advantage of a FORM-based approach lies in its computational efficiency relative to alternative approaches such as MCS (typically, the number of evaluations of the *LSF* required by a FORM-based approach is several orders of magnitude less than that required by a MCS-based approach). MCS avoids the need to compute gradients (which can be difficult to compute), but at the expense of an increased number of evaluations of the *LSF*. Several variations of MCS methods that reduce the required number of evaluations of *LSF* have been developed. These include importance sampling and directional simulation methods and are collectively referred to as variance reduction techniques (VRTs) (Cho, 2007). However, VRTs still require many more evaluations of the *LSF* than a FORM-based approach. Sensitivity measures, which can be used to rank the relative importance of the basic random variables, are also available within a MCS framework.

Finally, in addition to the physical uncertainty present in the basic random variables, FORM and MCS-based approaches can also incorporate statistical uncertainty (due to the use of limited sample sizes for estimating the parameters that define the probability distributions of the basic random variables) and modelling uncertainty (due to use of imperfect models and the interpretation of the accepted limit state).

Notwithstanding, the full probabilistic approach has its inherent problems, the first of which is the interpretation of the acceptable (target) probability of failure, $P_{target, ILS}$.

$P_{target, ILS}$ was found to take on various values depending on various situations with Table 2.6 giving the indicative intervals of P_{target} and β_{target} values adopted for this study. The reason for the variability in P_{target} arises from the fact that different researchers have different interpretations of the initiation limit state (ILS). There is no clarification in literature, on what the practical meaning of a certain probability of corrosion initiation is in terms of either amount of de-passivated steel, damaged concrete surface area or maintenance costs. Consequently, the accepted probability for corrosion initiation $P_{target, ILS}$ varies between different standards depending on the interpretation of the ‘probability of corrosion initiation’.

The second setback of the probabilistic approach arises from the fact that the method relies on characterising each parameter in terms of mean, standard deviation and statistical distribution. This is a problem due to the fact that the amount of data available for most of the parameters in the LSF was limited.

Thirdly, the method relies heavily on numerical methods for analysis. It requires the use of statistical software packages that incorporate numerical methods such as Monte Carlo simulation.

Performance Verification using Semi- Probabilistic (Partial Safety Factor) Philosophy

This philosophy is frequently used in structural design and is a practical compromise between the old prescriptive methods and new fully probabilistic concepts of reliability design. The semi-probabilistic approach at present forms the basis of durability design in the FIB Model code for service life design and is also a basis of structural design codes, including the EN206.

The semi-probabilistic philosophy enables the durability design for a particular deterioration mechanism (chloride induced corrosion) to be carried out as a simple calculation without additional considerations concerning the probabilistic distributions of input parameters – as is

the case in a full-probabilistic approach. The approach utilizes partial factors, characteristic values and design values in representing a stochastic variable.

In the durability design of chloride induced corrosion, $S_{\mathbf{C}}$ and S_{lim} are chosen as characteristic values which is normally a quantile such as 5th percentile value for $S_{\mathbf{C}}$ or 95th percentile value for S_{lim} of their respective stochastic distributions. The characteristic values of both $S_{\mathbf{C}}$ and S_{lim} are simply represented by the Equations 2-41 and 2-42 respectively.

$$S_{\text{lim},char} = \mu_{\text{lim}} + 1.645 \cdot \sigma_{\text{lim}} \quad (2-41)$$

$$S_{\mathbf{C},char} = \mu_{\mathbf{C}} - 1.645 \cdot \sigma_{\mathbf{C}} \quad (2-42)$$

Partial safety factors γ , determined from engineering judgement and experience or from the reliability-based FORM method (as explained in Appendix G), are applied to the appropriate characteristic values of $S_{\mathbf{C}}$ and S_{lim} to obtain the respective design values, $S_{\mathbf{C},d}$ and $S_{\text{lim},d}$ (as shown in Equations 2-43 and 2-44).

$$S_{\mathbf{C},d} = \frac{S_{\mathbf{C},char}}{\gamma} \quad (2-43)$$

$$S_{\text{lim},d} = \gamma \cdot S_{\text{lim},char} \quad (2-44)$$

The partial factors take account of unfavourable deviations of $S_{\mathbf{C}}$ and S_{lim} from their representative values and the effects of model uncertainties that may cause concrete material to behave differently than it is foreseen in normal conditions during its use (FIB Model Code for Service Life Design).

The relationship between characteristic values, design values and partial factors of $S_{\mathbf{C}}$ and S_{lim} is illustrated in Figure 2.6.

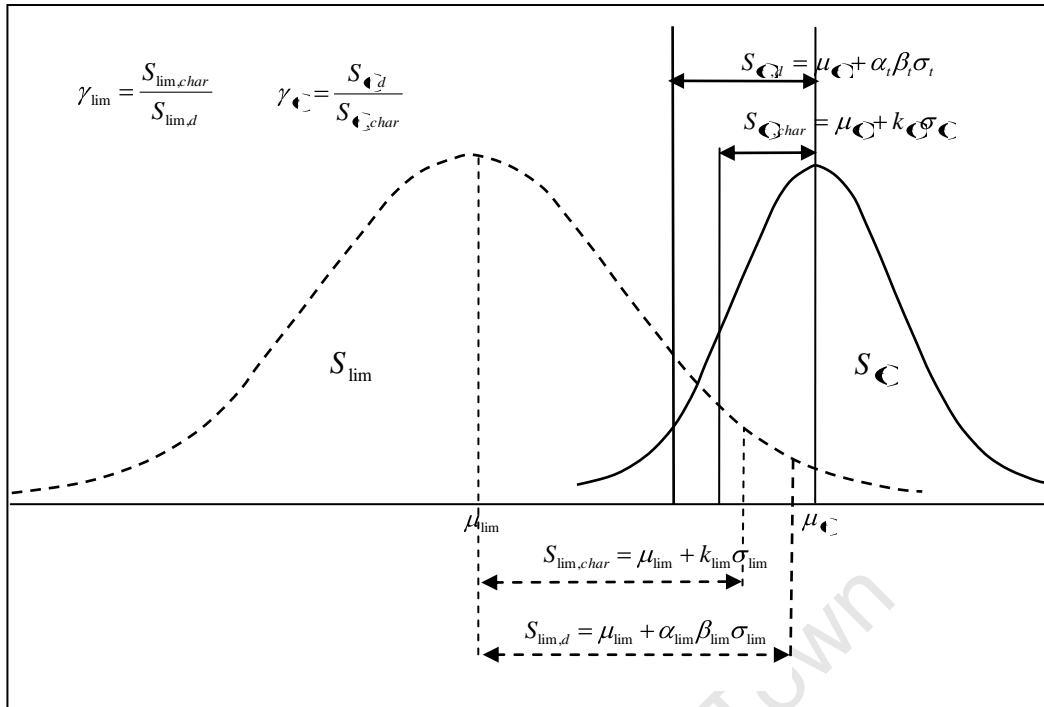


Figure 2.6: Relation between characteristic values, design values and partial factors of safety

The verification of a structure for reinforcement corrosion initiation, due to ingress of chloride ions, using the semi-probabilistic approach is conducted by ensuring that (FIB Model Code for Service Life Design):

$$\gamma_i \frac{S_{C,d}}{S_{lim,d}} \leq 1.0 \quad (2-45)$$

Where, γ_i is the final partial factor applied as the product of other partial factors which express influence of different single effects for each parameter representing measurement or model uncertainty as shown by Equation 2-46:

$$\gamma_i = \gamma_{i1} \times \gamma_{i2} \times \gamma_{i3} \times \gamma_{i4} \times \gamma_{i5} \dots \quad (2-46)$$

The design value $S_{lim,d}$ is calculated from Equation 2-47.

$$S_{lim,d} = \frac{S_{lim,char}}{\gamma_{S_{lim}}} \quad (2-47)$$

where, $\gamma_{s_{lim}}$ is the partial factor (≥ 1).

Similarly, the design value of chloride ion concentration at the depth of the reinforcement S_{cl} is calculated as:

$$S_{cl} = \gamma_{cl} \cdot C_{sd} \left[1 - \operatorname{erf} \left(\frac{x_d}{2\sqrt{D_{id}t^{(1-m)}}} \right) \right] \quad (2-48)$$

(i) γ_{cl} is a safety factor taking account of the variation in the function S_{cl}

(ii) x_d is the design value of the concrete cover (mm) and is given as by:

$$x_d = x_{min} + \Delta x \quad (2-49)$$

Where, x_{min} is the characteristic (minimum) concrete cover (mm), and

Δx is the margin of the concrete cover (mm)

(iii) D_{id} is the design value for the diffusion coefficient given as:

$$D_{id} = \gamma_d \cdot D_{i_{char}} \quad (2-50)$$

(iv) and C_{sd} is the design value of surface chloride concentration given by:

$$C_{sd} = \frac{C_{s_{char}}}{\gamma_c} \quad (2-51)$$

In Equation 2-50 and 2-51, $D_{i_{char}}$ and $C_{s_{char}}$ are the characteristic values of the initial diffusion coefficient (mm^2/year) and surface chloride concentration (g/m^3) respectively. Whereas, γ_d and γ_c are partial safety factors to account for the material properties of concrete and the exposure conditions respectively.

Thus a structural element will meet its durability requirements w.r.t chloride induced corrosion if the limit state (Equation 2-52) is fulfilled.

$$\frac{\gamma_{cl} \cdot C_{S,d} \left[1 - \operatorname{erf} \left(\frac{x_d}{2\sqrt{D_d t^{(1-m)}}} \right) \right]}{C_{crit,d}} \leq 1 \quad (2-52)$$

Since the underlying principles of the partial safety factor method are used in structural engineering, it makes it easier for engineers to understand and apply the basic concepts behind this approach. The most important advantage of the partial factor method is the possibility to take into account uncertainty of individual basic variables by adjusting (calibrating) the relevant partial factor (Holický, 2007).

2.4.2.5 Summary of Service Life Design Approaches

The flow diagram (Figure 2.7) gives a summary of the flow of decisions and design activities when using the deemed-to-satisfy, avoidance of deterioration, the partial safety factor and the full-probabilistic approaches.

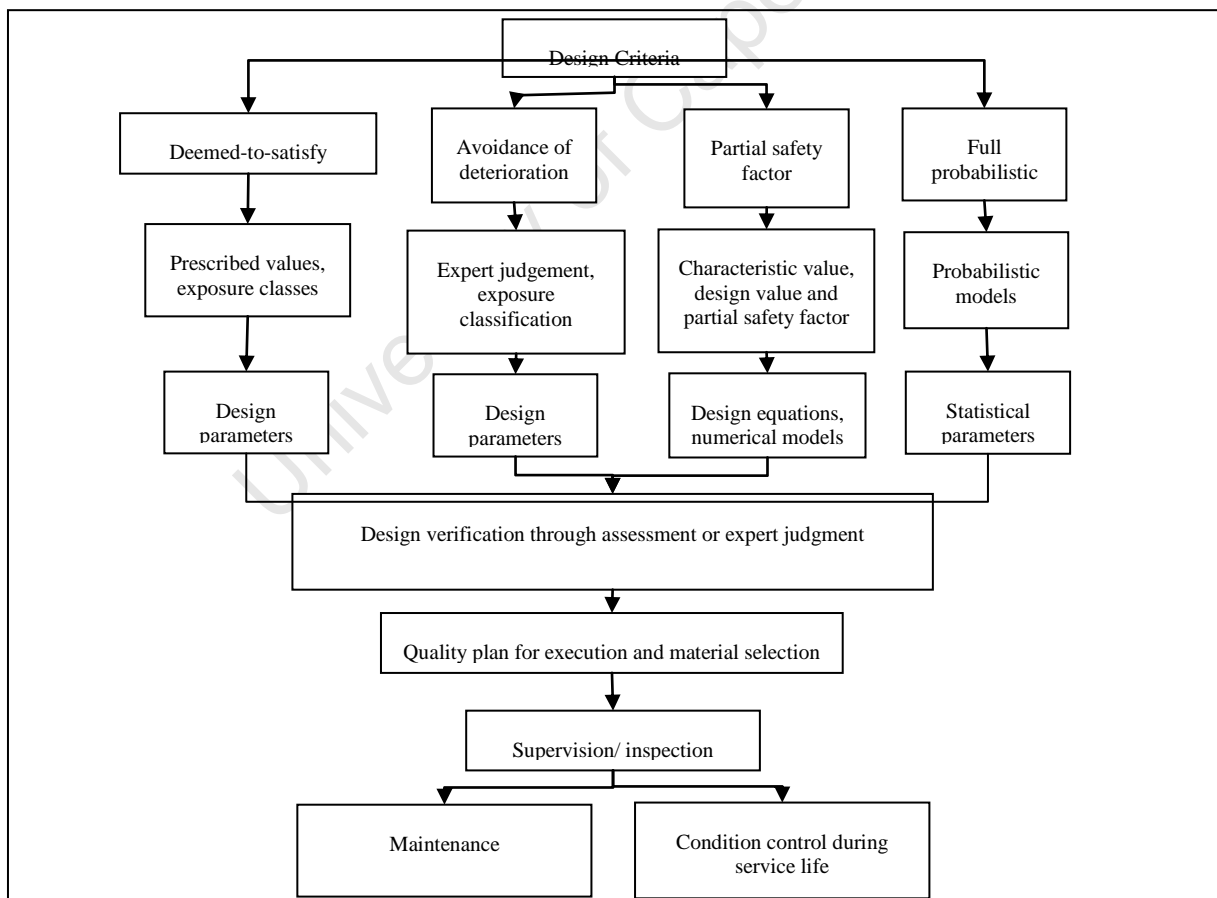


Figure 2.7: Summary of service life design approaches (ISO 13823, 2008)

An example of a SLD of a concrete pier using three of the SLD approaches i.e. the deemed-to-satisfy, avoidance of deterioration and the partial safety factor approaches is illustrated in Appendix H. The full-probabilistic approach to SLD forms the basis of this study and is covered in the next two chapters of the thesis.

2.5 SUMMARY

Concrete transport properties have been shown to be important in the durability and service life design of concrete structures. In particular, the chloride ion penetration in cementitious materials is one of the processes widely responsible for the degradation of RC structures.

Owing to the problems associated with chloride-induced corrosion in RC structures, mathematical models based on Fick's second law have been developed to model chloride ingress in concrete and to predict the time to depassivation. Existing Fickian models have been reviewed in this chapter. The time-dependent diffusion coefficient is a useful parameter in the SA Fickian model and is used in assessing the concrete cover quality. The diffusion coefficient in this study will be derived from the chloride conductivity test (CCT) which is one of South Africa's durability index tests. The CCT is used as an engineering measure of the potential resistance of concrete cover to chloride diffusion.

Finally, the chapter gives a brief overview of some of the design approaches to SLD give by design standards. Of importance to this study is the full-probabilistic approach which combines the SA Fickian degradation model and CCT results for service life prediction. The probabilistic approach classifies parameters in the degradation model as structural dimensions, environmental and material parameters that correspond to the load and resistance variables of reliability-based design (RBD) as used in the structural design.

RBD utilizes probability theory to quantify and analyse the influence of different random variables (and processes due to variation in time) in SLD. The RBD methodology thus provides a rational criterion for service life prediction under uncertainty and will be covered in the next two chapters of the thesis.

2.6 REFERENCES

AASHTO T260 (1997), Sampling and Testing for Chloride Ion in Concrete

ACI Committee 201 (1994), Guide to Durable Concrete, Chapter 4-Corrosion of Steel and other Materials Embedded in Concrete, *Manual of Concrete Practice*, Part 1.

Alexander, M. G. Ballim, Y Stanish, K. (2007) A Framework for Use of Durability Indexes in Performance-based Design and Specifications for Reinforced Concrete Structures, *Materials and Structures Journal*, 41(5), pp. 921-936.

Alexander, M.G., Ballim, Y., Mackechnie, J.R., Horton, J., (2001) Durability Index Tests- Further notes on the aspects related to testing and variability, *Research monograph No. 4*, UCT/Wits, 1999.

Alexander, M.G., Mackechnie, J.R. and Ballim, Y. (1999) Guide to the use of durability indexes for achieving durability in concrete structures. *Research Monograph No 2*, Department of Civil Engineering, University of Cape Town, 35 pp.

Alexander, M.G., Mindess, S., (2006), *Aggregate in Concrete*, Taylor and Francis, pp. 288

Alexander, M.G., Stanish, K., (2001) Durability design and specification of reinforced concrete structures using a multi-factor approach, *Conference Proceedings in Honour of Sidney Mindess*.

Andrade, C., Castellote, M., Alonso C. and Gonzalez C. (2000) Non-steady-state chloride diffusion coefficients obtained from migration and natural diffusion tests. Part I: Comparison between several methods of calculation, *Materials and Structures*, 33(2000), pp. 21-28

Ann, K. Y., Song, H. W., (2007) Chloride Threshold level for Corrosion Initiation of Steel in Concrete, *Corrosion Science*, doi:10.1016/j.corsci.2007.05.007, pp. 1-21

Architectural Institute of Japan (1993) Guide for Service life planning of buildings

ASTM C 802 (1987), Standard Practice for Conducting an Inter-laboratory Test program to determine the Precision of Test Methods for Construction Materials, ASTM book of standards, 04.02.

- Atkinson, A., and Nickerson, A.K., (1984)** The diffusion of ions through water-saturated cement, *Journal of Material Science*, 19(1984), pp. 3068-3078.
- Ballim, Y., Basson, J., (2001)** Durability of Concrete, *Fulton Concrete Technology*, Eighth Edition, Eds. B. Addis B. and G. Owens G. (Cement Concrete Institute, South Africa), pp. 135-161.
- Baroghel-Bouny, V. (2002)** Which toolkit for durability evaluation as regards chloride ingress into concrete? Part II, Development of a performance approach based on durability indicators and monitoring parameters, *In Proceedings 3rd Internal RILEM Workshop, Testing and modelling chloride ingress into concrete, Madrid, Spain, 2004*, Eds. C. Andrade and J. Kropp, Bagnaux, RILEM Publication, PRO 38, pp.137-163.
- Basheer, L., Kropp, J., Cleland, D.J., (2001)**, Assessment of the Reliability of Concrete from its Permeation Properties: A Review, *Construction and Building Materials*, 15(2001), pp. 93-103.
- Baykal, M., (2000)** *Implementation of Durability Model for Portland cement Concrete in to Performance-Based Specifications*, Austin, TX, the University of Texas at Austin College of Engineering.
- Bentz, E., (2003)**, Probabilistic modelling of Service Life for Structures Subjected to Chlorides, *American Concrete Institute Materials Journal*, Sept-Oct 2003, pp. 390-397.
- Borsoi, S. Collepardi, L. Coppola, R. Troli and Collepardi, M., (2001)** Strength and Durability of Concretes with Slag-Fly Ash-Portland Cement, *American Concrete Institute Materials journal*, pp. 115-126
- Bourke, K., and Davies, H., (1997)**, Factors Affecting Service Life predictions of buildings: A discussion paper, Laboratory report, Building Research Establishment, Garston, Watford, U.K.
- BS 8110-1:1997, (1997)**, *Structural use of concrete- Code of practice for design and construction*.
- Castellote, M., Andrade, C., (2006)**, Round-Robin Test on Methods for Determining Chloride Transport Parameters in Concrete, *Materials and Structures*, 39(2006), pp. 955-990.
- Castellote, M., Andrade, C., Alonso, C., (2001)** Measurements of the Steady and Non-steady-state Chloride Diffusion Coefficients in a Migration Test by means of Monitoring the conductivity

in the Anolyte Chamber. Comparison with Natural Diffusion Tests, *Cement and Concrete Research*, 31(2002), pp. 1411-1420.

CEB-FIP Comité Euro-International du Béton (1988), General principles on reliability for structures, Bulletin Information, pp.191.

Cho, S.E., (2007), Effects of Spatial Variability of Soil Properties on Slope Stability, *Engineering Geology*, 92(3-4), pp. 97-109.

Colleparidi, M., Marcialis, A., Turriziani, R., (1972) Penetration of Chloride ions into Cement Pastes and Concretes, *Journal of American Concrete Society*, pp. 534-535.

Crank, J., (1975), *The Mathematics of Diffusion*, Oxford University Press, 2nd Edition.

Detwiler, R., Taylor, P., (2005) Guide to Durable Concrete, *The Indian Concrete Journal*, 79(10), pp. 3-5.

DuraCrete, (1999a) *Compliance Testing for Probabilistic Design Purposes*, BE95- 1347/R0, The European Union – Brite EuRam III, Contract BRPR-CT95-0132, Project BE95-1347.

DuraCrete, (1999b), *Probabilistic Methods for Durability Design*, Document BE95- 1347/R0, The European Union – Brite EuRam III, Contract BRPR-CT95-0132, Project BE95-1347.

Edvardsen C. and Mohr L., (1999) *DURACRETE –Structures a guideline for Durability-based Design of Concrete*, Prepared by COWI Consulting Engineers and Planners AS, Denmark.

EN 1990 (2000) Eurocode: Basis of structural design. British Standards Institution.

EN 206 (2000) Concrete - Part 1: Specification, performance, production and conformity. British Standards Institution: 70 pp.

European Committee for Standardization (2004) BS EN 1992-1-1 Eurocode 2: Design of Concrete Structures – Part 1-1: General rules and rules for buildings (European standard prEN1992-1-1). CEN, Brussels, Belgium

Faber, M., H., Sørensen, J., D, (2002), *Reliability Based Code Calibration Joint Committee on Structural Safety*, Paper for the Joint Committee on Structural Safety Draft.

Ferreira, R. M., (2006), *Improving Durability through Probabilistic Design*, Doctorate Thesis, University of Minho, Portugal.

- FIB Model Code for Service Life Design (2006)** *fib* Bulletin 34, EPFL Lausanne, 116 pp.
- Garboczi, E.J., and Bentz, D.P., (1996)**, Modelling of the Microstructure and Transport Properties of Concrete, *Construction and Building Materials*, 10 (5), pp. 293-300.
- Gardner, T.J., (2006)**, *Chloride Transport Through Concrete and Implications for Rapid Chloride Testing*, Masters Thesis, University of Cape Town.
- Gjørsv, O. E., (1995)**, Effect of Condensed Silica Fume on Steel Corrosion in Concrete, *American Concrete Institute Materials Journal*, 92(6), pp. 591-598.
- Gouws, S.M., Alexander, M.G., Maritz, G., (2001)**, Use of Durability Index Tests for the Assessment and Control of Concrete Quality on Site, *Concrete Beton*, 98(2001)
- Hamad, S.B., and Itani, S. M., (1998)**, Bond Strength of Reinforcement in High-Performance Concrete, The Role of Silica Fume, Casting Position, and Superplasticizer Dosage, *American Concrete Institute Materials Journal*, 95(5).
- Hansson C. M., Poursae, A., Jaffer, S. J., (2007)**, *Corrosion of Reinforcing bars in Concrete*.
- Hasofer A.M. and Lind, N.C. (1974)** Exact and invariant second-moment code format, *Journal of the Engineering Mechanics Division, ASCE* 100 (1974), pp. 111–121.
- HETEK-53 (1996)** Chloride Penetration into Concrete, State of the art, Transport processes, Corrosion Initiation, Test Methods and Prediction Models, Road Directorate, 1020, Copenhagen, Denmark, pp. 102.
- Hobbs, D. W., (1996)** Chloride Ingress and Chloride Induced Corrosion In Reinforced Concrete Members, *Proceedings of Fourth International Symposium on Corrosion of Reinforcement in Concrete Construction*, Edited by Page C.L, Bamforth P.B and Figg, J.W., pp. 124-135.
- Holický M., (2007)** Probabilistic design of structures for durability, *Proceedings of the SEMC Seminar*.
- Hooton, R.D., Thomas, M.D.A. and Stanish, K. (2001)** Testing the Chloride Penetration Resistance of Concrete: A Literature Review, Prediction of Chloride Penetration in Concrete, publication No. FHWA-RD-00-142, US Department of Transportation, Federal Highway Administration, McLean, VA., USA.

- Hovde, P.J., (2005)**, The Factor method- A simple tool to service life estimation, Proceedings of the 10th DBMC International Conference on Durability of Building Materials and Components, Lyon (France).
- ISO 13823 (2008)** *General Principles on the Design of Structures for Durability*, ISO TC98/SC2, Final Draft.
- ISO 15686-1:2000, (2000)**, Buildings and constructed assets -- Service life planning -- Part 1: General Principles.
- ISO 15686-8 (2008)** Buildings and Constructed Assets – Service life planning -Part 8: Reference service life and service life estimation
- ISO 2394 (1998)** General Principles on Reliability for Structures for Durability, pp. 73
- ISO 5725-2 (1994)** Accuracy (Trueness and Precision) of Measurement Methods and Results. Basic methods for the determination of repeatability and reproducibility of a standard measurement method.
- Knudsen A, Jensen FM, Klinghoffer O, Skovsgaard T. (1998)** Cost-effective enhancement of durability of concrete structures by intelligent use of stainless steel reinforcement, *Proceedings of International Conference on corrosion and rehabilitation of reinforced concrete structures*, Orlando, FL, 8–11 December 1998 [on CD-ROM]. Orlando (FL): Federal Highway Administration.
- Kropp J., (1995)**, Chlorides in concrete, Performance Criteria for Concrete Durability (edited by Kropp and Hilsdorf), *RILEM Report 12*, 1st edition.
- Kwan and Wong Henry H.C., Albert, K.H., (2006):**, *Durability of Reinforced Concrete Structures, Theory vs. Practice*, Department of Civil Engineering, The University of Hong Kong, Hong Kong.
- Li, C. Q., (1997)**, Deterioration of concrete building structures, *Building Research and Information*, 25(4), pp.196 – 201.
- Lindvall, A., (2006a)** Chloride Ingress data from Field and Laboratory Exposure –Influence of Salinity and Temperature, *Cement and Concrete Composites*, 29(2007), pp. 88-93.

- Lindvall, A., (2006b)**, Models for Environmental Actions for Reinforced Concrete Structures in Marine and Road Environments, Alexander (Editions) International conference on Concrete Repair, Rehabilitation and Retrofitting (ICRRR), 21-23 November 2005, Cape Town, pp. 119-120
- Liu P.L. and Der Kiureghian, A. (1990)** Optimization algorithms for structural reliability, *Structural Safety* 9 (1990), pp. 161–177.
- Liu, Y., Weyers, R.E., (1998)**, Modeling the time-to-corrosion cracking in chloride contaminated reinforced concrete structures, *American Concrete Institute Materials Journal*, 95(6), pp 675-681.
- Lu, X., (1997)** Application of the Nernst-Einstein Equation to Concrete, *Cement and Concrete Research*, 27(2), pp.293–302.
- Luping, T., Gulikers, J., (2007)**, On the Mathematics of Time-Dependent Apparent Chloride Diffusion Coefficient in Concrete, *Cement and Concrete Research Journal* 37, pp. 589–595
- Luping, T., Nilsson, L.O., (2001a)**, Ionic Migration and its Relation to Diffusion, *Ion and Mass Transport in Cement-Based Materials, Material Science of Concrete* (Eds.) Hooton, R.D., Thomas, MDA, Marchand, J., Beaudoin, J.J, Skalny, J.P., pp. 81-95.
- Luping, T., Nilsson, L.O., (2001b)**, Rapid Determination of Chloride Diffusivity of Concrete by Applying an Electric Field, *American Concrete Institute Materials Journal*, 89(1).
- Mac Donald, K., (1992)**, *The Diffusion of Chloride Ion In Cement Paste*, MSc. Thesis, Department of Mechanical Engineering, University of Windsor.
- Mackechnie, J. R., Alexander, M. G., (1997)** Durability Findings from Case Studies of Marine Concrete Structures, *Cement, Concrete and Aggregates*, 19(1), pp. 22-25
- Mackechnie, J.R., (1996)** *Prediction of Reinforced Concrete Durability in the Marine Environment*, University of Cape Town, PhD Thesis.
- Mackechnie, J.R., and Alexander, M.G. (2002)** Durability Predictions Using Early-Age Durability Index Testing, *In Proceedings of the Ninth Durability and Building Materials Conference*, Australian Corrosion Association, Brisbane, Australia, 11 pp.

- Mangat, P., and Molloy, B., (1994)** Prediction of Long Term Chloride Concentration in Concrete, *Materials and Structures*, 27, pp. 338-346.
- Marchand, J., Gernrd, B. and Delagrave, A., (1998)** Ion transport mechanisms in cement-based materials, *Materials Science of Concrete*, 5(1998), pp. 307-400.
- Marteinsson, B., (2005)**, *Service Life Estimation in the Design of Buildings a Development of the Factor Method*, Doctoral Thesis, Department of Technology and Built Environment, University of Gävle, Sweden.
- Martin-Perez, B., Zibara, H., Hooton, R.D., Thomas, M.D.A., (2000)**, A study of the effect of chloride binding on service life predictions, *Cement and Concrete Research*, 30(2000), pp. 1215-1223.
- Mehta, P. K., (2006)**, *High-Performance, High-Volume Fly Ash Concrete for Sustainable Development*, University of California, Berkeley, USA.
- Mehta, P.K., (1999)** Advancements in Concrete Technology, *Concrete International*, pp. 68-76.
- Mehta, P.K., and Burrows, R.W., (2001)** Building Durable Structures in the 21st Century, *Concrete International*, 23(3), pp. 57-63.
- Melchers, R.E., (1999)** *Structural Reliability Analysis and Prediction*, John Wiley, –XVIII; 437 ISBN 0-471-98324-1.
- Mele, I., (2006)** *Service life design of concrete structures -Predicting time dependent reinforcement corrosion due to chloride ingress*, Thesis for the Master degree of Civil Engineering, TU Delft
- Mikulic, D., Guainnoki, N., (2001)** *Blacktop Resurfacing of Bridge Decks*, Department of Civil Engineering, Center for Advanced Infrastructure and Transportation (CAIT), Rutgers, New Jersey.
- Nanukuttan, S.V., Basheer, L., McCarter, W.J., Robinson D.J., Basheer, P.A.M., (2008)** Full Scale Marine Exposure Tests on Treated and Untreated Concretes-Initial 7-year Results, *American Concrete Institute*, 105(1), pp 81-88
- Neville, A.M., (1995)** *Properties of Concrete*, Prentice Hall, 4th Edition, pp. 864.

- Noguchi, T., Kanematsu, M., Masuda, Y., (2006)**, Outline of Recommendations for Durability Design and Construction Practice of Reinforced Concrete Buildings in Japan, *Proceedings Of The Seventh Canmet/American Concrete Institute International Conference On Durability Of Concrete*, Greece, Malhotra, V.M. (eds).
- Nokken, M., Boddy, A., Hooton, R.D. and Thomas M.D.A., (2006)**, Time Dependent Diffusion in Concrete—Three Laboratory Studies, *Cement and Concrete Research*, 36 (1), pp. 200-207.
- Pandey J.L. and Banerjee, M.K. (1998)** Concrete Corrosion and Control Practices-an Overview, *Anti-corrosion Methods and Materials*, 45(1), pp. 5-15.).
- Phoon, K.K., Kulhawy, F.H., and Grigoriu, M.D., (2000)**, Reliability-Based Design for Transmission Line Foundations, *Computers and Geotechnics*, 26(3-4), pp. 169-185.
- Powers, T.C., Brownyard, T.L., (1947)**, Studies of the Physical Properties of Hardened Portland Cement Paste, *Journal of American Concrete Institute*, Parts 1-9, 18(2-8).
- Rackwitz R. and Fiessler, B. (1978)** Structural reliability under combined load sequences, *Computers and Structures* 9 (1978), pp. 489–494.
- Richardson, M. G., (2002)**, *Fundamentals of Durable Concrete*, First Edition, Spoon Press- Taylor and Francis group, pp. 38-50.
- Rooij, M.R., Polder R.B., (2004)**, What Diffusion Coefficient is Used for Chloride Diffusion Modelling?, *Advances in Concrete through Science and Engineering, Proceedings of RILEM International Symposium, Evanston*
- SANS 10100-2 (2005)** South African National Standard: The Structural use of Concrete, Part 2: Materials and Execution Work, 3rd Edition, pp. 66.
- Shiessl, P., (1996)**, Durability of Reinforced Concrete Structures, *Construction and Building Materials*, 10(5), pp. 289-292.
- Siemes T., Edvardsen, C., (1999)** Duracrete: Service Life Design for Concrete Structures-A Basis for Durability of Other Building Materials and Components? *Durability of Building Materials and Components 8*, Edited by M.A. Lacasse and D.J. Vanier. Institute for Research in Construction, Ottawa ON, K1A 0R6, Canada, pp. 1343-1356
- Smith, W.F. (2004)** *Foundations of Materials Science and Engineering*, 3rd Edition, McGraw-Hill

- Stanish K., Alexander, M.G., Ballim, Y., (2006)**, Assessing the Repeatability and reproducibility of South African Durability Index Tests, *Journal of the South African Institution of Civil Engineering*, 48(2), pp. 10-17.
- Stanish, K., Alexander, M. G., Ballim, Y., (2007)**, A Framework for Use of Durability Indexes in Performance-based Design and Specifications for Reinforced Concrete Structures, *Materials and Structures Journal*, DOI 10.1617/s11527-007-9295-0
- Stanish, K.D., Hooton, R.D. and Thomas, M.D.A., (1997)**, Testing the Chloride Penetration Resistance of Concrete: A Literature Review, Department of Civil engineering, University of Toronto
- Streicher, P. E, (1997)**, *The Development of a Rapid Chloride Test for Concrete and its use in Engineering Practice*, PhD Thesis, University of Cape Town.
- Streicher, P.E., and Alexander, M.G., (1994)**, A Critical Evaluation of Chloride Diffusion Test Methods for Concrete, *In Proceedings of 3rd CANMET/ACI International Conference on Durability of Concrete*, Supplementary papers, pp. 517-530.
- Streicher, P.E., and Alexander, M.G., (1995)**, A Chloride Conduction Test, *Cement and Concrete Research*, 25(6), pp. 1284-1295
- Suryavanshi, A.K., Swamy, R.N., Cardew, G.E., (2002)**, Estimation of Diffusion Coefficients for Chloride Ion Penetration into Structural Concrete, *American Concrete Institute*, 99(5), pp 441-450.)
- Takewaka, K., and Mastumoto, S., (1988)**, Quality and cover thickness of concrete based on the estimation of chloride penetration in marine environments, in V.M. Malhotra (Ed.), *Proceedings of the 2nd International Conference Marine Environment*, American Concrete Institute SP-109, pp. 381-400.
- Tang, L. and Nilsson, L.O., (1992)**, Rapid Determination of the Chloride Diffusivity in Concrete by Applying an Electric Field, *American Concrete Institute Materials Journal*, 89(1), pp. 49-53
- Tikalsky, P.J., Pustka, D. and Marek, P., (2005)** Statistical Variations in Chloride Diffusion in Concrete Bridges, *American Concrete Institute Structural Journal*, May-June 2005, pp. 481-487.

Truc, O., Olivier, J.P., Carcassè, M., (2000) A new way for determining the chloride diffusion coefficient in concrete from steady state migration test, *Cement and Concrete Research*, 30 (2000), pp.217–226

Zhang, M., H., Chia, K., S., (2006), Water Permeability and Chloride Penetration in Lightweight and Normal weight Aggregate Content, *Proceedings of the 7th CANMET/American Concrete Institute conference*.

University of Cape Town

CHAPTER 3: METHODOLOGY

3.1 INTRODUCTION

This chapter gives an overview of the procedures to be followed in developing a probabilistic model for the durability design of RC structures. In this study, probabilistic modelling will involve representing parameters that have an influence on the durability of a RC structure as stochastic quantities. The relationship between the parameters will then be expressed using a mathematical model/ limit state function. An analysis of the model is carried out using Monte Carlo simulation (MCS). The results of the analysis are described in terms of the probability of durability failure.

3.2 OBJECTIVES OF THE STUDY

1. The first task in this study will be to define the limit-state function (LSF) for RC structures in a marine environment. The LSF is derived from modified Fick's second law and will be used to predict the time to corrosion initiation for new structures. The parameters in the LSF are classified as environment, geometric or material parameters. The surface chloride concentration C_s represents the environmental load parameter. C_s is generated from the marine environment and is the force driving chlorides into the concrete towards the reinforcement. Determining a value of C_s for concrete elements in different marine environments is carried out through laboratory testing. The geometric parameter refers to the cover depth and is determined from in-situ testing of existing RC structures/elements. The diffusion coefficient D_i determines the potential resistance of concrete cover with respect to chloride diffusion and is used to represent the material parameter in the LSF. D_i is determined from the chloride conductivity values obtained from the chloride conductivity test which was aforementioned in Chapter 2 as one of South Africa's durability index tests.
2. The second step involves carrying out a statistical quantification of the variability in the LSF parameters by specifying their statistical distributions and associated parameters such as mean and standard deviation. The statistical quantification is carried out using data obtained from measurements and/or from literature.

3. The third step shows the application of structural reliability design philosophy to compute the probability of durability failure. Reliability-based design philosophy involves the use of probability theory and numerical techniques in evaluating the LSF. Monte Carlo simulation technique is used to analyse the durability LSF and to predict, with an acceptable level of confidence, the probability that corrosion is initiated during the service life of the RC structure. Results of the reliability-based design (RBD) give the design parameters (i.e. the chloride conductivity value and the cover depth) that will ensure the RC structure meets its performance requirements with a required probability level.
4. The final step involves carrying out an analysis of the sensitivity of LSF parameters to failure probability. The sensitivity analysis assigns sensitivity factors to each model parameter. The sensitivity factors give the designer insight to the parameters of the LSF that are more influential in the design. The designer can then use this information to define future research and development needs.

A schematic representation of all the tasks involved in the study are summarised in Figure 3.1.

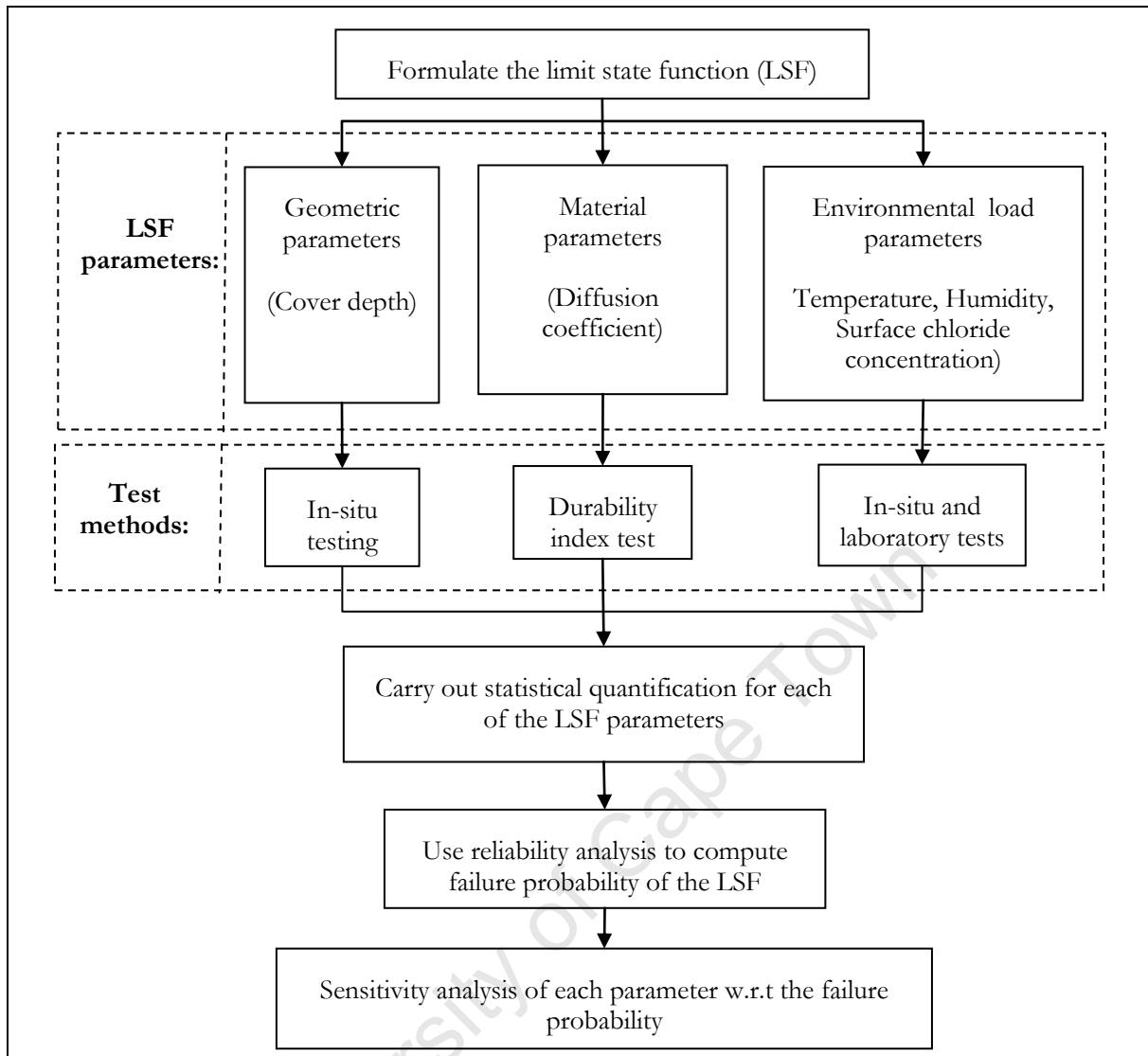


Figure 3.1: Flow chart of the methodology followed in the study

3.3 LIMIT-STATE DURABILITY DESIGN

3.3.1 Introduction

The probabilistic service life design methodology presented in this study follows the same principles of reliability and performance given in structural design standards such as ISO 2394 (1998). The methodology takes into consideration the scatter of the influencing parameters of durability and represents these parameters in the form of a limit-state function (LSF).

The limit state is the border that separates desired states from the undesired or adverse states which a structure may be subjected to during its lifetime (Edvardsen and Mohr, 1999). Three

types of limit-states are defined by ISO 13823 (2008) namely the ultimate limit state (ULS), the serviceability limit state (SLS) and the initiation limit state (ILS). ULS depicts the point at which the safety of the RC structure is considered (for example the risk of collapse) while SLS defines the point at which the functionality of the structure is considered (for example the limitation of crack widths). ILS precedes both the occurrence of ULS and SLS, and is used to describe the onset of deterioration such as corrosion initiation. The decision on specifying the type of limit state may be based on technical reasons but other aspects, such as economical, functional, and social reasons also need to be considered (Marteinsson, 2005).

This study dwells on the durability design of RC structures and hence the appropriate limit-state is the ILS. The LSF will therefore have variables representing the degradation of the RC structure with time up till the ILS. The time-varying variables in the LSF are classified as load S_C and resistance variables R_C similar to structural design.

The reliability of the structure against degradation is then evaluated by ensuring that the probability of the load being greater than the resistance during the structure's design service life is lower than the allowable failure probability, $P_{target,ILS}$ given in durability standards (Table 2.6) (Sarja and Vesikari, 1996). Figure 3.2 shows the reduction of resistance R_C with time due to deterioration as the load S_C increases.

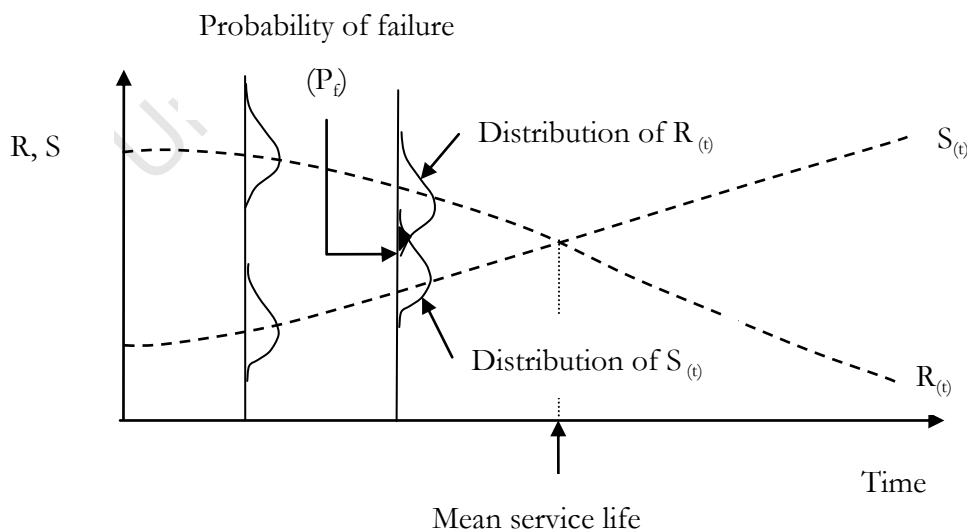


Figure 3.2: Illustration of the decrease of resistance with time and increase of load with time (Rostam, 2005)

The interaction between the two probability density functions (PDF) of the load and resistance variables in Figure 3.2 constitutes the probability of failure P_f . This P_f is nil at the beginning of the structure's service life but continuously increases with time due to deterioration of the structure. The dotted lines represent the mean values of S_c and R_c at any particular time and are used in a deterministic format. The probabilistic (reliability) method takes into consideration not only the mean values but also the PDF of S_c and R_c . The format taken by the probabilistic method is illustrated by the following equation (ISO 13823, 2008):

$$P_f = \phi(\beta) = P(R_c - S_c = 0) < P_{target,LLS} \quad (3-1)$$

All the terms in the equation have been previously defined.

The probabilistic design method has been applied to several degradation models, such as in the Brite-EuRam project BE95-1347, called DuraCrete project (1996-1999) where the approach was subsequently applied in the design of high relevance structures such as the Western Scheldt Tunnel in 2000. Within the Duracrete model the Rapid Chloride Migration test was adopted as the standard laboratory test method to quantify the potential chloride transport properties of a concrete mix (DuraCrete, 2000).

The study presented in this thesis is similar in principle to the DuraCrete approach but differs in two ways. First the study applies a South African prediction model developed by Mackechnie (1996) to specify material parameters that will ensure that the RC structure remains durable within its service life. Secondly, the model used applies the chloride conductivity (durability index) test to determine values for the material resistance parameter.

3.3.2 Durability Design Procedure

An example will be given in the study on the durability design of a RC element based on the probabilistic service life design methodology. The procedure to be followed in the design is illustrated in Figure 3.3.

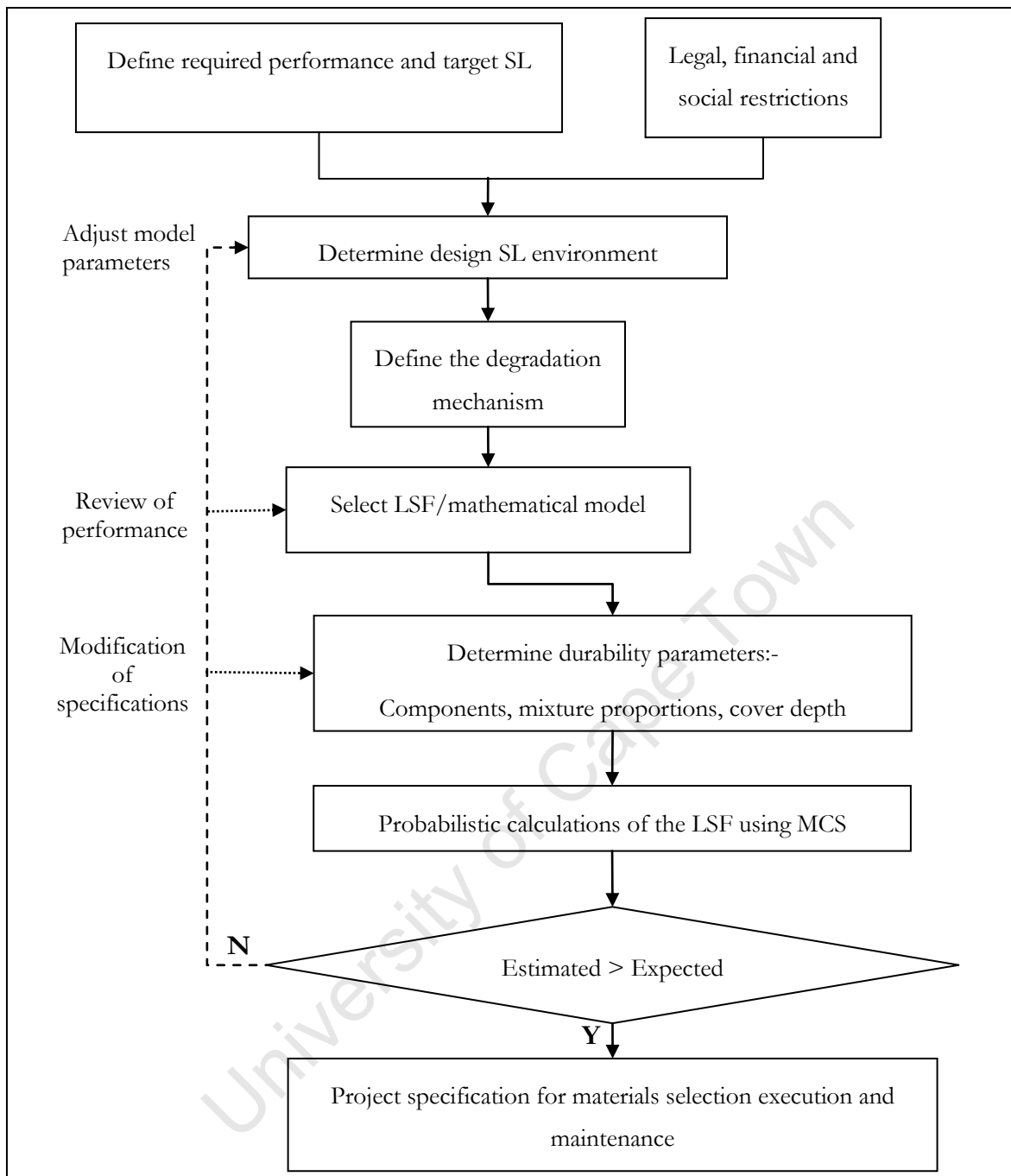


Figure 3.3: Flow chart of the durability design procedure (Adapted from Sarja, 2002)

The first step in durability design involves defining the desired service life of the structure, and is carried out mainly by the client/owner of the structure. In this step, the client specifies a deterministic quantity referred to as the design working life of the structure \mathbf{C}_d (Table 2.3 of Chapter 2), having given consideration to the performance requirements of the structure.

The second step in the design involves the appraisal of environmental actions acting on the structure in order to show their significance in relation to durability (Siemes and Edvardsen, 1999). Environmental actions are those chemical and physical actions to which the concrete is exposed and that result in effects on the concrete or reinforcement that are not considered as loads in structural design (EN206-1, 2000). For this study, the main environmental action is chloride-induced corrosion, of RC structures, by chlorides from seawater. This type of environmental action usually occurs for RC structures near a marine environment. The relevant marine environments are given in Table 3.1 which gives EN 206 marine classifications modified for South African conditions.

Table 3.1: Marine Environmental Classes (Natural environments only) (after EN206-1 as cited in Alexander *et al.*, 2001)

Corrosion Induced by Chlorides from Seawater	
Designation	Description
XS1	Exposed to airborne salt but not in direct contact with seawater
XS2a [#]	Permanently submerged
XS2b [#]	XS2a + exposed to abrasion
XS3a [#]	Tidal, splash and spray zones Buried elements in desert areas exposed to salt spray
XS3b [#]	XS3a + exposed to abrasion

[#] These sub clauses have been added for South African coastal conditions

Proper definition of the environmental classes is important as it assists in identifying the dominant transfer processes of aggressive agents into concrete. The transport processes are modelled using deterioration mechanisms. For example, chloride penetration in the concrete structure/ component can be modelled using Fick's second law of diffusion.

The Fickian type model applicable to South Africa marine environment and which will be used in this study is represented as:

$$C_{(x,t)} = C_s \left(1 - \operatorname{erf} \left(\frac{x}{2\sqrt{D_i t^{1-m}}} \right) \right) \quad (3-2)$$

where:

C_s - chloride concentration at the surface of the concrete

C_x - chloride concentration at depth x

x - depth of chloride penetration (mm)

D_i - initial diffusion coefficient determined theoretically from the chloride conductivity test (mm²/year)

m - diffusion coefficient reduction factor

erf - error function

t - time (years)

The durability design focus using reliability-based design approach will be to present the degradation of a RC structure over time due to reinforcement corrosion in the form of an *initiation limit-state function* (ISO 13823, 2008):

$$S_{\text{lim}} > S \quad (3-3)$$

S_{lim} is the barrier effect represented by C_{crit} , which is the critical (threshold) chloride concentration at the rebar level and which when exceeded leads to corrosion initiation. S is the action effect represented by the modified Fickian model $C_{(x,t)}$ (Equation 3-2). The relationship between $C_{(x,t)}$ and C_{crit} is modelled mathematically as a function of basic variables, g , representing concrete dimensions, material properties and the environment of the RC structure as shown by Equation 3-4.

$$Z = C_{\text{crit}} - C_{(x,t)} = g(C_s, D_i, t, m, C_{\text{crit}}) \quad (3-4)$$

Consequently, the ILS will be deemed to occur when $C_{(x,t)}$ is equal to C_{crit} .

$$\Rightarrow C_{\text{crit}} - C_{(x,t)} = 0 \quad (3-5)$$

$$\Rightarrow C_{\text{crit}} - C_S \left[1 - \text{erf} \left(\frac{x}{2\sqrt{\theta_i \cdot \theta_{D_i} \cdot t^{1-m}}} \right) \right] = 0 \quad (3-6)$$

The Equations 3-5/ 3-6 represent the ILS of the RC structure with θ_{D_i} representing the parameter that accounts for model uncertainties in D_i . This model uncertainty arises from the use of an idealised relationship during the conversion of the 28-day chloride conductivity value to a diffusion coefficient representing the concrete material quality. The effect of the model uncertainty parameter will be to increase the scatter in the model output (see Section 4.6 of Chapter 4).

The functions C_{crit} and $C_{(x,t)}$ are represented as probability density functions (PDFs) as illustrated in Figure 3.4, with the interaction between the two PDFs representing the probability of durability failure.

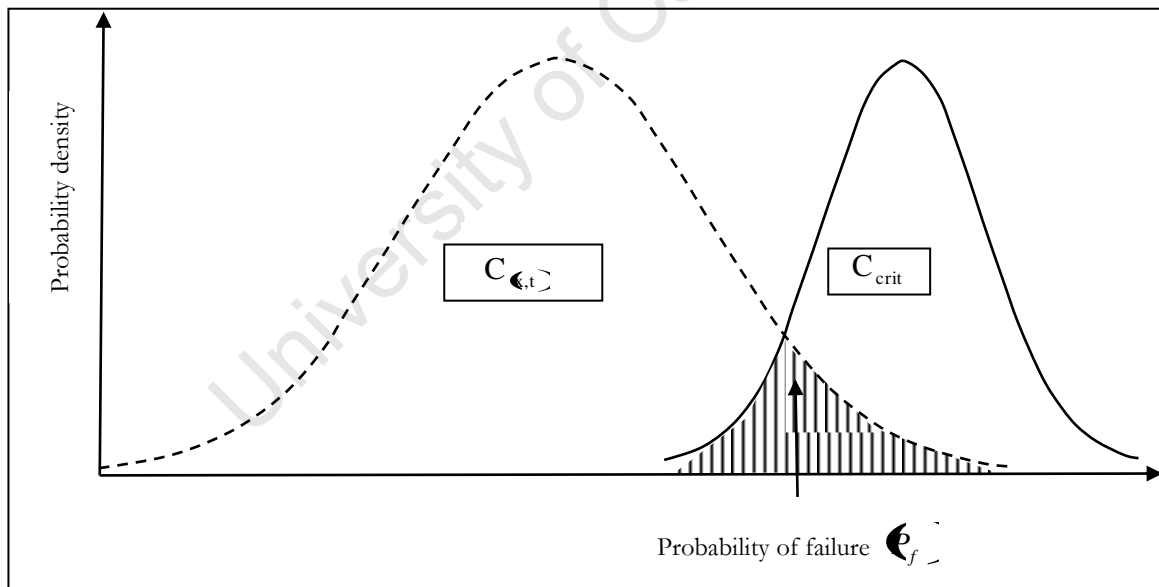


Figure 3.4: Illustration of PDF showing relation of the action effect, resistance and probability of failure

Having formulated the ILS function (Equation 3-6), the next task in durability design involves selecting an optimal material composition and structural detailing that will reliably resist the environmental actions threatening the structure, and if possible, prolong the period to the attainment of the initiation limit state. This involves:

- Making a choice of a concrete mix that will provide a low permeation for the chloride ions from the sea water.
- Choosing a large concrete cover to the reinforcement by finding an optimum between the advantage of a large cover with the increased risks of cracking
- Ensuring that the structural dimensions and detailing of the reinforcement leave adequate space for placing concrete.

Aforementioned, reliability-based design is concerned with not only the probability of failure but also with the risk of the RC structure/component not achieving its expected performance at the ILS based on the choice of parameters. The acceptable risk $P_{target,ILS}$ associated with ILS is given in Table 2.6 (of Chapter 2).

The ILS represented by Equation 3-6, will therefore be verified by ensuring that the condition represented in Equation 3-7 holds.

$$P_f = P \left\{ \xi_{(x,t)} - C_{crit} < 0 \right\} P_{target,ILS} \quad (3-7)$$

If the choice of values for material and geometry parameters does not meet the condition specified by Equation 3-7, then the selection should be adjusted appropriately until the condition is satisfied.

In conclusion, it can be observed that durability design of RC structures at the design stage involves not only selecting appropriately the materials and the mix proportion of concrete and deciding structural details of the structure but also ensuring the reliability of performance of the designed structure throughout the service life.

3.3.3 Limit-State Function Parameters

From the LSF (Equation 3-6), the parameters C_{crit} , C_s , D_i , x and m have been identified as key parameters, which will be further categorised as structural (geometric), material or environmental parameters as illustrated in Table 3.2. The material parameters are determined from durability index tests and the environment and execution parameters are determined from either laboratory or in-situ testing and they will be covered next.

Table 3.2: Basic random variables in the initiation limit-state function

Parameters		Section
Material parameters	Diffusion coefficient D_i	3.3.4.1
	Reduction factor η	3.3.4.2
	Critical chloride content C_{crit}	3.3.4.3
Environmental parameter	Surface chloride concentration C_s	3.3.5
Structural parameter	Concrete cover depth x	3.3.6

3.3.4 Material Parameters

3.3.4.1 Diffusion coefficient

The diffusion coefficient used in the LSF is the initial diffusion coefficient D_i . The value of D_i is determined theoretically from the chloride conductivity value of the concrete determined by the chloride conductivity test (CCT) (Figure 2.4 of Chapter 2). An overview of the test procedure was given in Section 2.3.2 of Chapter 2.

The CCT gives a rate of conduction of the concrete material characterised by conductivity σ , and is equal to the charge flux (current density) under a unit electric field. The chloride conductivity value is determined by measuring the electric current flowing through the concrete specimen and applying Equation 3-8.

$$\sigma = \frac{i \cdot t}{V \cdot A} \quad (3-8)$$

where,

$\sigma \Rightarrow$ Chloride conductivity (mS/cm)

$i \Rightarrow$ Measured current (mA)

$V \Rightarrow$ voltage (V)

$t \Rightarrow$ Specimen thickness (cm)

$A \Rightarrow$ Cross-sectional area (cm²)

D_i is calculated using the relation:

$$Q = \frac{D_i}{D_o} = \frac{\sigma}{\sigma_o} \quad (3-9)$$

where,

1. Q is the diffusibility ratio.
2. σ is the conductivity of concrete (calculated from Equation 3-8)
3. σ_o is the conductivity of the pore solution: - as aforementioned, (Section 2.3.2 of Chapter 2), σ_o results from both the saturating salt solution and also from mobile ions such as K^+ , Na^+ and OH^- which are present in concrete pores. To measure the conductivity of the latter would involve pore expression measurements which are difficult and impractical for routine rapid testing, and hence the value of σ_o is assumed to be that of the 5M *NaCl* saturating solution (Streicher, 1997).
4. D_o is the diffusivity of chloride ions in the pore solution (m²/s) as given by:

$$D_o = \frac{RT}{ZF} \cdot \frac{l \cdot J_c}{E \cdot c} \quad (3-10)$$

where,

$R \Rightarrow$ Gas constant $R = 8.314 \text{ J} \cdot \text{K}^{-1} \cdot \text{mol}^{-1}$

$T \Rightarrow$ Absolute temperature (K)

$Z \Rightarrow$ Valency of chloride ion ($Z = -1$) (eq/mol)

$F \Rightarrow$ Faraday constant $F = 9.648 \cdot 10^4 \text{ J} \cdot \text{V}^{-1} \cdot \text{mol}^{-1}$

$\frac{E}{l} \Rightarrow$ Gradient of the electric field (V/m)

$c \Rightarrow$ Concentration of chloride ions (mol/m^3)

$$\text{and } J_c = \frac{i}{ZF} \quad (3-11)$$

where:

$i \Rightarrow$ Current density (ampere / m^2)

$Z \Rightarrow$ Valency of ion ($Z = +1, +2, \dots$) (eq/mol)

$F \Rightarrow$ Faraday constant (Coul/eq)

5. Finally, D_i is the effective diffusivity of chloride ions through concrete (m^2/s) given as:

$$D_i = \frac{D_o \sigma}{\sigma_o} \quad (3-12)$$

The diffusion coefficient D_i does not necessarily represent the actual diffusion coefficient represented in the service life prediction model (Equation 3.6). This is because the 28-day chloride conductivity value, σ does not allow for long-term chemical interactions between ingressing agents and the constituents of concrete (i.e. continued hydration and chloride binding). Mackechnie, (1996) established that for σ to be representative of true conditions, it needed to be adjusted using a modification factor. The modification factor depended on the concrete type and was derived from two different techniques (Mackechnie *et al.*, 1996b):

- (i) Correlation between 28-day conductivity index values and chloride ingress in structures in the Western Cape Province.
- (ii) Laboratory-based experimental correlations between 28-day conductivity index values and chloride diffusion coefficients.

Mackechnie (1996) established a correlation between the modified chloride conductivity and diffusion coefficients (for different binder types) recorded after two years, and presented this correlation in the form of a nomogram excel spread sheet, *concur.xcl*. The spreadsheet essentially computes the modified chloride conductivity from the 28-day chloride conductivity value (input) and gives an output of both the corresponding 2 year diffusion coefficient $D_{2\text{years}}$ and the reference (initial) diffusion coefficient D_i at 28 days.

This nomogram sheet, that represents the idealised relationship between 28-day chloride conductivity and 2 year diffusion coefficient will be used in this study to obtain D_i values for the service life prediction model.

3.3.4.2 Diffusion coefficient reduction factor

A reduction factor $\left(\frac{t_i}{t}\right)^m$ is applied to D_i , to allow for a change in diffusion coefficient with time, such that at any given time t the diffusion coefficient D_t can be represented as a function of the initial diffusion coefficient, D_i (Mackechnie, 1996):

$$D_t = D_i \left(\frac{t_i}{t} \right)^m \quad (3-13)$$

Mackechnie (1996) found m to be a constant dependent on the binder types. The values he obtained for the different binder types and which are also adopted for this study are given in Table 3.3.

Table 3.3: Chloride diffusion coefficient reduction factor
(Adopted from Mackechnie, 1996)

Binder type	m
# 100 % PC	0.29
Fly ash (FA)	0.68
Slag	0.68

100 % PC – 100 % Portland cement

From Table 3.3 it can be seen that the magnitude of m is small for PC concrete compared to the blended cements (FA and slag). This means that a decrease in diffusion coefficient with time is noticeable for concretes containing blended cements such as fly ash but for 100 % Portland cement the diffusion coefficient remains nearly constant with time. This concept is illustrated in Figure 3.5 in which values of D_i for different binders types (i.e. for: -

OPC $\rightarrow D_i = 9.48E - 08 \text{ cm}^{-2} / \text{s}$, FA $\rightarrow D_i = 8.62E - 09 \text{ cm}^{-2} / \text{s}$ and

GGBS $\rightarrow D_i = 2.55E - 08 \text{ cm}^{-2} / \text{s}$) are substituted into Equation 3-13 to compute corresponding D_t at various time intervals.

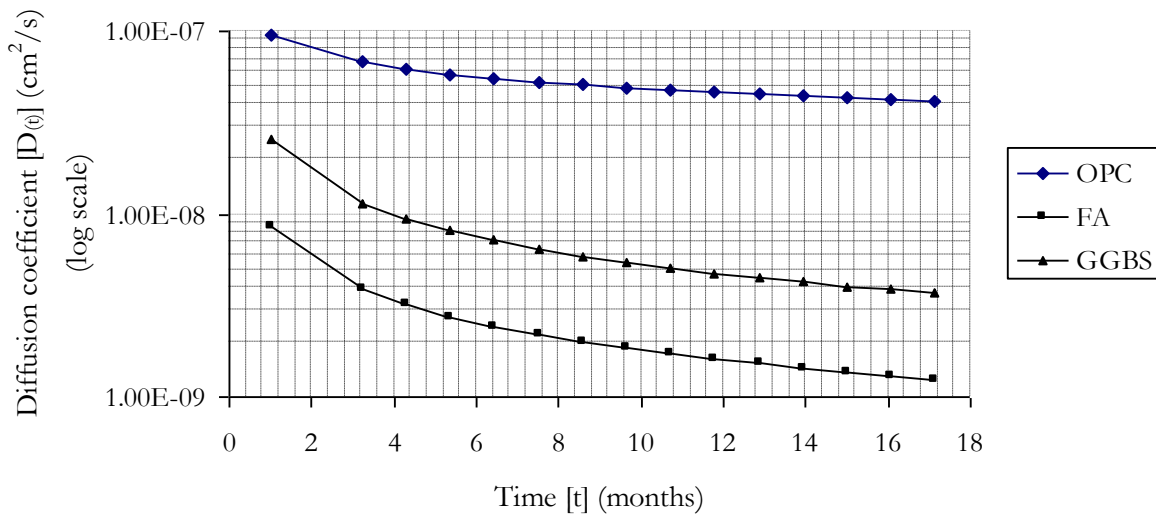


Figure 3.5: Illustration of decrease in diffusion coefficient (log-scale) with time (normal scale) for different binder types

The reason for the negligible decrease of diffusion coefficients with time of OPC concrete may be ascribed to its lower chloride binding capacity as compared to blended cements containing FA and GGBS (Arya *et al.*, 1989). The FA (a pozzolanic material) and GGBS (a latent hydraulic material) binders are able to bind greater proportions of chloride ions hence cause the rapid decrease of diffusion coefficient with time.

It can thus be concluded that the long term performance of OPC concrete in a marine environment is not as good as that of concrete containing FA or GGBS binders.

3.3.4.3 Critical chloride content

The critical chloride content (C_{crit}) is defined in two ways; the first definition refers to the content of chlorides at the steel depth that is necessary to sustain local passive film breakdown, irrespective of whether it leads to visible corrosion damage on the concrete surface (Schiessl and Raupach, 1990; Duracrete, 2000). The second definition of C_{crit} refers to the chloride content which leads to deterioration or damage of the concrete structure (Duracrete, 2000). The former definition of C_{crit} is applicable for durability design in this study as it considers lower chloride concentrations and ensures that the RC structure does not undergo significant deterioration during its design working life. Furthermore, the chloride threshold value definition is relevant as was seen in Chapter 2 in that it plays a role in the

selection of the appropriate target reliability index β_{target} . For durability design purposes, β_{target} is selected by considering the economic, social and environmental consequences associated with the damage state of a structure at the initiation limit state.

The threshold level is not fully established because the critical level at which passivity is lost and corrosion commences is difficult to define (Richardson, 2002). Studies carried out by Alonso *et al.* (2000) show that C_{crit} is not a unique value but takes on a number of values depending on factors that affect concrete quality such as; concrete mix proportions, binder type and C₃A content of cement. Currently, no work has been successfully completed to model the variation of the threshold value as a function of each of the parameters affecting it. For these reasons, there exists a wide variation in the reported values for the critical chloride content at the reinforcing steel level necessary to initiate corrosion under specific conditions (Sandberg, 1995). Table 3.4 summarises a range of C_{crit} values reported by various researchers expressed in terms of the total chloride content as a percentage by mass of binder.

Table 3.4: Critical chloride content levels

Reference	Critical chloride content (% mass of binder)
Berke (1986)	2.0 - 2.5
Browne (1982)	0.4
ACI (1994)	0.15

This study will review the statistical values given in literature to represent C_{crit} and consequently adopt one of these. This is because there is lack of local data relating to C_{crit} making it difficult to carry out a statistical quantification on the same.

3.3.5 Environmental Parameter

The temperature, relative humidity and concentration of chlorides on the surface of concrete all constitute environmental parameters. The surface chloride concentration C_s will be considered in this study as the environmental load on concrete and is expressed in terms of concentration of chlorides by mass of cement or concrete. The value of C_s is influenced by

the curing method, binder type, binder content, the location of the structure and its orientation in the marine environment (Song *et al.*, 2008).

For the statistical quantification of C_s , published data for C_s were used in the study. The data were obtained from previous in-depth inspections of marine structures, which were built between 1920 and 1977 and from concrete samples placed in two sites at the Cape Peninsula i.e.: a site at Simonstown, which is sheltered from wave action and prevailing winds, and a site at Granger bay which is exposed to heavy wave action. Simonstown is located within a shallow bay that traps warmer water resulting in sea temperatures between 13 and 20°C, while Granger bay is exposed to the open sea with colder water of between 12 and 15°C (Mackechnie and Alexander, 1997).

The values of C_s were obtained from chloride profiling tests where the chloride content of the concrete was determined. The chloride profiling test begins with the grinding the concrete to varying depths from concrete surface to the steel level. The chloride concentration of each sample is often given in parts per million, which is then converted to the percentage weight of concrete and finally as the percentage of chloride by weight of cement which is calculated by assuming a uniform distribution of cement through the cover concrete (Song *et al.*, 2008). The error function solution (Equation 2-4) is then fitted to chloride profiles and technically C_s would be taken as the y-co-ordinate of the profile. However, difficulty arises in obtaining a value of C_s as the chloride content within millimetres inside the outer surface of cover concrete decreases, because the concrete skin has a different composition, compared to the internal concrete, due to phenomena such as a contact with the moulds, segregation of aggregates or washing away of chlorides at the surface of cover concrete during preparation of samples (Song *et al.*, 2008). Thus, the value of C_s reported is an extrapolated value of the fitted curve and not the actual value as shown in Figure 3.6.

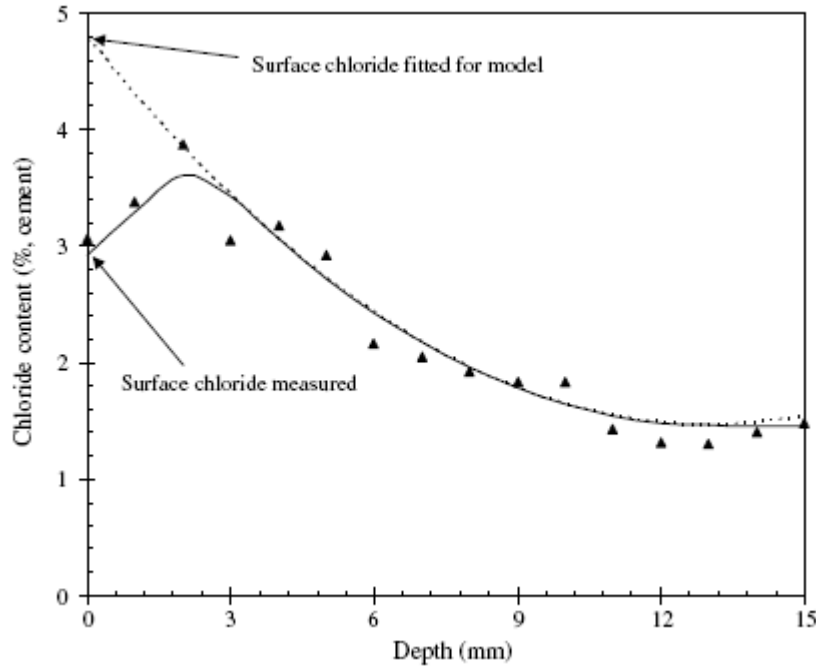


Figure 3.6: Chloride profile with fitted curves for C_s (Song *et al.*, 2008)

In literature, different researchers have found C_s to behave differently with time. Weyers *et al.* (1994) showed that the surface chloride concentration increases as a function of the square root of time (Equation 3-14).

$$C_{s(0,t)} = C_o \sqrt{t} \quad (3-14)$$

where,

$C_{s(0,t)} \Rightarrow$ Near surface chloride concentration

$C_o \Rightarrow$ A surface chloride concentration coefficient

$t \Rightarrow$ time

Studies carried out by Swamy *et al.* (1994) showed that the increase in surface chloride concentration, $C_{s(0,t)}$ tends to be attenuated over time as shown:

$$C_{s(0,t)} = C_1 t^n \quad (3-15)$$

Where C_1 is the surface chloride content after one year, and n is an empirical coefficient.

Other researchers such as Collins, *et al.* (1997) have found C_s to remain constant with time. In this study an assumption of constant chloride accumulation at the surface (i.e., a constant C_s) is made during the statistical quantification of C_s and in solving the LSF. However, a recommendation is made for further research to be conducted on the parameter to investigate its behaviour with time for RC structures in SA marine conditions.

3.3.6 Structural Parameter: Cover depth

SANS 10100-2 (1994) defines the term “concrete cover” as the thickness of concrete between the outer surface of the reinforcing steel and the face of the concrete (as cast) as illustrated in Figure 3.7.

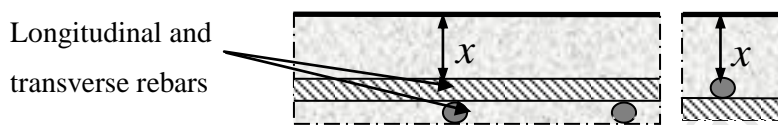


Figure 3.7: Cover depth measurements

Other technical terms such as nominal cover and minimum cover are also used to describe concrete cover. Nominal cover x_{nom} refers to the dimension used in design and is indicated on engineering drawings, whereas minimum cover is specified in codes and building standards to cover for durability and fire provisions (Ronne, 2005). x_{nom} constitutes of the minimum cover x_{min} , plus an allowance in design for deviation, Δx_{dev} as illustrated by Equation 3-16 (EN 1992-1, 2004). EN 1992, 2004 recommends a value of 10 mm for Δx_{dev} .

$$x_{nom} = x_{min} + \Delta x_{dev} \quad (3-16)$$

Concrete cover plays an important role in protecting the embedded reinforcement against corrosion. Failure to achieve adequate cover during construction has been found to be the single most important factor in the premature deterioration of reinforced and prestressed concrete structures (Sharp, 1997). This shortfall in concrete cover may be due to three reasons; first failure to appreciate the severity of the exposure conditions by the designer may result in a design error when specifying the cover, secondly, workmanship error during

construction and lastly, a design and detailing error which occurs when the designer specifies rebar details and bar lapping that are complex and do not allow for adequate compaction of the concrete as illustrated in Figure 3.8.

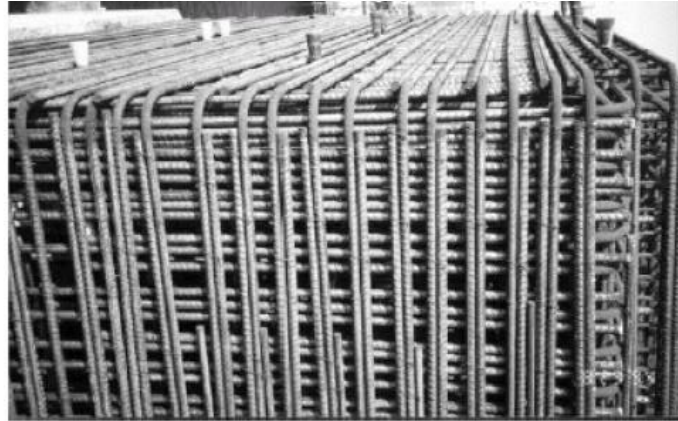


Figure 3.8: Complex reinforcement detailing which does not allow for adequate compaction (Rostam, 2005)

The cover depth achieved during construction is measured using non-destructive equipment (NDE) such as the digital covermeter (Alexander *et al.*, 2007). The cover meter or proformeter is able to detect rebar size, direction and position (Song and Saraswathy, 2007) and comprises of a probe and indicator unit as shown in Figure 3.9. The first step involved in taking cover depth measurements is to allocate a numbering system for the area under investigation. Secondly, the depth of reinforcing steel below the concrete surfaces and the diameter of the steel reinforcement is determined using the cover and diameter probes of the cover meter. The bar diameter reading is estimated first and used as an input into the rebar locator. To achieve an accurate cover reading, at least three cover readings are taken at each measurement point. The average of these three readings is then used in the statistical quantification process.

Figure 3.9 shows an example of a typical available commercial cover meter. BS 1881: Part 204 (1988) stipulates the accuracy of measurement likely to be obtained when an electromagnetic cover meter is used “on the average site” as $\pm 15\%$ for reinforcement covers of less than 100 mm. However, this equipment is not efficient where rebar details are

complex, such as at bar lapping or where there is interference from other metal work in a concrete element (Figure 3.8).



Figure 3.9: Cover meter (Song and Saraswathy, 2007)

The SA cover depth data available for this study were in post-processed form (raw data were unavailable for this study) and represented in the form of COV for the various nominal cover depths. This information is relayed in Chapter 4 where two statistical distributions: Normal and lognormal distribution were selected from literature to represent high cover depth (>40 mm) and low cover depths (<40 mm) respectively.

3.4 FITTING DISTRIBUTIONS TO DATA

3.4.1 Uncertainty in LSF parameters

The LSF (Equation 3-6) exhibits uncertainty arising from three possible sources i.e. statistical, model and physical uncertainty, as illustrated in Figure 3.10 (Khatri and Sirivivatnanon, 2004).

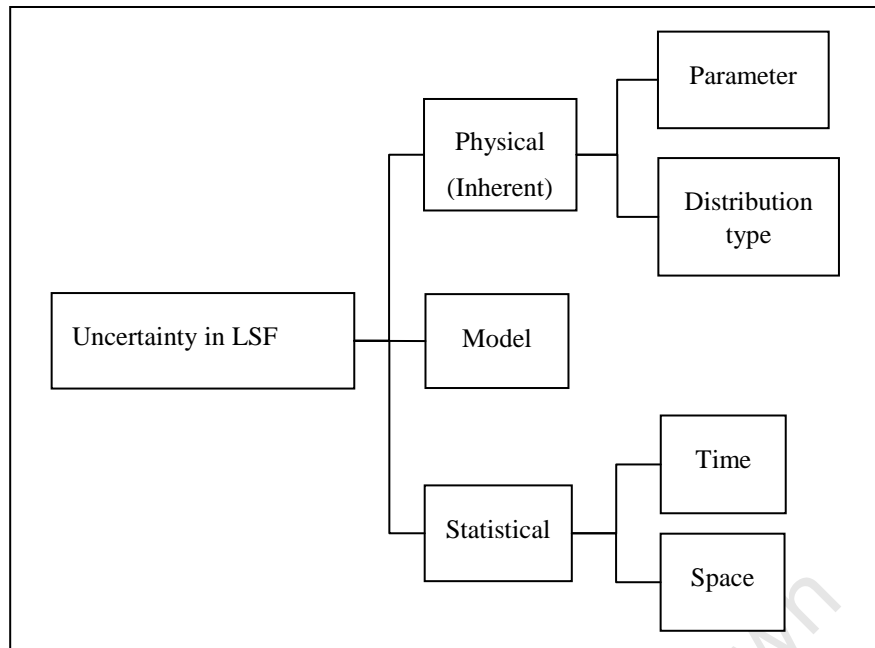


Figure 3.10: Types of uncertainty

These three sources of uncertainty are taken into account in the analysis of the LSF and are defined next.

Physical uncertainties result from natural variability in the (i) material properties of concrete, such as its permeability (ii) variability of structural geometry such as concrete cover depth and (iii) variability of micro-environment such as its surface chloride concentration. Concrete is a heterogeneous material made under variable conditions with variable materials. Therefore, it is inevitable that there will be fluctuations in its characteristics such as its quality due to variations in chemical composition of cement, level of compaction and extent of curing (Bentz, 2003).

Statistical uncertainties taken into account are anticipated to result from use of a limited number of specimens due to time and space limitations, measurement errors, data handling and transcription errors depending on the quality assurance observed during the chloride conductivity testing and the other in-situ tests on other parameters.

Model uncertainties are associated with the use of the simplified Fickian models or relationships between the basic variables to represent the actual physical phenomena of chloride ingress and corrosion initiation (Zhang and Lounis, 2006). This may be made due to lack of knowledge of the behaviour of materials in their service environment. For example, the conversion of the chloride conductivity value to the diffusion coefficient value based on

the idealised relationship between the two values creates errors in the prediction capability of the SLP model. In addition, the SLP model limits the number of basic variables, leaving out an infinite set of parameters which during the model idealization were judged as secondary or of negligible importance to corrosion initiation.

The aforementioned sources of uncertainty in concrete material affect the predictive capability of the SLP model. The uncertainties make it difficult or rather impossible to say with any conviction that there is a uniquely defined value for each of the variables in the LSF. It is more likely that for each parameter, there is a certain range of possible values that the designer can define with using the respective laboratory or in-situ testing. In general, some of these values can have a greater likelihood of occurring than others.

The range of possible values for each parameter (random variable) and the different likelihood of realization will be represented using various descriptors, such as their mean, standard deviation and probability distribution functions or probability density functions. To account for model uncertainties a variable (with statistical descriptors) will be introduced into the model. The effect of this ‘model uncertainty variable’ will be to increase the scatter of the predictions made using the SLP model.

3.4.2 Main Descriptors of Random Variables

The physical uncertainty associated with each parameter in the LSF will be represented in the form of a histogram. The histogram is a plot of the number of observed values for respective intervals of values of the parameter in question (Ang and Tang 2007). The histogram is obtained by splitting the range of the data into equal-sized bins (B) using the rule of thumb, $B = \sqrt{n}$ where n is the sample size. In addition, other formula’s may be used for setting the number of bins which includes (Kun and Meeden, 1997):

$$B = \frac{Range}{W} \quad (3-17)$$

where W is the bin width determined using Scotts (1979) formula:

$$W = 3.49 \times s \times n^{1/3} \quad (3-18)$$

s in Equation 3.18 is the standard deviation of the sample.

A probability distribution function will be used to show the following information of the data (Ang and Tang, 2007; Quinn and Keough, 2002 and Holický, 2007):

3.4.2.1 Location

Based on sample data of size n , an estimate for the center (location) of the distribution will be calculated using the sample mean \bar{x} which is an unbiased estimator of the population mean μ . For example, a normal distribution $N(\mu, \sigma^2)$ has location $\bar{x} = \frac{1}{n} \sum_i X_i$.

3.4.2.2 Scale

The scale parameter s indicates how widely or narrowly the values in sample are clustered

around the sample mean value. For a normal distribution $s = \sqrt{\frac{1}{n-1} \sum_i (X_i - \bar{x})^2}$.

Based solely on the value of standard deviation s , it may be difficult to state the degree of dispersion, and for this reason, the coefficient of variation (COV) will be used. The COV (Equation 3-19) is a measure of the dispersion relative to the mean \bar{x} and is usually calculated only when all the mean values under consideration are positive $\bar{x} > 0$.

$$COV = \frac{s}{\bar{x}} \quad (3-19)$$

3.4.2.3 Sample skewness α and kurtosis

The skewness is the degree of the symmetry or non-symmetry of a random variable X . It is measured by the skewness coefficient α which is given by:

$$\alpha = \frac{n}{(n-1)(n-2)} \left[\frac{\sum (X - \bar{x})^3}{s^3} \right] \quad (3-20)$$

3.4.2.4 Presence of outliers

The skewness is very sensitive to extreme values of a sample and may easily be affected by gross errors (outliers). A large sample $n > 30$ is usually preferred for estimating the skewness.

All these features of a histogram will be used in this study to provide indications of the proper distributional model for the data. The goodness-of-fit test will then be used to verify the distributional model.

3.4.3 Goodness-of-fit-tests

When only incomplete statistical data are available, the location and scale parameter of each dataset will be specified, without providing a specific probability distribution. However for a parameter with a large dataset ≥ 30 a number of probability distribution functions exist, such as the Normal, Lognormal, Gamma or Gumbel distribution, which can be used to describe the parameter. A selection of the most appropriate distribution for each parameter is carried out using a goodness-of-fit (GOF) test.

In the GOF test, an assumption is first made on the distribution type by examining the shape of the histogram of the random variable, and then selecting a distribution type that closely bears this shape. Statistical tests are then used to decide whether or not the adequacy of a selected distribution should be rejected *a priori* with a confidence level (Van Gelder, 2008). Such tests include Chi-Square test and the Kolmogorov-Smirnov test (Ang and Tang, 2007). The Chi-Square test is described further in Appendix D.

3.4.4 Tail sensitivity

When assigning distribution functions, the data available are mainly of the central part of the distribution and there will not be many observations from the tails of the distributions to be fit.

The “tail” of a distribution refers to the extreme regions of the distribution i.e. both left and right (EDA, 2006). The tail length indicates how fast these extremes approach zero. For a short-tailed distribution, the tails approach zero very fast and vice versa. The shape of the tail assists in the selection process for an appropriate distribution. For example:

- For a short-tailed distribution, the tails approach rapidly the effect of which the distribution has a truncated (“sawn-off”) look. The uniform (rectangular) distribution would be appropriate for describing the distribution of the data.
- In the case where the tails decline to zero moderately, the corresponding distribution is the normal (Gaussian) distribution.
- For a long-tailed distribution where the tails decline to zero slowly, the corresponding long-tailed distribution is the Cauchy distribution.

- Where the right tail of the distribution is considerably longer relative to the other tail (right-skewed distribution) the data may be described using the weibull, gamma, Chi-square or lognormal distributions.

From a reliability standpoint, the selection of one or other distribution for the central part is not very significant and only the lower distribution tail is of interest: this is the domain where the smallest values are found. This is so because, the probability distribution assigned to any variable can have an important influence on the estimated probabilities of failure. This problem is called the tail sensitivity problem and can be overcome by accurately determining the probability distribution of random variables, especially at the significant tails.

3.5 MONTE-CARLO SIMULATION

The analysis of the LSF will be carried out using Monte Carlo Simulation (MCS) techniques, specifically the bootstrapping technique.

The concept of bootstrapping was first introduced by Efron (1979) and is a more specific case of the general class of MCS techniques (Dudewicz, 1992). Two types of bootstrapping are used in this study, i.e. the parametric bootstrap and the simple (non-parametric) bootstrap.

The parametric bootstrap uses a known distribution that provides the best fit to the observed data (Efron and Tibshirani, 1993). Random values are then sampled from each of the defined distributions to be used in the resampling process. The parametric bootstrap makes the underlying assumption that the shape of the population fits some known distribution, and the observed sample defines the parameters of the distribution.

The simple (non-parametric) bootstrap eliminates the need to assign a known distribution to the observed data (Chernick, 1999). Instead, the shape of the observed sample is assumed to represent the shape of the entire population. In this way, individual observed data points are randomly sampled from each input variable during the resampling process. Because the simple bootstrap eliminates the need to assign a known distribution to the observed data, it is particularly effective when the observed data does not match any known distribution or when the dataset is too small ($N < 30$).

For each of the input variables in the LSF $\{C_s, D_i, t, m, C_{crit}\}$ MCS analysis will be applied to solve the time to corrosion initiation $\{t_i\}$ and to estimate the probability of failure $\{P_f\}$. The

process will be repeated a sufficient number of trials (10, 000 times) to define a distribution of t_i and to reduce the inherent error involved in the MCS process. This means that the accuracy of the results increases as the number of simulation cycles increases (Ang and Tang, 2007)

For each trial, the variables in the LSF will be randomly sampled from the probability distribution function or from the sample itself, depending on the bootstrapping technique applied for each variable, and the LSF evaluated. Figure 3.11 shows a summary of the MCS procedure that will be followed in computing P_f .

The P_f is given by the ratio between the number of trials resulting in the negative performance of the LSF \hat{P}_f and the total number of trials N (Equation 3-21).

$$P_f = \frac{n}{N} \quad (3-21)$$

The accuracy of estimating P_f using MCS techniques will be calculated using the variance of the estimated P_f as shown:

$$\text{Var} \hat{P}_f = \frac{P_f \hat{P}_f}{N} \quad (3-22)$$

Furthermore, the statistical accuracy of the estimated P_f will be measured using the COV:

$$\text{COV} \hat{P}_f = \frac{\sqrt{\text{Var} \hat{P}_f}}{P_f} \quad (3-23)$$

Finally, the design parameters are adjusted to ensure that the estimated P_f does not exceed the acceptable target value $P_{\text{target,ILS}}$ for the ILS (Table 2.6).

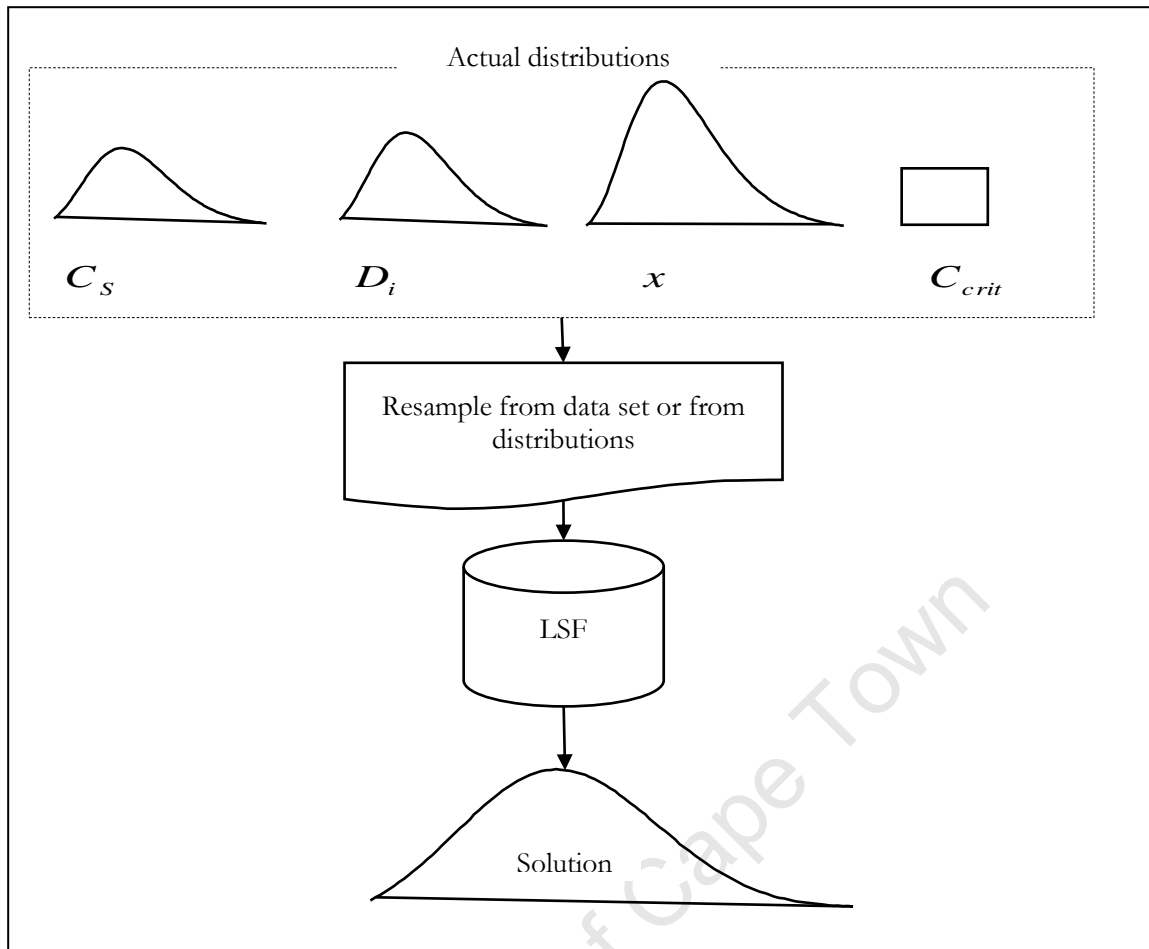


Figure 3.11: Flow chart of the MCS procedure service-life design

3.6 SENSITIVITY ANALYSIS

A sensitivity analysis will be carried out to identify parameters in the LSF which have the most influence on the probability of meeting a pre-specified target. This is particularly important if a target could not be satisfied with a required probability level. In such a case, a sensitivity analysis indicates where to spend effort and provides the decision maker with information regarding which parameters to control to achieve a given design life (Zhang *et al.*, 2006).

A number of methods have been developed for sensitivity analysis namely (Zhang *et al.*, 2006): (i) Nominal range sensitivity analysis (ii) Monte Carlo simulation (MCS) (iii) differences in log-odds ratio (iv) differential analysis (v) response surface methods (vi) Fourier amplitude sensitivity test (FAST) and (vii) Bayesian sensitivity analysis. These methods vary in level of complexity, data requirements, representation of the sensitivity and specific uses (Zhang *et al.*, 2006).

In this study, the MCS is used to investigate the sensitivity of the probability of corrosion initiation during the design service life to the basic variables in the LSF. This method provides relevant information on the impact of different parameters on the model output and a ranking of their relative importance. It requires data related to the governing parameters, namely their mean values, standard deviations and their probabilistic distributions.

In summary, the sensitivity analysis will assist in understanding the effect of each of the variables in the LSF and provide the insight necessary to make decisions regarding which variables to optimize in order to achieve improved concrete durability.

University of Cape Town

3.7 REFERENCES

- ACI Committee 201 (1994)**, Guide to Durable Concrete, Chapter 4-Corrosion of Steel and other Materials Embedded in Concrete, *Manual of Concrete Practice*, Part 1.
- Alexander, M. G. Ballim, Y Stanish, K. (2007)** A Framework for Use of Durability Indexes in Performance-based Design and Specifications for Reinforced Concrete Structures, *Materials and Structures Journal*, 41(5), pp. 921-936.
- Alexander, M.G., Ballim, Y., Mackechnie, J.R., Horton, J., (2001)** Durability Index Tests- Further notes on the aspects related to testing and variability, *Research monograph No. 4*, UCT/Wits, 1999.
- Alexander, M.G., Mackechnie, J.R. and Ballim, Y. (1999)** Guide to the use of durability indexes for achieving durability in concrete structures. *Research Monograph No 2*, Department of Civil Engineering, University of Cape Town, 35 pp.
- Alonso, C. Andrade, M. Castellote and Castro, P., (2000)** Chloride Threshold Values To Depassivate Reinforcing Bars Embedded In A Standardized Ordinary Portland Cement Mortar, *Cement And Concrete Research*, 30(7), pp. 1047-1055.
- Ang, A.H.S., Tang, W., H., (2007)**, *Probability Concepts in Engineering-Emphasis on Applications to Civil and Environmental Engineering*, John Wiley & Sons, 2nd Edition, pp. 406
- Ann, K. Y., Song, H. W., (2007)** Chloride Threshold level for Corrosion Initiation of Steel in Concrete, *Corrosion Science*, doi:10.1016/j.corsci.2007.05.007, pp.1-21
- Arya, C., Buenfield, N.R., Newman, J.B., (1989)** Factors influencing chloride binding in concrete, *Cement and concrete research*, 2(1989), pp. 291-300.
- Bentz, E., (2003)**, Probabilistic modelling of Service Life for Structures Subjected to Chlorides, *American Concrete Institute Materials Journal*, Sept-Oct 2003, pp. 390-397.
- Berke, N.S., (1986)**, Corrosion Rates of Steel in Concrete, *ASTM Standardization News*, 14(3), pp. 57-61.
- Browne, R., (1982)**, Design Prediction of the Life for Reinforced Concrete in a Marine and other Chloride Environment, *Durability of Building Materials*, 1(2), pp. 113-125.

- BS 1881: Part 204 (1988)**, Testing Concrete-Recommendations on the use of Electromagnetic Cover meters.
- Chernick, M.R., (1999)**, *Bootstrap methods, a practioners guide*, Wiley, New York
- Collins, F.G. Grace, W.R. (1997)** Specification and testing for corrosion durability of marine concrete, The Australian perspective, in: V.M. Malhotra (Ed.), *Proceedings of the 4th CANMET/American Concrete Institute International Conference on Durability of Concrete*, Sydney, Australia, August 1997, SP 170-39, American Concrete Institute, 1997, pp. 757–776.
- Committee of Land Transport Officials (COLTO), (1998)**, Standard Specifications for Road and Bridge Works for State Road Authorities. Halfway House: South African Institution of Civil Engineering, pp. 6300-6302.
- Concrete Society (1996)**, Developments in Durability Design & Performance-based Specification of Concrete, *Discussion document*, pp. 69.
- Dudewicz, E.J., (1992)**, the generalised bootstrap, in *Bootstrapping and related Techniques*, (Eds.) K-H Joche, G., Rothe, & Sendler, Springer-Verlag, Berlin.
- Duprat, F., (2007)**, Reliability of RC beams under chloride ingress, *Construction and Building Materials*, pp. 1605-1616
- Duracrete, (2000)**, *Statistical Quantification of the Variables in the Limit State Functions*, The European Union - Brite EuRam III, Project BE95-1347/R9, Probabilistic Performance-Based Durability Design of Concrete Structures.
- Edvardsen C. and Mohr L., (1999)** *DURACRETE –Structures a guideline for Durability-based Design of Concrete*, Prepared by COWI Consulting Engineers and Planners AS, Denmark.
- Efron, B., & Tibshirani, R.J., (1993)**, *An introduction to the bootstrap*, Chapman & Hall, New York
- Efron, B., (1979)**, Bootstrap methods: another look at the jackknife, *The annals of statistics*, 7(1979), pp. 1-26
- EN 206 (2000)**, Concrete - Part 1: Specification, performance, production and conformity. British Standards Institution: 70 pp.

Exploratory Data Analysis (EDA) (2006), *Engineering Statistics Handbook*, Internet edition: <http://www.itl.nist.gov/div898/handbook/eda/eda.htm> [Downloaded 11/091/2008 9:56:13 AM]

FIB Model Code for Service Life Design (2006) *fib Bulletin 34*, EPFL Lausanne, 116 pp.

Holický M., (2007) Probabilistic design of structures for durability, *Proceedings of the SEMC Seminar*.

Holický M., (2007b) Introduction to Reliability and Risk Analysis, *Lecture Notes in Reliability based design course held at University of Stellenbosch, 2007*.

ISO 13823 (2008) *General Principles on the Design of Structures for Durability*, ISO TC98/SC2, Final Draft.

ISO 2394 (1998) *General Principles on Reliability for Structures for Durability*, pp. 73

Khatri, R.P., Sirivivatnanon, V., (2004) Characteristic Service Life for Concrete Exposed To Marine Environments, *Cement and Concrete Research*, 34 (2004), pp. 745–752.

Maage, M., Helland, S and Carlsen, J.E., (2000) Prediction of Long Term Chloride Concentration in Concrete, *Materials and Structures*, 27, pp. 338-346.

Mackechnie, J. R., Alexander, M. G., (1997) Durability Findings from Case Studies of Marine Concrete Structures, *Cement, Concrete and Aggregates*, 19(1), pp. 22-25

Mackechnie, J.R., (1996) *Prediction of Reinforced Concrete Durability in the Marine Environment*, University of Cape Town, PhD Thesis.

Mackechnie, J.R., Alexander, M., G., (2002), A Pragmatic Model for Chloride ingress into Concrete, *Rilem Conference Proceedings Madrid*.

Marteinsson, B., (2005), *Service Life Estimation in the Design of Buildings a Development of the Factor Method*, Doctoral Thesis, Department of Technology and Built Environment, University of Gävle, Sweden.

McGee R., (2000), Modelling of durability performance of Tasmanian bridges. In: Melchers RE, Stewart MG, editors. *Applications of statistics and probability in civil engineering*, Rotterdam: Balkema; 2000. p. 297–306.

- Quinn, G.P. and Keough, M.J., (2002)**, *Experimental Design and Data Analysis for Biologists*, Cambridge University Press, pp. 537.
- Richardson, M. G., (2002)**, *Fundamentals of Durable Concrete*, First Edition, Spoon Press- Taylor and Francis group, pp. 38-50.
- Ronne, P.D., (2005)**, Variation in Cover to Reinforcement: Local and International Trends, *Concrete Beton*, 111.
- Rostam, S., (2005)**, Service Life Design of Concrete Structures-A Challenge to Designers as well as to Owners, *Asian Journal of Civil Engineering (Building and Housing)*, 6(5), pp. 423-445.
- Sandberg, P., (1995)**, *Critical Evaluation of Factors Affecting Chloride Initiated Reinforcement Corrosion in Concrete*, Licentiate Thesis, University of Lund, Sweden.
- SANS 10100-2 (2004)** Structural use of concrete Part 2 -materials and execution work.
- Sarja, A., (2002)**, *Integrated life cycle design of structures*, 1st Edition, London Spon Press
- Sarja, A., Vesikari, E., (1996)**, *Durability design of concrete structures*, 1st Edition, London Spon Press
- Sharp, B., (1997)**, Criteria for Cover –A Blackhole, *Concrete for the Construction Industry*, 31(6), pp. 34-38.
- Shiessl, P., Raupach, M., (1990)** Influence of Concrete Composition and Micro-climate on the Critical Chloride Content in Concrete, Page C.L., Treadway, K.W.J., Bamforth P.B., (Eds.), *Corrosion of Reinforcement in Concrete*, Elsevier Applied Science, London UK, pp. 49-58.
- Siemes A.J.M., and Edvardsen, C., (1999)**, Duracrete service life, design for concrete structures –A basis for durability of other building materials and components, *Proceedings 8th conference on Durability of Building Materials and Components (8DBMC)*, Vancouver, pp. 1343-1356.
- Song and Saraswathy, (2007)**, Corrosion Monitoring of Reinforced Concrete Structures- A Review, *International Journal of Electrochemical Science*, 2(2007), pp.1-28.
- Song, H.W., Lee, C.H., Ann, K.Y., (2008)** Factors Influencing Chloride Transport in Concrete Structures Exposed to Marine Environments, *Cement and Concrete Composites*, 30(2008), pp. 113-121.

- Streicher, P. E. (1997)**, *The Development of a Rapid Chloride Test for Concrete and its use in Engineering Practice*, PhD Thesis, University of Cape Town.
- Swamy, I.L. N., Hamada, H. and Laiw, J. C., (1994)**, A Critical Evaluation of Chloride Penetration into Concrete in Marine Environment, Corrosion and Corrosion Protection of Steel in Concrete, *Proceedings of an International Conference*, University of Sheffield, England, pp. 404-419.
- Tikalsky, P.J. Pustka, D. and Marek, P. (2005)**, Statistical Variations in Chloride Diffusion in Concrete Bridges, *American Concrete Institute Structural Journal*, May-June 2005, pp. 481-487.
- Van Gelder, J.M., (2008)** The Importance of Statistical Uncertainties in Selecting Appropriate Methods for Estimation of Extremes, *International Journal River Basin Management*, 6(1), pp. 1-9.
- Weyers, R.E. and Liu, Y. (1998)**, Modelling the Time-to-Corrosion Cracking in Chloride Contaminated Reinforced Concrete Structures, *American Concrete Institute-Materials-Journal*, 95(6), pp 675-681.
- Weyers, R.E., Fitch, M.G, Larsen, E.P., Al-Qadi, I., Chamberlin W.P. and Hoffman, P.C., (1994)** *Concrete Bridge Protection and Rehabilitation: Chemical and Physical Techniques. Service Life Estimates*, Strategic Highway Research Program, National Research Council, Washington, DC, SHRP-S-668.
- Zhang, J., Lounis, Z., (2006)**, Sensitivity Analysis of Simplified Diffusion-Based Corrosion Initiation Model of Concrete Structures Exposed to Chlorides, *Cement and Concrete Research*, 36(2006), pp. 1312-1323.

CHAPTER 4: STATISTICAL QUANTIFICATION and RELIABILITY ANALYSIS

4.1 INTRODUCTION

This chapter deals with the statistical quantification of the variability in the limit state function (LSF) parameters by specifying their statistical distributions and associated parameters such as mean and standard deviation. The statistical quantification of the environment influence and geometric parameters is carried out using data obtained from laboratory and/or in-situ testing as summarised in Table 4-1. The material parameters are determined from the chloride conductivity test (CCT) which is one of South Africa's durability index tests. The CCT is used as an engineering measure of the potential resistance of concrete cover to chloride diffusion.

Table 4.1: Basic random variables in the initiation limit-state function

Parameters		Tests	Section
Environmental load parameter	Surface chloride concentration C_s	Chloride profiling	4.2
Material parameters	Critical chloride content C_{crit}	Laboratory testing	4.3
	Diffusion coefficient D_i	Chloride conductivity test	4.4
Structural parameter	Concrete cover depth c	In-situ test	4.5

The stochastic quantities (shape and scale parameter for the respective statistical distributions –see Section 3.4.2) for each random variable, are then substituted into the LSF and a numerical method, namely the Monte Carlo Simulation technique (MCS), is applied to compute the probability of durability failure. The results of the simulation are used to give the design specifications, i.e. concrete quality (given by the chloride conductivity value) and the cover depth, that will ensure the RC structure meets its performance requirements with a required/target probability level.

Finally, an analysis of the sensitivity of the LSF parameters to failure probability using MCS technique is carried out. The sensitivity analysis assigns sensitivity factors to each model parameter. These sensitivity factors are useful as they give the designer insight to the LSF

parameters which are more influential in the design. The designer can then use this information to define future research and development needs.

4.2 SURFACE CHLORIDE CONCENTRATION

4.2.1 Collection of data

Published data for surface chloride concentration (C_s) was used in the study. The data were obtained from two sources, the first of which was from previous in-depth inspections of marine structures, which were built between 1920 and 1977 along the South African coastline. The second source of C_s data was obtained from concrete samples placed in two sites in the Cape Peninsula namely: a site in Simonstown, which is sheltered from wave action and prevailing winds, and a site at Granger Bay which is exposed to heavy wave action. Simonstown is located within a shallow bay that traps warmer water resulting in sea temperatures between 13 and 20°C, while Granger Bay is exposed to the open sea with colder water of between 12 and 15°C (Mackechnie and Alexander, 1997). Table 4.2 gives details of the marine structures and field samples investigated for C_s whereas Figure 4.1 gives the geographical locations of the exposure sites.

Table 4.2: Concrete Structures investigated for surface chloride concentration (Mackechnie, 1996)

Name	Abb.	Age at survey (years)	Strength grade (MPa)	Binder Type	Concrete condition #	Exposure Environment
Camps Bay Pump Station	CBPS	18	45	OPC	Good	Severe-spray
East London Breakwater	ELBW	28	25	OPC+Slag	Poor	Extreme-tidal
East London Breakwater 2	ELBW2	28	25	OPC	Poor	Extreme-tidal
Hout Bay Marina	HBM	6	40	OPC	Poor	Extreme-tidal
Koeberg Power Station	KPS	12	30	OPC	Repaired	Severe-spray
Kogel Bay Tidal Pool	KBTP	3	55	OPC	Good	Extreme-tidal
Muizenberg Bridges	MZB	38	30	OPC	Repaired	Very severe-spray
Oudekraal Retaining Wall	ORW	19	35	OPC	Poor	Very severe-tidal
Sea Point Aquarium	SPA	55	25	OPC	Demolished	Very severe-splash
Sea Point Toilet Block	SPTB	48	25	OPC	Poor	Very severe-splash
Simonstown Jetty	STJ	75	25	OPC	Repaired	Very severe-tidal
Steenbras River Bridge	SRB	67	25	OPC	Poor	Very severe-splash
Strandfontein Tidal Pool	SFTP	13	35	OPC	Fair	Extreme-tidal
Table Bay Breakwater	TBBW	6	50	LASRC	Fair	Extreme-tidal
Walvis Bay Syncrolift	WBS	25	30	OPC	Poor	Very severe-tidal
Wilderness Bridges	WB	46	30	OPC	Fair	Very severe-spray

Abb. = Abbreviation

Concrete condition# = Based on visual assessment of the structure for cracks and spalling

OPC= Ordinary Portland cement; LASRC =Low Alkali Sulphate Resistance Concrete, Slag =Ground granulated blast furnace slag

Details of the concrete composition used for each of the structures are given in Appendix A. However, relevant information such as the cement content, water-cement ratio and curing was not well documented for most of the structures.

The experimental procedure followed in determining the surface chloride content in the structural elements of each of the structures is given in Mackechnie (1996): Concrete powder was extracted from structures using a plastic tube and sample packet held around the 20 mm drill bit of a rotary hammer drill. The outer 5 mm of each drilling was discarded due to local and seasonal fluctuations of surface chloride concentration. The concrete powder was extracted at 25 mm depth increments to a depth of 100 mm with powder from three 20 mm holes combined to form a sample. Thereafter, the powder was analyzed in accordance with BS 1881 Part 124 but using a potentiometric titration, and the acid-soluble chloride concentration of chlorides, expressed in terms of the cement content, determined.

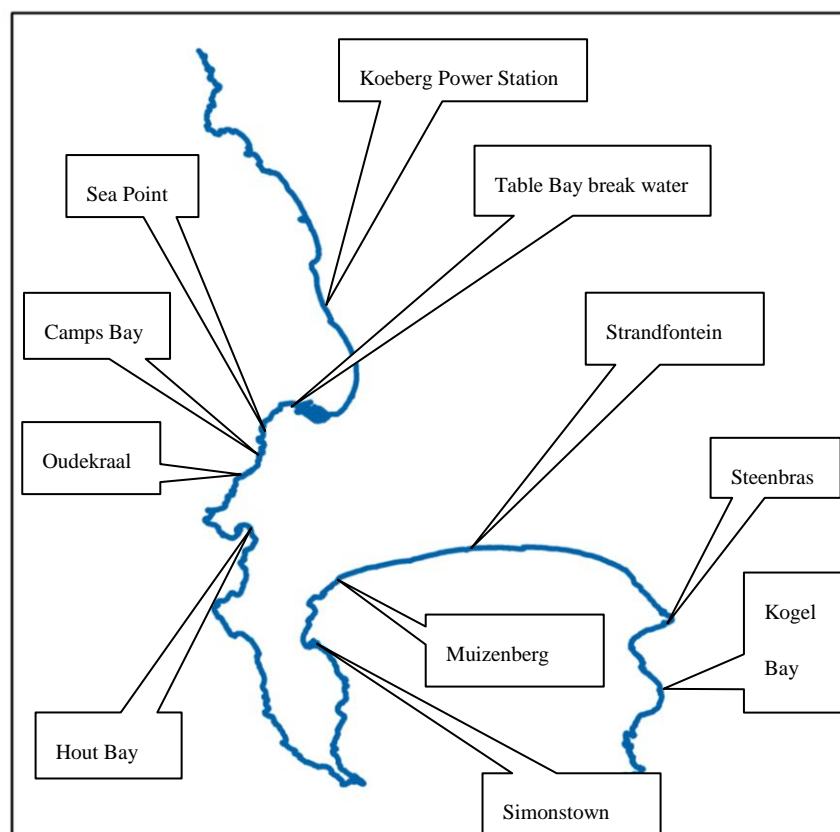


Figure 4.1: Detail of the geographical locations of the marine structures investigated and sample exposure sites along the Cape Peninsula and environs

4.2.2 Classification of data

From past research (Bamforth and Price, 1993) it has been noted that the level of chloride build up on the surface of concrete exposed to a marine environment is largely dependent on the location of the structure and the degree of exposure to salt. The classification of data available in the database was therefore made in the following four steps:

- a) Type of binder
- Portland cement (OPC)
 - Portland cement with Blast furnace slag (OPC + GGBS)
 - Portland cement with Fly ash (OPC + FA)
 - Portland cement with Silica fume (OPC + SF)

Due to shortage of data in the various binder classes, only C_s data for OPC concrete structures were used in the statistical quantification.

- b) Exposure environment (Macro level description)

The C_s data for statistical quantification were available for the marine environments represented by the shaded regions in Table 4.3. The marine exposure categories are based on SABS 0100 (1992).

Table 4.3: Marine exposure categories for South African conditions (*Adopted from: SABS 1992, as cited in Mackechnie, 1996*)

	Marine tidal and splash zones	Marine spray zones
Extreme	Exposed to sea water, heavy wave action	Not applicable
Very Severe	Exposed to sea water, sheltered location	Within 500m of shore in an exposed location
Severe	Not applicable	Near shore (>500m) in an exposed location
Moderate	Not applicable	Anywhere else within 30 km of the coast

However, the above classification has since been revised and the EN 206-1 (2000) environmental classification modified for South African marine conditions adopted. Hence, the task involved in this section was to re-classify the data to match the current environmental classification system. This process would also assist in future recommended studies of updating the C_s database. Table 4.4 gives the environmental classification based on SABS - 0100 (1992) and the corresponding marine classification zones based on EN 206-1 (2000) (modified for South African marine conditions).

Table 4.4: Marine Environmental Classes EN206-1 Vs SABS-2 (1992)

SANS 10100-2 (2005)	Description	Corresponding environmental class in EN 206
Moderate , very severe spray and severe spray zones	Exposed to airborne salt but not in direct contact with seawater	XS1
Very severe tidal and splash zones	Tidal, splash and spray zones Buried elements in desert areas exposed to salt spray	XS3a [#]
Extreme – tidal, splash and spray zones	XS3a [#] + exposed to abrasion	XS3b [#]

[#] These sub clauses have been added for South African coastal conditions

c) Local conditions (Meso level description)

The orientation and configuration of the structure, in any given marine environmental zone, with respect to the source of the chlorides is an important parameter to consider when classifying C_s data. This information describes the structure at a ‘meso level’ and is used to show the ‘systematic spatial variation’ of the C_s data (i.e. fluctuation pattern of the data in space) (Li, 2004) and should be indicated during the collection of concrete specimens from the structure. For example, the chloride content of a concrete sea wall at the side of the wall facing the sea is normally higher than the rear side of the wall. For this case, the wall is divided into sections with different properties and data from each section (with zero systematic spatial variation) recorded separately.

The surface concentrations also fluctuate due to local and seasonal variations (Mackechnie, 2006) hence, an indication should be made of the season in which the concrete specimens were collected.

Classifying data w.r.t spatial variation is important during the application of the data in a service life model since if there is zero spatial variability within the elements, then the probability of corrosion initiation calculated would relate to that section and not to the entire structure. This also means that when corrosion initiation occurs it does so for the entire section having a zero systematic spatial variation and not for a percentage of the section. This would be useful when planning for expected repair costs or maintenance of the structure.

Therefore, it is important to find the right spatial variation so as to improve on the precision of the service life model.

The aspect of spatial variability was not considered in the collection of data available for this study but, it is recommended that in future data collection processes this aspect be considered due to the aforementioned merits.

d) Quality of data

The fourth and final step in the classification process involved checking the quality of data. DuraCrete (2000b) recommends the removal of data from the database of any data which differs significantly from the expected values through two different ways; either by examining if the mean value of the chosen distribution is too small or large, or if the standard deviation of the chosen distribution is too large. For this study, a quality check was carried out using box-plots which are useful tools in detecting and illustrating location and variation changes between different groups of data (Chambers, 1983). The box-plot shows the median (center of the sample data), the 25% and 75% quartiles, and the “outliers”. The “outliers” are defined in literature as data points that are greater than 1.5 times the inter-quartile range (IQR) above the 75% quartile mark or below the 25% quartile mark as shown in Figure 4.2 (Quinn and Keough, 2002). The unbiased estimator of the population mean used when plotting the box-plot is the median rather than the sample mean as it is more resistant to outliers, thus the shape of the box-plot will not be significantly affected by the outliers (Quinn and Keough, 2002).

The box-plot indicates several aspects of the sample (Quinn and Keough, 2002):

- The variability of the data indicated through a line that extends to the most extreme value up to 1.5 times the IQR. This line is also referred to as the ‘whisker’.
- The shape of the sample i.e. whether it is symmetrical or skewed (see Section 3.4.2.3 of Chapter 3). If the median is positioned toward the lower end of the data, then the data are positively skewed.
- The presence of outliers, which are extreme values and very different from the rest of the sample.

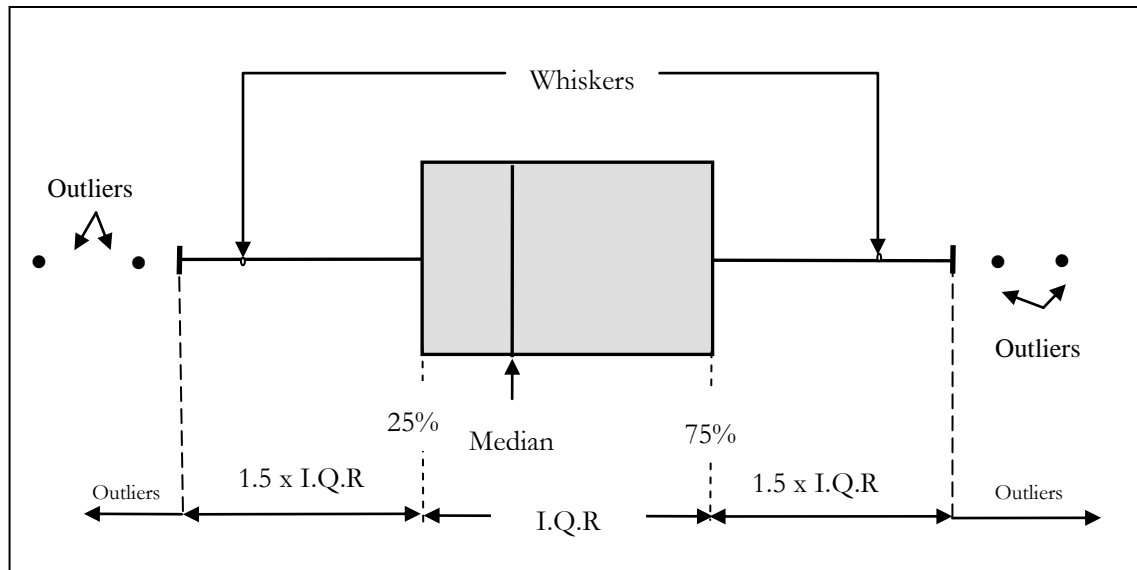
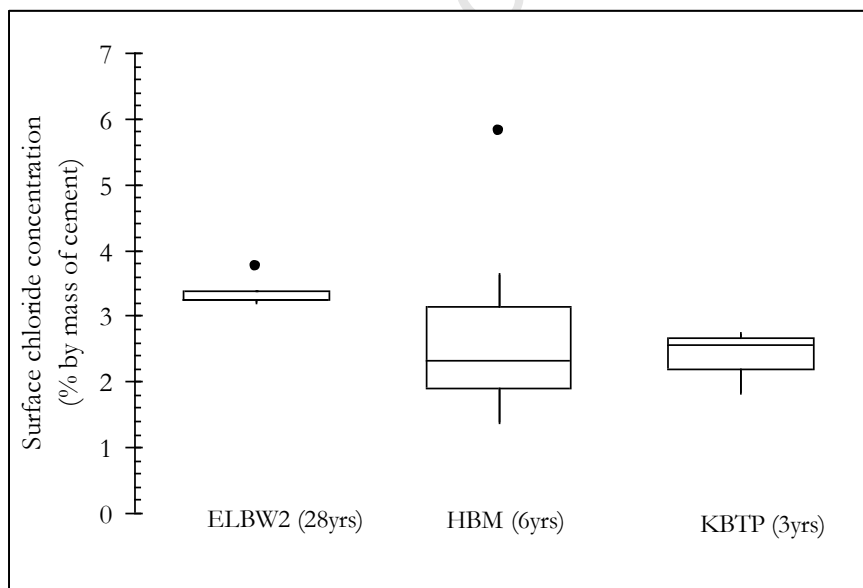


Figure 4.2: Illustration of box and whisker plot

The variability of C_s data for all the structures in the different environmental classifications, are represented by the comparative box-plots in Figures 4.3 to 4.5.

Figure 4.3: Comparative box-plots of C_s data for PC concrete structures in XS3b[#] marine zone

From Figure 4.3, it is observed that the C_s values for the oldest structure (ELBW2) are higher than for the other structures, this may be an indicator that it takes many years for C_s to stabilise. In addition, the C_s data from ELBW2 is the least variable with about 50% of the values falling within 1 C_s unit.

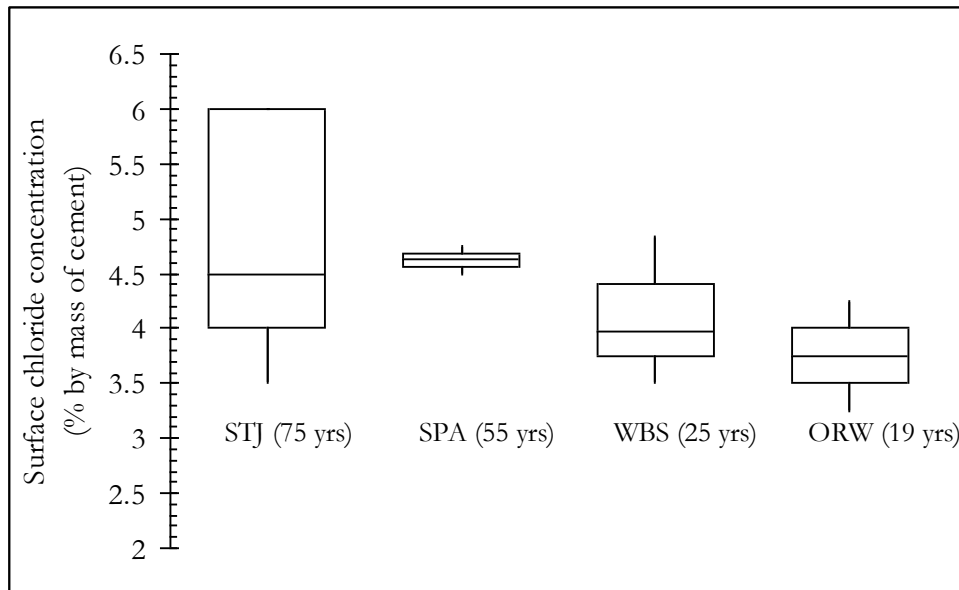


Figure 4.4: Comparative box-plots of C_s data for PC concrete structures in XS3a[#] marine zone

The SRB and SPTB although initially classified as structures in the very severe splash and tidal (XS3a[#]) environment, have been excluded from this class due to their low values and will be classified in the very severe spray environment (XS1) for the analysis. This is because the observed environmental conditions surrounding the structures are prevalent of a very severe spray environment (XS1) (Alexander, 2008).

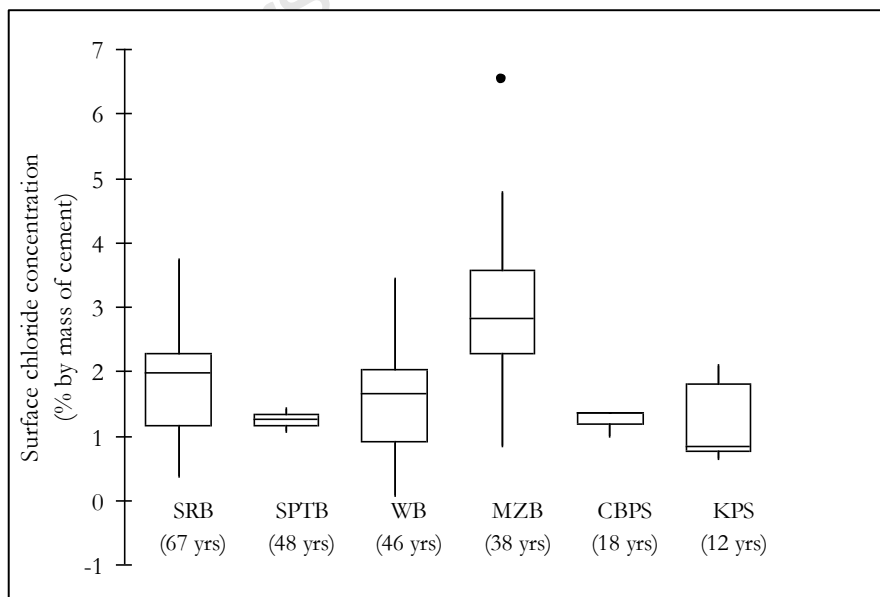


Figure 4.5: Comparative box-plots of C_s data for PC concrete structures in XS1 marine zone

From the comparative box-plots, Figures 4.3 to 4.5, it is observed that though the C_s data were derived from similar environments and from structures of the same material (OPC concrete type), a wide range of variability in the data of most of the structures still exist.

Although these data exhibit large variability, they will be used in the quantification process owing to lack of other sources of C_s data, and only the outliers are discarded in the analysis. However, it is the recommendation of this study that upon acquiring better (less variable) data the quantification can be reviewed by following the same procedure laid out. It is worth noting that the aim of this study is not to give the exact statistical quantities taken by durability parameters, but to provide a framework that will be used in later studies on the statistical quantification of durability parameters.

In this study an assumption of constant chloride level at the surface of the RC element over time is made during the statistical quantification of C_s and in solving the LSF.

4.2.3 Statistical quantification of C_s data

The surface chloride concentration data for the different classes (given in Appendix A) were analysed. The histogram of C_s for ordinary Portland cement exposed to very severe spray marine environment (XS1) (sample size $n = 59 - 1 \text{ outlier} = 58$), is shown in Figure 4.6. The number of bins/classes B for the histogram was determined using the rule of thumb:

$$B = \sqrt{n} \quad (4-1)$$

or an integer close to this, but should be at least 5 and not more than 25 (Kottegoda *et al.*, 1997).

For this case:

$$B = \sqrt{58} = 7.62 \approx 7 \text{ bins} \quad (4-2)$$

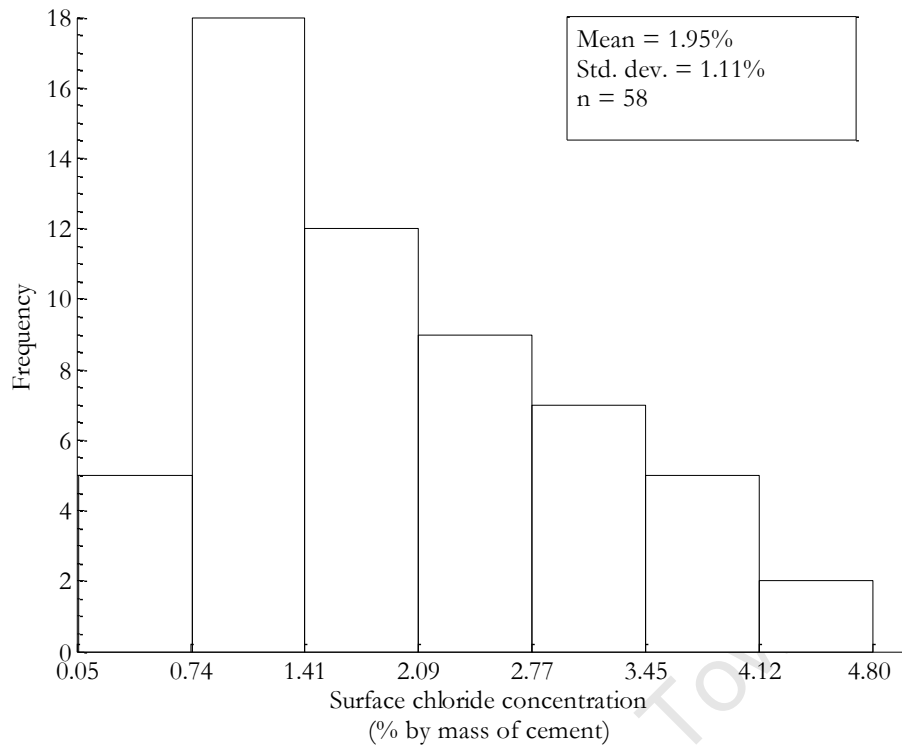


Figure 4.6: Histogram of surface chloride concentration of OPC concrete in XS1 marine environment

From the dataset, the first two moments were estimated to be, $\bar{x} = 1.95\%$ and $s = 1.11\%$ chlorides by mass of cement.

From Figure 4.6 it is observed that the data was positively skewed i.e. the right tail of the distribution is considerably longer relative to the left tail.

To fit the C_s data into a distribution the probability distribution functions of two theoretical distribution models: the lognormal and the gamma distributions (which have their right tails considerably longer relative to the other tail and lower bounds at zero) are selected and superimposed on the histogram using Matlab application program (dfittool command) (Figure 4.6).

Selecting a distribution with lower bounds at zero is practical as it eliminates the occurrence of non-negative values in data.

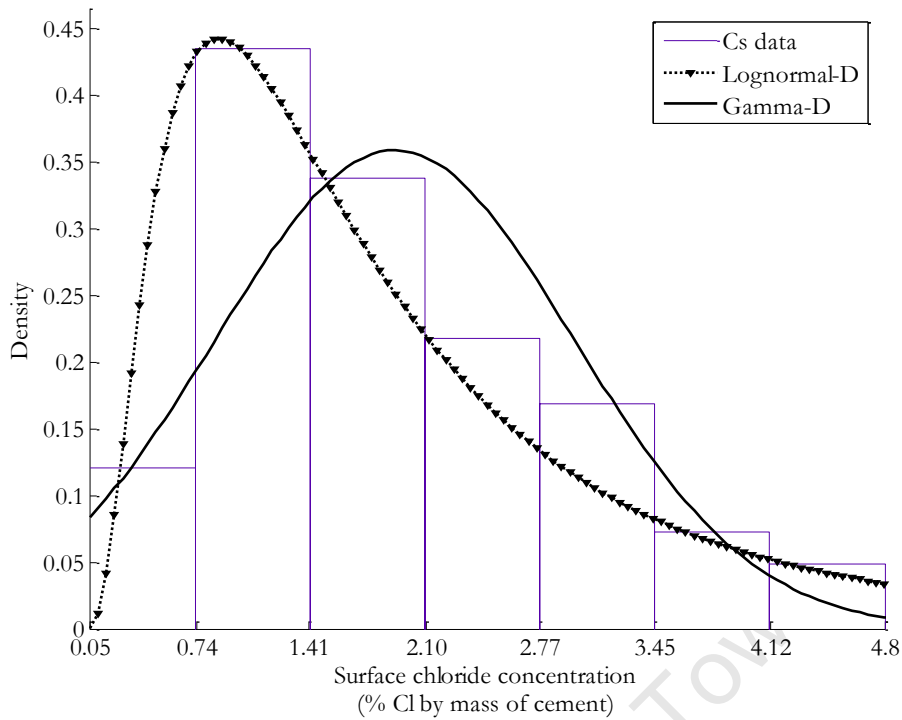


Figure 4.6: Histogram and distribution fit of surface chloride concentration of OPC concrete in very severe spray marine environment

Figure 4.6 shows that the gamma distribution closely fits most of the classes of the C_s distribution as compared to the lognormal distribution. To ascertain the best distribution for the data a goodness-of-fit test (Appendix D) was carried out using an Excel spreadsheet developed for this study (goodness_of_fit.xls); the results of which are tabulated in Table 4.5.

Table 4.5: Chi-squared tests of two distributions for OPC concrete in XS1 marine environment

Interval C_s (% #)	Observed Frequency n_i	Theoretical Frequencies e_i		$\sum_{i=1}^k \frac{(n_i - e_i)^2}{e_i}$	
		Lognormal	Gamma	Lognormal	Gamma
0 - 0.05	0	0.00	0.00	0.00	0.003
0.05 - 0.74	5	3.37	5.93	0.79	0.145
0.74 - 1.41	18	17.88	15.34	0.00	0.460
1.41 - 2.10	12	16.70	14.87	1.32	0.556
2.10 - 2.77	9	9.79	10.22	0.06	0.145
2.77 - 3.45	7	5.04	5.88	0.77	0.212
3.45 - 4.12	5	2.52	3.06	2.43	1.235
4.12 - 4.80	2	1.27	1.48	0.41	0.181
4.80 - 10.0	0	1.41	1.21	1.41	1.212
Σ	58	58	58	7.20	4.15

(% #) = % of chlorides by mass of cement

From Table 4.5 the gamma distribution would be chosen as it gives the lowest $\sum_{i=1}^k \frac{e_i - e_i^2}{e_i}$ value of the two distributions. To ensure that the correct distribution is not rejected, a hypothesis test is carried out on the chi-squared results (see Appendix D for details of a hypothesis test). At the significance level of $\alpha = 0.5\%$ and degree-of-freedom ($d.o.f = 7 - 3 = 4$), a critical value of $C_{0.95,4} = 7.78$, for both the distributions, is obtained from Table D.1 (Appendix D). The Chi-squared values of both distributions are less than the critical and hence they can be accepted for describing the distribution of C_s with a confidence level of at least 95%.

This study adopts the gamma distribution for use in modelling the surface chloride concentration in OPC concrete in XS1 environmental zone, due to its smaller $\sum_{i=1}^k \frac{e_i - e_i^2}{e_i}$ value (see Table 4.5). The shape, α and scale, β parameters used to describe the gamma distribution are defined in Appendix D.

A similar analysis was carried out on the other data from structures in the XS3a and XS3b marine zone and the results obtained are shown in Table 4.6. The calculations are appended in Appendix B.

Table 4.6: Summary of statistics for surface chloride concentration parameter

Environment	Binder Type	Sample size	Mean (% #)	Std. dev. # (% #)	Distribution type	α #	β #
XS1	OPC	58	1.95	1.11	Gamma	3.09	0.63
Very severe splash and tidal (XS3a)	OPC	16	4.5	0.91	Gamma	24.45	0.18
Extreme tidal and splash (XS3b)	OPC	17	2.61	0.74	Gamma	12.44	0.21

(% #) = % of chlorides by mass of cement

Std. dev. # = Standard deviation

α # = Shape parameter

β # = Scale parameter

4.2.4 How C_s distribution compares to others in literature

Ideally, a comparison of statistical quantification of C_s should be made with results from other researchers who have used the same type of concrete, analysis method (representing C_s in terms of % by mass of cement) and similar classification of exposure conditions. A review

of reported distributions for C_s based on studies carried out internationally on marine structures was carried out.

Typical locations of the structures investigated are given in Table 4.7.

Table 4.7: Concrete Structures investigated for surface chloride concentration

Name	Location (Country)	Age at survey (years)
This study	South African coastline	3-75
Collins <i>et al.</i> (1997)	Tasmanian coast (Australia)	-
Duracrete (2000)	Europe structures	-

The study carried out by Collins and Grace (1997) to investigate the distribution of surface chloride content using data of structures on offshore and onshore RC structures along the Victorian and Tasmanian coast of Australia.

The investigations were based on a similar assumption made in this study: that surface chloride levels increase with time only during the first few years of exposure, after which the surface chloride content stabilize and remains almost constant over the rest of the service life of a structure.

Collins and Grace (1997) found that C_s parameter is well described by a lognormal distribution. The mean and COV of the surface chloride content for the various marine zones investigated are reported in Table 4.8.

Table 4.8: Statistical quantities of surface chloride concentration from literature for OPC

Reference	Unit	Marine environmental zone	Distribution type	Mean value	Standard deviation	Shape parameter (α)	Scale parameter (β)
This study	# % m/m	XS3b	Gamma-D	1.95	1.11	3.09	0.63
		XS3a	Gamma-D	4.5	0.91	24.45	0.18
		XS1	Gamma-D	2.61	0.74	12.44	0.21
Collins <i>et al.</i> (1997)	kg/m ³	Splash	LN	7.35	5.15	-	-
		Atmospheric (Severe spray)	LN	2.95	2.07	-	-
		Atmospheric (Moderate spray)	LN	1.15	0.58	-	-

% m/m = % chlorides by mass of cement

A similar study was carried out by Duracrete (2006) on structures located in Europe. However, the C_s was modelled as a linear function of water/binder ratio (w/b) and an error term:

$$C_s = A_{C_s} \cdot (w/b) + \varepsilon_{C_s} \quad (4-2)$$

Table 4.9 shows the distributions of two regression parameters (A_{C_s} and ε_{C_s}) for OPC in marine environments found in the study.

Table 4.9: Statistical quantities for surface chloride concentration regression parameters (Duracrete, 2000) (Values given in % by weight of binder)

Environment	Distribution	$\mu_{A_{C_s}}$	$\sigma_{A_{C_s}}$	$\mu_{\varepsilon_{C_s}}$	$\sigma_{\varepsilon_{C_s}}$
Submerged	Normal	10.35	0.71	0	0.58
Tidal and Splash	Normal	7.76	1.36	0	1.11
Atmospheric	Normal	2.57	0.36	0	0.41

From this review it is observed that there is a wide variability between the mean values of C_s reported for similar marine zones in different locations. This highlights the difficulty of choosing one particular distribution to model the C_s parameter for concrete structures in different locations.

Both this study and that undertaken by Collins *et al.* (1997) are comparable in that similar assumptions are made in quantifying C_s and also in both studies, right skewed distributions are selected to represent the distribution of C_s . This is done to eliminate the occurrence of negative values for low C_s concentrations.

4.2.5 Summary of C_s results

During the quantification, statistical uncertainties arose due to the limited number of observations. It is the recommendation of this study that further chloride profiling tests be carried out on marine structures to build up the database and hence provide more representative results.

The process of obtaining additional data from a structure should first take into account the spatial variability of certain elements in the structure. It is proposed that concrete structures be represented by means of concrete surfaces belonging on different categories. The surfaces are categorised depending on their orientation to the source of the chlorides. The individual

concrete surfaces are divided into zones with similar initial condition indicators and bear the same risk to corrosion. Samples should then be taken repeatedly from the respective zones in the structure being monitored. The advantage of using this approach in sampling of mature concretes is that it is possible to establish a more realistic assessment of the chloride ingress with time i.e. information about the short-term to long-term trends becomes available. In addition, it is possible to check the accuracy of the data. The accuracy will be limited by local variations in the presumed uniform area, the exposure variations over the years and the accuracy of the Fickian model used in the curve fitting process (Goltermann, 2003)

4.3 CRITICAL CHLORIDE CONTENT

For a probabilistic evaluation, various values of the critical chloride concentration C_{crit} necessary to cause steel depassivation have been suggested in literature as shown in Table 3.4 (Chapter 3). However, some of the C_{crit} values shown do not indicate whether the threshold concentration is represented as total or free chloride content. Table 4.10 gives a report of stochastic parameters used to describe C_{crit} from literature.

Table 4.10: Statistical quantities of critical chloride content for OPC binder (% by mass of cement)

Reference	Distribution	Mean	Standard deviation	Shape parameter (α)	Scale parameter (β)
<i>Fib</i> Model Code (2006)	Beta	0.60	0.15	2.00	0.20
Duracrete (2000b)	Normal	0.48	0.15	-	-
Vassie (1984)	Truncated Normal	0.95	0.375	0.1	-

The values reported in Table 4.10 apply to Portland cement concrete. There is lack of reliable statistically quantified values for the critical chloride content in literature for Blast furnace slag, Silica fume or Fly ash cement concrete. Further, only Duracrete (2000b) states the effect of the corresponding chloride critical level in a structure: i.e. the chloride content of 0.48 ± 0.15 % chlorides by mass of binder will cause the depassivation of the steel and will not necessarily lead to visible corrosion damage on the concrete surface. This information is important when establishing the target reliability index for the initiation limit state (see Section 2.4.2-4)

Consequently, this study adopts the statistical values given by Duracrete (2000b) which assumes C_{crit} to have a normal distribution with mean value of 0.48% and standard deviation of 0.15. These values will be applied for all binder types. However, the study recommends further studies to be carried out to determine appropriate values of C_{crit} for various binder types in South Africa.

4.4 CHLORIDE CONDUCTIVITY & DIFFUSION COEFFICIENT

4.4.1 Collection and Classification of Chloride Diffusion Data

4.4.1.1 Collection of Chloride Diffusion Data

The chloride conductivity test (CCT) as aforementioned in Section 3.2.3 (of Chapter 3) is useful in obtaining data characterizing the concrete quality and is required to support the use of the chloride-induced SLP model. The CCT measures the physical resistance of the concrete to chloride conduction at early ages (28 days) under the action of an applied voltage across the concrete specimen.

Published data for chloride conductivity from a single source of data (Du Preez, 2002) were obtained from CCT carried out on a series of wall and slab elements that were cast and cured on two test sites at the mouth of the Buffalo River in the Port of East London (South Africa). The first test site was at the high-water mark and the site was characterised as being in a severe exposure site subjected to salt spray but no wave action. The second test site was at approximately 2 km from the mouth of the river and was less exposed. The mixture proportions of all the concrete elements used in the tests is summarised in Table 4.11.

Table 4.11: Mix proportions (g/m^3) of concrete (*adopted from Du Preez, 2002*)

Element	Mix Type	W/C ratio	Cement OPC-42.5	FA #	CSF #	GGBS #	Coarse aggregate	Fine Aggregate	Water
Wall	WA	0.50	190	-	-	190	1230	764	190
	WB	0.50	240	105	-	-	1280	764	180
	WC	0.57	320	-	20	-	1200	805	195
Slab	SA1-SA4	0.46	209	-	-	209	1230	630	190
	SB1-SB4	0.47	265	115	-	-	1280	703	180
	SC1-SC4	0.54	340	-	24	-	1200	762	195

GGBS # = Ground Granulated Blast Furnace Slag; CSF # = Condensed Silica Fume; FA # = Fly Ash

4.4.1.2 Determining chloride diffusion from chloride conductivity data

All the concrete elements in Table 4.11 were tested for chloride conductivity at 28 days before exposure and thereafter at 12 months and at 18 months. For this study, only the 28-day chloride conductivity results (Appendix C) are used as they are suitable for quality control purposes of new structures. However, 28-day chloride conductivity values do not allow for long-term chemical interactions between ingressing agents and the constituents of concrete (i.e. continued hydration and chloride binding), and need to be adjusted using a modification factor to ensure the reliable predictions of durability (Mackechnie, 1996). The modification factor is derived from either accelerated laboratory techniques or by use of empirical data from site and effectively allows the rapid chloride test results to be adjusted depending on the concrete type (Mackechnie *et al.*, 1996b).

Mackechnie (1996) established a correlation between the modified chloride conductivity and diffusion coefficients (for different binder types) recorded after two years, and presented this correlation in the form of a nomogram Excel spread sheet, *concur.xcl*. The spreadsheet essentially computes the modified chloride conductivity from the 28-day chloride conductivity value (input) and gives an output of both the corresponding 2 year diffusion coefficient $D_{2\text{years}}$ and the reference (initial) diffusion coefficient D_i at 28 days.

D_i is required as an input parameter in the SLP model and is derived from the two year diffusion using the following relationship:

$$D_t = D_i \left(\frac{t_i}{t} \right)^m \quad (4-3)$$

Hence, from the Equation 4.3 D_i is given as:

$$D_i = D_{2\text{years}} \cdot \left(\frac{2 \times 365}{28} \right)^m \quad (4-4)$$

where m is the diffusion reduction factor (see Table 3.3 of Chapter 3).

Figures 4.7 to 4.11 show the idealized relationship between the 28 day chloride conductivity value and corresponding reference (28 day) diffusion coefficients, D_i for different binder types and curing methods. The m values used for the different binder types are shown in Table 3.3 (Chapter 3). For the CSF concrete binder the diffusion coefficient reduction factor,

m, has not been established in literature for SA marine conditions, hence the data relating to CSF was excluded in the analysis.

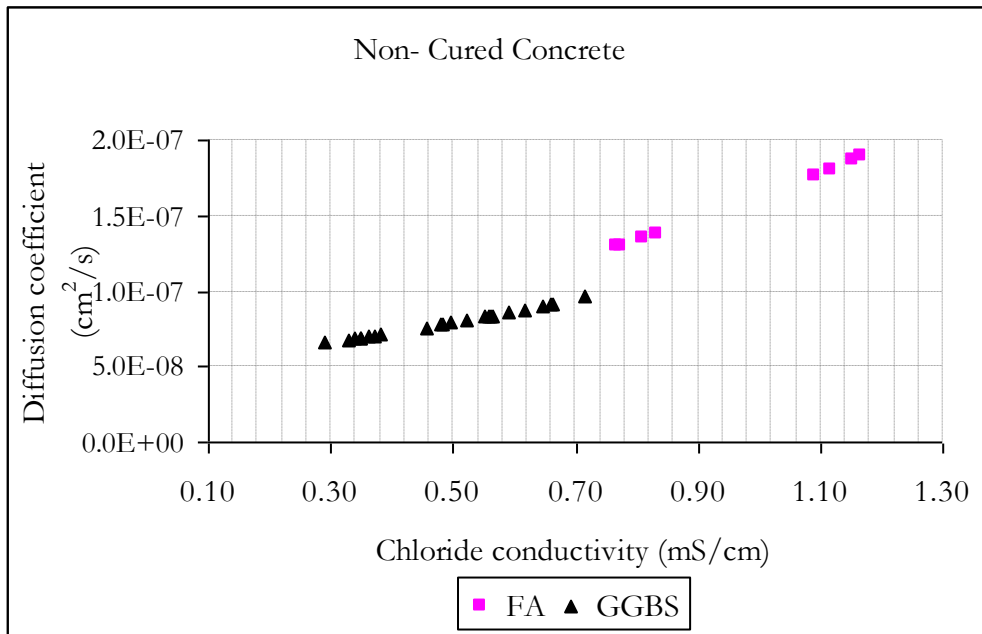


Figure 4.7: Correlation of 28-day chloride conductivity and D_i for CSF

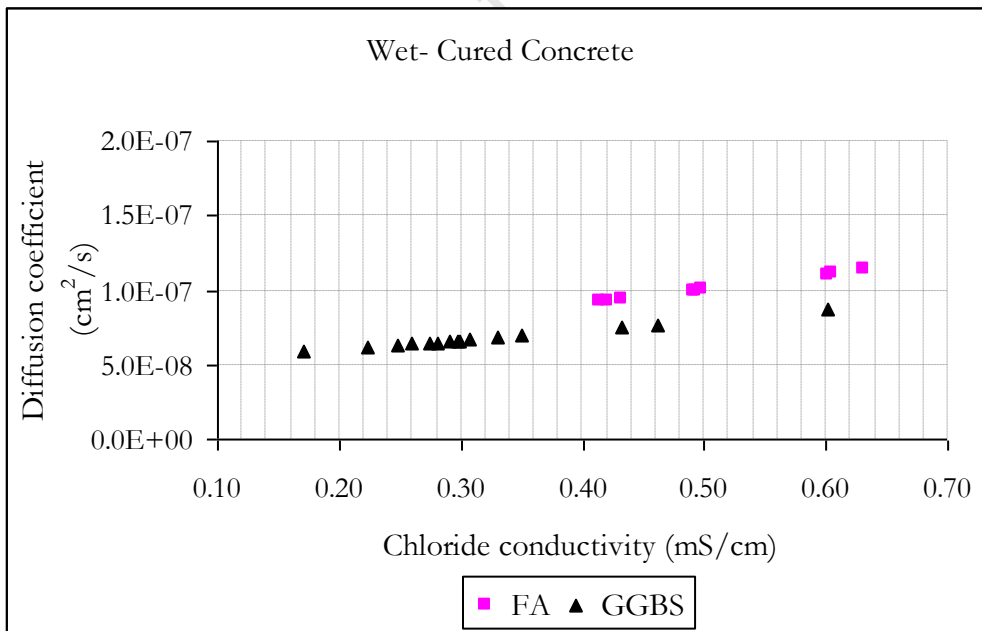


Figure 4.8: Correlation of 28-day chloride conductivity and D_i for FA

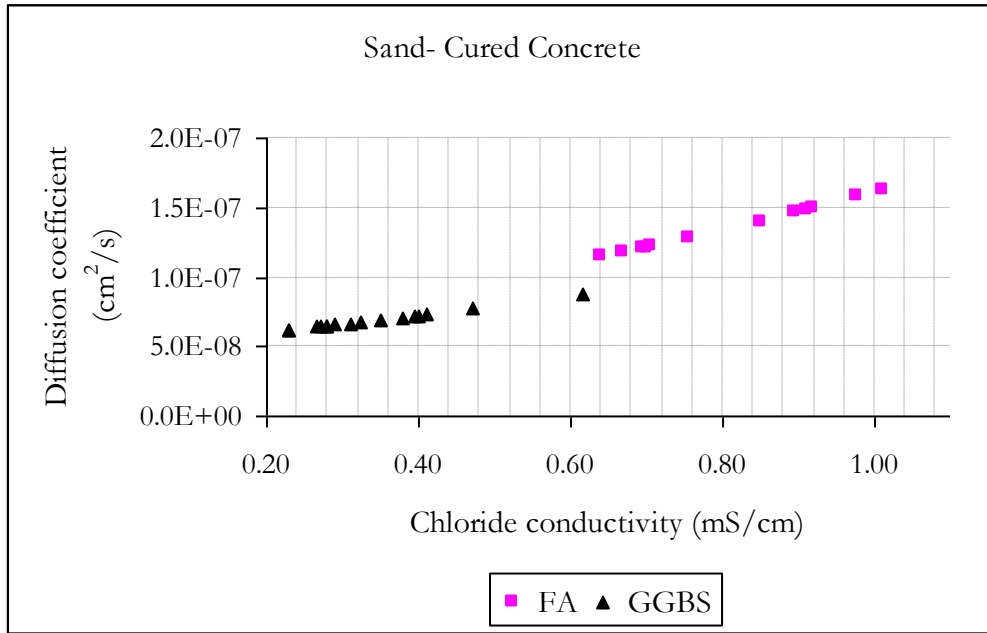


Figure 4.9: Correlation of 28-day chloride conductivity and D_i for FA

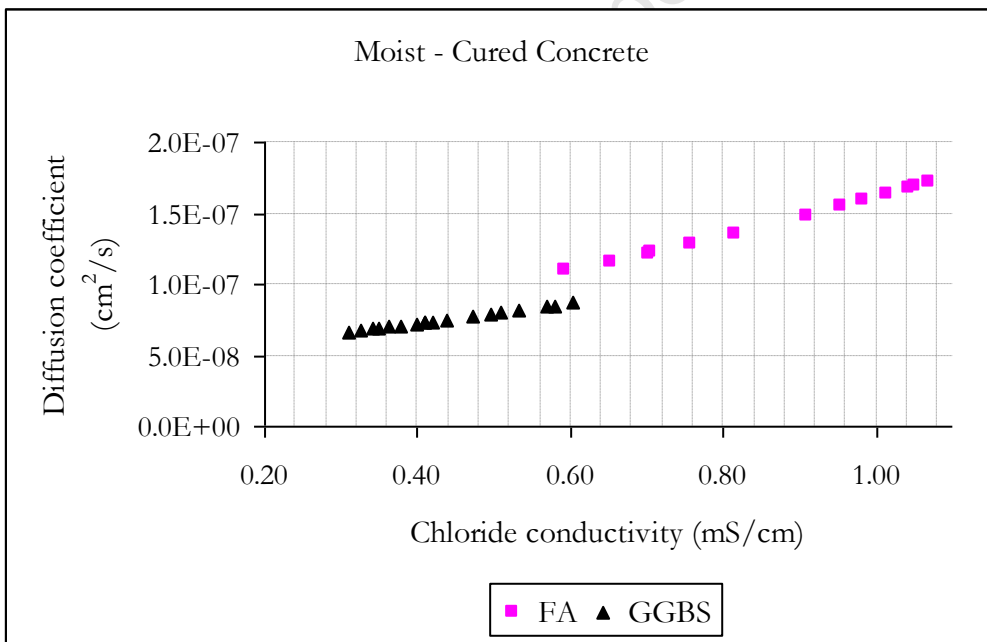


Figure 4.10: Correlation of 28-day chloride conductivity and D_i for FA

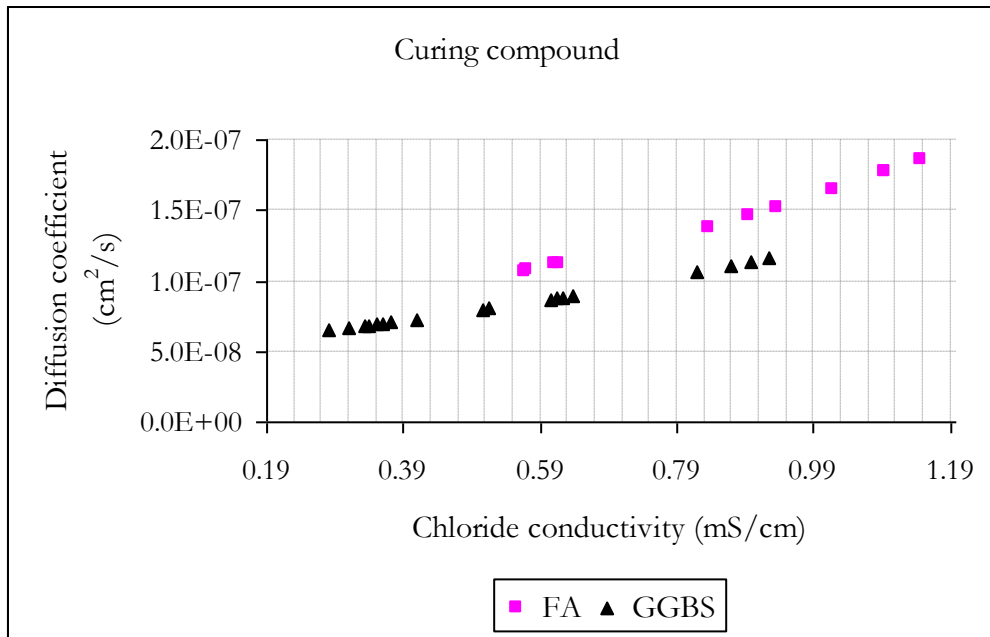


Figure 4.11: Correlation of 28-day chloride conductivity and corresponding D_i for FA

In general non-cured concrete has a high diffusivity value compared to wet cured concrete for each binder type. This is because curing allows continued hydration reactions which lead to a reduction in the permeability of concrete. In addition, the diffusion coefficients obtained for FA binder are higher than those of GGBS. This may be explained as due to the higher chloride binding capacity of GGBS.

From Figures 4.7 to 4.11, it can be concluded that diffusion is influenced by a number of factors: w/c, cementitious materials content and type of curing in addition to other factors such as compaction practice. These factors result in a large scatter on the diffusion coefficient value. It is therefore not straightforward to state only the mean value of the chloride diffusion in service life prediction but to consider the variability due to the factors influencing it. Both 28-day chloride conductivity and D_i parameters were statistically quantified. Data relating to both parameters was classified into data sets of concrete with the similar properties as explained next.

4.4.1.3 Classification of chloride diffusion data

The classification of 28-day chloride conductivity and D_i values available in the database was made by considering factors that affect diffusion (see Chapter 2) summarized as:

- a) Binder type

The use of supplementary cementing materials such as fly ash in the concrete causes a refinement of the pore structure in which coarser pore volumes are decreased due to being filled up by secondary C-S-H gel generated through pozzolanic reaction (Swamy, 1997 as cited in Suryavanshi *et al.*, 2002), making the concrete less permeable to ingress of aggressive agents. For this reason the data are classified under the following sub-sets:

- Portland cement (OPC)
- Portland cement with Blast furnace slag (OPC + GGBS)
- Portland cement with fly ash (OPC + PFA)
- Portland cement with silica fume (OPC + SF)

b) Curing type

The type and extent of curing significantly affects the extent of cement hydration. A lower degree of hydration of the cementing materials close to the surface will result in higher porosity and a more connected capillary pore system (Hooton *et al.*, 2002). Well-cured concrete reduces permeability resulting in a lower diffusion coefficient. Type of curing in the database includes:

- Wet cured (W)
- Moist cured (M)
- Dry curing (D)
- Curing compound (C)
- No curing (N)

c) Water cement ratio (w/c)

The w/c ratio of the concrete influences the capillary porosity of the concrete. Low w/c ratios (below 0.38), reduce the penetrability of the cement paste considerably due to the greater extent of calcium-silicate-hydrate (C-S-H) gel formation which fills up the available capillary pore space (Neville, 1995; McDonald, 1992; Ballim, 2001).

For w/c ratios between 0.38 and 0.6, the amount of C-S-H gel formation is usually significant enough to disrupt the continuity of the capillary pores, provided that substantial hydration of the cement is allowed to occur.

For w/c ratios higher than 0.6, gel formation is insufficient to block the capillary pores even with complete hydration. Tests have shown that concrete penetrability decreases by up to four orders of magnitude as the w/c ratio is reduced from 0.75 to 0.26 (Ballim, 2001).

d) Quality of execution

The quality of compaction and curing has a major role to play on the resulting penetrability of the structure. The quality of the structure can be determined at the initial stages using the water permeability test which is one of the DI's (see Appendix F).

4.4.2 Statistical quantification of chloride diffusion data

The statistical quantification of chloride conductivity and D_i data (see Appendix C) was carried out to get the statistical quantities: mean and standard deviation. The results obtained for each dataset of chloride conductivity and D_i data are reported in Tables 4.12 and 4.13 respectively.

Table 4.12: Summary of statistical quantities of chloride conductivity values ($\mu\text{S}/\text{cm}$) for $w/c=0.5$

Type of Curing	Binder Type	Sample size	Mean	Std Dev. #	COV #
Curing compound	OPC	-	-	-	-
	FA	14	0.98	0.33	0.34
	GGBS	18	0.54	0.22	0.41
	CSF	16	1.05	0.21	0.20
Water curing	OPC	-	-	-	-
	FA	12	0.74	0.42	0.57
	GGBS	15	0.32	0.11	0.34
	CSF	8	1.04	0.58	0.56
Hessian (Moist) curing	OPC	-	-	-	-
	FA	18	1.13	0.50	0.44
	GGBS	18	0.44	0.09	0.20
	CSF	12	1.16	0.35	0.30
Sand (Dry) curing	OPC	-	-	-	-
	FA	16	0.99	0.35	0.35
	GGBS	16	0.34	0.10	0.29
	CSF	6	1.14	0.51	0.45

Cont...

Cont... Table 4.12: Summary of statistical quantities of chloride conductivity values ($\mu\text{S}/\text{cm}$) for $w/c=0.5$

Type of Curing	Binder Type	Sample size	Mean	Std Dev. #	COV #
----------------	-------------	-------------	------	------------	-------

No curing	OPC		-	-	-
	FA	15	1.29	0.46	0.36
	GGBS	23	0.49	0.13	0.27
	CSF	12	1.59	0.43	0.27

COV # = Coefficient of variation; Std. dev. # = Standard deviation

Table 4.13: Summary of statistical quantities of effective diffusion coefficients (m^2/s) for $w/c=0.5$

Type of Curing	Binder Type	Sample size	Mean	Std Dev. #	COV #
Curing compound	OPC	-	-	-	-
	FA	14	1.82E-08	5.89E-09	0.32
	GGBS	18	9.13E-09	1.87E-09	0.20
	CSF	16	3.40E-08	1.01E-08	0.30
Water curing	OPC	-	-	-	-
	FA	12	1.49E-08	6.98E-09	0.47
	GGBS	15	7.38E-09	7.52E-10	0.10
	CSF	8	4.38E-08	3.47E-08	0.79
Hessian (Moist) curing	OPC	-	-	-	-
	FA	18	2.26E-08	1.48E-08	0.65
	GGBS	18	8.19E-09	6.84E-10	0.08
	CSF	12	4.43E-08	2.36E-08	0.53
Sand (Dry) curing	OPC	-	-	-	-
	FA	16	1.84E-08	6.83E-09	0.37
	GGBS	16	7.52E-09	7.19E-10	0.10
	CSF	6	4.8E-08	3.36E-08	0.70
No curing	OPC	-	-	-	-
	FA	15	2.55E-08	1.26E-08	0.49
	GGBS	23	8.67E-09	9.79E-10	0.11
	CSF	12	9.48E-08	6.62E-08	0.70

COV # = Coefficient of variation
Std. dev. # = Standard deviation

From Tables 4.12 and 4.13 it is observed that the COV of chloride conductivity in all sub-classes differs from that of the corresponding diffusion coefficients sub-classes. This may be explained as due to error propagation during the conversion process (using the aforementioned idealised relationship).

Due to the limited sample sizes ($n < 30$) for all classes, a non-parametric boot-strapping technique was used in this study to generate sub-samples from the original data sets. (The concept of bootstrapping was covered in Section 3.4 of Chapter 3).

A non-parametric bootstrap is used to estimate the uncertainty of a statistic (mean or standard deviation) from a set of data. For example, to estimate the uncertainty of the mean from a dataset with 10 elements, the following procedure is used (EDA, 2006):

- (i) A sub-sample of a size less than or equal to 10 is generated from the data, and the mean calculated. This sub-sample is generated “with replacement” so that any data point can be sampled multiple times or not sampled at all.
- (ii) This process is repeated at least 500 times so as to have at least 500 values for the mean.
- (iii) Computed values for the mean form an estimate of the sampling distribution of the mean. A confidence interval of 90% $\left(\bar{\sigma}\right)$, 95 % $\left(\bar{\sigma}\right)$ or 98 % $\left(\bar{\sigma}\right)$ of the sampling distribution for the mean is reported to show the uncertainty of the mean.

The bootstrap method was carried out using a Matlab subroutine.

An example is illustrated in Figures 4.12 and 4.13 of the results of 999 non-parametric simulations of chloride conductivity and D_i respectively represented in form of histograms.

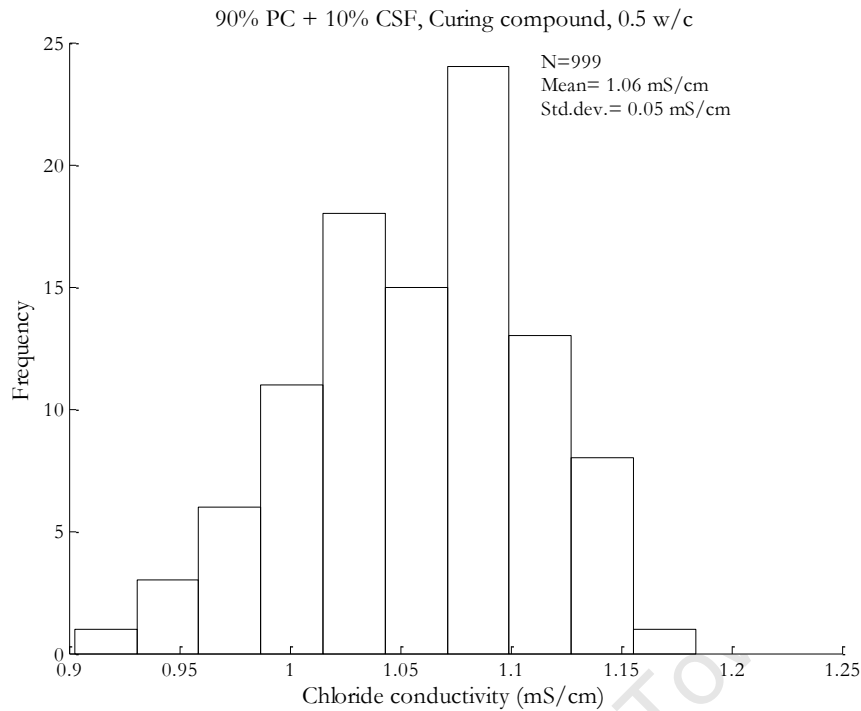


Figure 4.12: Histogram of chloride conductivity of CSF concrete **cured with a curing compound** based on 999 non-parametric simulations

From the generated data set, the first two moments for chloride conductivity were estimated to be, $\bar{x} = 1.06$ mS/cm and $s = 0.05$ mS/cm.

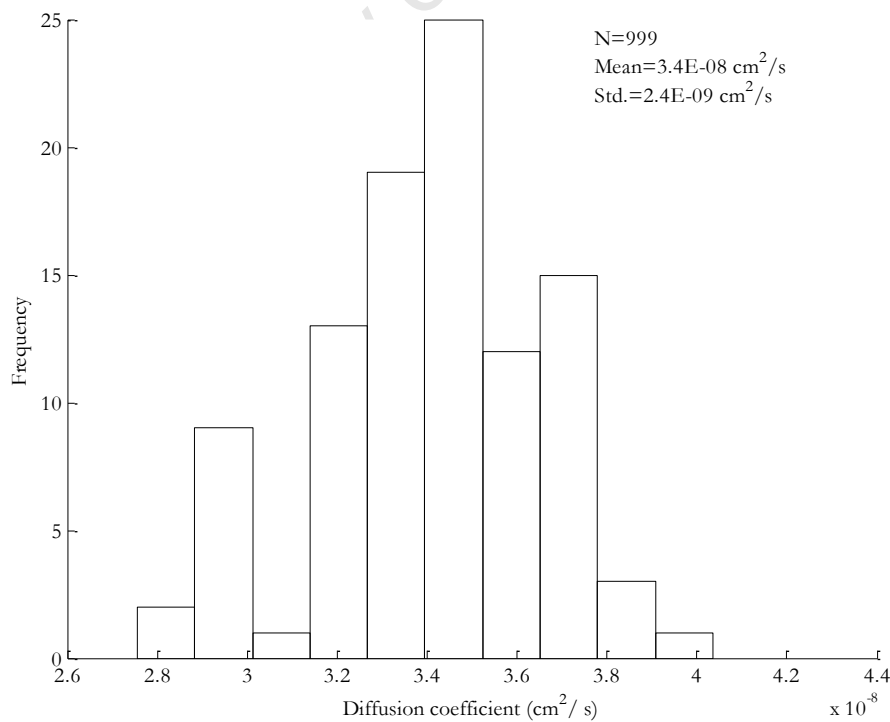


Figure 4.13: Histogram of diffusion coefficient of CSF concrete **cured with a curing compound** based on 999 non-parametric simulations

From the generated dataset, the first two moments for D_i were estimated to be, $\bar{x} = 3.4\text{E-}08 \text{ cm}^2 / s$, $s = 2.4\text{E-}09 \text{ cm}^2 / s$ and a $\text{COV} = 0.07$.

The value of standard deviation obtained from the parametric simulation of $s = 2.4 \text{ E-}09 \text{ cm}^2 / s$ is less than that obtained from the original data ($s = 1.01 \text{ E-}08 \text{ cm}^2 / s$). This is due to the fact that the values used in plotting the histogram are the mean values from the re-sampled datasets.

4.4.3 Summary of D_i results

The D_i data was divided into subsets of information such as binder type and processing influences such as type and degree of curing. The expanded suite of parameter classes was carried out to ensure a better reflection on specific concrete properties of D_i in the database. However, subdividing the available data into the additional subclasses meant reducing the class size of the data, which led to problems in the next stage of statistical quantification. In addition, not all the data at hand had fields representing all of the sub-classes.

It is the recommendation of this study that additional data be obtained to allow for the accurate quantification of the D_i parameter.

4.5 COVER DEPTH

During the design of RC structures, the nominal cover (x_{nom}) is usually specified as the design value for concrete cover depth. x_{nom} is defined as the minimum cover (x_{min}), plus an allowance in design for deviation, (Δx_{dev}) as illustrated by Equation 4-5 (EN 1992-1, 2004). EN 1992, 2004 recommends a value of 10 mm for Δx_{dev} .

$$x_{nom} = x_{min} + \Delta x_{dev} \quad (4-5)$$

Due to construction quality practices the actual cover achieved during construction varies from the recommended x_{nom} , and hence cover depth has to be considered as a stochastic variable rather than a constant value. For this reason, a statistical quantification of cover depth measurements is essential in order to obtain the statistical quantities necessary for representing the parameter adequately in a SLP model.

South African data on cover depths for both bridge and building structures representing various elements on each structure are presented in Figure 4.14 (Ronne, 2005). The actual data were however not available for use in this study.

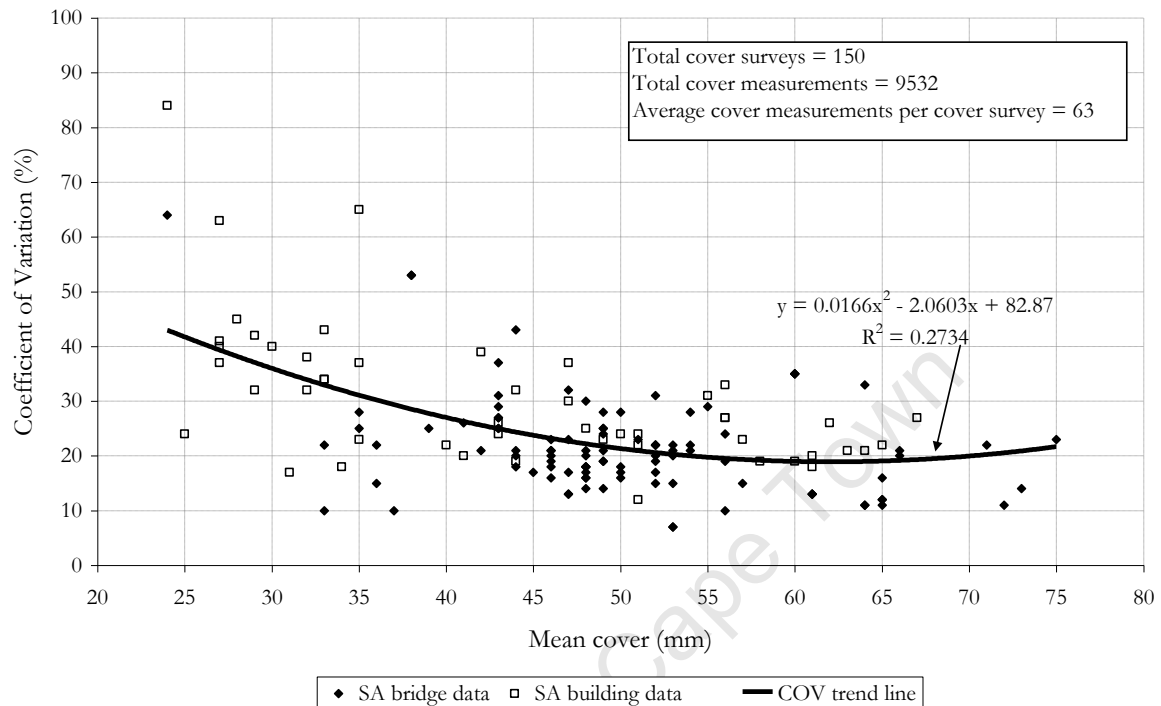


Figure 4.14: Scatterplot for cover depth data in South African (Ronne, 2005)

From the scatterplot, it is observed that the coefficients of variation (COV) are more significant at low cover depths than at greater cover depths. Further, the trendline on the graph shows that the COV decreases with increasing depth. The high COV in low cover depths (20 mm to 40 mm) of 48% to 27% may be due to poor standards of control (see Table 4.14).

Table 4.14: Suggested COV values for various standards of control for typical British construction practice (Sharp, 1997 as cited in Ronne and Beushausen, 2008)

Standard of control	COV #
Near laboratory precision	10
Good	15
Moderate	20
Poor	30

For mean covers between 55 mm and 80 mm, the COV was approximately constant at 20% representing moderate control during construction. Table 4.15 gives a summary of expected COV from the scatterplot.

Table 4.15: COV of cover depths \bar{c} from South African data (Ronne, 2005)

Cover depth (mm)		COV (%)
Low cover depths	20	48
	30	36
	40	27
High cover depths	>40	20

Since the COV is more significant at low covers (cover depth < 40 mm) than at high covers the study will adopt FIB Model Code for SLD (2006) recommendations on assigning statistical distributions to the cover depth data.

For concrete covers with low cover depths, a right skewed lognormal distribution is adopted to avoid the probability of negative values occurring during the statistical analysis. For mean covers larger than 40 mm, the COV is low and hence, the effect of negative values occurring becomes negligible. Hence, a normal distribution function will be used for describing large concrete covers.

The quantities adopted for the statistical quantification of cover depth are summarised in Table 4.16.

Table 4.16: Statistical quantities of cover depth \bar{c} in mm for this study

Distribution type		Mean value	COV
Low cover depths <40 mm	Lognormal	$X_{\text{nom}}^{\#}$	0.40
High cover depths > 40 mm	Normal	$X_{\text{nom}}^{\#}$	0.20

$X_{\text{nom}}^{\#}$ = Nominal design cover depth value (mm)

4.6 MODEL UNCERTAINTIES

The accuracy of the aforementioned mathematical model (represented by Equations 3-6 and 4-6) used in the study is limited to the assumptions and approximations made in its formulation. These assumptions and approximations in the model in effect introduce errors into the results.

In probabilistic models, this error is partially taken into account by increasing the scatter of the results obtained from the model (Ferreira, 2006). A model uncertainty parameter is used to take into account the uncertainties that arise due to the simulation of the real phenomenon process (Leira *et al.*, 2000 *as cited in* Ferreira, 2006). For example an inherent error occurs during the conversion of chloride conductivity values to corresponding diffusion coefficients. The model uncertainty parameter θ_{D_i} is included in the LSF to account for error in the diffusion coefficient value.

$$Z = \frac{S_{lim} - S_{cr} - C_{crit} - C_s}{\sigma} \left[1 - \operatorname{erf} \left(\frac{x}{2\sqrt{C_i \cdot \theta_{D_i} \cdot t^{1-m}}} \right) \right] = 0 \quad (4-6)$$

The parameters in the Equation 4-6 have been previously defined in Equation 3-6. Due to lack of a suitable value for this parameter, this study assumes the statistical values for θ_{D_i} given in Table 4.17.

Table 4.17: Assumed factor for conversion of chloride conductivity to diffusion coefficient

Modelling uncertainty	Distribution type	Mean value	Standard deviation
$\theta_{D_i}^{\#}$	Normal	1.0	0.01

$\theta_{D_i}^{\#}$ = modelling uncertainty in the calculation of material resistance

4.7 RELIABILITY ANALYSIS

Having determined the stochastic quantities of the parameters in the LSF, the problem remains to evaluate the reliability against depassivation of reinforcement. The reliability analysis will be carried out using Monte Carlo simulation techniques.

4.7.1 Monte Carlo Simulations

From the statistical quantification, the probability density functions (PDFs) for most of the variables in the LSF was established. The diffusion coefficient and chloride conductivity data were found insufficient in assigning a PDF to the parameters. Hence, non-parametric bootstrapping was carried out on the parameters during the LSF analysis.

For the surface chloride concentration, a gamma distribution was found to match the field data. The mean, standard deviation and shape factors are the parameters that best describe gamma distribution. The critical chloride content is taken to have a normal distribution, whereas the cover depth distribution was taken as lognormal for low cover depths (<40 mm)

and a normal distribution for high cover depth (>40 mm). The stochastic quantities obtained from the statistical quantification are summarised in Table 4.18.

Table 4.18: Summary of statistics for LSF variables

Reference section	Parameter	Units		Distribution type	Mean value	COV [#]	α [#]	β [#]
4.2.3	C_s	%	XS1	Gamma	1.95	0.57	3.09	0.63
			XS3a	Gamma	4.5	0.2	24.45	0.18
			XS3b	Gamma	2.61	0.28	12.44	0.21
4.5	x	mm	$x_{nom}^{\#} < 40$	Lognormal	$x_{nom}^{\#}$	0.4	-	-
			$x_{nom}^{\#} > 40$	Normal	$x_{nom}^{\#}$	0.2	-	-
4.4	D_i	mm ² /year		Non-parametric bootstrapping on sample data				
4.6	θ_{D_i}	-		Normal	1	0.01	-	-
4.3	C_{crit}	% m/m		Normal	0.48	0.31	-	-
3.3.4-2	m	-		Deterministic	Table 3.3			

$\theta_{D_i}^{\#}$ = modelling uncertainty in the calculation of diffusion coefficient

$x_{nom}^{\#}$ = Nominal design cover depth value (mm)

COV[#] = Coefficient of variation

$\alpha^{\#}$ = Shape parameter of distribution

$\beta^{\#}$ = Scale parameter of distribution

Having determined the stochastic quantities representing each variable in the LSF (C_{crit} , C_s , x and D_i), the Monte Carlo simulation technique was applied to generate random samples from the distributions or from the sample set, as was the case for the D_i parameter. Each of the generated set of numbers for each variable was then substituted into the LSF and the probability of failure P_f computed. This process was repeated for 10, 000 iterations to improve the accuracy of the result. The process of carrying out the MCS analysis for service life design is illustrated in Figure 3.11 of Chapter 3 and was carried out using a Matlab subroutine developed for this study.

4.7.2 Example: Reliability Analysis of a RC Pier

The example given in this section is aimed at illustrating the use of probabilistic modelling in determining the chloride conductivity index value for material specification using the limit-state design (performance) principle introduced in Chapter 3.

4.7.2.1 Example: Limit-State Principle

Problem Statement

The reliability analysis methodology introduced in Section 2.4.2.4 (Chapter 2) is exemplified for a concrete pier to be cast in-situ in an extreme splash and tidal marine environment using a cement blend of Portland cement and ground granulated blast furnace slag - OPC: GGBS (50:50). GGBS has been selected as it has been found to be beneficial in the marine environment in that it is able to bind chlorides with time and resist the ingress of chlorides (Alexander *et al.*, 1999).

The designers' task is to specify the required material resistance against chloride penetration in terms of a chloride conductivity value and/or corresponding diffusion coefficient given the parameters in Table 4.19.

Analysis:

The problem solution will follow that given by the design flow chart in Figure 3.11 of Chapter 3.

- (i) The first step in the durability design involves defining the desired life of the structure, and is carried out mainly by the client/owner of the structure. In this step, the client specifies a deterministic quantity referred to as the design working life of the structure t_d (Table 2.3 of Chapter 2), having given thoughtful consideration to the performance requirements of the structure. For this example, the concrete element is a pier which is a common structural element in marine structures (such as jetties) and other concrete structures such as bridges which have a design service life of 50+ years. Thus from Table 2.3 the design life is selected as 100 years.
- (ii) The second step in the design involves the appraisal of environmental actions acting on the structure in order to show their significance in relation to durability (Siemes and Edvardsen, 1999). For this example, concrete material degradation is assumed to occur solely as a result of corrosion of steel in the concrete, by chlorides from marine exposure. The extreme splash and tidal marine environment is classified as XS3b exposure class based on EN 206-1 modified for South African conditions (Table 3.1 of Chapter 3).

- (iii) Proper definition of the environmental class is important as it assists in the third step of identifying the dominant transfer processes of chloride ions into concrete. From Chapter 2 the relevant transport mechanism is chloride diffusion (which is the dominant transport mechanism for chloride ions in concrete) and is modelled using a Fickian type model applicable to South Africa marine environment represented in Equation 2-22 (Chapter 2).
- (iv) For probabilistic analysis the Fickian model is represented as a LSF (see Equation 4-7) and a solution of the LSF is obtained using the aforementioned MCS techniques.

The statistical quantities for the LSF parameters data relating to OPC: GGBS in XS3b environmental condition are represented in Table 4.19.

Table 4.19: Input parameters for reliability analysis of a RC pier

Reference	Parameter	Units	Mean	COV	Distribution type	$\alpha^{\#}$	$\beta^{\#}$
Section 4.5	Concrete cover, x	mm	50	0.2	Normal	50	10
Section 4.3	Critical chloride content, $C_{crit}^{\#}$	%	0.40	0.3125	Normal	0.40	0.125
Table 2.3	Design service life (t)	years	100	-	Deterministic	50	-
Table 4.17	θ_{D_i}	-	1	0	Normal	-	-
Table 3.3	Reduction factor, m	-	0.68	-	Deterministic	0.68	-
Mackechnie (1996) [#]	Surface chloride concentration, C_s	%	4.13	0.21	Gamma	24.46	0.17

$\alpha^{\#}$ = Shape parameter of distribution

$\beta^{\#}$ = Scale parameter of distribution

Mackechnie (1996)[#] = only the mean values relating to this parameter were obtained from this reference. The corresponding statistical distribution was adopted from this study.

$C_{crit}^{\#}$ = Value relates to OPC binder but is adopted due to lack of a suitable value for GGBS binder

Design verification:

The design target is to calculate a set of values for material resistance against chloride penetration (D_i or chloride conductivity values) corresponding to the probability of the event ‘corrosion initiation’ using the set of parameters in Table 4.19.

The material resistance value selected for design specification will be that corresponding to a probability of failure of 6.7% for the 100 year service life of the structure –which is the target

probability of failure, $P_{\text{target,ILS}}$, specified by EN 1990 (2000). This value corresponds to a target reliability index ($\beta_{\text{target,ILS}}$) of 1.5 (Table 2.6 of Chapter 2).

In addition, the D_i (or chloride conductivity) value specified for design will ensure that the structure meets its performance requirement (50 years service life) for the cover depth of 50 mm. If during the analysis the choice of the geometry parameter (cover depth) results in a chloride conductivity value that cannot be economically attained for the specified performance, then a trade off is made by adjusting either parameter appropriately until the condition specified by Equation 4-7 is satisfied.

$$P_f = P \left\{ \xi_{(x,t)} \cdot \theta_R - C_{\text{crit}} \cdot \theta_S < 0 \right\} P_{\text{target,ILS}} \quad (4-7)$$

The design verification for Equation 4-7 was carried out using MCS bootstrapping techniques. A Matlab sub-routine program (MonteCarlo2_PerformancePrinciple.m) developed for this study (attached CD) was applied in carrying out MCS on the respective statistical distributions of the parameters in Table 4.19.

The simulated values were then substituted into Equation 4-8 and the diffusion coefficient calculated.

$$D_i = \left[\frac{2}{x} \text{erf}^{-1} \left(1 - \frac{C_{\text{crit}}}{C_S} \right) \right]^{-2} \cdot \frac{1}{\theta_{D_i} t^{\left(\frac{m}{2} \right)}} \quad (4-8)$$

Figure 4.15 shows the cumulative density function (CDF) obtained from the analysis. For a failure probability of 0.067, a diffusion coefficient value of 44.5 mm²/year was obtained.

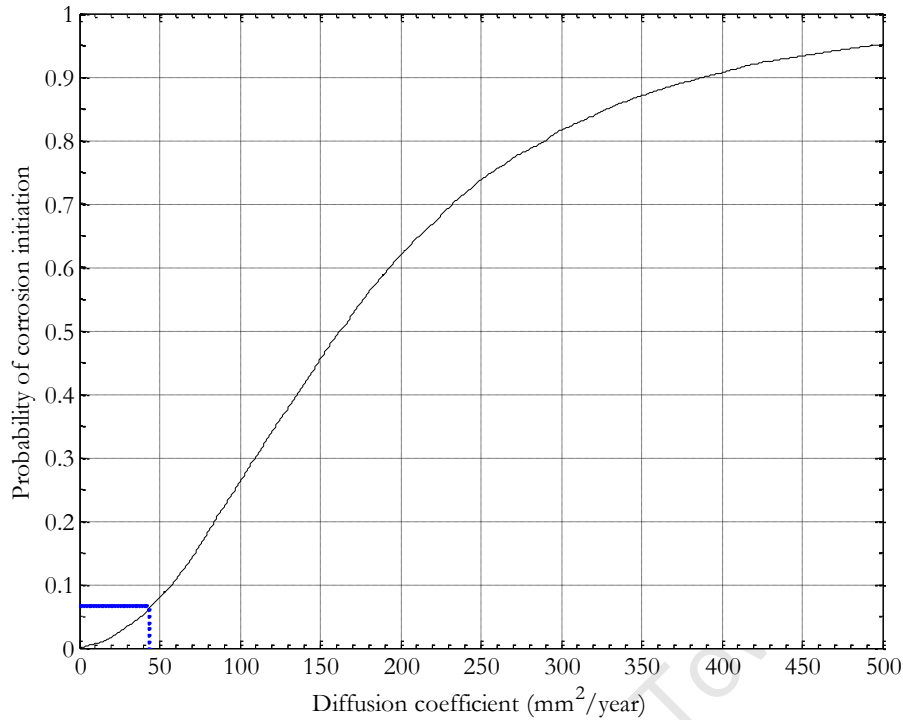


Figure 4.15: CDF of probability of failure for diffusion coefficient values

The diffusion coefficient value of $44.5 \text{ mm}^2/\text{year}$ ($1.41 \times 10^{-12} \text{ m}^2/\text{s}$) corresponds to a chloride conductivity value of 0.9 mS/cm (determined using Concur.xcl spreadsheet). This chloride conductivity value is lower than that specified by the deemed-to-satisfy approach of 1.05 mS/cm as shown in Table 4.20.

Table 4.20: Maximum Chloride Conductivity Values (mS/cm) for Different Classes and Binder Types: Deemed to Satisfy Approach – Monumental Structures (Cover = 50 mm) (Alexander *et al.*, 2007)

EN 206 class	70:30 CEM I:Fly Ash	50:50 CEM I:GGBS	50:50 CEM I:GGCS	90:10 CEM I:CSF
XS1	2.50	2.80	3.50	0.80
XS2a	2.15	2.30	2.90	0.50
XS2b, XS3a	1.10	1.35	1.60	0.35
XS3b	0.90	1.05	1.30	0.25

In conclusion, for the RC pier to have a 6.7% probability of corrosion initiation during its 100 year life time, the designer should specify a chloride conductivity value of not greater than 0.9 mS/cm and cover depth of 50 mm .

4.7.3 Method of Sensitivity Analysis

The sensitivity analysis was carried out by varying the parameter of interest over the valid range (i.e. $\approx \bar{x} \pm 3s$), and maintaining the other variables at their respective base case settings. Table 4.21 shows the parameter information needed for the analysis.

Table 4.21: Range of parameters for sensitivity analysis

Parameter	Base case (mean value)	Range of values	COV
x (mm)	50.0	0 → 100	0.3
D_i (mm ² /year)	98.3	58.3 → 158.3	0.1
C_{cr} (% mass of cement)	0.40	0.2 → 0.8	0.375
C_s (% mass of cement)	4.50	1.5 → 7.5	0.2
t (years)	50.0	-	0
m	0.64	-	0

The diffusion coefficients are presented in units of mm²/year (1 mm²/year = 3.171×10^{-14} m²/s). These units were chosen to simplify the presentation of the results, and can be directly used in the service life calculations because the unit measure for concrete cover is mm and the unit for service life is years.

The results of the sensitivity of the estimated service life to changes in the parameters (Table 4.21) are presented next.

4.7.3.1 Sensitivity to cover depth

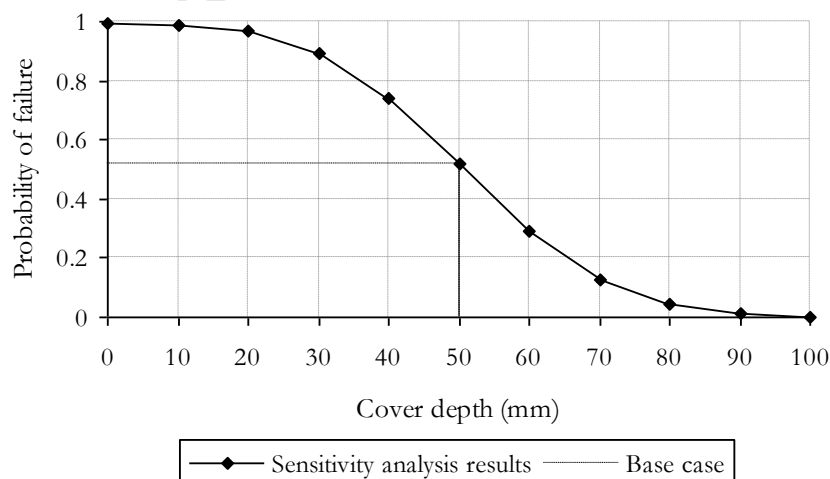


Figure 4.16: Sensitivity of cover depth to probability of corrosion initiation

Figure 4.16 represents a graph of probability of corrosion initiation against cover depth. The probability values correspond to the number of model iterations in the simulation that predict corrosion initiation in the RC element during its service life.

From the graph it can be observed that an increase in the cover depth leads to a decrease in the probability of failure. For example, increasing the cover depth by increments/decrements of $\pm 20\%$ (each step from 50 mm base case whilst holding other parameters constant) reduces the probability of failure by a rate of 0.47% ~ 77.05 % (see Table 4.22). This effect results from the fact that a deeper cover allows a greater reduction in diffusivity to occur before corrosion is initiated.

Table 4.22: Sensitivity of concrete cover depth to P_f

Cover depth	P_f	Rate of change of P_f (%)
0	0.994	-
10	0.989	0.47
20	0.965	2.41
30	0.893	7.46
40	0.738	17.35
50 [#]	0.516	30.10
60	0.290	43.81
70	0.125	56.76
80	0.042	66.59
90	0.012	70.88
100	0.003	77.05

Base case[#] = 50 mm cover depth

4.7.3.2 Sensitivity to surface chloride concentration

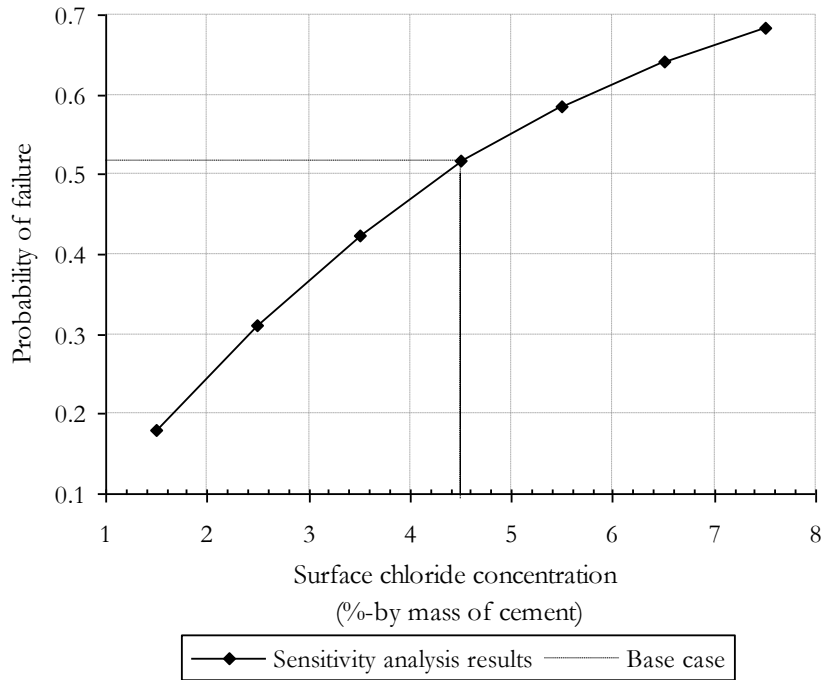


Figure 4.17: Sensitivity of surface chloride concentration to probability of corrosion initiation

From Figure 4.17, it is observed that when the surface chloride concentration increases/decreases 10% each step from 4.5% (with other parameters held constant), the rate of change of probability of failure ranges from 4.3% ~ 13.15 % as summarized in Table 4.23.

Table 4.23: Sensitivity of surface chloride concentration to P_f

C_s	P_f	Rate of change of P_f
1.5	0.179	13.15
2.5	0.310	11.33
3.5	0.423	9.33
4.5 [#]	0.517	6.94
5.5	0.586	5.49
6.5	0.641	4.30
7.5	0.684	-

Base case[#] = 4.5 % of chlorides by mass of cement

4.7.3.3 Sensitivity to critical chloride content

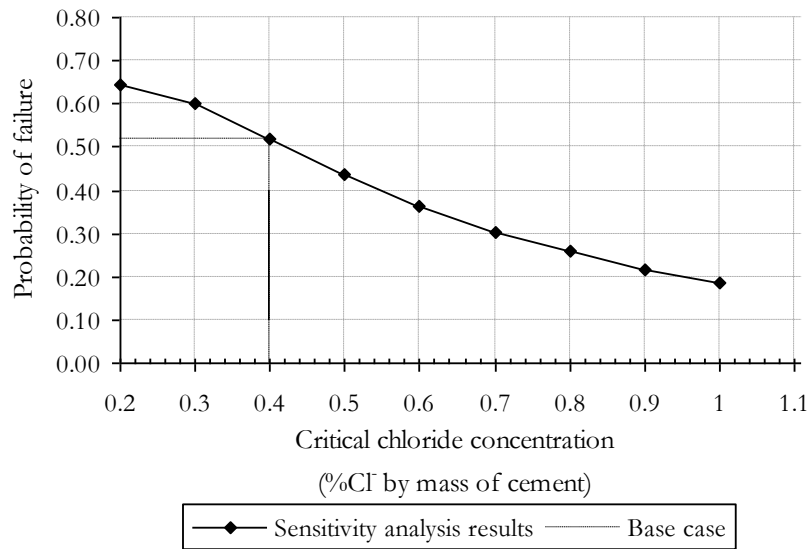


Figure 4.18: Sensitivity of critical chloride content to probability of corrosion initiation

Figure 4.18 shows that an increase in the critical chloride content leads to a decrease in the probability of failure. When C_{crit} increases/decreases 10% each step from 0.4% (the other parameters held constant), the probability of failure reduces by 6.87%~15.47% as summarized in Table 4.24.

Table 4.24: Sensitivity of critical chloride content to P_f

C_{crit}	P_f	Rate of change of P_f (%)
0.2	0.64	-
0.3	0.60	6.87
0.4 [#]	0.52	13.53
0.5	0.44	16.00
0.6	0.36	16.55
0.7	0.30	16.22
0.8	0.26	15.34
0.9	0.22	15.55
1.0	0.18	15.47

Base case[#] = 0.4% of chlorides by mass of cement

4.7.3.4 Sensitivity to diffusion coefficient

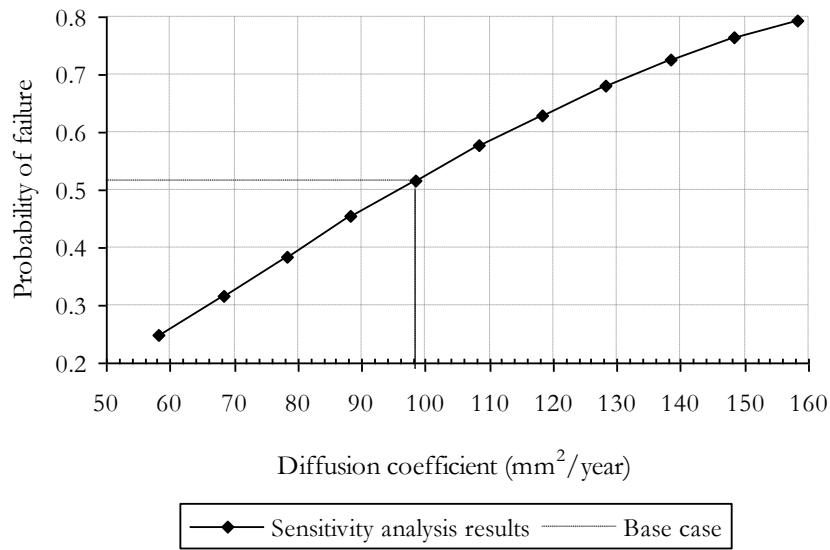


Figure 4.19: Sensitivity of diffusion coefficient to probability of corrosion initiation

Figure 4.19 shows that when the chloride diffusion coefficient increases/decreases 10% each step from 98.3 mm²/year (and the other parameters are constant), the rate of probability of failure increase ranged from 3.85%~21.47% as summarized in Table 4.25.

Table 4.25: Sensitivity of diffusion coefficient to P_f

D_i	P_f	Rate of change of P_f
58.3	0.248	21.47
68.3	0.316	17.75
78.3	0.385	15.29
88.3	0.454	12.05
98.3 [#]	0.516	10.77
108.3	0.579	7.91
118.3	0.628	7.74
128.3	0.681	5.99
138.3	0.724	5.17
148.3	0.764	3.85
158.3	0.794	-

Base case[#] = 98.3 mm²/year

4.7.3.5 Conclusion to Sensitivity Analysis

From section 4.7.3.1 to 4.7.3.4, it is obvious that the parameter, which has maximal effect on probability of corrosion initiation during the design life of a RC structure in a chloride environment, is the thickness of concrete cover. The chloride diffusion coefficient, critical chloride content and surface chloride concentration, are next as summarized in Table 4.26.

Therefore, in durability design of RC structures it is important to work out a reasonable thickness of concrete cover for adequate protection in the marine environment. At the same time, other factors such as water-cement ratio, concrete compressive strength and protection condition etc, which will affect the quality of concrete cover, should also be taken into consideration.

Table 4.26: Sensitivity of parameters to P_f

Number	Parameter	Sensitivity
1	x (mm)	0.47% ~ 77.05 %
2	D_i ($mm^2/year$)	3.85%~21.47%
3	C_{cr} (% mass of cement)	6.87%~15.47%
4	C_s (% mass of cement)	4.3% ~ 13.15 %

Decreasing
↓
sensitivity

4.8 CONCLUSION

4.8.1 Discussion

The proposed probabilistic-based design approach involved identifying the geometric, material and environmental parameters that have an influence on the durability of a RC structure and representing them as stochastic quantities. The relationship between the parameters was then expressed in the form of a limit-state function (LSF) similar to structural reliability theory. Data for the parameters representing environmental influence and the RC structure's geometry were obtained from previous in-depth studies in either laboratory or in-situ testing in South Africa. The chloride conductivity test (CCT) which is one of South Africa's durability index tests (DI's) was found useful in obtaining material parameter data required to support the use of the LSF. The 28 day chloride conductivity values were adjusted using a modification factor to allow for long-term chemical interactions between ingressing agents and the constituents of concrete. An idealised relationship between the modified

chloride conductivity values and diffusion coefficients was then used in computing the latter. This process was carried out with the help of an Excel spreadsheet (Concur.xcl).

Data for each parameter were classified under different datasets having the same concrete material properties e.g. material parameters were divided into sub-sets such as binder type and processing influences such as type and degree of curing. The expanded suite of classes was carried out to ensure a better reflection on specific concrete properties for each parameter.

However, subdividing the available data into the additional subclasses meant reducing the class size of the data, which led to problems in the next stage of statistical quantification. In addition, not all the data at hand had fields representing all of the sub-classes.

During the classification of the data sets, the box plot was found as an effective tool for summarising large quantities of data and identifying the variability of the data. The box plot was used to check the quality of the data by identifying outliers for each data set.

The datasets for each parameter were then presented in histograms. However, not all the data sets had sufficient data to allow for the subsequent construction of histograms as was the case for the diffusion coefficient parameter. For this case non-parametric bootstrapping techniques were applied to generate additional datasets using a Matlab sub-routine program. The tail of the distribution represented by the histogram was an important parameter in considering suitable distribution types for the data. Depending on the observed skewness a number of possible distributions were selected to represent the data. For example, during the quantification of PC binder concrete in XS1 marine zone, the histogram was found to have a right skew (the right tail was longer than the left). For this reason, possible distribution types were selected as lognormal and gamma distributions as they have right skews.

Having selected representative distributions based on the shape of the histogram, a chi-squared goodness-of-fit test was applied to obtain the most suitable statistical distribution for the data. During the test process it was noted that results of goodness-of-fit tests should never be depended on solely whilst selecting the analytic form for a distribution. Generally, goodness-of-fit tests were found best at rejecting poor distribution fits rather than for identifying good fits. This was especially so for the surface chloride concentration parameter (for the extreme tidal and splash marine zone in Appendix B) where the normal distribution was at first considered to be a suitable distribution followed by the gamma distribution, from the chi-squared goodness-of-fit results. However, it was noted that the normal distribution

would not be a suitable distribution since it would take up negative values. To avoid the occurrence of negative values the gamma distribution in this case proved to be more realistic.

Having selected suitable distribution fits for each parameter, the next step followed was the application of reliability principles in analysing the service life model. An example was used to illustrate the application of the limit-state principle in carrying out reliability design of RC elements. The design target in the example was to calculate a set of values for material resistance against chloride penetration (D_i or chloride conductivity values) corresponding to the probability of the event 'corrosion initiation' given the stochastic values for the other parameters in the LSF.

The diffusion coefficient value selected of $44.5 \text{ mm}^2/\text{year}$ corresponded to a 6.7 % probability of failure which is the acceptable target probability of failure given by EN 2000 for the serviceability-limit state. Specifying this D_i value for design meant that there would be a 6.7% probability of corrosion initiation during the element's design life.

The D_i value is equivalent to a chloride conductivity value of 0.9 mS/cm. This chloride conductivity value was found to be lower than that specified by the deemed-to-satisfy approach, of 1.05 mS/cm, for the same set of design conditions (service life and cover depth). From this example, it was concluded that the deemed-to-satisfy design is less conservative in durability design. In addition the deemed-to-satisfy design does not give the design risk involved for the durability failure. Information relating to the design risk assists the owner of the structure to plan for expected repair costs or maintenance of the structure.

Finally, a sensitivity analysis was carried out to investigate the influence of the basic parameters to the probability of failure, P_f . The most influential parameter was the concrete cover, where small changes in the average value resulted in significant variations in P_f . This was closely followed by the diffusion coefficient, the critical chloride content and the surface chloride concentration respectively. This shows that in the durability design of RC structures it is important to work out a reasonable thickness of concrete cover for adequate protection in the marine environment. At the same time, other factors such as water-cement ratio and protection condition, which will affect the quality of concrete cover, should also be taken into consideration.

4.8.2 Specific Conclusions

The idealised formula in the excel spreadsheet *concur.xls* used in computing the diffusion coefficient from modified chloride conductivity value is based on chloride data analysed a decade ago by Mackechnie (1996). However, concrete material properties have since changed, for example, due to a change in the Portland cement manufacture specification (SABS 471) in 2001, cement manufactures now produce CEM I which has different chemical composition from that of OPC. Thus the idealised relationship presented by the Excel spreadsheet is not a true representation of current material properties. For this reason, it is recommended that the spreadsheet be revised and updated to allow for more accurate predictions of diffusion coefficient from chloride conductivity data.

Lack of sufficient data for most of the parameters proved to be the main hindrance during the statistical quantification process. The distribution of the critical chloride concentration C_{crit} parameter was adopted from literature due to lack of local available data. However, the value adopted was applicable only to Portland cement. Other distribution types or statistical quantities representing C_{crit} for other binder types such as Fly Ash were not available. This in turn made it difficult to use the probabilistic model effectively in predicting time to corrosion initiation for other binder types other than Portland cement. It is therefore recommended that a further study on the parameter be carried out so as to acquire data for its quantification.

For the surface chloride concentration (C_s), additional data should be collected by sampling repeatedly from selected positions in the monitored structure. This will allow for the availability of information relating to short-term and long-term trends of C_s which in turn leads to the improvement of the SLP model.

4.8.3 General conclusion

The probabilistic approach presented in this study considers uncertainties in the SLP model parameters and hence leads to more accurate predictions of service life. The basic approach used in the model is similar to several other probabilistic prediction models but the proposed model applies the chloride conductivity (durability index) test to determine values for the material resistance parameter.

Further, using a probabilistic approach makes it possible to carry out a sensitivity analysis of the SLP model parameters. The results of a sensitivity analysis offer the designer useful

insights of the importance of different input parameters to the overall failure probability. Such knowledge is essential in identifying the important parameters to which attention should be given to so as to have a better assessment of their values and, accordingly, to reduce the overall uncertainty of the failure probability.

The methodology presented in this study for the durability design of RC structures prone to chloride-induced corrosion can similarly be applied to design of other forms of deterioration using their respective deterioration models. This recommendation is presented in Chapter 5 where the application of the probabilistic approach is recommended for the SA corrosion initiation prediction model for carbonation-induced corrosion.

University of Cape Town

4.9 REFERENCES

- Alexander, M.G., (2008)**, Personal Communication on 8th September.
- Alexander, M.G., Ballim, Y., Stanish, K., (2007)** Specifying Durability Index Limits for Reinforced Concrete Construction, (Current recommendations as at August 2007)
- Alexander, M.G., Mackechnie, J.R. and Ballim, Y. (1999)** Guide to the use of durability indexes for achieving durability in concrete structures. *Research Monograph No 2*, Department of Civil Engineering, University of Cape Town, 35 pp.
- Ang, A.H.S., Tang, W.,H., (2007)**, *Probability Concepts in Engineering-Emphasis on Applications to Civil and Environmental Engineering*, John Wiley & Sons, 2nd edition, pp. 406
- Ballim, Y., Basson, J., (2001)** Durability of Concrete, *Fulton Concrete Technology*, Eighth Edition, Eds. B. Addis B. and G. Owens G. (Cement Concrete Institute, South Africa), pp. 135-161.
- Bamforth and Price, (1993)**, Factors Influencing Chloride Ingress into Marine Structures, Edited by Ravindra, Dhir, Jones, E&F Spoon.
- BS 1881: Part 204 (1988)**, Testing Concrete-Recommendations on the use of Electromagnetic Cover meters.
- Chambers, J., Cleveland, W., Kleiner, V., and Tukey, P., (1983)**, *Graphical Methods for Data Analysis*, Wadsworth
- Collins, F.G. Grace, W.R. (1997)**, Specification and testing for corrosion durability of marine concrete, The Australian perspective, in: V.M. Malhotra (Ed.), *Proceedings of the 4th CANMET/American Concrete Institute International Conference on Durability of Concrete*, Sydney, Australia, August 1997, SP 170-39, American Concrete Institute, 1997, pp. 757–776.
- Concrete Society (1996)**, Developments in Durability Design & Performance-based Specification of Concrete, *Discussion document*, pp. 69.
- CONCUR.xcl (1996)**, Spreadsheet for SLP, Available in www.uct.civil.ac.za webpage

- Crowder, M.J., Kimber, A.C., Smith, R.L., Sweeting, T.J., (1991)**, *Statistical Analysis of Reliability Data*, Chapman and Hall, London.
- Du Preez, A.A., (2002)**, A Site Based Study of Durability Indexes for Concrete in Marine Conditions, Masters thesis, University of Cape Town.
- Duprat, F., (2007)**, Reliability of RC beams under chloride ingress, *Construction and Building Material*, 21(8), pp. 1605-1616.
- DuraCrete, (1997)**, *Design Framework*, Document BE95-1347/R1, the European Union – Brite EuRam III, Contract BRPR-CT95-0132, Project BE95-1347.
- DuraCrete, (1998)**, *Modelling of degradation*, The European Union – Brite EuRam III, Project BE95-1347, Probabilistic performance based durability design of concrete structures.
- DuraCrete, (1999)**, *Probabilistic Methods for Durability Design*, Document BE95-1347/R0, The European Union – Brite EuRam III, Contract BRPR-CT95-0132, Project BE95-1347.
- DuraCrete, (2000a)**, *General Guidelines for Durability Design and Redesign*, The European Union – Brite EuRam III, Project BE95-1347/R15, Probabilistic Performance based Durability Design of Concrete Structures.
- Duracrete, (2000b)**, *Statistical Quantification of the Variables in the Limit State Functions*, The European Union - Brite EuRam III, Project BE95-1347/R9, Probabilistic Performance-based Durability Design of Concrete Structures.
- EN 1990 (2000)** Eurocode: Basis of structural design. British Standards Institution.
- EN 1992-1, (2002)** Eurocode 2: Design of Concrete Structure - Part 1: General rules and rules for buildings, CEN (European Committee for Standardization), Brussels, 2002.
- EN 206 (2000)** Concrete - Part 1: Specification, performance, production and conformity. British Standards Institution: 70 pp.
- Exploratory Data Analysis (EDA) (2006)**, *Engineering Statistics Handbook*, Internet edition: <http://www.itl.nist.gov/div898/handbook/eda/eda.htm> [Downloaded 11/09/2008 9:56:13 AM]
- Faber, M.H., Straub, D., (2006)** A Computational Framework for Risk Assessment of RC Structures Using Indicators, *Computer-Aided Civil and Infrastructure Engineering* 21, pp. 216–230.

- Ferreira, R. M., (2006)**, *Improving Durability through Probabilistic Design*, Doctorate Thesis, University of Minho, Portugal.
- FIB Model Code for Service Life Design (2006)** *fib Bulletin* 34, EPFL Lausanne, 116 pp.
- Ghods, P., Alizadeh, R., Chini, M., Hoseini, M., Ghalibafian, M., Shekarchi. M., (2007)**, Durability-Based Design in the Persian Gulf, *Concrete International*, Dec. 2007 pp. 50-55.
- Glanville, J. Neville, A. (Editors) (1997)**, Prediction of concrete durability, *Proceedings of STATS 21st Anniversary Conference*, E&FN Spon, London UK, pp. 185.
- Goltermann, P., (2003)** Chloride Ingress in Concrete Structures: Extrapolation of Observations, *ACI Materials Journal*, 100(2), pp.114-120
- Gregory W. G., (2007)**, Service Life Modelling Of Virginia Bridge Decks, *Virginia Polytechnic Institute and State University PhD Thesis*, 2007.
- Holický M., (2007b)** Introduction to Reliability and Risk Analysis, *Lecture Notes in Reliability based design course held at University of Stellenbosch*, 2007 .
- Hooton, R.D., Geiker, M.R., Bentz, E.C., (2002)**, Effects of curing on chloride ingress and implications on service life, *ACI Materials Journal*, 99(2), pp. 201-207.
- Kun, H., Meeden, G., (1997)**, Selecting the number of bins in a histogram: A decision Theoretic Approach, *Journal of Statistical Planning and Inference*, 61(1997), pp. 59.
- Kottegoda, N.T., Rosso, R., (1998)**, Statistics, Probability and Reliability for Civil and Environmental Engineers, McGraw-Hill Edition, pp. 735.
- Leira, B. J., Hynne, T., Lindgård, J., (2000)**, Marine Concrete Structures Subjected to Chloride Attack: Probabilistic Lifetime Assessment, *Proceedings of the ETCE/OMAE2000 Joint Conference: Energy for the New Millennium. American Society of Mechanical Engineers (ASME)*, New Orleans, USA, 2000
- Li, Y., (2004)**, *Effect of spatial variability on maintenance and repair decisions for concrete structures*, Doctorate Thesis, University of Delft.
- Mac Donald, K., (1992)**, *The Diffusion of Chloride Ion In Cement Paste*, MSc. Thesis, Department of Mechanical Engineering, University of Windsor.

- Mackechnie, J.R., (1996)**, Prediction of reinforced concrete durability in the marine environment, *University of Cape Town, PhD thesis*, 1996.
- Mackechnie, J.R., Alexander M. G., (1997)**: Exposure of concrete in different marine environments, *Journal of materials in civil engineering*, 9(1), pp. 41-44
- Mackechnie, J.R., Alexander, M.G., (1996b)**, Marine Exposure of Concrete under selected South African Conditions, *3rd CANMET/ACI International conference on performance of concrete in marine environment*
- McGee R., (2000)**, Modelling of durability performance of Tasmanian bridges. In: Melchers RE, Stewart MG, editors. *Applications of statistics and probability in civil engineering*, Rotterdam: Balkema, p. 297–306.
- Neville, A.M., (1995)** *Properties of Concrete*, Prentice Hall, 4th Edition, pp. 864.
- Nokken, M., Boddy, A., Hooton, R.D., Thomas, M.D.A., (2004)**: Time Dependent Diffusion in Concrete- Three Laboratory Studies, *Cement and Concrete Research*, 36(2006), pp. 200-207
- Quinn, G.P. and Keough, M.J., (2002)**, *Experimental Design and Data Analysis for Biologists*, Cambridge University Press, pp. 537.
- Ronne, P., Beushausen, H.D., (2008)**, Concrete cover depth-variations observed in practice and reliability of measurement techniques, *Concrete Plant International*, pp. 82-89.
- Ronne, P.D., (2005)**, Variation in Cover to Reinforcement: Local and International Trends, *Concrete Beton*, 111.
- SABS (1997)**, Portland cement (ordinary rapid-hardening and sulphate resisting)
- SABS 0100-2 (1992)** South African National Standard: The Structural use of Concrete, Part 2: Materials and Execution of Work.
- Scott, D. W., (1979)**, On optimal and data-based histograms, *Biometrika*, 66(1979), pp.605-610.
- Sharp, B., (1997)**, Criteria for Cover- ‘a black hole’, *Concrete for the Construction Industry*, 31(6), pp.34-38
- Suryavanshi, A.K., Swamy, R.N., Cardew, G.E., (2002)**, Estimation of diffusion coefficients for chloride ion in penetration into structural concrete, *American Concrete Institute Journal*, 99(5), pp. 441-450.

Swamy, R. N., (1997), Design for Durability and Strength through the Use of Fly Ash and Slag in Concrete, Advances in Concrete Technology, *Proceedings of the Third CANMET/American Concrete Institute International Conference*, SP-171, V. M. Malhotra, ed., American Concrete Institute, Farmington Hills, Michigan, pp. 1-72.

Tikalsky, P.J. Pustka, D. and Marek, P. (2005), Statistical Variations in Chloride Diffusion in Concrete Bridges, *American Concrete Institute Structural Journal*, May-June 2005, pp. 481-487.

Vassie PR., (1984) Reinforcement corrosion and the durability of concrete bridges, *Proceedings of the Institution of Civil Engineers*, 76(8), pp.713–23.

Zemajtis, J., (1998), Modelling the time to corrosion initiation for concretes with mineral admixtures and/ or corrosion inhibitors in chloride-laden environments, Dissertation in Civil Engineering, Virginia Polytechnic Institute and State University, 1998

CHAPTER 5: CONCLUSION and RECOMMENDATIONS

5.1 SUMMARY

5.1.1 Service Life Prediction

Many reinforced concrete (RC) structures in the marine environment fail to fulfill their design working life due to chloride-induced reinforcement corrosion. As a result, reliable and practical service life design methods have been sought to effectively design new RC structures which will require less maintenance and repair over their lifetime.

This study identified a number of service life design (SLD) approaches to durability that are incorporated in current standards and codes of practice such as the FIB Model Code (Service Life Design) and ISO 15686-8 (2008) The SLD approaches reviewed were:

- (i) avoidance of deterioration approach
- (ii) a reference factor method,
- (iii) partial factor design approach,
- (iv) deemed to satisfy approach and,
- (v) the full probabilistic approach,

The avoidance-of-deterioration approach enhances the durability of RC by reducing the risk of reinforcement corrosion, through the use of materials that will not deteriorate, based on expert judgement.

Both the reference factor method (ISO 15686) and the partial factor design method (FIB model code) use partial safety factors determined from engineering judgement and experience to account for deviations that may occur between the estimated and the actual service life.

The design against chloride ingress for RC structures in South Africa is currently carried out using the deemed-to-satisfy approach. The approach gives the limits of the chloride conductivity (durability index) values and cover depths, for given environmental classes and selected binder types, which will ensure the structures durability. The limiting chloride conductivity values are derived from a Fickian-type service life prediction (SLP) model developed by Mackechnie (1996). The main set-back of this model is that it gives a deterministic output which contrasts with the well known fact that concrete properties are

quite variable both throughout the structure and in terms of quality of construction and materials used. Thus, there has been an increasing need to adopt the full probabilistic approach and hence the reason for this study.

The full-probabilistic approach was applied in this study to account for variability in:

- (i) Concrete material properties (diffusivity) which was represented by a diffusion variable derived from chloride conductivity measurements taken from the chloride conductivity test (CCT). The CCT characterises the microstructure of the cover concrete and has been shown to be sensitive to most of the quality related concrete material parameters such as binder type, processing influences (such as type and degree of curing), and environmental influences (such as temperature and relative humidity).
- (ii) Structural geometry represented by the cover depth.
- (iii) Micro-environmental load which was represented by the surface chloride concentration for each environmental condition.

The range of possible values for each random variable and the different likelihood of realizations were represented using various statistical descriptors which included: sample mean, standard deviation and probability distribution function. In addition, a variable representing the model uncertainty due to use of the idealised relationship between the diffusion variable and the 28-day chloride conductivity value was applied. The effect of this 'model uncertainty variable' was to increase the scatter of the predictions made using the SLP model.

These variables were effectively represented in a LSF analogous to structural design theory. The design was carried out using Monte Carlo simulations to give values for material resistance against chloride penetration (diffusion coefficient and chloride conductivity values) that were expected to meet the requirements for service life of the RC members under the influence of chloride ion ingress. The design specifications were kept within an acceptable target probability value Φ_{target} corresponding to the degree or risk of failure (corrosion initiation) that may occur during the design service life.

A number of advantages relating to probabilistic design methods have been identified. The probabilistic methods:

- (i) Provide the means of dealing with uncertainties in concrete durability parameters.
- (ii) Result in efficient and possibly economical use of materials.
- (iii) Allow for future changes as a result of additional information gained in SLP models, material and load characterisation.
- (iv) Provide sensitivity factors that can be used for defining future research and development needs.

Notwithstanding, the full probabilistic approach was found to have its inherent problems which are presented in the next sub-sections.

5.1.1.1 Different interpretations of target probability of failure

In literature, there is no clarification on what the practical meaning of a certain probability of corrosion initiation is in terms of either degree of steel depassivation, damaged concrete surface area or maintenance costs. Consequently, the accepted probability for corrosion initiation $P_{target,ILS}$ varies between different standards depending on the interpretation made of the ‘probability of corrosion initiation’.

There is therefore a need to establish a standard criterion to be used in determining the acceptable probability of exceeding the durability limit state.

5.1.1.2 Lack of data for statistical quantification

The second setback of the probabilistic approach was found to arise from the fact that the method relies on characterising each parameter in terms of mean, standard deviation and statistical distribution. When sufficient data are available, probability theory is the dominant and effective way to model uncertainties. However, in most circumstances especially in this study, the amount of data available for most of the parameters in the LSF are limited, this then creates a hindrance in the subsequent statistical quantification process.

5.1.1.3 Reliance on numerical methods

The probabilistic method relies heavily on numerical methods for analysis. It requires the use of statistical software packages that incorporate numerical methods such as Monte Carlo simulation. For this study both the Monte Carlo simulation technique and the First Order Reliability method (FORM) were illustrated for use in analysis. For the FORM (illustrated in Appendix G), the additional number of variables introduced from the Maclaurin expansion of the error function up to the 8th polynomial made the method labour intensive and complex.

5.1.2 Importance of the study

5.1.2.1 Accounting for Uncertainties in Service Life Prediction

The probabilistic (reliability) approach considers not only the mean values of durability parameters but also their scatter. The approach combines the use of deterioration models and compliance tests to predict the occurrence of a limit state for a given set of durability parameters. The probabilistic design method has been applied to several degradation models, such as in the Brite-EuRam project BE95-1347, called DuraCrete project (1996-1999) where the approach was subsequently applied in the design of structures such as the Western Scheldt Tunnel in 2000. Within the Duracrete model the Rapid Chloride Migration test was adopted as the standard laboratory test method to quantify the potential chloride transport properties of a concrete mix (DuraCrete, 2000).

This study follows similar principles to design as the DuraCrete approach except in two ways. First the study applies a South African prediction model to specify material parameters that will ensure the concrete remains durable within its service life. Secondly, the model used applies the chloride conductivity (durability index) test to determine values for the material resistance parameter.

The findings of this work are potentially valuable in that they provide an understanding on the use of the chloride conductivity test in probabilistic modelling for durability design of RC members. The chloride conductivity test (CCT) is one of South Africa's durability index (DI) tests and measures the resistance of concrete to chloride conduction under the action of an applied voltage across the specimen. The high precision (repeatability and reproducibility) and the short duration of the CCT make it useful in obtaining the material parameter data required to support the use of degradation models.

In addition, the probabilistic approach assists in accounting for the inherent variability in concrete. The study demonstrated the application of Monte Carlo simulation technique to predict, the probability of failure (corrosion initiation) during the service life of a RC element. Results of the reliability-based design (RBD) gave the design parameters (i.e. the chloride conductivity value and the cover depth) that would ensure the RC element met its performance requirements with an acceptable probability level.

5.1.2.2 Sensitivity Analysis

The probabilistic method is not restricted to predicting the probability of failure due to chloride ingress. It was shown to be useful for evaluating the sensitivity of the SLP model parameters to the probability of failure. The sensitivity study performed indicated the most influential parameter, to failure probability, to be concrete cover, followed by the diffusion coefficient, critical chloride content and lastly surface chloride concentration.

Therefore, during design attention should be given to cover depth so as to reduce the overall uncertainty of the failure probability. At the same time, other factors such as water-cement ratio and protection condition, which will affect the quality of concrete cover, should also be taken into consideration.

5.2 LIMITATIONS AND FUTURE RESEARCH

5.2.1 Limitations in analysis

Accurate/reliable statistical quantification of any parameter in the LSF depends on the availability of data. This aspect could not be covered adequately for all durability parameters in this study. During the quantification of surface chloride concentration (C_s) data statistical uncertainties arose due to the limited number of observations. It is the recommendation of this study that further chloride profiling tests be carried out on marine structures to build up the database and hence provide more representative results. The process of obtaining additional data from a structure should first take into account the spatial variability of certain elements in the structure. It is proposed that concrete structures be represented by means of concrete surfaces belonging to different categories. The surfaces are categorised depending on their orientation to the source of the chlorides. The individual concrete surfaces are divided into zones with similar initial condition indicators and bear the same risk to corrosion. Samples should then be taken repeatedly from the respective zones in the structure being monitored.

The advantage of using this approach in sampling of mature concretes is that it is possible to establish a more realistic assessment of the chloride ingress with time i.e. information about the short-term to long-term trends becomes available. In addition, it is possible to check the accuracy of the data. The accuracy will be limited by local variations in the presumed uniform area, the exposure variations over the years and the accuracy of the Fickian model used in the curve fitting process.

During the classification of the data for each parameter into datasets (with similar properties) it was noted that relevant information on construction practices such as curing was not well documented for most of the structures investigated. It is recommended that in future studies the water sorptivity test, (see Appendix F) would be useful in obtaining data on new structures for some of the material parameter sub-sets e.g. the degree of curing and quality of construction. The water sorptivity test has been found sensitive to the effects of initial moist curing and can thus be used to characterise the quality of early age (28-day) concrete (Ballim *et al.*, 2000).

The distribution of the critical chloride concentration (C_{crit}) was adopted from literature due to lack of local data. However, the value adopted was applicable only to Portland cement. Other distribution types or statistical quantities representing C_{crit} for other binder types such as Fly Ash were not available. This in turn made it difficult to use the probabilistic model effectively in predicting time to corrosion initiation for other binder types other than Portland cement. It is therefore recommended that a further study on the parameter be carried out so as to acquire data for its quantification.

5.2.2 Limitations in the service life prediction model

The design against chloride induced corrosion using chloride conductivity values is based on empirical relationships between 28-day chloride conductivity value and 2 year diffusion coefficients' and was established from 2 different techniques (Mackechnie, 1996b):

- (i) Correlation between 28-day conductivity index values and chloride ingress in structures in the Western Cape Province.
- (ii) Laboratory-based experimental correlations between 28-day conductivity index values and chloride diffusion coefficients.

This idealised relationship introduces errors in the prediction capability of the model. Further, the idealised relationship does not take into account the various marine environmental

conditions in South Africa. Chloride ingress is dependent on environmental conditions such as sea water and air temperature and relative humidity. These conditions vary widely along the South African coastline, for example sea temperatures along the Atlantic side of the Cape Peninsula were found to be on average 5°C lower than the adjacent False Bay while sea temperatures at East London (side bordering the Indian ocean) were on average several degrees warmer than those in False Bay (Mackechnie, 1996).

Further work is necessary to test 28-day conductivity index values against chloride ingress in various marine environments in South Africa. A study is currently in place at the University of Cape Town, to investigate the ingress of chlorides into various different types of concrete based on site exposure in the Cape Town and Durban harbours. In this study, measurements taken on site-exposed samples are correlated to laboratory-based measurements of chloride conductivity index values and diffusion coefficients. These correlations are expected to refine the existing service life models and make it applicable to various regions in South Africa.

5.3 CONCLUSIONS

Based on this thesis work the following main conclusions can be drawn:

1. This work has demonstrated the importance of accounting for the high variability that exists in basic variables for durability design. Uncertainties in concrete material properties, structural geometry and micro-environmental load were successfully accounted for and represented using stochastic quantities (mean, coefficient-of-variation and probability density function).
2. The application of a probabilistic model to design for durability not only involves selecting appropriately the materials and the mix proportion of concrete and deciding structural details of the structure but also ensuring the reliability of performance of the designed structure throughout the service life.
3. The probabilistic methods allow for sensitivity studies to be carried out of the response of LSF parameters to the failure probability. The sensitivity study is useful as it gives the designer insight to the parameters of the LSF that are more influential in the design. The designer would then use this information to define future research and development needs.

5.4 RECOMMENDATIONS

Based on this thesis work the following main recommendations are given:

5.4.1 Bayesian updating of probability distribution functions

When additional data are obtained from further laboratory or in-situ studies, then the distribution functions recommended for the respective parameters can be updated using Bayesian theory.

5.4.2 Validating the probabilistic model

The proposed probabilistic SLP model for chloride-induced corrosion should be sufficiently verified on existing concrete structures. The model should be calibrated against uncertainties in material properties and environmental influences using data gathered from existing structures. The calibrated model would then be applied during the design and construction phases of new structures to give realistic and representative results of material resistance parameters, in the form of appropriate combination of concrete quality (DI value) and cover.

5.4.3 Probabilistic carbonation model

The main cause of deterioration of RC elements or structures was identified in this study as due to reinforcement corrosion caused by ingress of chlorides or carbon dioxide gas (CO_2). The former cause was adequately covered in this study whereby it was shown that the main process of chloride ingress for RC elements was due to diffusion. The diffusion process was modelled using Fick's second law of diffusion. The chloride conductivity test was found useful in theoretically determining a diffusion coefficient value for the Fickian model.

Carbonation induced corrosion affects structures in the XC4 environmental class (EN 206 classifications-see Table 5.2), which are exposed to moist conditions during the cyclic wetting of the concrete (Mackechnie, 2004).

Table 5.2: Carbonation Exposure Classes (Natural environments only) (after EN206-1 as cited in Alexander *et al.*, 2001)

Carbonation Induced Corrosion		
Designation	Description	Range of average RH* (%)
XC1	Permanently dry or permanently wet	≤ 65
XC2	Wet, rarely dry	91-100
XC3	Moderately humid	60 -80
	(External concrete sheltered from rain)	
XC4	Cyclic wet and dry	80-90

RH[#] = Relative humidities within the concrete proposed in a Concrete society discussion document (1996)

A proposal is made for future research to carry out a reliability based design of RC structures that are prone to carbonation induced corrosion. The design will follow the same general procedure for chloride induced corrosion presented in this thesis. This will involve selecting a carbonation model that allows for the expected service life of a structure to be predicted based on considerations of environmental conditions, cover thickness and concrete quality.

5.5 REFERENCES

- Alexander, M.G., Ballim, Y., Mackechnie, J.R., Horton, J., (2001)** Durability Index Tests- Further notes on the aspects related to testing and variability, *Research monograph No. 4*, UCT/Wits, 1999.
- Ballim, Y. and Alexander, M.G., (2000)**, Research in concrete deterioration and durability, in 'A review and some thoughts on future developments', *Proceedings of a Colloquium on South African research needs in cement and concrete*, Pretoria, 2000 (NRF) 44.
- Concrete Society (1996)**, Developments in Durability Design & Performance-based Specification of Concrete, *Discussion document*, pp. 69.
- Duracrete, (2000)**, *Statistical Quantification of the Variables in the Limit State Functions*, The European Union - Brite EuRam III, Project BE95-1347/R9, Probabilistic Performance-based Durability Design of Concrete Structures.
- EN 206 (2000)** Concrete - Part 1: Specification, performance, production and conformity. British Standards Institution: 70 pp.
- Mackechnie, J.R., Alexander, M.G., (1996b)**, Marine Exposure of Concrete under selected South African Conditions, *3rd CANMET/ACI International conference on performance of concrete in marine environment*
- Mackechnie, J.R., Alexander, M.G., (2004)**, Durability predictions using early-age durability index testing, *9th DBMC proceedings*.
- Mackechnie, J.R., Alexander, M.G., Heiyantuduwa, R., Rylands, T., (2004)**, The effectiveness of organic corrosion inhibitors for reinforced concrete, *Research monograph No.7*, UCT, 2004.

APPENDIX A: SURFACE CHLORIDE CONCENTRATION DATA

I. EXTREME SPLASH and TIDAL ENVIRONMENT
Table A.1: Surface chloride concentration of CEM I + Slag concrete in extreme splash and tidal environment

Samples	Structure #	Element Number	Cement (g/m^3)	Slag (g/m^3)	W-B	Age (Years)	C_s (% by mass of binder)
1	EL BW 2	E5	148	148	0.7	28	3.25
2	EL BW 2	E6	148	148	0.7	28	3.50
3	EL BW 2	E7	148	148	0.7	28	5.53
4	EL BW 2	E8	148	148	0.7	28	7.65
5	EL BW 2	E9	148	148	0.7	28	9.75

Table A.2: Surface chloride concentration of OPC + FA concrete in extreme splash and tidal environment

Samples	Structure #	Element Number	Cement (g/m^3)	FA (g/m^3)	W-B	Age (Years)	C_s (% by mass of binder)
1	SFTP	S1	265	114	0.61	13	3.50
2	SFTP	S2	265	114	0.61	13	4.50
3	SFTP	S4	265	114	0.61	13	6.25
4	SFTP	S5	265	114	0.61	13	4.75
5	SFTP	S6	265	114	0.61	13	4.25
6	SFTP	S7	265	114	0.61	13	4.50
7	SFTP	S8	265	114	0.61	13	4.90

Table A.3: Mix composition of **OPC** concrete structures in extreme splash and tidal environment (adopted from Mackechnie, 1996)

Samples	Structure #	Element Number	Cement (g/m^3)	W-B	Age (years)	C_s (% by mass of binder)
1	ELBW 2	E1	295	0.68	28	3.2
2	ELBW 2	E2	295	0.68	28	3.25
3	ELBW 2	E3	295	0.68	28	3.75
4	ELBW 2	E4	295	0.68	28	3.25
5	HBM	M13A	NG	NG	6	3.4
6	HBM	M14A	NG	NG	6	5.8
7	HBM	S31A	NG	NG	6	3.65
8	HBM	P1A	NG	NG	6	1.38
9	HBM	P2A	NG	NG	6	1.57
10	HBM	P3A	NG	NG	6	2.71
11	HBM	P5A	NG	NG	6	1.81
12	HBM	P6A	NG	NG	6	2.88
13	HBM	P11A	NG	NG	6	2.32
14	HBM	P12A	NG	NG	6	1.98
15	HBM	P33A	NG	NG	6	2.12
16	KBTP	K1	438	0.4	3	1.83
17	KBTP	K2	438	0.4	3	2.56
18	KBTP	K3	438	0.4	3	2.76

Structure # = refer to Table 4.1 for details of structure

NG= Not given

Outlier

Table A.4: Mix composition of **LASRC** concrete structures in extreme splash and tidal environment (adopted from Mackechnie, 1996)

Samples	Structure #	Element Number	Cement (g/m^3)	W-B	Age (years)	C_s (% by mass of binder)
1	TBBW	D1	NG	0.47	6	1.7
2	TBBW	D2	NG	0.47	6	1.65
3	TBBW	D3	NG	0.47	6	2.1
4	TBBW	D1	NG	0.47	6	1.7
5	TBBW	D2	NG	0.47	6	1.65
6	TBBW	D3	NG	0.47	6	2.1
7	TBBW	D1	NG	0.47	6	1.7
8	TBBW	D2	NG	0.47	6	1.65
9	TBBW	D3	NG	0.47	6	2.1
10	TBBW	D7	NG	0.47	6	1.35
11	TBBW	D8	NG	0.47	6	1.25
12	TBBW	D9	NG	0.47	6	1.35
13	TBBW	D4	NG	0.47	6	1.85
14	TBBW	D5	NG	0.47	6	1.8
15	TBBW	D6	NG	0.47	6	1.55
16	TBBW	D10	NG	0.47	6	1.35
17	TBBW	D11	NG	0.47	6	1.25
18	TBBW	D13	NG	0.47	6	2

II. VERY SEVERE SPLASH and TIDAL ENVIRONMENT

Table A.5: Mix composition of **OPC** concrete structures in very severe splash and tidal marine environment (adopted from Mackechnie, 1996)

Samples	Structure #	Element Number	Cement g/m^3	W-B	Age (years)	C_s (% by mass of binder)
1	STJ	J1	325	0.75	75	6.00
2	STJ	J2	325	0.75	75	6.00
3	STJ	J4	325	0.75	75	6.00
4	STJ	J5	325	0.75	75	4.50
5	STJ	J6	325	0.75	75	3.50
6	STJ	J7	325	0.75	75	4.50
7	STJ	J8	325	0.75	75	4.00
8	STJ	J9	325	0.75	75	3.50
9	STJ	J10	325	0.75	75	5.00
10	ORW	O1	360	0.56	19	4.25
11	ORW	O2	360	0.56	19	3.25
12	SPA	Q1	270	0.75	55	4.75
13	SPA	Q3	270	0.75	55	4.50
14	SPTB	T6	NG	0.75	48	1.43
15	SPTB	T7	NG	0.75	48	1.07
16	WBS	W4	NG	NG	25	4.83
17	WBS	W5	NG	NG	25	3.97
18	WBS	W7	NG	NG	25	3.51
19	SRB	S1	NG	NG	67	3.26
20	SRB	S2	NG	NG	67	3.75
21	SRB	S4	NG	NG	67	2.62
22	SRB	S5	NG	NG	67	2.03
23	SRB	S6	NG	NG	67	2.33
24	SRB	S9	NG	NG	67	0.36
25	SRB	S10	NG	NG	67	1.35
26	SRB	S11	NG	NG	67	0.93
27	SRB	S12	NG	NG	67	2.13
28	SRB	S13	NG	NG	67	1.72
29	SRB	S14	NG	NG	67	2.25
30	SRB	S15	NG	NG	67	1.99
31	SRB	S16	NG	NG	67	0.36
32	SRB	S17	NG	NG	67	0.99
33	SRB	S18	NG	NG	67	1.93

Structure # = refer to Table 4.1 for details of structure
 NG = Not given

III.VERY SEVERE SPRAY ENVIRONMENT

Table A.6: Mix composition of PC concrete structures in very severe spray environment (adopted from Mackechnie, 1996)

Samples	Structure #	Element Number	Cement (g/m^3)	W-B	Age (years)	C_s (% by mass of binder)
1	MZB	M1	NG	0.67	38	3.53
2	MZB	M2	NG	0.67	38	3.42
3	MZB	M3	NG	0.67	38	3.35
4	MZB	M4	NG	0.67	38	1.88
5	MZB	M5	NG	0.67	38	0.91
6	MZB	M6	NG	0.67	38	2.85
7	MZB	M7	NG	0.67	38	2.40
8	MZB	M8	NG	0.67	38	3.65
9	MZB	M9	NG	0.67	38	2.80
10	MZB	M10	NG	0.67	38	6.52
11	MZB	M11	NG	0.67	38	4.80
12	MZB	M12	NG	0.67	38	2.50
13	MZB	Z1	NG	0.67	38	3.80
14	MZB	Z2	NG	0.67	38	1.72
15	MZB	Z3	NG	0.67	38	2.48
16	MZB	Z4	NG	0.67	38	2.65
17	MZB	Z5	NG	0.67	38	3.08
18	MZB	Z8	NG	0.67	38	0.85
19	MZB	Z9	NG	0.67	38	0.88
20	MZB	Z10	NG	0.67	38	4.53
21	WB	T1	NG	0.75	46	0.91
22	WB	T2	NG	0.75	46	1.67
23	WB	T4	NG	0.75	46	1.00
24	WB	T5	NG	0.75	46	3.10
25	WB	T6	NG	0.75	46	3.45
26	WB	L1	NG	0.75	46	0.23
27	WB	L2	NG	0.75	46	1.95
28	WB	L3	NG	0.75	46	2.04
29	WB	L4	NG	0.75	46	0.06

Structure # = refer to Table 4.1 for details of structure

NG= Not given

Outlier

IV. SEVERE SPRAY ENVIRONMENT

Table A.7: Mix composition of OPC concrete structures in severe spray environment (adopted from Mackechnie, 1996)

Samples	Structure #	Element Number	Cement (g/m^3)	W-B	Age (years)	C_s (% by mass of binder)
1	KPS	K1	NG	0.67	12	1.75
2	KPS	K2	NG	0.67	12	0.85
3	KPS	K3	NG	0.67	12	0.75
4	KPS	K4	NG	0.67	12	0.80
5	KPS	K5	NG	0.67	12	2.10
6	KPS	K6	NG	0.67	12	1.85
7	KPS	K7	NG	0.67	12	0.65
8	CBPS	C1	420	0.47	18	1.00
9	CBPS	C2	420	0.47	18	1.35
10	CBPS	C3	420	0.47	18	1.35

Structure #= refer to Table 4.1 for details of structure
 NG= Not given

V. SUBMERGED ENVIRONMENT

Table A.8: Surface chloride concentration of submerged OPC concrete

Samples	Structure #	Element Number	Cement (g/m^3)	W-B	Age (years)	C_s (% by mass of binder)
1	SS1	S2	180	0.4	1	1.31
2	SS1	S13	180	0.4	1	2.53
3	SS1	S20	180	0.4	1	2.56
4	SS1	S4	297	0.6	1	1.99
5	SS1	S7	297	0.6	1	1.87
6	SS1	S14	297	0.6	1	2.62
7	SS1	S4	297	0.6	1	3.43
8	SS1	S11	297	0.6	1	3.87

Structure #= refer to Table 4.1 for details of structure

Table A.9: Surface chloride concentration of submerged OPC + FA concrete

Sample	Structure #	Element Number	Cement (g/m^3)	FA (g/m^3)	W-B	Age (years)	C_s (% by mass of binder)
1	SFTP	S4	265	114	0.61	13	6.21

Structure #= refer to Table 4.1 for details of structure

APPENDIX B: FITTING DISTRIBUTIONS TO SURFACE CHLORIDE DATA

I. EXTREME TIDAL AND SPLASH ENVIRONMENT (XS3b)

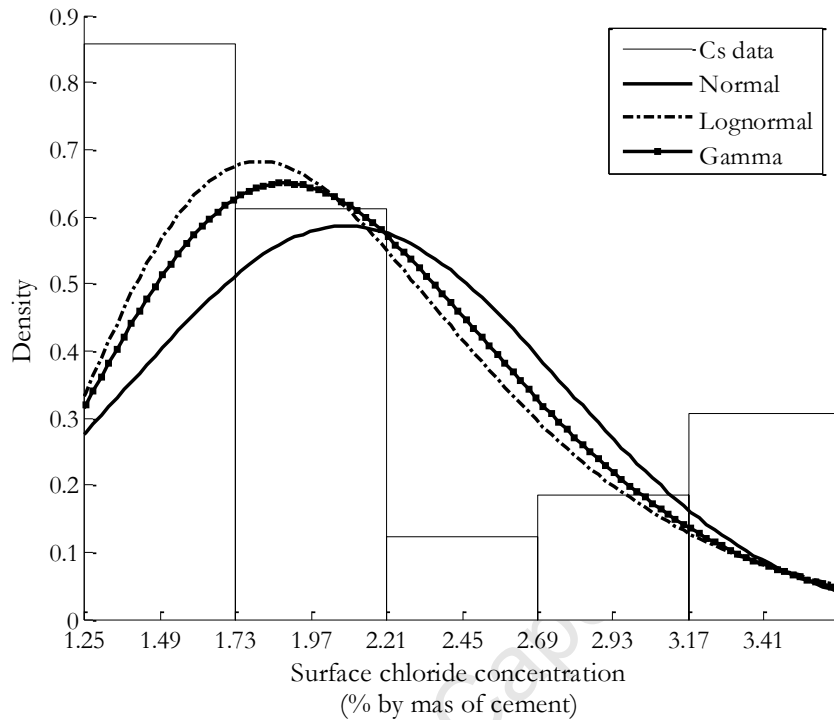


Figure B.1: Histogram and distribution fit of surface chloride concentration of OPC concrete in **extreme tidal and splash marine** environment

Table B.1: Computation of Chi-square tests of three distributions of OPC concrete in **extreme tidal and splash** marine environment

Interval C_s (% #)	Observed Frequency e_i	Theoretical Frequencies e_i			$\sum_{i=1}^k \frac{(e_i - e_i)^2}{e_i}$		
		Normal	Lognormal	Gamma	Normal	Lognormal	Gamma
0 - 1.25	0	0.56	0.10	0.23	0.56	0.10	0.23
1.25 - 1.73	2	1.43	1.43	1.54	0.23	0.23	0.14
1.73 - 2.21	4	3.01	3.96	3.63	0.32	0.00	0.04
2.21 - 2.69	2	4.23	4.67	4.46	1.17	1.53	1.36
2.69 - 3.17	3	3.95	3.42	3.55	0.23	0.05	0.09
3.17 - 3.65	5	2.46	1.90	2.07	2.63	5.06	4.13
3.65 - 10	1	1.36	1.52	1.52	0.09	0.18	0.18
Σ	17	17	17	17	5.23	7.15	6.15

(% #)= % of chlorides by mass of cement

From the chi-square test results in Table B.1 the normal distribution would be chosen as it gives the lowest value of $\sum_{i=1}^k \frac{O_i - e_i}{e_i}$ amongst the three distributions. To ensure that the correct distribution is not rejected, a hypothesis test is carried out on the chi-squared results (see Appendix D for details of a hypothesis test). At the significance level of $\alpha = 0.5\%$ and degree-of-freedom ($d.o.f = 7 - 3 = 4$), a critical value of $C_{0.95,4} = 7.78$, for all the distributions, is obtained from Table D.1 (Appendix D). The Chi-squared values of all three distributions are less than the critical and hence all the three distributions can be accepted for describing the distribution of C_s with a confidence level of at least 95%. However, even with both the Chi-squared value and the hypothesis test supporting the use of a normal distribution to describe C_s a critical physical examination of the data still needs to be carried out. The physical examination shows that the sample had a large variability ($COV=0.55 > 0.3$) that could be attributed to the small sample size. Hence, during the statistical analysis of the LSF a confidence interval of $3\sigma = \pm 3.72\%$ would have C_s , taking up negative values $C_s = 2.26\% \pm 3.72\%$, which in reality is not possible. For this reason, the normal distribution is disqualified and the next option of a non-negative distribution function would be to use the gamma distribution (which has a lower bound at zero) to model the surface chloride concentration in OPC concrete exposed to extreme tidal and splash marine environment as indicated by the next best value of $\sum_{i=1}^k \frac{O_i - e_i}{e_i}$ in Table B.1.

II. VERY SEVERE TIDAL AND SPLASH ENVIRONMENT

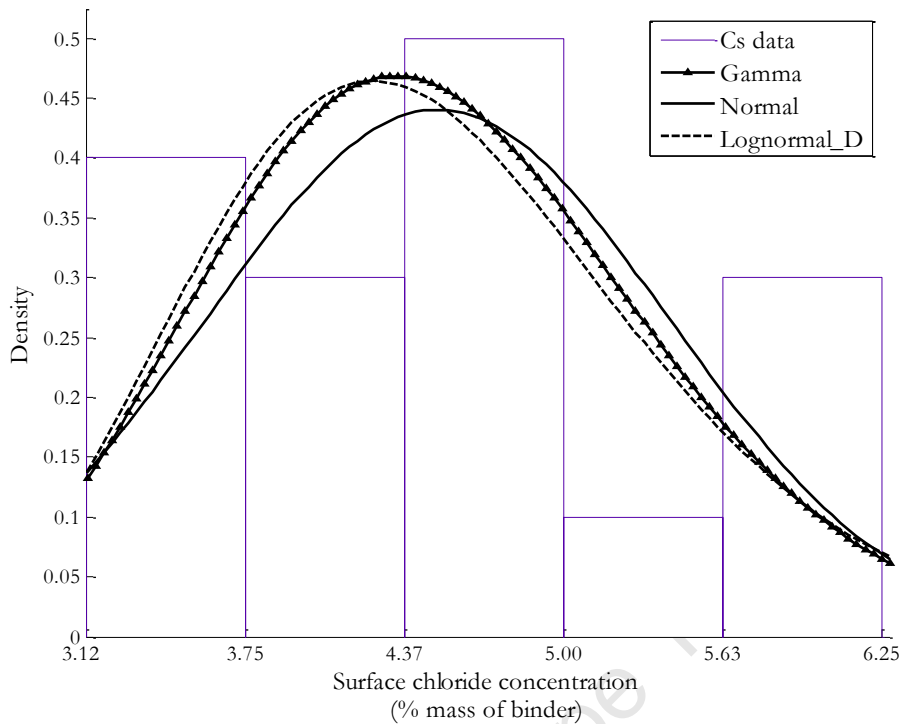


Figure B.2: Histogram and distribution fit of surface chloride concentration of OPC concrete in **very severe tidal and splash (XS3a)** marine environment

Table B.2: Computation of Chi-square tests of three distributions for OPC concrete in **very severe tidal and splash (XS3a)** marine environment

Interval C_s (% #)	Observed Frequency ϕ_i	Theoretical Frequencies e_i			$\sum_{i=1}^k \frac{(\phi_i - e_i)^2}{e_i}$		
		Normal	Lognormal	Gamma	Normal	Lognormal	Gamma
0 - 3.12	0	1.04	0.67	0.81	1.04	0.67	0.81
3.12 - 3.75	4	2.22	2.65	2.52	1.42	0.69	0.86
3.75 - 4.37	3	3.85	4.41	4.20	0.19	0.45	0.34
4.37 - 5.00	5	4.22	4.02	4.06	0.14	0.24	0.22
5.00 - 5.63	1	2.94	2.46	2.61	1.28	0.87	0.99
5.63 - 6.25	3	1.29	1.14	1.21	2.25	3.02	2.66
6.25 - 10.00	0	0.43	0.65	0.59	0.43	0.65	0.59
Σ	16	16	16	16	6.75	6.59	6.48

(% #) = % of chlorides by mass of cement

APPENDIX C: DIFFUSION COEFFICIENT DATA

I. MOIST CURED CONCRETE

Table C.1: Steady state (Effective) diffusion coefficient of **moist cured OPC+ CSF** concrete

Element Number	Element #	W/C	Chloride conductivity $\mu\text{S} / \text{cm}$	$D_{\text{effective}}$ m^2 / s
1	SC2:H(7)	0.455	1.61	7.92E-08
2	SC2:H(8)	0.455	1.65	8.39E-08
3	SC2:H(5)	0.455	1.51	6.70E-08
4	SC3:H(8)	0.455	1.20	4.12E-08
5	SC4:H(6)	0.455	0.76	2.03E-08
6	SC2:H(6)	0.455	1.47	6.34E-08
7	SC4:H(7)	0.455	0.83	2.28E-08
8	SC3:H(5)	0.455	1.24	4.39E-08
9	SC3:H(6)	0.455	1.12	3.58E-08
10	SC4:H(8)	0.455	0.71	1.86E-08
11	SC3:H(7)	0.455	1.12	3.61E-08
12	SC4:H(5)	0.455	0.74	1.95E-08

Element[#] = Refer to Table 4.11Table C.2: Steady state (Effective) diffusion coefficient of **moist cured OPC+ FA** concrete

Element Number	Element #	W/C	Chloride conductivity $\mu\text{S} / \text{cm}$	$D_{\text{effective}}$ m^2 / s
1	SB4:H(7)	0.455	0.91	1.61E-08
2	SB4:H(5)	0.455	0.81	1.47E-08
3	SB1: H(5)	0.455	0.98	1.73E-08
4	SB1: H(6)	0.455	1.04	1.83E-08
5	SB1: H(7)	0.455	1.07	1.88E-08
6	SB3:H8	0.455	0.59	1.19E-08
7	SB4:H(8)	0.455	1.01	1.78E-08
8	SB3:H7	0.455	0.65	1.26E-08
9	SB3:H6	0.455	0.70	1.32E-08
10	SB3:H5	0.455	0.70	1.33E-08
11	SB2: H(5)	0.455	1.67	3.33E-08
12	SB2: H(7)	0.455	1.67	3.31E-08
13	SB2: H(8)	0.455	1.67	3.33E-08
14	SB1: H(8)	0.455	0.95	1.68E-08
15	SB4:H(6)	0.455	0.76	1.40E-08

Element[#] = Refer to Table 4.11

Table C.3: Steady state (Effective) diffusion coefficient of **moist cured OPC+ GGBS** concrete

Element Number	Element #	W/C	Chloride conductivity ($\mu S / cm$)	$D_{effective}$ (m^2 / s)
1	SA3:H(6)	0.455	0.49	8.59E-09
2	WA: H(h)	0.455	0.53	8.87E-09
3	SA1: H(6)	0.455	0.34	7.47E-09
4	WA: H(g)	0.455	0.58	9.27E-09
5	SA4:H(6)	0.455	0.33	7.37E-09
6	SA4:H(7)	0.455	0.38	7.72E-09
7	SA1: H(7)	0.455	0.35	7.54E-09
8	SA1: H(5)	0.455	0.31	7.27E-09
9	SA4:H(5)	0.455	0.36	7.62E-09
10	SA3:H(5)	0.455	0.44	8.16E-09
11	SA2: H(3)	0.455	0.40	7.88E-09
12	WA: H(f)	0.455	0.57	9.19E-09
13	WA: H(e)	0.455	0.60	9.47E-09
14	SA2: H(4)	0.455	0.42	8.03E-09
15	SA2: H(2)	0.455	0.41	7.95E-09
16	SA1: H(8)	0.455	0.41	7.95E-09
17	SA3:H(7)	0.455	0.51	8.70E-09
18	SA3:H(8)	0.455	0.47	8.40E-09

Element[#] = Refer to Table 4.11

II. DRY CURED CONCRETE

Table C.4: Steady state (Effective) diffusion coefficient of **dry cured OPC+ CSF** concrete

Element Number	Element #	W/C	Chloride conductivity ($\mu S / cm$)	$D_{effective}$ (m^2 / s)
1	SC2:S(8)	0.455	1.55	7.13E-08
2	SC2:S(7)	0.455	1.59	7.62E-08
3	SC2:S(5)	0.455	1.68	8.76E-08
4	SC4:S(5)	0.455	0.69	1.81E-08
5	SC4:S(8)	0.455	0.70	1.83E-08
6	SC4:S(7)	0.455	0.64	1.68E-08

Element[#] = Refer to Table 4.11

Table C.5: Steady state (Effective) diffusion coefficient of **dry cured OPC+ FA** concrete

Element Number	Element #	W/C	Chloride conductivity $\mu S / cm$	$D_{effective}$ m^2 / s
1	SB3:S7	0.455	0.67	1.28E-08
2	SB1: S(5)	0.455	0.91	1.61E-08
3	SB2: S(5)	0.455	1.43	2.66E-08
4	SB3:S5	0.455	0.69	1.31E-08
5	SB2: S(6)	0.455	1.68	3.34E-08
6	SB1: S(8)	0.455	0.92	1.63E-08
7	SB1: S(7)	0.455	0.98	1.72E-08
8	SB1: S(6)	0.455	1.01	1.77E-08
9	SB2: S(7)	0.455	1.44	2.66E-08
10	SB2: S(8)	0.455	1.58	3.05E-08
11	SB3:S8	0.455	0.64	1.25E-08
12	SB4:S(8)	0.455	0.85	1.52E-08
13	SB4:S(7)	0.455	0.70	1.32E-08
14	SB4:S(6)	0.455	0.71	1.33E-08
15	SB4:S(5)	0.455	0.90	1.59E-08
16	SB3:S6	0.455	0.76	1.39E-08

Element# = Refer to Table 4.11

Table C.6: Steady state (Effective) diffusion coefficient of **dry cured OPC+ GGBS** concrete

Element Number	Element #	W/C	Chloride conductivity $\mu S / cm$	$D_{effective}$ m^2 / s
1	SA1: S(5)	0.455	0.38	7.74E-09
2	SA2: S(1)	0.455	0.27	7.01E-09
3	SA2: S(2)	0.455	0.23	6.76E-09
4	SA4:S(5)	0.455	0.61	9.57E-09
5	SA4:S(7)	0.455	0.39	7.84E-09
6	SA2: S(4)	0.455	0.28	7.08E-09
7	SA2: S(3)	0.455	0.23	6.76E-09
8	SA1: S(6)	0.455	0.35	7.54E-09
9	SA3:S(5)	0.455	0.27	6.99E-09
10	SA3:S(6)	0.455	0.32	7.36E-09
11	SA3:S(7)	0.455	0.28	7.07E-09
12	SA3:S(8)	0.455	0.29	7.13E-09
13	SA1: S(7)	0.455	0.40	7.88E-09
14	SA1: S(8)	0.455	0.31	7.27E-09
15	SA4:S(8)	0.455	0.41	7.96E-09
16	SA4:S(6)	0.455	0.47	8.40E-09

Element# = Refer to Table 4.11

III. WET CURED CONCRETE

Table C.7: Steady state (Effective) diffusion coefficient of **wet cured OPC+ CSF** concrete

Element Number	Element #	W/C	Chloride conductivity $\mu S / cm$	$D_{effective}$ m^2 / s
1	SC4:Cube(4)	0.455	0.43	7.73E-09
2	SC4:Cube(3)	0.455	0.55	1.45E-08
3	SC4:Cube(2)	0.455	0.48	9.84E-09
4	SC4:Cube(1)	0.455	0.58	1.51E-08
5	SC2:Cube(3)	0.455	1.67	8.68E-08
6	SC2:Cube(2)	0.455	1.52	6.84E-08
7	SC2:Cube(1)	0.455	1.53	6.95E-08
8	SC2:Cube(4)	0.455	1.61	7.84E-08

Element# = Refer to Table 4.11

Table C.8: Steady state (Effective) diffusion coefficient of **wet cured OPC+ FA** concrete

Element Number	Element #	W/C	Chloride conductivity $\mu S / cm$	$D_{effective}$ m^2 / s
1	SB3:Cube(4)	0.455	0.50	1.09E-08
2	SB2:Cube(3)	0.455	1.42	2.63E-08
3	SB4:Cube(4)	0.455	0.63	1.24E-08
4	SB4:Cube(2)	0.455	0.60	1.21E-08
5	SB4:Cube(1)	0.455	0.60	1.20E-08
6	SB3:Cube(1)	0.455	0.49	1.09E-08
7	SB3:Cube(4)	0.455	1.45	2.69E-08
8	SB2:Cube(2)	0.455	1.41	2.60E-08
9	SB1:Cube(4)	0.455	0.41	1.01E-08
10	SB1:Cube(2)	0.455	0.43	1.02E-08
11	SB1:Cube(1)	0.455	0.42	1.01E-08
12	SB3:Cube(2)	0.455	0.49	1.08E-08

Element# = Refer to Table 4.11

Table C.9: Steady state (Effective) diffusion coefficient of **wet cured OPC+ GGBS** concrete

Element Number	Element #	W/C	Chloride conductivity $\mu S / cm$	$D_{effective}$ m^2 / s
1	SA3:Cube(4)	0.455	0.35	7.53E-09
2	SA1:Cube(1)	0.455	0.26	6.95E-09
3	SA1:Cube(2)	0.455	0.28	7.08E-09
4	SA1:Cube(3)	0.455	0.17	6.41E-09
5	SA1:Cube(4)	0.455	0.33	7.40E-09
6	WA:Cube(2)	0.5	0.31	7.25E-09
7	WA:Cube(1)	0.5	0.46	8.33E-09
8	SA3:Cube(3)	0.455	0.30	7.20E-09
9	WA:Cube(3)	0.5	0.22	6.73E-09
10	SA4:Cube(1)	0.455	0.60	9.45E-09
11	SA4:Cube(2)	0.455	0.25	6.87E-09
12	SA3:Cube(1)	0.455	0.27	7.04E-09
13	SA4:Cube(3)	0.455	0.29	7.15E-09
14	SA4:Cube(4)	0.455	0.43	8.11E-09
15	SA3:Cube(2)	0.455	0.30	7.19E-09

Element[#]= Refer to Table 4.11

IV. NON-CURED CONCRETE

Table C.10: Steady state (Effective) diffusion coefficient of **non-cured OPC+ CSF** concrete

Element Number	Element #	W/C	Chloride conductivity $\mu S / cm$	$D_{effective}$ m^2 / s
1	SC4:N(6)	0.455	1.51	6.74E-08
2	SC4:N(7)	0.455	1.11	3.56E-08
3	SC4:N(8)	0.455	1.03	3.11E-08
4	SC2:N(8)	0.455	2.17	1.92E-07
5	SC2:N(6)	0.455	2.15	1.87E-07
6	SC2:N(5)	0.455	2.10	1.73E-07
7	SC2:N(7)	0.455	2.12	1.79E-07
8	SC3:N(5)	0.455	1.46	6.20E-08
9	SC4:N(5)	0.455	1.31	4.85E-08
10	SC3:N(6)	0.455	1.53	6.98E-08
11	SC3:N(7)	0.455	1.17	3.89E-08
12	SC3:N(8)	0.455	1.37	5.35E-08

Element[#]= Refer to Table 4.11

Table C.11: Steady state (Effective) diffusion coefficient of **non-cured OPC+ FA** concrete

Element Number	Element #	W/C	Chloride conductivity $\mu S / cm$	$D_{effective}$ cm^2 / s
1	SB1: N(7)	0.455	1.25	2.23E-08
2	SB1: N(6)	0.455	1.26	2.26E-08
3	SB1: N(5)	0.455	1.17	2.06E-08
4	SB2: N(5)	0.455	2.02	4.62E-08
5	SB1: N(8)	0.455	1.29	2.33E-08
6	SB4:N(7)	0.455	1.15	2.03E-08
7	SB4:N(8)	0.455	1.09	1.91E-08
8	SB2: N(7)	0.455	1.76	3.63E-08
9	SB2: N(8)	0.455	1.81	3.80E-08
10	SB2: N(6)	0.455	2.21	5.54E-08
11	SB3:N8	0.455	0.81	1.47E-08
12	SB3:N6	0.455	0.77	1.41E-08
13	SB3:N5	0.455	0.77	1.42E-08
14	SB3:N7	0.455	0.83	1.50E-08
15	SB4:N(6)	0.455	1.12	1.97E-08

Element[#] = Refer to Table 4.11Table C.12: Steady state (Effective) diffusion coefficient of **non cured OPC+ GGBS** concrete

Element Number	Element #	W/C	Chloride conductivity $\mu S / cm$	$D_{effective}$ cm^2 / s
1	SA3:N(6)	0.455	0.59	9.37E-09
2	SA4:N(7)	0.455	0.50	8.60E-09
3	SA4:N(5)	0.455	0.52	8.80E-09
4	SA2: N(4)	0.455	0.37	7.67E-09
5	SA2: N(1)	0.455	0.29	7.14E-09
6	SA3:N(7)	0.455	0.71	1.05E-08
7	SA4:N(6)	0.455	0.46	8.28E-09
8	SA3:N(5)	0.455	0.62	9.58E-09
9	SA2: N(2)	0.455	0.34	7.47E-09
10	SA2: N(3)	0.455	0.35	7.54E-09
11	WA: F(e)	0.455	0.56	9.09E-09
12	WA: F(f)	0.455	0.56	9.14E-09
13	WA: F(g)	0.455	0.48	8.50E-09
14	WA: F(h)	0.455	0.48	8.46E-09
15	WA: N(e)	0.500	0.66	1.00E-08
16	WA: N(f)	0.500	0.55	9.04E-09
17	WA: N(g)	0.500	0.56	9.12E-09
18	SA3:N(8)	0.455	0.66	9.95E-09
19	WA: N(h)	0.500	0.65	9.84E-09
20	SA1 : N(7)	0.455	0.38	7.74E-09
21	SA1 : N(8)	0.455	0.35	7.54E-09
22	SA1 : N(6)	0.455	0.33	7.40E-09

23	SA1 : N(5)	0.455	0.36	7.60E-09
----	------------	-------	------	----------

Element[#] = Refer to Table 4.11

V. CURING COMPOUND

Table C.13: Steady state (Effective) diffusion coefficient of **OPC+ CSF** concrete cured using a curing compound

Element Number	Element #	W/C	Chloride conductivity $\mu\text{S} / \text{cm}$	$D_{\text{effective}}$ m^2 / s
1	SC3:S(5)	0.455	1.31	4.90E-08
2	SC3:C(8)	0.455	1.15	3.76E-08
3	SC3:C(7)	0.455	1.19	4.00E-08
4	SC3:C(6)	0.455	1.17	3.93E-08
5	SC3:C(5)	0.455	1.13	3.66E-08
6	SC3:S(8)	0.455	1.25	4.42E-08
7	SC4:C(5)	0.455	0.96	2.78E-08
8	SC3:S(6)	0.455	1.22	4.23E-08
9	SC3:Cube(4)	0.455	0.97	2.82E-08
10	SC3:Cube(3)	0.455	0.62	1.63E-08
11	SC3:Cube(2)	0.455	0.71	1.87E-08
12	SC3:Cube(1)	0.455	0.77	2.05E-08
13	SC3:S(7)	0.455	1.22	4.22E-08
14	SC4:C(7)	0.455	1.24	4.34E-08
15	SC4:C(6)	0.455	0.90	2.52E-08
16	SC4:C(8)	0.455	1.07	3.31E-08

Element[#] = Refer to Table 4.11

Table C.14: Steady state (Effective) diffusion coefficient of **OPC+ FA** concrete cured using a curing compound

Element Number	Element #	W/C	Chloride conductivity $\mu\text{S} / \text{cm}$	$D_{\text{effective}}$ m^2 / s
1	SB4:C(5)	0.455	0.84	1.51E-08
2	SB3:C5	0.455	0.57	1.16E-08
3	SB4:C(8)	0.455	1.35	2.44E-08
4	SB4:C(7)	0.455	1.15	2.02E-08
5	SB4:C(6)	0.455	1.10	1.92E-08
6	SB1: C(5)	0.455	0.94	1.65E-08
7	SB1: C(6)	0.455	0.90	1.59E-08
8	SB1: C(7)	0.455	1.10	1.93E-08
9	SB2: C(6)	0.455	1.53	2.90E-08
10	SB3:C8	0.455	0.57	1.17E-08
11	SB3:C7	0.455	0.61	1.22E-08
12	SB3:C6	0.455	0.62	1.22E-08
13	SB2: C(8)	0.455	1.52	2.89E-08
14	SB1: C(8)	0.455	1.02	1.79E-08

Element[#] = Refer to Table 4.11

Table C.15: Steady state (Effective) diffusion coefficient of **OPC+ GGBS** concrete cured using a curing compound

Element Number	Element #	W/C	Chloride conductivity $\mu\text{S} / \text{cm}$	$D_{\text{effective}}$ m^2 / s
1	SA4:C(5)	0.455	0.61	9.55E-09
2	SA2: C(2)	0.455	0.37	7.69E-09
3	SA2: C(3)	0.455	0.28	7.08E-09
4	WA: C(h)	0.5	0.92	1.26E-08
5	WA: C(g)	0.5	0.82	1.15E-08
6	SA3:C(7)	0.455	0.64	9.76E-09
7	SA1: C(6)	0.455	0.36	7.60E-09
8	WA: C(f)	0.5	0.87	1.20E-08
9	WA: C(e)	0.455	0.90	1.24E-08
10	SA2: C(4)	0.455	0.35	7.55E-09
11	SA1: C(5)	0.455	0.31	7.27E-09
12	SA4:C(6)	0.455	0.51	8.74E-09
13	SA2: C(1)	0.455	0.33	7.43E-09
14	SA4:C(7)	0.455	0.51	8.67E-09
15	SA3:C(6)	0.455	0.62	9.65E-09

Element[#]= Refer to Table 4.11

APPENDIX D: GOODNESS-OF-FIT TEST

Goodness-Of -Fit Test

When a particular distribution has been specified to model the random variables, determined perhaps on the basis of the shape of the histogram, the validity of the assumed distribution model may be verified statistically using the goodness-of-fit tests (Ang and Tang, 2007). Three tests used widely are the chi-square, the Kolmogorov-Smirnov (K-S), and the Anderson-Darling (or A-D) methods; one or the other of these methods may be used to test the validity of the specified or assumed distribution model. (Ang and Tang, 2007). This study applied the chi-square test to get the best distribution fit for the data.

Chi-Square method

The chi-square method for goodness-of-fit compares the observed frequencies $\{O_i\}$ with corresponding theoretical frequencies $\{E_i\}$ calculated from the assumed theoretical distribution.

$$\sum_{i=1}^k \frac{(O_i - E_i)^2}{E_i} \quad (D-1)$$

If the assumed distribution yields

$$\sum_{i=1}^k \frac{(O_i - E_i)^2}{E_i} < C_{1-\alpha, f} \quad (D-2)$$

In which $C_{1-\alpha, f}$ is the critical value of the χ_f^2 distribution at the cumulative probability of $(1-\alpha)$, then the assumed theoretical distribution is deemed to be an acceptable model at the significance level of α . Otherwise if Equation D-2 is not satisfied, the assumed distribution is not substantiated by the observed data at the significance level α .

Expected frequency

The expected frequency can be computed from the histogram by calculating the probability $P(a < X < b)$, for each assumed distribution, and multiplying this with the number of observations N . The probability $P(a < X < b)$ is calculated differently for different

distributions. This appendix gives ways of calculating $P(a < X < b)$ for the normal, lognormal and gamma distribution.

a) Normal distribution parameters (μ and σ)

The probability is evaluated as follows

$$P(a < X < b) = \Phi\left(\frac{b-\mu}{\sigma}\right) - \Phi\left(\frac{a-\mu}{\sigma}\right) \tag{D-3}$$

Where a and b are the upper and lower limits of the class interval respectively.

b) Log-normal distribution

The lognormal distribution with the lower bound at zero always has a positive skewness (Holichky *et al.*, 2006). Its skewness γ is given by the value of the coefficient of variation V as:

$$\gamma = 3V + V^3 \tag{D-4}$$

The scale, ζ^2 , and shape, λ , parameters of the lognormal distribution are represented by Equations D-5 and D-6 respectively.

$$\zeta^2 = \ln\left[1 + \left(\frac{\sigma_x}{\mu_x}\right)^2\right] \tag{D-5}$$

$$\lambda = \ln \mu_x - \frac{1}{2} \zeta^2 \tag{D-6}$$

The probability for the log-normal distribution is evaluated as follows:

$$P(a < X < b) = \int_a^b \left(\frac{1}{\sqrt{2\pi}\zeta x} \exp\left[-\frac{1}{2}\left(\frac{\ln x - \lambda}{\zeta}\right)^2\right] \right) dx \tag{D-7}$$

If $s = \left(\frac{\ln x - \lambda}{\zeta}\right)$ such that $dx = \zeta x ds$ then,

$$P(a < X < b) = \frac{1}{\sqrt{2\pi}} \int_{(\ln a - \lambda/\zeta)}^{(\ln b - \lambda/\zeta)} e^{-\zeta/2 s^2} ds \tag{D-8}$$

Equation D-8 when simplified yields Equation D-9.

$$P(a < X < b) = \Phi\left(\frac{\ln b - \lambda}{\zeta}\right) - \Phi\left(\frac{\ln a - \lambda}{\zeta}\right) \tag{D-9}$$

c) Gamma distribution

The gamma distribution is a type III Pearson distribution with lower limit at zero (Holichky *et al.*, 2006). It is useful in cases where there is significant skewness in the data and has the following PDF:

$$f(X) = \frac{\lambda^k x^{k-1} e^{-\lambda x}}{\Gamma(k)} \tag{D-10}$$

Where $\Gamma(k)$ is the gamma function of parameter k given by:

$$\Gamma(k) = \int_0^\infty u^{k-1} e^{-u} du \tag{D-11}$$

The mean and the variance are:

$$\mu_x = \frac{k}{\lambda} \tag{D-12}$$

$$\sigma_x^2 = \frac{k}{\lambda^2} \tag{D-13}$$

Where, $\frac{1}{\lambda}$ is a scale parameter and k is a shape parameter (Crowder *et al.*, 1991). Gamma distributions are positively skewed, though the skewness tends to zero for large k , in which the density resembles a normal density distribution (Crowder *et al.*, 1991). The skewness ϖ is given by:

$$\varpi = 2V \tag{D-14}$$

The skewness is less than that of the lognormal distribution, for this reason, the gamma distribution is more convenient for describing variable actions that do not have great skewness (Holichky *et al.*, 2006).

The probability is given by:

$$P(a < X < b) = \frac{\lambda^k}{\Gamma(k)} \int_a^b x^{k-1} e^{-\lambda x} dx \tag{D-15}$$

$$P(a < X < b) = \frac{1}{\Gamma(k)} \left[\int_0^{\lambda b} (\lambda x)^{k-1} e^{-\lambda x} d(\lambda x) - \int_0^{\lambda a} (\lambda x)^{k-1} e^{-\lambda x} d(\lambda x) \right] \tag{D-16}$$

If $y = \lambda x$ then,

$$P(a < X < b) = \frac{1}{\Gamma(k)} \left[\int_0^{\lambda b} y^{k-1} e^{-y} dy - \int_0^{\lambda a} y^{k-1} e^{-y} dy \right] \tag{D-17}$$

$$P(a < X < b) = I(\lambda b, k) - I(\lambda a, k) \tag{D-18}$$

One-Sided Hypothesis Test

The steps involved in a one sided hypothesis test for a goodness-of-fit test are (Bolstad, 2007):

1. Set up a null hypothesis

$$H_0 : \mu \leq \mu_0 \tag{D-19}$$

2. Choose a level of significance α , which can be 0.10, 0.05 or 0.01.
3. Read out the *p-value* from statistical tables (Table D.1) which is the probability of observing what was observed in the Goodness-of-fit test, given that the null hypothesis $H_0 : \mu \leq \mu_0$ is true.
4. If the *p-value* $\leq \alpha$, then the null hypothesis is rejected, otherwise it is accepted.

Table D.1: Critical Values χ^2 of the Distribution at Probability Level α (Ang and Tang, 2007)

d.o.f.	$\alpha = 0.001$	$\alpha = 0.005$	$\alpha = 0.01$	$\alpha = 0.025$	$\alpha = 0.05$	$\alpha = 0.10$	$\alpha = 0.20$
1	0	0	0.0002	0.0010	0.0039	0.0158	0.0642
2	0.0020	0.0100	0.0201	0.0506	0.1026	0.2107	0.4463
3	0.0243	0.0717	0.1148	0.2158	0.3518	0.5844	1.0052
4	0.0908	0.2070	0.2971	0.4844	0.7107	1.0636	1.6488
5	0.2102	0.4117	0.5543	0.8312	1.1455	1.6103	2.3425
6	0.3811	0.6757	0.8721	1.2373	1.6354	2.2041	3.0701
7	0.5985	0.9893	1.2390	1.6899	2.1673	2.8331	3.8223
8	0.8571	1.3444	1.6465	2.1797	2.7326	3.4895	4.5936
9	1.1519	1.7349	2.0879	2.7004	3.3251	4.1682	5.3801
10	1.4787	2.1559	2.5582	3.2470	3.9403	4.8652	6.1791
11	1.8339	2.6032	3.0535	3.8157	4.5748	5.5778	6.9887
12	2.2142	3.0738	3.5706	4.4038	5.2260	6.3038	7.8073
13	2.6172	3.5650	4.1069	5.0088	5.8919	7.0415	8.6339
14	3.0407	4.0747	4.6604	5.6287	6.5706	7.7895	9.4673
15	3.4827	4.6009	5.2293	6.2621	7.2609	8.5468	10.3070
16	3.9416	5.1422	5.8122	6.9077	7.9616	9.3122	11.1521
17	4.4161	5.6972	6.4078	7.5642	8.6718	10.0852	12.0023
18	4.9048	6.2648	7.0149	8.2307	9.3905	10.8649	12.8570
19	5.4068	6.8440	7.6327	8.9065	10.1170	11.6509	13.7158
20	5.9210	7.4338	8.2604	9.5908	10.8508	12.4426	14.5784
21	6.4467	8.0337	8.8972	10.2829	11.5913	13.2396	15.4446
22	6.9830	8.6427	9.5425	10.9823	12.3380	14.0415	16.3140
23	7.5292	9.2604	10.1957	11.6886	13.0905	14.8480	17.1865
24	8.0849	9.8862	10.8564	12.4012	13.8484	15.6587	18.0618
25	8.6493	10.5197	11.5240	13.1197	14.6114	16.4734	18.9398
26	9.2221	11.1602	12.1981	13.8439	15.3792	17.2919	19.8202
27	9.8028	11.8076	12.8785	14.5734	16.1514	18.1139	20.7030
28	10.3909	12.4613	13.5647	15.3079	16.9279	18.9392	21.5880
29	10.9861	13.1211	14.2565	16.0471	17.7084	19.7677	22.4751
30	11.5880	13.7867	14.9535	16.7908	18.4927	20.5992	23.3641
31	12.1963	14.4578	15.6555	17.5387	19.2806	21.4336	24.2551
32	12.8107	15.1340	16.3622	18.2908	20.0719	22.2706	25.1478
33	13.4309	15.8153	17.0735	19.0467	20.8665	23.1102	26.0422
34	14.0567	16.5013	17.7891	19.8063	21.6643	23.9523	26.9383
35	14.6878	17.1918	18.5089	20.5694	22.4650	24.7967	27.8359
36	15.3241	17.8867	19.2327	21.3359	23.2686	25.6433	28.7350
37	15.9653	18.5858	19.9602	22.1056	24.0749	26.4921	29.6355
38	16.6112	19.2889	20.6914	22.8785	24.8839	27.3430	30.5373
39	17.2616	19.9959	21.4262	23.6543	25.6954	28.1958	31.4405
40	17.9164	20.7065	22.1643	24.4330	26.5093	29.0505	32.3450
45	21.2507	24.3110	25.9013	28.3662	30.6123	33.3504	36.8844
50	24.6739	27.9907	29.7067	32.3574	34.7643	37.6886	41.4492
55	28.1731	31.7348	33.5705	36.3981	38.9580	42.0596	46.0356
60	31.7383	35.5345	37.4849	40.4817	43.1880	46.4589	50.6406
65	35.3616	39.3831	41.4436	44.6030	47.4496	50.8829	55.2620
70	35.3616	43.2752	45.4417	48.7576	51.7393	55.3289	59.8978
75	42.7573	47.2060	49.4750	52.9419	56.0541	59.7946	64.5466
80	46.5199	51.1719	53.5401	57.1532	60.3915	64.2778	69.2069
90	54.1552	59.1963	61.7541	65.6466	69.1260	73.2911	78.5584
100	61.9179	67.3276	70.0649	74.2219	77.9295	82.3581	87.9453

(Continued)

Table D.1: (*Continued*) Critical Values χ^2 of the Distribution at Probability Level ($1-\alpha = p$) (Ang and Tang, 2007)

d.o.f.	$p = 0.800$	$p = 0.900$	$p = 0.950$	$p = 0.975$	$p = 0.990$	$p = 0.995$	$p = 0.999$
1	1.6424	2.7055	3.8415	5.0239	6.6349	7.8794	10.8276
2	3.2189	4.6052	5.9915	7.3778	9.2103	10.5966	13.8155
3	4.6416	6.2514	7.8147	9.3484	11.3449	12.8382	16.2662
4	5.9886	7.7794	9.4877	11.1433	13.2767	14.8603	18.4668
5	7.2893	9.2364	11.0705	12.8325	15.0863	16.7496	20.5150
6	8.5581	10.6446	12.5916	14.4494	16.8119	18.5476	22.4577
7	9.8032	12.0170	14.0671	16.0128	18.4753	20.2777	24.3219
8	11.0301	13.3616	15.5073	17.5345	20.0902	21.9550	26.1245
9	12.2421	14.6837	16.9190	19.0228	21.6660	23.5894	27.8772
10	13.4420	15.9872	18.3070	20.4832	23.2093	25.1882	29.5883
11	14.6314	17.2750	19.6751	21.9200	24.7250	26.7568	31.2641
12	15.8120	18.5493	21.0261	23.3367	26.2170	28.2995	32.9095
13	16.9848	19.8119	22.3620	24.7356	27.6882	29.8195	34.5282
14	18.1508	21.0641	23.6848	26.1189	29.1412	31.3193	36.1233
15	19.3107	22.3071	24.9958	27.4884	30.5779	32.8013	37.6973
16	20.4651	23.5418	26.2962	28.8454	31.9999	34.2672	39.2524
17	21.6146	24.7690	27.5871	30.1910	33.4087	35.7185	40.7902
18	22.7595	25.9894	28.8693	31.5264	34.8053	37.1565	42.3124
19	23.9004	27.2036	30.1435	32.8523	36.1909	38.5823	43.8202
20	25.0375	28.4120	31.4104	34.1696	37.5662	39.9968	45.3147
21	26.1711	29.6151	32.6706	35.4789	38.9322	41.4011	46.7970
22	27.3015	30.8133	33.9244	36.7807	40.2894	42.7957	48.2679
23	28.4288	32.0069	35.1725	38.0756	41.6384	44.1813	49.7282
24	29.5533	33.1962	36.4150	39.3641	42.9798	45.5585	51.1786
25	30.6752	34.3816	37.6525	40.6465	44.3141	46.9279	52.6197
26	31.7946	35.5632	38.8851	41.9232	45.6417	48.2899	54.0520
27	32.9117	36.7412	40.1133	43.1945	46.9629	49.6449	55.4760
28	34.0266	37.9159	41.3371	44.4608	48.2782	50.9934	56.8923
29	35.1394	39.0875	42.5570	45.7223	49.5879	52.3356	58.3012
30	36.2502	40.2560	43.7730	46.9792	50.8922	53.6720	59.7031
31	37.3591	41.4217	44.9853	48.2319	52.1914	55.0027	61.0983
32	38.4663	42.5847	46.1943	49.4804	53.4858	56.3281	62.4872
33	39.5718	43.7452	47.3999	50.7251	54.7755	57.6484	63.8701
34	40.6756	44.9032	48.6024	51.9660	56.0609	58.9639	65.2472
35	41.7780	46.0588	49.8018	53.2033	57.3421	60.2748	66.6188
36	42.8788	47.2122	50.9985	54.4373	58.6192	61.5812	67.9852
37	43.9782	48.3634	52.1923	55.6680	59.8925	62.8833	69.3465
38	45.0763	49.5126	53.3835	56.8955	61.1621	64.1814	70.7029
39	46.1730	50.6598	54.5722	58.1201	62.4281	65.4756	72.0547
40	47.2685	51.8051	55.7585	59.3417	63.6907	66.7660	73.4020
45	52.7288	57.5053	61.6562	65.4102	69.9568	73.1661	80.0767
50	58.1638	63.1671	67.5048	71.4202	76.1539	79.4900	86.6608
55	63.5772	68.7962	73.3115	77.3805	82.2921	85.7490	93.1675
60	68.9721	74.3970	79.0819	83.2977	88.3794	91.9517	99.6072
65	74.3506	79.9730	84.8206	89.1771	94.4221	98.1051	105.9881
70	79.7146	85.5270	90.5312	95.0232	100.4252	104.2149	112.3169
75	85.0658	91.0615	96.2167	100.8393	106.3929	110.2856	118.5991
80	90.4053	96.5782	101.8795	106.6286	112.3288	116.3211	124.8392
90	101.0537	107.565	113.1453	118.1359	124.1163	128.2989	137.2084
100	111.6667	118.498	124.3421	129.5612	135.8067	140.1695	149.4493

An Excel program spreadsheet (Chi_Squared_Goodness_of_fit_test.xls) in the attached CD is provided to assist users in carrying out chi-square goodness-fit-tests on data.

References D:

Ang, A.H.S., Tang, W.H., (2007), *Probability Concepts in Engineering-Emphasis on Applications to Civil and Environmental Engineering*, John Wiley & Sons, 2nd edition, pp. 406

Bolstad, W.M., (2007), *Introduction to Bayesian Statistics*, John Wiley & Sons, 2nd edition, pp. 437

Crowder, M.J., Kimber, A.C., Smith, R.L., Sweeting, T.J., (1991), *Statistical Analysis of Reliability Data*, Chapman and Hall, London

University of Cape Town

APPENDIX E: MCS PROGRAM DOCUMENTATION

Two Matlab programs have been developed in this study to carry out Monte Carlo simulation and first order reliability analysis on the LSF. This appendix serves to show the algorithm followed by both programs during the analysis of the LSF.

Monte Carlo Simulation (MCS) ANALYSIS

Program Flow Chart

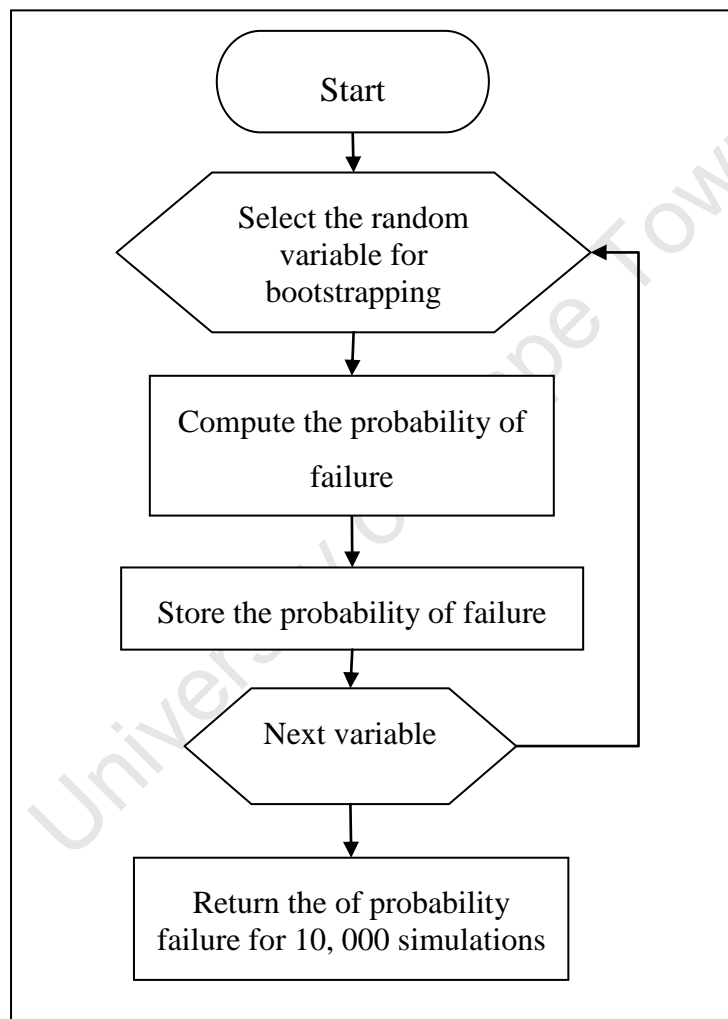


Figure E.1: Flow chart of the MCS program used for the reliability analysis

First Order Reliability Method (FORM) ANALYSIS

The FORM_method.m Matlab program was designed to assist users in carrying out a First order reliability analysis on data pertaining to chloride ingress diffusion. The FORM algorithm follows the procedure outlined in Figure E.2.

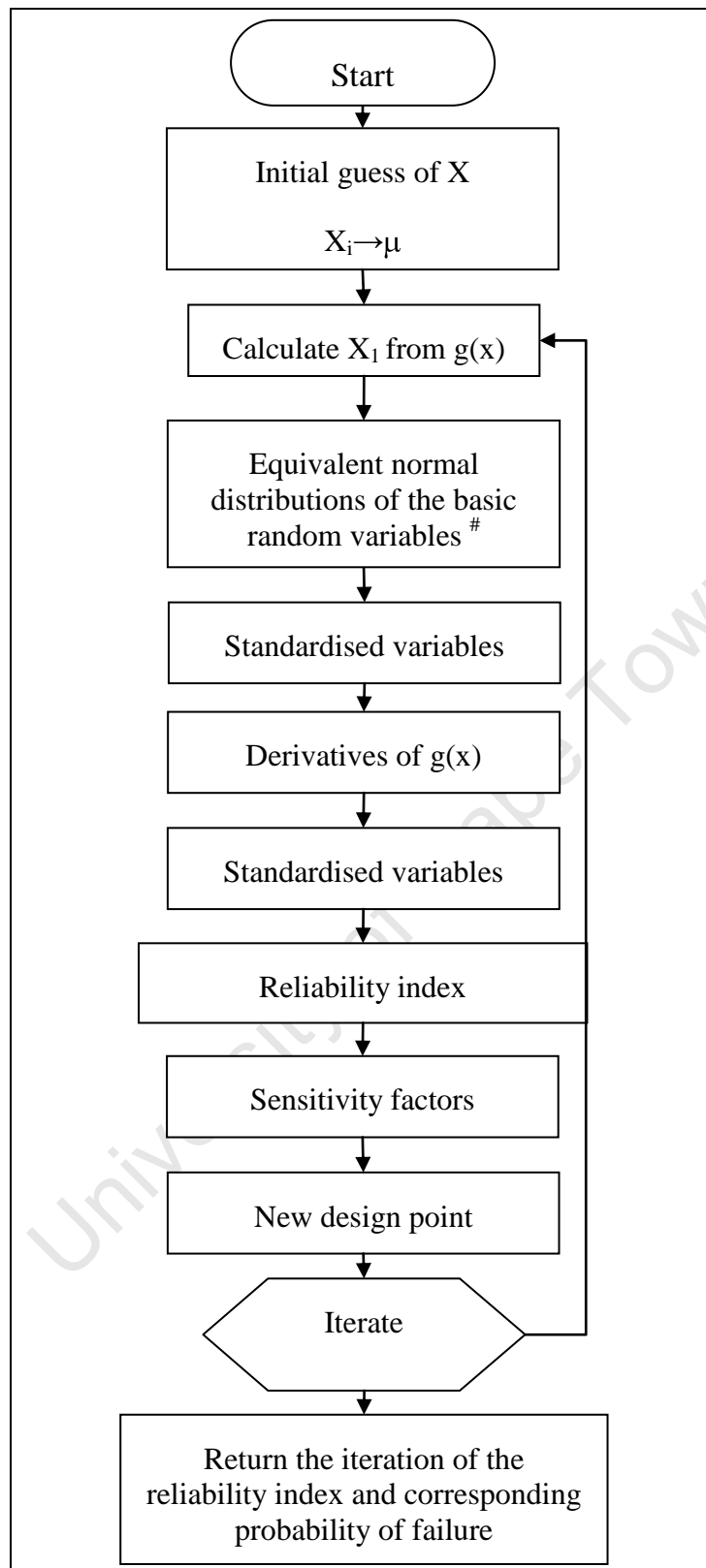


Figure E.2: Flow chart of the FORM program used for the reliability analysis

Advantages of the program

FORM.m Matlab program gives an output of the partial safety factors that serve as important input parameters in the semi-probabilistic SLD approach. The FORM program also gives sensitivity measures to each basic variable in the LSF. This helps in illustrating the relative importance of each parameter w.r.t the reliability index.

Limitations of the program

1. The FORM analysis is carried out based on the assumption that there is no correlation between the basic variables in the LSF. However, this assumption need not be true and there is need to carry out further research on the correlation between the various parameters in the LSF, for instance, the relationship between surface chloride concentration and critical chloride content parameters or between surface chloride concentration and diffusion coefficient. The findings from such research if applied, would improve on the accuracy of results given by the FORM program.
2. The basic random variables are assumed to be normally distributed hence the step of converting the variables to the equivalent normal distributions is not illustrated in the program application (see Figure E.2). Further work needs to be carried out in this part once the actual probability density functions have been established for each of the variables.

APPENDIX F: DURABILITY INDEX TESTS

This appendix section covers two durability index tests i.e. the water sorptivity test and the oxygen permeability test. The two tests were found useful in this study for application in future research.

Water Sorptivity Test

The fluid is drawn into the porous, unsaturated material through the action of capillary forces. The amount of water drawn into the concrete under capillary suction is determined by carrying out a water sorptivity test.

The test procedure is given in the durability index testing manual (2007) and begins with the oven drying of concrete specimens $70 \pm 2 \text{ mm}$ \varnothing by $25 \pm 2 \text{ mm}$ thick (representing the cover layer of concrete) at $50 \pm 2 \text{ }^\circ\text{C}$ for $7 \text{ days} \pm 2 \text{ hours}$.

The specimens are then placed in a vacuum saturation facility as shown in Figure F.1. Following this, the specimens are placed in water contained in a stainless steel tray which is 20 mm deep. The test face represents the side of the sample that would be exposed to wetting and drying cycles. At regular intervals the specimens are removed from the water and the mass of water absorbed is determined by weighing the sample. Measurements are stopped before saturation is reached, and the concrete is then vacuum-saturated in water to determine the effective porosity.

A linear relationship exists between the mass of water absorbed and the square root of time. The sorptivity index is determined from the slope of the straight line produced.



Figure F.1: Water sorptivity test apparatus (Page and Badenhorst, 2007)

Oxygen Permeability Test

The test procedure is given in the durability index testing manual (2007) and begins with the oven drying of concrete specimens $70 \pm 2 \text{ mm } \varnothing$ by 25 to 30 mm thick (representing the cover layer of concrete) at $50 \pm 2 \text{ }^\circ\text{C}$ for 7 days ± 2 hours. The samples are placed in rubber collars secured on top of a permeability cell as illustrated in Figure F.2 for approximately 5 hours. The cell is pressurized with oxygen gas to 100kPa before testing.

The pressure decay is monitored and measured at constant time intervals and is used to determine the Darcy coefficient of permeability (k). The test output is referred to as an oxygen permeability index, which has a logarithmic scale and is defined as the negative logarithm of k as expressed by Equation F-1.

$$OPI = -\log k \quad (F-1)$$

The higher the value of the OPI, the more permeable the material is.

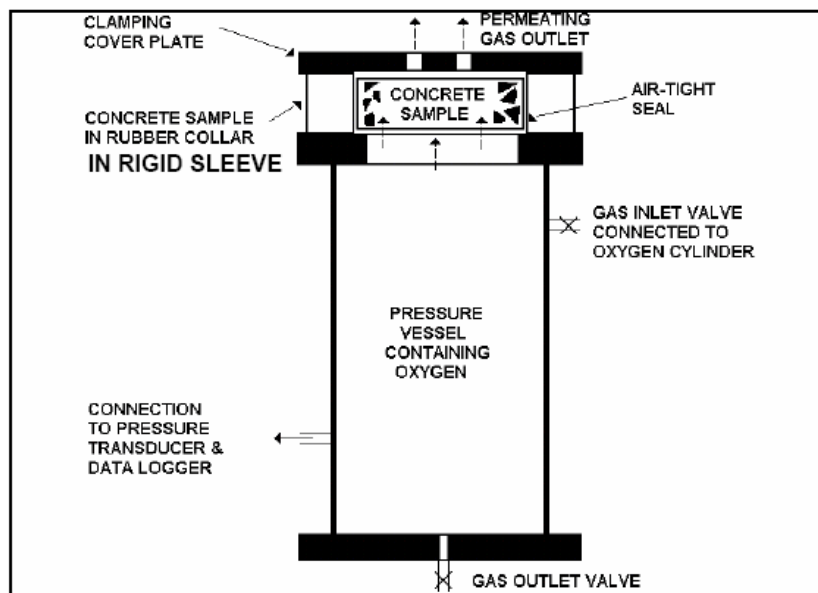


Figure F.2: Oxygen permeability test set-up (Durability index testing manual, 2007)

References F:

Page, R., Badenhorst, S., (2007), Practical Considerations and Constraints in Durability Testing, Proceedings of Concrete Society of SA Durability Workshop, October 2007

Durability index testing manual (2007), Concrete Durability Index Testing

APPENDIX G: First Order Reliability Method (FORM)

Introduction

This appendix section gives two procedures:

- (i) The first order reliability method (FORM) procedure for the analysis of the LSF to obtain a reliability index against the durability failure. The section also illustrates how sensitivity factors are obtained using the FORM to describe the influence of the specific parameters on the reliability index.
- (ii) The use of the FORM in obtaining the partial factors of safety used in the semi-probabilistic approach to SLD.

G1: Form Order Reliability Method (FORM) Procedure

Recalling from Section 3.2 of Chapter 3 that the limit effect, $C_{(x,t)}$ and the action effect, C_{crit} are modelled mathematically as a function of basic variables, $g(C_1, X_2, \dots)$, representing concrete dimensions, material properties and the environment of the RC structure as shown by Equation G-1.

$$Z = C_{crit} - C_{(x,t)} = g(C_s, D_i, t, m, C_{crit}) \quad (G-1)$$

At the durability failure point, $g(C_s, D_i, t, m, C_{crit}) = 0$, the initiation limit state (ILS) is given by:

$$Z = g(C_s, D_i, t, m, C_{crit}) = C_{crit} - C_s \left[1 - \operatorname{erf} \left(\frac{x}{2\sqrt{D_i t^{1-m}}} \right) \right] = 0 \quad (G-2)$$

The error function $\operatorname{erf}(\cdot)$ in Equation G-2 can be further expanded using Maclaurin expansion of the form (Blair *et al.*, 1976; Carlitz, 1963):

$$\operatorname{erf}(y) = \frac{2}{\sqrt{\pi}} \int_0^y e^{-t^2} dt = \frac{2}{\sqrt{\pi}} \left(y - \frac{y^3}{3 \cdot 1!} + \frac{y^5}{5 \cdot 2!} - \frac{y^7}{7 \cdot 3!} + \dots \right) \quad (G-3)$$

An approximation of up to the 8th order polynomial will serve as a best fit for Equation G-3 and would result in an error of 1E-06. The polynomial coefficients $A_0 \rightarrow A_8$ of the expansions up to the 8th order are summarised in Table G.1.

$$erf(y) = k \left(A_1 y - A_2 y^3 + A_3 y^5 - A_4 y^7 + \dots \right)$$

Where $k = \frac{2}{\sqrt{\pi}}$

Table G.1: Polynomial expansion coefficients

Coefficient	Value	Coefficient	Value
A_1	1	A_5	4.63E-03
A_2	3.33E-01	A_6	7.58E-04
A_3	1.0E-01	A_7	1.07E-04
A_4	2.38E-02	A_8	1.32E-05
Normal residue			1.0E-6

The polynomial expansion coefficients in Table G.1 will be used in further analysis of Equation G-2 with the help of a Matlab program. However, for ease of further illustrating the FORM procedure, only the first coefficient is applied. From this, the approximate expanded form of Equation G-2 is:

$$Z = g(\mu, C_S, D_i, t, m, C_{crit}) = C_{crit} - C_S \left[1 - A_1 \left(\frac{x}{2\sqrt{\mu} t^{1-m}} \right) \right] = 0 \tag{G-4}$$

To solve the limit state function (Equation G-4) using FORM method, first, the basic random variables μ, C_S, D_i and C_{crit} (which will alternatively be referred to as X_1, X_2, X_3, X_4 respectively) are transformed into a space of standardised normal variables X'_1, X'_2, X'_3, X'_4 using the equation (Ayyub):

$$X'_i = \frac{X_i - \mu_i}{\sigma_i} \tag{G-5}$$

Where μ_i and σ_i are the mean and standard deviation of the basic random variables respectively. The limit state function is thus transformed to:

$$g(\mu'_1, X'_2, X'_3, X'_4) \geq 0 \text{ OR } g(\mu'_s, C'_s, D'_i, t, m, C'_{crit}) \geq 0 \quad (G-6)$$

The function (G-6) is non-linear i.e. the distance from the failure hyper-surface to the origin of the reduced variables may not be unique as illustrated in Figure G.1.

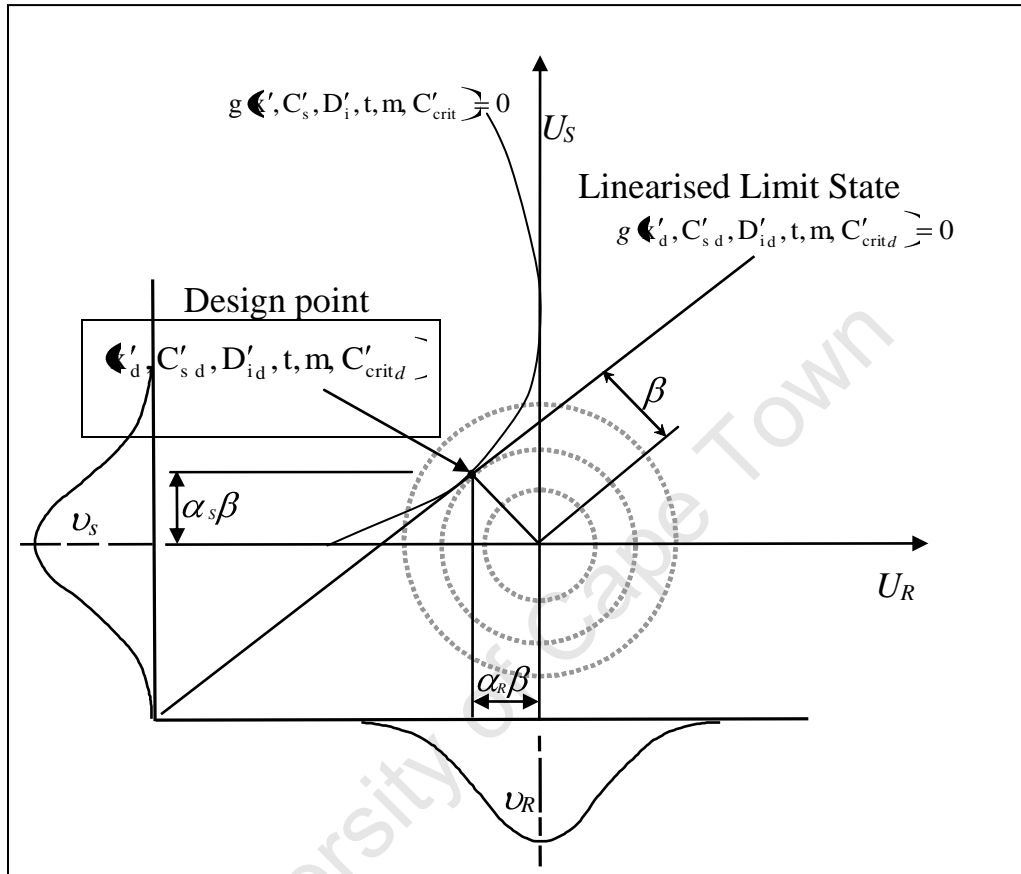


Figure G.1: Illustration of the reliability index β (Ljungquist, 2005; Holichky, 2007)

The second part of the FORM procedure aims at obtaining a *design point* $(X'_{d1}, X'_{d2}, X'_{d3}, X'_{d4})$ (OR $(\mu'_d, C'_{s,d}, D'_{i,d}, t, m, C'_{crit,d})$) which is the point lying on the failure boundary closest to the origin as illustrated in Figure G.1 (Holichky, 2007).

Due to the non-linearity of the failure plane, $g(\mu'_s, C'_s, D'_i, t, m, C'_{crit}) \geq 0$ an approximate mean (μ'_d) and variance (σ'^2_d) of the design point is obtained by the use of a tangent hyperplane to the function $g(\mu'_s, C'_s, D'_i, t, m, C'_{crit}) \geq 0$.

The tangent hyperplane function is approximated by means of a Taylor series expansion of the function $g(\mu'_1, X'_2, X'_3, X'_4) \geq 0$ about the mean values of X_i such that (Ang and Tang, 2007):

$$Z = g(X_1, X_2, \dots, X_n) \approx g(\mu_{X_1}, \mu_{X_2}, \dots, \mu_{X_n}) + \sum_{i=1}^n (X_i - \mu_{X_i}) \frac{\partial g}{\partial X_i} + \frac{1}{2} \sum_{i=1}^n \sum_{j=1}^n (X_i - \mu_{X_i})(X_j - \mu_{X_j}) \frac{\partial^2 g}{\partial X_i \partial X_j} + \dots \quad (G-7)$$

Equation G-7 is truncated at the linear terms to give:

$$g(X_1, X_2, \dots, X_n) \approx g(\mu_{X_1}, \mu_{X_2}, \dots, \mu_{X_n}) + \sum_{i=1}^n (X_i - \mu_{X_i}) \frac{\partial g}{\partial X_i} \quad (G-8)$$

Based on the assumption that all the variables are uncorrelated (or statistically independent) the first-order approximate mean and the standard deviation of the design point can be obtained as:

$$E(Z) \approx g(\mu_{X_1}, \mu_{X_2}, \dots, \mu_{X_n}) \quad (G-9)$$

$$\sigma_z^2 \approx \sum_{i=1}^n \left(\frac{\partial g}{\partial X_i} \right)^2 \sigma_i^2 \quad (G-10)$$

By this method, the minimum distance from the origin to the design point is represented by the reliability index β as:

$$\beta = \frac{E(Z)}{\sigma_z} = \frac{g(\mu_{X_i})}{\sqrt{\sum_{i=1}^n \left(\left(\frac{\partial g}{\partial X_i} \right)^2 \sigma_i^2 \right)}} \quad (G-11)$$

Hence from Equations G-11 and G-12 the following expression is obtained:

$$X'_i = - \frac{\frac{\partial g}{\partial X_i} \sigma_i}{\sqrt{\sum_{i=1}^n \left(\left(\frac{\partial g}{\partial X_i} \right)^2 \sigma_i^2 \right)}} \beta = -\alpha_i \beta \quad (G-12)$$

Where α_i are the direction cosines of the component axes. The directional cosine for the variable say X_1 is given as:

$$\alpha_1 = \frac{\sigma_1}{\sqrt{\sigma_1^2 + \sigma_2^2 + \sigma_3^2 + \sigma_4^2}} = \frac{\frac{\partial g}{\partial X_1} \sigma_1}{\sqrt{\sum_{i=1}^n \left(\left(\frac{\partial g}{\partial X_i} \right)^2 \sigma_i^2 \right)}} \quad (G-13)$$

Assuming that there is no correlation between the variables, the partial derivatives of the LSF w.r.t each of the variables evaluated at the failure point are shown in Equations G-14 to G-17.

$$\left. \frac{\partial g}{\partial C_{crit}} \right|_{C_S, D_i, x} = \sigma_{crit} \quad (G-14)$$

$$\left. \frac{\partial g}{\partial C_S} \right|_{C_{crit}, D_i, x} = - \left[1 - A_1 \left(\frac{x}{2\sqrt{D_i t^{1-m}}} \right) \right] \cdot \sigma_{C_S} \quad (G-15)$$

$$\left. \frac{\partial g}{\partial x} \right|_{C_{crit}, C_S, D_i} = - \left[C_S \left[1 - A_1 \left(\frac{1}{2\sqrt{D_i t^{1-m}}} \right) \right] \right] \cdot \sigma_x \quad (G-16)$$

$$\left. \frac{\partial g}{\partial D_i} \right|_{C_{crit}, C_S, x} = - \left[C_S \left[1 - A_1 \left(\frac{1}{2\sqrt{D_i^3 t^{1-m}}} \right) \right] \right] \cdot \sigma_{D_i} \quad (G-17)$$

Thus the new design point is given as (Vrijling and Gelder, 2000):

$$X'_{di(new)} = \mu_i + X'_i \sigma_i = \mu_i - \alpha_i \beta \sigma_i \quad (G-18)$$

The revised limit state function can be expressed as:

$$g(\mu_1 - \alpha_1 \sigma_1 \beta, \mu_2 - \alpha_2 \sigma_2 \beta, \mu_3 - \alpha_3 \sigma_3 \beta, \mu_4 - \alpha_4 \sigma_4 \beta) = 0 \quad (G-19)$$

The limit-state equation is given by Equation G-20 and can be solved to give a value for β

$$g(\mu_1 - \alpha_1 \sigma_1 \beta) + (\mu_2 - \alpha_2 \sigma_2 \beta) + (\mu_3 - \alpha_3 \sigma_3 \beta) - (\mu_4 - \alpha_4 \sigma_4 \beta) = 0 \quad (G-20)$$

To perform the next iteration, the value of β obtained from G-20 is substituted into the Equation G-18 to obtain the new failure point.

The procedure G-12 to G-20 is repeated until the value of β converges.

G2: Deriving partial factors from FORM Procedure

The FORM procedure outlined in Section G1 can be used to determine the partial safety factors for the load and resistance variables of the LSF in the semi-probabilistic approach to SLD. The semi-probabilistic approach utilizes partial factors, characteristic values and design values in representing the load and resistance variables of a LSF.

The design point obtained in Equation G-12 is illustrated again by Equations G-21 and G-22 for the resistance and load variables respectively (Duracrete, 1999).

$$X_{d, \text{resistance}} = \mu_{X_i} - \alpha_i \beta \sigma_{X_i} \quad (\text{G-21})$$

$$X_{d, \text{load}} = \mu_{X_i} + \alpha_i \beta \sigma_{X_i} \quad (\text{G-22})$$

The partial factor for the action (load) function is obtained by dividing the design value by the characteristic value as shown in Equation G-23.

$$\gamma_{\text{load}} = \frac{X_{d, \text{load}}}{X_{\text{char}}} \quad (\text{G-23})$$

Similarly, the partial factor for the limiting (resistance) variable is obtained by dividing the characteristic value by the design value as shown in Equation G-24.

$$\gamma_{\text{resistance}} = \frac{X_{\text{char}}}{X_{d, \text{resistance}}} \quad (\text{G-24})$$

In both Equations G-23 and G-24, X_{char} is the characteristic value which is normally taken as a quantile such as 5th percentile value for the load function or 95th percentile value for the resistance function of their respective stochastic distributions.

References G:

Ang, A.H.S., Tang, W.,H., (2007), *Probability Concepts in Engineering-Emphasis on Applications to Civil and Environmental Engineering*, John Wiley & Sons, 2nd edition, pp. 406

Ayyub, B., M., (2006) *Methodology for developing reliability –based load and resistance factor design (LRFD) guidelines for ship structures.*

Blair J. M.; Edwards C. A.; Johnson J. H. (1976), Rational Chebyshev Approximations for the Inverse of the Error Function, *Mathematics of Computation*, 30 (136), pp. 827-830.

Carlitz, L., (1963), The Inverse Error Function, *Pacific Journal of Mathematics*, 13(2), pp. 459-470.

DuraCrete, (1999), *Probabilistic Methods for Durability Design, Document BE95- 1347/R0*, The European Union – Brite EuRam III, Contract BRPR-CT95-0132, Project BE95-1347.

Ljungquist, K. (2005), *A Probabilistic Approach to Risk Analysis-A comparison between undesirable indoor events and human sensitivity*, Doctorate thesis, Lulea University of Technology.

Vrijling, J.K., Gelder, P.H.A.J.M., (2000) Probabilistic Design, lecture notes, IHE-Delft

APPENDIX H: Service Life Design Examples

The example given in this section is aimed at illustrating the use of the three SLD approaches i.e. the deemed-to-satisfy, avoidance of deterioration and the partial safety factor approaches introduced in Sections 2.4.2.1, 2.4.2.2 and 2.4.2.4 respectively.

Problem Statement

The aforementioned three SLD approaches introduced in Chapter 2 are exemplified for a concrete pier to be cast in-situ in an extreme splash and tidal marine environment using a cement blend of Portland cement and ground granulated blast furnace slag - OPC: GGBS (50:50). GGBS has been selected as it has been found to be beneficial in the marine environment in that it is able to bind chlorides with time and resist the ingress of chlorides (Alexander *et al.*, 1999). In this illustration, concrete material degradation is assumed to occur solely as a result of diffusion of chlorides in the concrete.

The designers' task is to specify the required material resistance against chloride penetration in terms of a chloride conductivity value and/or corresponding diffusion coefficient given the design requirements in Table H.1.

Table H.3: Design requirements

Parameter	Design requirement	Reference
Type of structure:	Civil structure	Table 2.3
Design life	50 years	
Exposure class (based on EN 206-1, 2000)	XS3b	Table 3.1
Cover depth	50 mm	Design specification
Binder type	50/50 CEM I:GGBS	Design specification

Analysis:

a) Deemed-to-satisfy approach

In this approach, the designer recommends limiting values which if met by the structure, result in the structure being 'deemed-to-satisfy' the design requirements.

The specific requirements for concrete material quality and cover for the deemed-to-satisfy method will be determined on the basis of calibrated values to long-term experience of building tradition in SA as represented in Table H.2. The table also shows the validity of the

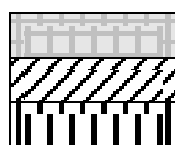
provisions by use of shaded regions i.e. the range of cement types and concrete grades covered by the calibration.

Thus, the values of chloride conductivity value and cover depth will be selected from Table H.2 based on expected environment class (XS3b) and desired service life of 50 years.

Table H.2: Deemed-to-satisfy parameters (Alexander *et al.*, 2007)

Marine Structure, 50-years design life		Maximum chloride conductivity (mS/cm) for various binder types		
Exposure class (based on EN 206-1, 2000)	Cover (mm)	100 % CEM I	30 % Fly ash	50 % Corex slag
XS3b: Tidal, splash and wetted spray zones, exposed to abrasion	40	0.45	0.75	1.05
	60	0.95	1.35	1.95
	80	1.3	1.8	2.6
XS0b: Airborne salt in an exposed near-shore marine location	40	1	1.85	2.5
	60	1.85	2.95	3.9
	80	2.5	3.75	4.8

Legend:



Impractical mixes; concrete grade > 60 MPa

Not recommended < 30 MPa, and/or w/b > 0.55

Acceptable: Grades from 30 to 60 MPa

From Table H.2, the recommended maximum chloride conductivity value for a CEM I: GGBS concrete column under XS3b environmental conditions is extrapolated from the given values as 1.6 mS/cm for a cover to reinforcing steel of 50 mm. The recommended material design values for the RC pier element are summarized in Table H.3.

Table H.3: Recommended material values (Table H.2)

Parameter	Design values
Minimum Cover	50 mm
Maximum chloride conductivity value	1.60 mS/cm
Water to binder ratio	0.55
Concrete grade	30 - 60 MPa

b) Avoidance of deterioration approach

The specific requirements for concrete material quality and cover using the avoidance of deterioration approach will be similar to those specified for the deemed-to-satisfy approach (see Table H.3).

In addition, the designer will select additional protective measures based on expert judgement that will reduce or negate the ingress of chloride ions in concrete. For this example, the designer could recommend the use of a surface applied corrosion inhibitor as a protection technique to delay and reduce the possibility of the onset of corrosion initiation.

A corrosion inhibitor is defined as a chemical substance that decreases the corrosion rate when present in the corrosion system at suitable concentration, without significantly changing the concentration of any other corrosion agents (ISO, 1989). Corrosion-inhibiting chemicals are either mixed in to the fresh concrete (admixed), or applied to the surface of hardened concrete (Heiyantuduwa, 2006).

Surface applied corrosion inhibitors (SACI) are brushed, spray applied or ponded onto the external surface of a RC structure and allowed to penetrate to the concrete /steel interface without the need to break out the concrete (Maeder *et al.*, 2006). The inhibitors penetrate the concrete by a combination of capillary absorption and diffusion up to the rebar level.

Upon penetration to the rebar, the corrosion inhibitor brings about the following beneficial actions (Richardson, 2006):

- Delay in the onset of corrosion
- Reduction of corrosion rates in chloride contaminated concrete
- Reduction of the incipient anode effect

Figure H.1 illustrates these beneficial actions that result from the use of a corrosion inhibitor.

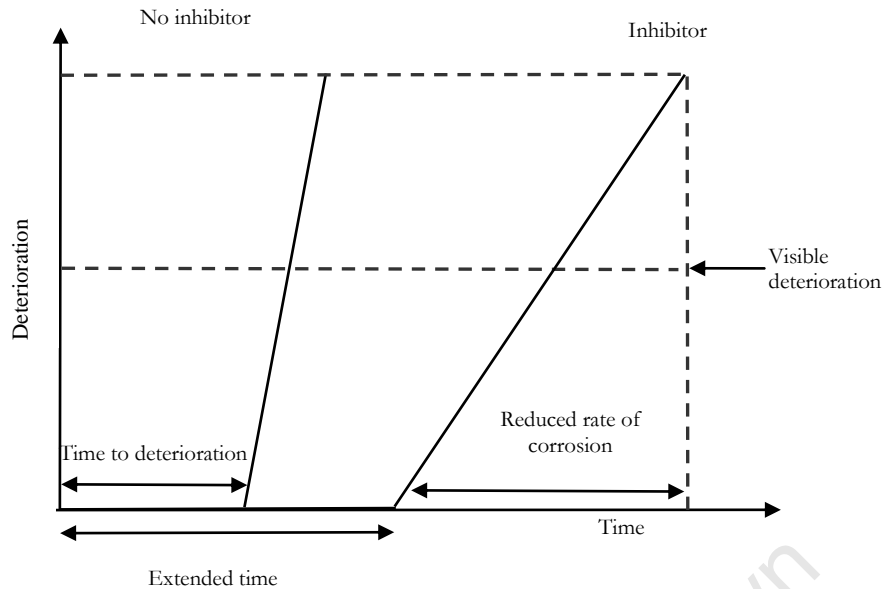


Figure H.1: Extension of the service life of a concrete structure with corrosion inhibitor treatment (Laamenen *et al.*, 1996).

The mechanisms of penetration of corrosion inhibitors responsible for bringing about the beneficial actions include (Richardson, 2005):

- The formation of a monomolecular layer on the steel surface, considered to be 100–1000 μm thick which reduces the dissolution of iron at the anodes and acts as a barrier to oxygen at the cathodes.
- The bounding of chloride to quaternary salt which results in an increase in the chloride ion threshold necessary to initiate corrosion.
- Displacement of chloride ions and other potentially deleterious ions on the reinforcement surface
- Gel formation due to the addition of the inhibitor to pore water solution leading to a pore blocking effect that causes a reduction in the penetration of chlorides, oxygen and water into the concrete.

Thus from the use of SACI it is presumed that there will be a delayed onset of time to corrosion initiation for the RC pier.

c) Partial safety factor approach

The partial factor approach is essentially a deterministic assessment that utilizes a model to carry out design calculations (Section 2.4.2.4). The approach utilizes characteristic values of input parameters of the model and partial safety factors to compute the required design values. The characteristic values are all defined in Table H.4 and are derived from their respective probability functions (quantified using the full-probabilistic approach), using the excel spreadsheet ModelFractiles.xcl (see attached CD). Table H.5 gives the partial factor applicable to each characteristic value for each individual parameter. The partial factors in Table H.5 are adopted from literature. For the concrete cover a margin Δx of 15 mm is applied.

Table H.4: Characteristic values for input parameters in the LSF

Parameter	Units	Distribution type [#]	Characteristic value (5 % percentile)	Characteristic value (50 % percentile)	Characteristic value (95% percentile)
x_{char}	mm	Normal(50,15,0.30)	-	47.891	-
$C_{crit,char}$	% m/m	Normal(0.48, 0.15)	-	0.40	-
m	-	Deterministic(0.68)	-	-	-
$C_{S,char}$	% m/m	Gamma(4.13, 0.87, 0.21, 24.46, 0.17)	0.985	-	4.069

Distribution type[#] = (mean, standard deviation, COV, $\alpha^{\#}$, $\beta^{\#}$)

COV[#] = Coefficient of variation

$\alpha^{\#}$ = Shape parameter of distribution

$\beta^{\#}$ = Scale parameter of distribution

Table H.5: Partial factors for parameters (adopted from Edvardsen, 1999)

Partial factor parameter	Units	Partial safety factor
Critical chloride content, $\gamma_{C_{cr}}$	-	1.05
Surface chloride concentration, γ_{C_s}	-	1.35

The design values for each parameter in the LSF are obtained by multiplying or dividing the characteristic values by the appropriate partial factors from Tables H.4 and H.5 respectively. Table H.6 gives a summary of the design values that serve as input values in the LSF (Equation H-1).

Table H.6: Design values for input parameters in the LSF

Parameter	Units	Design value
$x_d = x_{char} - \Delta x$	mm	$47.89 - 15 = 32.89$
$C_{crit,d} = \frac{C_{crit,char}}{\gamma_{C_{crit}}}$	% m/m	$0.4 \times 1.05 = 0.42$
m	-	0.68
$C_{s,d} = C_{s,Char} \cdot \gamma_{C_s}$	% m/m	$4.07 \times 1.35 = 5.49$

$$Z = C_{crit,d} - C_{(x,t),d} = 0 \tag{H-1}$$

Where, $C_{(x,t),d}$ is the design value of chloride ion concentration at a distance x from the concrete surface after exposure to a saline environment for a period of time t ;

Equation H-1 can be further represented as:

$$Z = C_{crit,d} - \gamma_{cl} \cdot C_{s,d} \left[1 - \operatorname{erf} \left(\frac{x_d}{2\sqrt{D_{i,d} t^{(1-m)}}} \right) \right] \tag{H-2}$$

By isolating the exposure time, the design diffusion coefficient can be estimated as:

$$D_{i,d} = \left[\left(\frac{2}{x_d} \operatorname{erf}^{-1} \left(1 - \frac{C_{crit,d}}{C_{s,d}} \right) \right)^{-2} \frac{1}{t^{(1-m)}} \right] \tag{H-3}$$

Substituting design values from Table H.6 into Equation H-3 gives:

$$D_{i,d} = \left[\left(\frac{2}{32.89} \operatorname{erf}^{-1} \left(1 - \frac{0.42}{5.49} \right) \right)^{-2} \frac{1}{100^{(1-0.68)}} \right] = 39.5 \text{ mm}^2 / \text{year} \tag{H-4}$$

= $1.25 \times 10^{-12} \text{ m}^2/\text{s}$ The diffusion coefficient value obtained was $39.5 \text{ mm}^2/\text{year}$ ($1.25 \times 10^{-12} \text{ m}^2/\text{s}$).

References H:

Ayyub, B., M., (2006) *Methodology for developing reliability –based load and resistance factor design (LRFD) guidelines for ship structures.*

CodeCal (2003), JCSS Code Calibration Program, www.jcss.ethz.ch

Edverdsen, C., Mohr, L., (1999) *DuraCrete– A Guideline for Durability Design of Concrete Structures*, COWI Consulting Engineers and Planners.

Heiyantuduwa R., Alexander, M.G., Mackechnie, J.R., and Rylands T., (2006), Performance of an organic corrosion inhibitor in concrete affected by both chloride and carbonation-induced corrosion, *Proceedings of Concrete Repair, Rehabilitation and Retrofitting Conference*, Alexander (Eds.), Taylor & Francis Group.

International Standards Organization (1989), Corrosion of metals and alloys – basic terms and definitions, ISO 8044

Laamenen. P. H. and Byfors, K., (1996), Corrosion inhibitors in concrete, AMA (alkanolamines) based inhibitor –State of the Art Report, *Nordic Concrete Research*, 19(1996), pp 29-40.

Maeder U., Wombacher, F., Marazzani, B., (2006), Concrete repair strategies including surface applied corrosion inhibitors, *Proceedings of Concrete Repair, Rehabilitation and Retrofitting Conference*, Alexander (Eds.), Taylor & Francis Group.

Richardson, M., (2005) Effectiveness of corrosion inhibitors in laboratory trials –Part A

Richardson, M., (2006) Test of effectiveness of corrosion inhibitors in field trials –Deliverable D21, Sustainable and advanced materials for road infrastructure report.

